PARAMETER-UNIFORM NUMERICAL METHODS FOR SINGULARLY PERTURBED DELAY PARABOLIC PARTIAL DIFFERENTIAL EQUATIONS

by

Abhishek Das

DEPARTMENT OF MATHEMATICS
INDIAN INSTITUTE OF TECHNOLOGY GUWAHATI
GUWAHATI-781039, INDIA

April, 2017

PARAMETER-UNIFORM NUMERICAL METHODS FOR SINGULARLY PERTURBED DELAY PARABOLIC PARTIAL DIFFERENTIAL EQUATIONS

A thesis submitted
in partial fulfillment of the requirements
for the degree of

DOCTOR OF PHILOSOPHY

by

Abhishek Das
(Roll Number: 126123005)

to the

DEPARTMENT OF MATHEMATICS
INDIAN INSTITUTE OF TECHNOLOGY GUWAHATI
April, 2017

DECLARATION

It is certified that the work contained in this thesis entitled **"Parameter-Uniform Numerical Methods for Singularly Perturbed Delay Parabolic Partial Differential Equations"** has done by me, under the supervision of **Dr. Natesan Srinivasan**, Professor, Department of Mathematics, Indian Institute of Technology Guwahati for the award of the degree of Doctor of Philosophy and this work has not been submitted elsewhere for a degree.

April, 2017

Abhishek Das
Roll No. 126123005
Department of Mathematics
Indian Institute of Technology Guwahati

CERTIFICATE

It is certified that the work contained in this thesis entitled **"Parameter-Uniform Numerical Methods for Singularly Perturbed Delay Parabolic Partial Differential Equations"** by **Abhishek Das,** a student of Department of Mathematics, Indian Institute of Technology Guwahati, for the award of the degree of Doctor of Philosophy has been carried out under my supervision and this work has not been submitted elsewhere for a degree.

April, 2017

Dr. Natesan Srinivasan
Professor
Department of Mathematics
Indian Institute of Technology Guwahati

Dedicated

to

my Parents

Acknowledgement

First and foremost, I would like to thank my supervisor Prof. Natesan Srinivasan. His encouragement, advice and patience during my research have been a great help for me throughout my research tenure. I have always looked up to him for inspiration. I am deeply indebted to him for his utmost care and making me feel free to express my views. I would like to thank him for carefully reading my thesis, providing useful feedback and posing interesting questions. Without his guidance and persistent help this dissertation would not have been possible.

I want to convey my sincere thanks to the members of my doctoral committee Prof. D. C. Dalal, Prof. R. K. Sinha and Prof. S. N. Bora for reviewing my research work periodically and giving valuable suggestions for the improvements of the same. Also, I would like to take the opportunity to thank all my teachers.

I would also like to thank Prof. A. Saikia and his family for making me feel at home.

I sincerely acknowledge Indian Institute of Technology Guwahati for facilities provided to me during my research work. I am most grateful to Ministry of Human Resource Development, Government of India, for providing me financial assistance for the completion of my thesis work.

I thank our technical superintendent Mr. Shantanu Majumdar and Mr. Pranpratim Borgohain and office staff members Mr. Sridhar Samal, Mr. Phatik Kumar and Mr. Saurav Choudhury of the department, for their assistance in various ways during my research period.

I take this opportunity to convey my gratitude to my friends and fellow research scholars for all their timely help, encouragement and support during this period. Thanks to my seniors and friends Kaushik, Murali, Kalyan, Barun, Himadri, Arnab, Santu, Chitralekha, Jhuma, Dishari, Debopam, Nasim, Anirudha, Hiranmoy, Swarup, Sougata, Swapnendu, Ankur, Koyel, Subhadeep, Shamik, Shyam and many others with whom I have shared some of the best moments of my life.

Special thanks to my friend Mr. Anirban Majumdar due to his friendly and wonderful company in my day to day research life. My juniors Mr. Maneesh Kumar Singh and Mr. Gautam Singh also deserve special gratitude.

I am thankful to my seniors Dr. Kaushik Mukherjee, Dr. Pratibhamoy Das and Dr. S. Gowrisankar. I am also grateful to Dr. Jugal Mohapatra, who always helped me to overcome many difficult situations during this period.

Finally, it is not possible for me to adequately express my heartfelt gratitude towards my parents (my mother Mrs. Anita Das and my father Mr. Debasish Das) and my brother (Mr. Kuntal Das) for everything they have done for me from the very first day of my life. I am also deeply indebted to Chandrani for her constant support and inspiration during this journey. I cannot thank them enough for their love which has been the driving force in every aspects of my life. I would also like to convey my deepest love to all my family members.

April, 2017

Abhishek Das

Abstract

The primary interest of this thesis is to provide some efficient numerical techniques for solving singularly perturbed delay parabolic initial-boundary-value problems (IBVPs) in one and two-dimensions. These types of problems are described by partial differential equations (PDEs) in which the highest-order derivative is multiplied by an arbitrarily small parameter ε and contain at least one delay term. Due to the parameter ε, the solution of such equation exhibits a thin layer where the solution varies rapidly, while away from the layer the solution varies slowly and behaves smoothly. Singularly perturbed PDEs model physical problems for which the evolution depend in the present state of the system. In contrast, singularly perturbed delay partial differential equations (DPDEs) relate an unknown function to its derivatives by the past history. Due to the layer phenomena, it is indeed a difficult task to provide ε-uniform numerical methods for singularly perturbed DPDEs, *i.e.*, methods in which the approximated solution converges (measured in supremum norm) to the exact solution of the corresponding continuous problem independently with respect to the parameter ε.

The purpose of this thesis is to apply, analyze and optimize the upwind based numerical methods on Shishkin-type meshes for solving singularly perturbed delay parabolic convection-diffusion problems.

We begin the thesis with general introduction along with the objective and the motivation for solving singularly perturbed delay parabolic PDEs. Then, we give some definitions and terminologies which are used throughout the thesis. Next, we move towards the main work of the thesis. A uniformly convergent hybrid scheme is proposed and analyzed for a 1D DPDE on the piecewise-uniform Shishkin mesh. The hybrid scheme used here, is a proper combination of the midpoint upwind scheme and the central difference scheme. Then, we consider the same problem and use a post-processing technique (Richardson extrapolation), which improves the first-order accuracy of the standard upwind scheme applied on the piecewise-uniform Shishkin mesh to second-order convergence. Numerical experiments are carried out for singularly perturbed linear and semilinear DPDEs.

Then we proceed towards two-dimensional parabolic PDEs. We use a fractional-step method to discretize the time-derivative of the singularly perturbed two-dimensional PDE. The resulting one-dimensional equations are solved by the classical upwind scheme along with the Richardson extrapolation technique. Next, we consider singularly perturbed two-dimensional DPDEs. We use the classical upwind scheme to discretize the spatial derivatives on the standard Shishkin mesh and the Bakhvalov-Shishkin mesh. By considering the fact that the fractional-step method allows us to reduce the computational cost, we use the fractional-step method along with the classical upwind scheme to solve singularly perturbed two-dimensional DPDE. We present numerical results to validate the theoretical findings.

A concise conclusion with possible future work is provided at the end of this thesis.

Contents

NOMENCLATURE

BVP	boundary-value problem
IBVP	initial-boundary-value problem
ODE	ordinary differential equation
PDE	partial differential equation
SPP	singular perturbation problem
DDE	delay differential equation
DPDE	delay partial differential equation
SPDDE	singularly perturbed delay differential equation
$\mathbb{R}$	set of real numbers
ε	singular perturbation parameter
τ	delay parameter
$O(\cdot)$, $o(\cdot)$	landau order symbol
N	number of mesh-intervals in the spatial direction
M	number of mesh-intervals in the time direction
T	final time
x, x_i, y, y_j	continuous and discrete spatial variables
t, t_n	continuous and discrete temporal variables
$h, h_{x,i}, h_{y,j}, H, H_x, H_y, h_x, h_y$	mesh-sizes in spatial direction
Δt	mesh-size in time direction
C	generic positive constant independent of mesh-points, mesh-sizes and ε
Q, $\overline{Q}$	bounded domain in $\mathbb{R} \times [0,T]$ and its colsure
$\|\cdot\|$ or $\|\cdot\|_\infty$	standard supremum norm on Q
$\mathfrak{C}^k(Q), \mathfrak{C}^\mu(Q), \mathfrak{C}^{k+\mu}(Q)$	function spaces
$\Omega_x, \overline{\Omega}_x, \Omega_y, \overline{\Omega}_y, \mathfrak{D}, \overline{\mathfrak{D}}$	continuous spatial domains
Λ_t, Λ_t^M	continuous and discrete time interval $(0,T]$
D	$\Omega_x \times \Lambda_t$
$\mathfrak{G}$	$\mathfrak{D} \times \Lambda_t$
$\overline{\Omega}_x^N, \overline{\Omega}_y^N, \overline{\mathfrak{D}}^N$	discrete spatial domains
$D^{N,M}$, $\mathfrak{G}^{N,M}$	discretization of domain D and $\mathfrak{G}$
Γ, Γ^N, Υ, Υ^N	boundary of given domains
$\mathscr{L}_\varepsilon$, $\mathcal{L}_\varepsilon$, $\mathcal{L}_{x,\varepsilon}$, $\mathcal{L}_{y,\varepsilon}$	differential operators
δ_x^+, δ_x^-, δ_x^0, δ_x^2, δ_y^+, δ_y^-, δ_y^0, δ_y^2, δ_t^-, $\mathscr{L}_{Hybrid}$, $\mathscr{L}_{mu}$, $\mathscr{L}_{cen}$, $\mathscr{L}_\varepsilon^N$, $\mathcal{L}_\varepsilon^N$, $\mathcal{L}_{x,\varepsilon}^N$, $\mathcal{L}_{y,\varepsilon}^N$	difference operators

ϕ_b, φ_b, s	initial data
ϕ_l, ϕ_r, $\tilde{s}$	boundary data
$e_\varepsilon^{N,\Delta t}$, $e^{N,\Delta t}$, $E_\varepsilon^{N,\Delta t}$, $E^{N,\Delta t}$, $\hat{e}_\varepsilon^{N,\Delta t}$, $\hat{e}^{N,\Delta t}$	maximum pointwise error
$p_\varepsilon^{N,\Delta t}$, $p^{N,\Delta t}$, $P_\varepsilon^{N,\Delta t}$, $P^{N,\Delta t}$, $\hat{p}_\varepsilon^{N,\Delta t}$, $\hat{p}^{N,\Delta t}$	order of convergence

List of Figures

List of Tables

CHAPTER 1

Introduction

1.1 Brief Background

The boundary layer phenomena have considerable importance in the area of fluid flow problems, chemical reactor theory, elasticity, heat and mass transfer, semi-conductor device modeling etc. From the mathematical perspective, such kind of problem is called singular perturbation problem (SPP) and the solution of such problem exhibits boundary layer(s) due to the small parameter (ε) multiplied with the highest-order derivative. When $\varepsilon \to 0$, the order of the differential equation is reduced, but the number of boundary conditions remain same and as a consequence, the problem becomes ill-posed. It can be observed that there is a thin layer where the solution varies rapidly, but away from the layer the solution behaves regularly and varies slowly. This class of problem is an attractive area for researchers due to its application nature.

For example, the Navier-Stokes equation of fluid dynamics, which governs the unsteady incompressible viscous fluid flow problem is given by

$$\begin{cases} \dfrac{\partial \mathbf{u}}{\partial t} + \mathbf{u} \cdot \nabla \mathbf{u} + \nabla p = \dfrac{1}{Re} \nabla^2 \mathbf{u}, \\ \nabla \cdot \mathbf{u} = 0, \end{cases} \tag{1.1.1}$$

subject to suitable initial and boundary conditions. Here, p is the pressure and $\mathbf{u}$ is the velocity field whose components are u_1, u_2 along x and y directions. The parameter $Re = |\mathbf{u}|L/\nu$ is the *Reynolds number* with L being the length scale and ν is the kinematic viscosity of the fluid. For sufficiently large Re ($\gg 1$), the equations given in (1.1.1) will be considered as singularly perturbed partial differential equation (PDE), and in such cases considerable amount of numerical difficulties arise due to the presence of boundary

layers. For more examples, one can refer the books of Morton [64], Murray [68] and the survey article of Lagerstrom and Casten [49].

In the Third International Congress of Mathematicians held at Heidelberg in 1904, Prandtl pioneered the subject of boundary layer theory for the first time. In his seven-page report, which was published in the proceedings [82], he explained how a quantity as small as the viscosity of common fluids such as water and air could play a crucial role in determining their flow. In that work, Prandtl had shown that the flow about a body can be dealt by dividing it into two regions: a very thin layer in proximity to the body (which he called the boundary layer) where the frictional effects are prominent and remaining as the outside regions. Afterwards, the boundary layer theory became the foundation stone for modern fluid dynamics. However, Friedrichs and Wasow [30] first commenced the term 'singular perturbation' in their paper on nonlinear vibrations, which was presented at New York University in 1946.

A differential equation is said to be singularly perturbed when the highest-order derivative is multiplied by a small parameter $0 < \varepsilon \ll 1$ (the so-called singular perturbation parameter). Due to the effect of ε, this topic got attention from mathematicians as well as physicists. When the parameter $\varepsilon \to 0$, the problem has a limiting solution, which is called the solution of the reduced problem [20] and the regions of nonuniform convergence lie near the boundary, which are known as boundary layers. Such problems have steep gradients in the narrow layer regions of the considered domain. In general, the analytic solution of these problems has multi-scale behavior. For singularly perturbed PDE, boundary layer can be broadly classified into two types, *i.e.*, parabolic boundary layer and regular boundary layer. If the characteristics of the reduced equation are parallel to the boundary, then it is called parabolic boundary layer otherwise such layer is called regular boundary layer. Another type of boundary layer near a corner, termed as corner layer, is also available in the literature. For better understanding, one can refer to the book of Farrell et al. [28], where these cases are explained nicely with graphs.

Numerical analysis and asymptotic analysis are two main approaches for solving SPPs. By numerical analysis one can get quantitative information about a particular problem, whereas asymptotic analysis provides an insight into the qualitative behavior of a family of problems. Quite a good number of books are available which deal with asymptotic approaches. To cite a few: Bender and Orszag [7], Bush [9], Eckhaus [22, 23], Kevorkian and Cole [42], Miller [61], Nayfeh [74, 75] and O'Malley [78, 79]. Several numerical methods have been developed over the last few decades for solving singularly perturbed stationary and non-stationary problems. For details, one may refer to the books of Doolan et al. [20], Farrell et al. [28] and Miller et al. [60] and the articles of Ewing and Wang [26], Farrell [27], Kadalbajoo and Patidar [35], Kopteva and Stynes

[45], Linß [56], Miller [58], Miller et al. [59] and Stynes [88].

In this thesis, we mainly focus on the numerical solution of singularly perturbed parabolic differential equation with a delay term. At the time of modeling a physical phenomenon, one may assume that the considered system is governed by a principle of causality, *i.e.*, the future state of the system solely depends on the present not on the past state. But, by thorough inspection, it becomes apparent that, more realistic model would involve some of the past history of the system. Such kind of phenomena are modeled by differential equations with delay arguments.

Delay differential equations (DDEs) are classified into four categories. In a DDE, if delay does not occur in the highest-order derivative then such type of DDE is called retarded type. For example, the following first-order ordinary differential equation (ODE)

$$\frac{du}{dx} + au(x) + bu(x - \tau(x)) = g(x),$$

is of retarded type.

If the delay appears in the highest-order derivative then that type of DDE is called neutral type. The example is

$$\frac{du}{dx} + a\frac{du(x - \tau(x))}{dx} + bu(x) + cu(x - \tau(x)) = g(x).$$

If the delay appears in the highest-order derivative and not in the next lower-order then such type of DDE is called advanced type. The following second-order ODE is of this type:

$$\frac{d^2u(x - \tau(x))}{dx^2} + a\frac{du}{dx} + bu(x) + cu(x - \tau(x)) = g(x).$$

Sometime the delay can be a function of an unknown function then that is called state dependent type. The example is

$$\frac{du}{dx} + au(x) + bu(x - \tau(x, u(x))) = g(x).$$

The general theory of DDEs is widely developed and we refer to the classical books by Bellman and Cooke [6], Diekmann et al. [19], Driver [21], El'sgol'ts and Norkin [24], Hale [33], Hale and Verduyn Lunel [34], Kolmanovskii and Myshkis [43], Kolmanovskii and Nosov [44], Kuang [46], Nelson and Perelson [76], Villasana and Radunskaya [93] and Zhao [96], which also include many real-life examples of DDEs.

Here, we consider retarded type DDE. A subclass of these equations is singularly perturbed delay differential equation (SPDDE), *i.e.*, the highest-order derivative term is multiplied by a small parameter (ε) and the equation contains at least one delay term.

For example, consider an automatically controlled furnace. The material strip to be heated is fed into the furnace by rollers whose speed is regulated by the speed controller.

The furnace temperature is varied by means of a heater actuated by a heater controller. The control objective is to maintain a desired spatial temperature distribution in the incoming material, which is fed into the furnace by rollers, the speed of which is regulated by a speed controller. This may be accomplished by placing temperature transducers along the material strip. A computer uses the information from the transducers to generate the appropriate control signals for the heater and feed roller controllers. Owing to the possible presence of time delays in actuation, and in information transmission and processing, the control signals may be delayed in time. A simplified mathematical description of the overall control system may be given by

$$\frac{\partial u(x,t)}{\partial t} = \varepsilon \frac{\partial^2 u(x,t)}{\partial x^2} + v\left(g(u(x,t-\tau))\right) \frac{\partial u(x,t)}{\partial x} + c\left[f(u(x,t-\tau)) - u(x,t)\right],$$

defined on a one-dimensional spatial domain $0 < x < 1$, subject to suitable initial and boundary conditions. Here, v is the instantaneous material strip velocity depending on a prescribed spatial average of the time-delayed temperature distribution $u(x, t-\tau)$, and f represents a distributed temperature source function depending on $u(x, t-\tau)$. More details can be seen in [95].

The so-called Britton model [8] in population dynamics is another example of delay problem, which is given by

$$u_t = \varepsilon \Delta u + u(1 - g * u)$$

with

$$g * u = \int_{t-\tau}^{t} \int_{\Omega} g(x-y, t-s) u(y,s) dy ds.$$

Here, $u(x,t)$ is the population density, which evolves through random migration (modeled by the diffusion term) and reproduction (modeled by the nonlinear reaction term). The latter part contains a convolution operator with a kernel $g(x,t)$, which models the distributed age-structure dependence of the evolution and its dependence on the population levels in the neighborhood.

In brief, the difference between singularly perturbed delay partial differential equations (DPDEs) and singular perturbed PDEs without time delay are:

(i) Singularly perturbed DPDEs can model the time-lag or after effect which cannot be done by conventional instantaneous PDEs.

(ii) If we replace $u(x, t-\tau)$ with the first few terms of the Taylor series expansion, then the solution of the approximated singularly perturbed PDE may behave quite differently from the original solution. Small lags can have large effects.

(iii) For singularly perturbed DPDEs, the initial condition is a function of x and t, defined on the interval $t \in [-\tau, 0]$, whereas in the case of singularly perturbed PDEs, the initial condition is given only on the x-axis, *i.e.,* along $t = 0$.

The boundary layer phenomenon causes severe hurdles in obtaining the numerical approximate solutions by the classical numerical methods on the uniform meshes. Two most reliable numerical methods for solving such type of equations which are available in the literatures are fitted operator methods (FOMs) and fitted mesh methods (FMMs). In FOMs, one uses an exponentially fitted difference scheme on the uniform meshes, which have coefficients of exponential type adapted to the SPP. The extension of FOMs to higher-dimensional problems are too difficult and in some cases it may not be even possible. Whereas, in FMMs, one can use the classical finite difference schemes on the piecewise-uniform mesh or any other layer-adapted nonuniform meshes. In FMMs, the meshes are constructed in such a way that the density of mesh-points will be more in the boundary layer regions compared to the outer regions. The well-known layer resolving fitted meshes are Bakhvalov meshes [4] and Shishkin meshes [60]. To generate the Bakhvalov meshes, one has to solve a nonlinear equation, which is comparatively difficult than generating the piecewise-uniform Shishkin mesh. In both the cases one requires *apriori* information about the width and location of the boundary layer. More information about the layer-adapted nonuniform meshes and the numerical schemes for SPPs can be found in the books of Farrell et al. [28], Miller et al. [60] and Roos et al. [85].

1.2 Objective and Motivation

The main aim of this thesis is to apply, analyze and optimize ε-uniform upwind based FMMs for solving singularly perturbed delay parabolic convection-diffusion problems. The theory and numerical solution of singularly perturbed DPDEs are still at the initial stage whereas numerical methods for singularly perturbed PDEs have been studied extensively by many authors. For details, one may refer the books by Doolan et al. [20], Farrell et al. [28], Miller et al. [60] and Roos et al. [85], where FOMs and FMMs are used for solving singularly perturbed problems in one and two-dimensions. Cai and Liu [10] and Stynes [88] developed uniformly convergent numerical methods on the Shishkin mesh for time dependent and steady-state convection-diffusion problems. One can also look into the articles [5, 69, 70, 71, 72, 91, 92], in which Natesan and his collaborators have proposed initial-value techniques and parallel boundary-value techniques to solve singularly perturbed boundary-value problems (BVPs).

However, constructing a parameter-uniform higher-order numerical method is always a challenging task. Here, we cite some articles, which dealt with such numerical methods, namely, the hybrid scheme and the Richardson extrapolation technique.

A hybrid scheme, which is a proper combination of the midpoint upwind scheme (for

the outer region) and the central difference scheme (for the inner region) was proposed in [65, 67, 89]. The midpoint upwind scheme was first introduced by Abrahamsson et al. [1] for system of singularly perturbed ODE. Stynes and Roos [89] combined this scheme with the central difference scheme to solve a singularly perturbed BVP. Mukherjee and Natesan [65, 67] used the hybrid scheme to solve a singularly perturbed parabolic convection-diffusion problem. The convection coefficient of the problem studied in [65] is continuous, whereas in [67], it is discontinuous. By using this scheme, they were able to obtain almost second-order spatial accuracy. Das and Natesan [17] proposed a higher-order scheme for solving system of reaction-diffusion ODE with mixed type boundary conditions. They used the cubic spline approximation for the inner region and the central difference scheme for the outer region and obtained almost second-order spatial accuracy.

Another method, which exists in the literature, to enhance the order of accuracy of the numerical solutions of SPPs is the Richardson extrapolation technique. This technique was used for singularly perturbed convection-diffusion BVP on the piecewise-uniform Shishkin mesh by Natividad and Stynes [73] and on equidistributed mesh by Das and Natesan [16], whereas Mohapatra and Natesan [62] applied this technique for singularly perturbed delay BVPs for ODEs. This technique was adapted to the system of convection-diffusion two-point BVPs by Deb and Natesan [18], and for parabolic PDEs (without the delay term) by Mukherjee and Natesan [66].

Any system involving a feedback control will almost involve delay since a finite time is required to sense information and then react to it. SPDDEs are very useful tool to model many phenomena in biophysics and mechanics [87, 90]. To solve a SPDDE having both the delay and shift terms, Lange and Miura [50, 51, 52, 53, 54] provided an asymptotic approach, moreover they showed that the effect of the delay and shift terms on the solutions cannot be neglected. Since SPDDE can model a wide range of biological problems, the computation for SPDDE is very important. Amiraliyev and Erdogan [2] suggested an implicit finite difference scheme on the piecewise-uniform Shishkin mesh to solve an initial-value problem (IVP) for a linear first-order DDE and also proved that the method has almost first-order convergence. Erdogan [25] proposed an implicit finite difference scheme on the special Bakhvalov mesh for an IVP. A hybrid finite difference scheme on the Shishkin mesh was suggested by Cen [11]. The FOMs or the FMMs was used by Kadalbajoo et al. [36, 37, 38, 39] and a non-standard finite difference scheme was used by Patidar and Sharma [80, 81] to solve BVPs. Mohapatra and Natesan [63] used the adaptive mesh generation method based on the idea of equidistribution to solve a BVP.

However, comparatively little work has been done for singularly perturbed delay

parabolic PDEs. Ansari et al. [3] considered a delay parabolic reaction-diffusion differential equation on a rectangular domain in the x, t plane. The second-order spatial derivative is multiplied by a small parameter, which gives rise to parabolic boundary layers on the two lateral sides of the rectangle. A numerical method comprising of a standard finite difference operator (central difference in space and implicit-Euler in time) on a rectangular piecewise-uniform fitted mesh condensing in the boundary layers, is proved to be robust with respect to the small parameter, or parameter-uniform, in the sense that its numerical solution converges to the exact solution in the maximum norm, uniformly for all $0 < \varepsilon \ll 1$.

Ramesh and Kadalbajoo [83] considered a class of time-dependent singularly perturbed convection-diffusion problems with retarded terms which often arise in computational neuroscience, *i.e.*, there is a delay term in the spatial variable. By using the Taylor series, they approximated the retarded terms, and finally with the help of a parameter-uniform numerical methods based on the implicit-Euler, upwind and midpoint upwind finite difference schemes, they solved their model problem.

Gowrisankar and Natesan [31] proposed a parameter-uniform computational technique to solve singularly perturbed delay parabolic reaction-diffusion problem. The domain was discretized with a nonuniform mesh obtained via equidistribution of a monitor function for the spatial variable and with a uniform mesh on the time direction. The numerical scheme consists of the implicit-Euler scheme for the time derivative and the classical central difference scheme for the spatial derivative. The proposed numerical scheme is of second-order accurate in space and first-order accurate in time.

In [32], Gowrisankar and Natesan considered a singularly perturbed delay parabolic convection-diffusion problem. They discretized the domain by using a piecewise-uniform Shishkin mesh in the spatial direction and uniform mesh in the temporal direction. The numerical scheme consists of the implicit-Euler scheme for the time derivative and the upwind finite difference scheme for the spatial derivative. The proposed numerical scheme is ε-uniformly convergent with first-order accurate in time and almost first-order (up to a logarithmic factor) accurate in space.

In [47], Kumar and Kadalbajoo considered a class of time-dependent singularly perturbed convection-diffusion problems with the delay in space. To approximate the retarded terms, the Taylor series expansion has been used and the resulting time-dependent SPP is approximated using parameter-uniform numerical method comprised of a standard implicit finite difference scheme to discretize in the temporal direction on the uniform mesh by means of the Rothe's method and a B-spline collocation method in the spatial direction on the piecewise-uniform Shishkin mesh. The method has shown to have almost second-order parameter-uniform convergence.

From the literature, one can observe that in most of the cases no higher-order parameter-uniformly convergent scheme was used to solve singularly perturbed delay parabolic convection-diffusion problem. Some works have been carried out where the delay parameters are involved in space, which is less usual phenomenon than delay in time. Again, the use of the Taylor series approximation for the delay term is not an effective way, because the solution of the approximated singularly perturbed PDE may behave quite differently from the original solution. By considering all these facts, we propose some higher-order parameter-uniformly convergent numerical schemes for solving singularly perturbed delay parabolic convection-diffusion problems.

1.3 Some Notations and Terminologies

In this section, we give some basic definitions, notations and terminology which will be used throughout the thesis.

We denote $\mathcal{C}^k(Q)$ as the space of all functions whose derivatives up to order $k(\geq 0)$ are continuous on Q, where Q is a bounded domain in $\mathbb{R}^n \times [0,T]$. Now, we define the Hölder continuous function.

Definition 1.3.1. *Let $\mu \in (0,1)$. A function $\chi : Q \to \mathbb{R}$ is said to be uniformly Hölder continuous with exponent μ in Q, if the quantity $[\chi]_{\mu,Q}$ is finite, where*

$$[\chi]_{\mu,Q} = \sup_{(\mathbf{x},t),\,(\mathbf{x}',t')\in Q} \frac{|\chi(\mathbf{x},t)-\chi(\mathbf{x}',t')|}{[dist((\mathbf{x},t),\,(\mathbf{x}',t'))]^{\mu}}, \quad dist((\mathbf{x},t),\,(\mathbf{x}',t')) = \left(\|\mathbf{x}-\mathbf{x}'\|^2 + |t-t'|\right)^{1/2},$$

with $\mathbf{x}$, $\mathbf{x}' \in \mathbb{R}^n$ and $\|\mathbf{x}\|$ is the euclidean norm $\left(\sum_{i=1}^{n} x_i^2\right)^{1/2}$.

This coincides with the definition of [29]. The space consisting of Hölder continuous functions is called Hölder continuous space, and it is denoted by $\mathcal{C}^{\mu,\mu/2}(Q)$. For each positive integer $k \geq 1$, the Hölder space $\mathcal{C}^{k+\mu,(k+\mu)/2}(Q)$ is defined as follows:

$$\mathcal{C}^{k+\mu,(k+\mu)/2}(Q) = \left\{ g : \frac{\partial^{i+j} g}{\partial \mathbf{x}^i \partial t^j} \in \mathcal{C}^{\mu,\mu/2}(Q), \text{ for all non-negative integers } i,\, j \text{ with } 0 \leq i+2j \leq k \right\},$$

where $\mathbf{x} = (x_1, x_2, \cdots, x_n)$, $\partial \mathbf{x}^i = \partial x_1^{i_1} \partial x_2^{i_2} \cdots \partial x_n^{i_n}$, and $i = i_1 + i_2 + \cdots + i_n$.

Note that for each integer $k \geq 0$, any function $g \in \mathcal{C}^{k+\mu,(k+\mu)/2}(Q)$ is uniformly continuous in Q and admits a unique extension on $\overline{Q}$. This permits us to speak about values on $\partial Q = \overline{Q} \backslash Q$ of a function $g \in \mathcal{C}^{k+\mu,(k+\mu)/2}(Q)$ and without ambiguity one can write $\mathcal{C}^{k+\mu,(k+\mu)/2}(Q) = \mathcal{C}^{k+\mu,(k+\mu)/2}(\overline{Q})$.

For the analysis, we use the standard supremum norm, which is denoted by $\|\cdot\|_\infty$ and is defined by

$$\|g\|_\infty = \sup_{(\mathbf{x},t)\in Q} |g(\mathbf{x},t)| .$$

Throughout the thesis, C has been used as a generic positive constant which is independent of ε, the mesh-points and the mesh-sizes. Note that C may take different values in different places.

In the analysis, we frequently assume that $\varepsilon \leq N^{-1}$ as it is the case of actual interest from the practical point of view. If $N^{-1} < \varepsilon$, then in practice the model problems considered in this thesis are not difficult to solve computationally, and the analysis can be carried out in the classical way.

Due to the boundary layer, obtaining an ε-independent error bound for a classical discretization methods applied on the uniform mesh is always a difficult task. To measure the performance and the robustness of a numerical method, let us introduce the concept of ε-uniform accuracy.

Definition 1.3.2. *(**ε-Uniform numerical method**) Consider a family of mathematical problems parameterized by a parameter ε where $0 < \varepsilon \ll 1$. Assume that each problem in the family has a unique solution denoted by u_ε and that of each u_ε is approximated by a sequence of numerical solution $\{(U_\varepsilon, \overline{Q}^{N,\Delta t})\}_{N=1}^{\infty}$, where U_ε is defined on the discrete space $\overline{Q}^{N,\Delta t}$ with the discretization parameters N and Δt. Now the numerical solution U_ε is said to converge ε-uniformly to the exact solution u_ε, if there exist a positive integer N_0 and positive number 'C', p and q such that for all $N \geq N_0$ and $M \geq M_0$, where $M = T/\Delta t$, we have*

$$\sup_{0<\varepsilon\ll 1} \|U_\varepsilon - u_\varepsilon\| \leq C\left(N^{-p} + \Delta t^q\right),$$

where N_0, M_0, C, p and q are independent of ε.

Here p and q are ε-uniform order of convergence with respect to the spatial and temporal variables, respectively, and C is called the ε-uniform error constant.

We choose the maximum norm for the measurement of the error, because we need to measure the error in a very small part of the domain where the boundary layer occurs. Other norms, such as the root mean square norm fails to capture the local behavior of the error inside the boundary layer regions. Further discussion on the choice of the norm can be found in the book of Miller et al. [60].

Now, we define the standard finite difference operators which are useful for describing the difference schemes in the subsequent chapters. For that, we consider the arbitrary meshes in the spatial direction as $\overline{\Omega}_x^N = \{0 = x_0 < x_1 < \cdots < x_N = 1\}$, and in the temporal direction as $\Lambda_t^M = \{0 = t_0 < t_1 < \cdots < t_m = T\}$.

For a given mesh function $q(x_i, t_n) = q_i^n$, define the forward, backward and central difference operators δ_x^+, δ_x^- and δ_x^0 in space by

$$\delta_x^+ q_i^n = \frac{q_{i+1}^n - q_i^n}{x_{i+1} - x_i}, \quad \delta_x^- q_i^n = \frac{q_i^n - q_{i-1}^n}{x_i - x_{i-1}} \quad \text{and} \quad \delta_x^0 q_i^n = \frac{q_{i+1}^n - q_{i-1}^n}{x_{i+1} - x_{i-1}},$$

respectively, and we define the second-order central difference operator δ_x^2 by

$$\delta_x^2 q_i^n = \frac{2(\delta_x^+ q_i^n - \delta_x^- q_i^n)}{x_{i+1} - x_{i-1}},$$

and define the backward difference operator δ_t^- in time by

$$\delta_t^- q_i^n = \frac{q_i^n - q_i^{n-1}}{t_n - t_{n-1}}.$$

In an analogous way, for a given mesh function $q(x_i, y, t_n) = q_{x_i,y}^n$, $y \in \Omega_y^N$, we define the forward difference operator δ_x^+, the backward difference operator δ_x^- (for first-order spatial derivative) and the central difference operator δ_x^2 (for second-order spatial derivative) in spatial x-direction by

$$\delta_x^+ q_{x_i,y}^n = \frac{q_{x_{i+1},y}^n - q_{x_i,y}^n}{x_{i+1} - x_i}, \; \delta_x^- q_{x_i,y}^n = \frac{q_{x_i,y}^n - q_{x_{i-1},y}^n}{x_i - x_{i-1}} \; \text{and} \; \delta_x^2 q_{x_i,y}^n = \frac{2(\delta_x^+ q_{x_i,y}^n - \delta_x^- q_{x_i,y}^n)}{x_{i+1} - x_{i-1}},$$

respectively.

Similarly, we define all the difference operators in y-direction. The backward difference operator δ_t^- is defined by

$$\delta_t^- q_{x_i,y_j}^n = \frac{q_{x_i,y_j}^n - q_{x_i,y_j}^{n-1}}{t_n - t_{n-1}}$$

to approximate the first-order time derivative.

Now, we provide the definition of an M-matrix, as given in the books [28, 85].

Definition 1.3.3. *A matrix $\boldsymbol{A} = (a_{i,j}) \in \mathbb{R}^{k,k}$ is an M-matrix if $\boldsymbol{A}$ is nonsingular, $\boldsymbol{A}^{-1} \geq 0$ and $a_{i,j} \leq 0$, for all $i \neq j$, $1 \leq i, j \leq k$.*

The next definition is of ***Landau's order symbols*** O (big-oh) and o (little-oh), which are used throughout the thesis. One can refer the books [42, 78] for further discussion of the following definitions. Let $f(\varepsilon)$ and $g(\varepsilon)$ be two real valued functions, where $0 < \varepsilon \leq \varepsilon_0 \ll 1$.

Definition 1.3.4. *The expression $f(\varepsilon) = O(g(\varepsilon))$ as $\varepsilon \to 0$, defines that there exist some positive constants C and ε_0 satisfying $\varepsilon \in (0, \varepsilon_0]$ such that*

$$|f(\varepsilon)| \leq C\,|g(\varepsilon)|\,, \quad \varepsilon \to 0.$$

Definition 1.3.5. *The expression $f(\varepsilon) = o(g(\varepsilon))$ as $\varepsilon \to 0$, defines that*

$$\lim_{\varepsilon \to 0} \frac{f(\varepsilon)}{g(\varepsilon)} = 0.$$

1.3.1 Shishkin-type meshes

To explain about the meshes used throughout the thesis, we consider the linear convection-diffusion two-point BVP for second-order ODE:

$$\begin{cases} -\varepsilon u''(x) - a(x)u'(x) + b(x)u(x) = f(x), \quad x \in \Omega_x := (0,1), \\ u(0) = 0 = u(1). \end{cases} \tag{1.3.1}$$

Moreover, we assume that the functions $a(x)$, $b(x)$ and $f(x)$ are continuous, $0 < \varepsilon \ll 1$ is the perturbation parameter and $a(x) \geq \alpha > 0$. The solution of (1.3.1) has an exponential boundary layer at $x = 0$ which behaves like $\exp(-\alpha x/\varepsilon)$.

Let $\rho = \rho_0 \varepsilon \ln N$ where $N \geq 4$ be an even positive integer. Following [84], we consider a mesh which is graded in $[0, x_{N/2}]$ and equidistant in $[x_{N/2}, 1]$, where $x_{N/2} = \rho$. Let φ be the mesh generating function on $[0, x_{N/2}]$ with the properties $\varphi(0) = 0$ and $\varphi(1/2) = \ln N$, where $\varphi(\sigma)$ is a monotonically increasing and piecewise continuously differentiable function. Then, the mesh-points are given by

$$x_i = \begin{cases} \rho_0 \varepsilon \varphi(\sigma_i), & \text{for } \sigma_i = i/N,\ i = 0,\ 1, \cdots, N/2, \\ 1 - (1-\rho)\dfrac{2(N-i)}{N}, & \text{for } i = N/2+1, \cdots, N. \end{cases}$$

Moreover, we assume that φ' does not decrease, which leads to a mesh that does not condense on $[0, \rho]$ as we move away from the layer. This condition ensures that $h_i \leq h_{i+1}$, for $i = 1, \cdots, N/2 - 1$, where $h_i = x_i - x_{i-1}$. For $i = N/2 + 1, \cdots, N$, we have $N^{-1} \leq h_i = H \leq 2N^{-1}$.

We now define a monotonically increasing function ψ, which is closely related to φ, such that $\varphi = -\ln \psi$, with $\psi(0) = 1$ and $\psi(1/2) = N^{-1}$. For different choices of mesh characterizing function ψ, we define three types of Shishkin-type meshes as follows:

The Shishkin mesh [60]:

$$\psi(\sigma) = \exp\left(-2(\ln N)\sigma\right);$$

The Bakhvalov-Shishkin mesh [55]:

$$\psi(\sigma) = 1 - 2(1 - N^{-1})\sigma;$$

Modified Bakhvalov-Shishkin mesh [94]:

$$\psi(\sigma) = \exp\left(-\sigma/(q-\sigma)\right) \quad \text{with} \quad q = \frac{1}{2} + \frac{1}{2\ln N}.$$

1.4 Model Problems

In this section, the model problems considered in this thesis are described briefly. For clarity of the presentation, we elaborately provide these model problems with suitable information on the given data at the beginning of the subsequent chapters.

The following types of model problems are considered and their concise descriptions are given below:

1.4.1 Singularly perturbed 1D delay parabolic convection-diffusion problem

Let $\Omega_x = (0,1)$, $\Lambda_t = (0,T]$, $D = \Omega_x \times \Lambda_t$, and $\Gamma = \Gamma_l \cup \Gamma_b \cup \Gamma_r$, where Γ_l and Γ_r are the left and right sides of the rectangular domain D corresponding to $x = 0$ and $x = 1$, respectively, and $\Gamma_b = \overline{\Omega}_x \times [-\tau, 0]$. Consider the following singularly perturbed delay parabolic initial-boundary-value problem (IBVP):

$$\begin{cases} \left(\dfrac{\partial}{\partial t} + \mathscr{L}_\varepsilon\right) u(x,t) = -c(x,t)u(x,t-\tau) + f(x,t), & (x,t) \in D, \\ u(x,t) = \phi_b(x,t), & (x,t) \in \Gamma_b, \\ u(0,t) = \phi_l(t), & \text{on } \Gamma_l = \{(0,t) : 0 \le t \le T\}, \\ u(1,t) = \phi_r(t), & \text{on } \Gamma_r = \{(1,t) : 0 \le t \le T\}, \end{cases} \tag{1.4.1}$$

where

$$\mathscr{L}_\varepsilon u(x,t) = -\varepsilon u_{xx}(x,t) + a(x)u_x(x,t) + b(x,t)u(x,t),$$

$0 < \varepsilon \ll 1$ is the singular perturbation parameter and $\tau > 0$ is the delay parameter. The coefficients $a(x)$, $b(x,t)$, $c(x,t)$, $f(x,t)$ on $\overline{D}$, and the boundary, initial values $\phi_l(t)$, $\phi_r(t)$, $\phi_b(x,t)$ on Γ, are sufficiently smooth and bounded functions such that $a(x) \ge \alpha > 0$, $b(x,t) \ge 0$ and $c(x,t)$ is nonzero on $\overline{D}$. The terminal time T is assumed to satisfy the condition $T = k\tau$ for some positive integer k. The solution of the IBVP (1.4.1) exhibits a boundary layer along $x = 1$.

1.4.2 Singularly perturbed 1D semilinear delay parabolic problem

Consider the following singularly perturbed semilinear delay PDE:

$$\begin{cases} u_t - \varepsilon u_{xx} + a(x)u_x = r(x,t,u(x,t),u(x,t-\tau)), & (x,t) \in D, \\ u(x,t) = \phi_b(x,t), & (x,t) \in \Gamma_b, \\ u(0,t) = \phi_l(t), & \text{on } \Gamma_l = \{(0,t) : 0 \le t \le T\}, \\ u(1,t) = \phi_r(t), & \text{on } \Gamma_r = \{(1,t) : 0 \le t \le T\}, \end{cases} \tag{1.4.2}$$

where $0 < \varepsilon \ll 1$ is the singular perturbation parameter and $\tau > 0$ is the delay parameter. Under sufficient smoothness and compatibility conditions imposed on the functions $a(x)$, $r(x,t,u(x,t),u(x,t-\tau))$, ϕ_b, ϕ_l and ϕ_r, the delay problem (1.4.2) admits a unique solution $u(x,t)$ which exhibits a boundary layer along $x = 1$ (for $a(x) \geq \alpha > 0$).

1.4.3 Singularly perturbed 2D parabolic convection-diffusion problem

Consider the following singularly perturbed 2D parabolic convection-diffusion IBVP posed on the domain $\mathfrak{G} = \mathfrak{D} \times \Lambda_t$, where $\mathfrak{D} = (0,1)^2$ and $\Lambda_t = (0,T]$:

$$\begin{cases} u_t + \mathcal{L}_\varepsilon u(x,y,t) = f(x,y,t), & (x,y,t) \in \mathfrak{G}, \\ u(x,y,0) = s(x,y), & (x,y) \in \overline{\mathfrak{D}}, \\ u(x,y,t) = 0, & (x,y,t) \in \partial\mathfrak{D} \times \overline{\Lambda}_t, \end{cases} \tag{1.4.3}$$

where

$$\mathcal{L}_\varepsilon u = -\varepsilon\Delta u + \mathbf{a}(x,y).\nabla u + b(x,y)u,$$

$0 < \varepsilon \ll 1$ is the singular perturbation parameter. We assume the functions $\mathbf{a} = (a_1, a_2)$, b, f and s are sufficiently smooth and bounded such that $a_1(x,y) \geq \alpha_{_x} > 0$, $a_2(x,y) \geq \alpha_{_y} > 0$ and $b(x,y) \geq 0$, on $\overline{\mathfrak{D}}$. The solution of the IBVP (1.4.3) exhibits boundary layers along the sides $x = 1$ and $y = 1$, and a corner layer at $(x,y) = (1,1)$.

1.4.4 Singularly perturbed 2D delay parabolic convection-diffusion problem

Consider the following singularly perturbed 2D delay parabolic convection-diffusion IBVP:

$$\begin{cases} u_t + \mathcal{L}_\varepsilon u(x,y,t) = -c(x,y)u(x,y,t-\tau) + f(x,y,t), & (x,y,t) \in \mathfrak{G}, \\ u(x,y,t) = \varphi_b(x,y,t), & (x,y,t) \in \Upsilon_b = \overline{\mathfrak{D}} \times [-\tau, 0], \\ u(x,y,t) = 0, & (x,y,t) \in \partial\mathfrak{D} \times \overline{\Lambda}_t, \end{cases} \tag{1.4.4}$$

where

$$\mathcal{L}_\varepsilon u = -\varepsilon\Delta u + \mathbf{a}(x,y).\nabla u + b(x,y)u,$$

$0 < \varepsilon \ll 1$ is the singular perturbation parameter and $\tau > 0$ is the delay parameter. We assume the functions $\mathbf{a} = (a_1, a_2)$, b, c, f and φ_b are sufficiently smooth and bounded such that $a_1(x,y) \geq \alpha_{_x} > 0$, $a_2(x,y) \geq \alpha_{_y} > 0$, $b(x,y) \geq 0$ and $c(x,y)$ is nonzero on $\overline{\mathfrak{D}}$. Under these assumptions, the solution of (1.4.4) exhibits boundary layers along the sides $x = 1$ and $y = 1$, and a corner layer at $(x,y) = (1,1)$.

1.5 General Outline of the Thesis

In this thesis, we focus on obtaining the numerical solution of singularly perturbed delay parabolic convection-diffusion problems in one and two-dimensions by some higher-order parameter-uniform numerical methods. First, we consider a one-dimensional singularly perturbed delay convection-diffusion problem, and we use the implicit-Euler scheme to discretize the time derivative and the hybrid scheme to discretize the spatial derivatives on the Shishkin mesh. We study the convergence of the scheme in the maximum norm, which shows the method converges uniformly with almost second-order accuracy in space and first-order accuracy in time. To validate the theoretical findings, numerical experiments are carried out.

It is well-known that the classical central difference scheme applied on the uniform mesh fails to provide satisfactory numerical solution for singularly perturbed convection-diffusion problems until we use unacceptably large number of mesh-points in comparison with the perturbation parameter ε. Therefore, special attention has to be paid to obtain second-order ε-uniformly convergent numerical solutions for singularly perturbed PDE having convection term. Due to this, we use the Richardson extrapolation technique, which gives second-order convergence not only in space, but also in time. Numerical experiments justify the theoretical results.

Then, we proceed towards two-dimensional parabolic PDEs. To solve the parabolic PDE, we use a fractional-step method along with the Richardson extrapolation technique. Fractional-step method allows us to convert the 2D problem into two 1D problems. As a consequence, one can obtain the numerical solution by solving only two tridiagonal matrices instead of a banded pentadiagonal matrix. By using the Richardson extrapolation technique, we are able to obtain second-order accuracy in space and time. Numerical experiments are carried out to show the convergence rate.

Next, we consider the singularly perturbed 2D delay parabolic convection-diffusion problem. We use the classical upwind scheme to discretize the problem on the Shishkin mesh. Also, we derive the error estimate, which shows that the method applied on the model problem is first-order convergence in space and time. Next, we use the Bakhvalov-Shishkin mesh instead of the Shishkin mesh, and we observe that error bound obtained for the scheme applied on the Bakhvalov-Shishkin mesh is optimal. Then, we consider the same problem and we use the fractional-step method to convert the 2D delay problem into two 1D delay problems. We solve the resulting 1D delay problems by the classical upwind scheme. Though, it gives almost first-order accuracy in space and time, but it is very efficient from the computational point of view.

The rest of this thesis consists of seven chapters and is organized as follows:

In **Chapter 2**, the singularly perturbed DPDEs of the form (1.4.1) is solved numerically on the uniform mesh in the temporal direction and the piecewise-uniform Shishkin mesh in the spatial direction. To discretize the temporal and spatial derivatives, we used the implicit-Euler scheme and the hybrid scheme, respectively. The method converges with almost second-order accurate in space and first-order accurate in time. Numerical experiments are carried out to validate the theoretical error estimates. We also carried out numerical experiment for singularly perturbed semilinear delay parabolic problem of the form (1.4.2).

The Richardson extrapolation technique is discussed in **Chapter 3**, which improves the accuracy of the upwind finite difference scheme on the piecewise-uniform Shishkin mesh, applied to the singularly perturbed DPDEs of the form (1.4.1). We proved theoretically that extrapolation provides second-order ε-uniform convergence in space as well as in time. The numerical results reveal the theoretical finding.

In **Chapter 4**, we solved a singularly perturbed 2D parabolic convection-diffusion problem of the form (1.4.3) on the uniform mesh in the temporal domain and a special piecewise-uniform Shishkin mesh in the spatial domains. First, we use a fractional-step method for the discretization of the time derivative, which gives a set of two 1D problems. Then, we use the upwind finite difference scheme to solve those 1D problems. To obtain a better approximate solution, we used the Richardson extrapolation technique. Theoretically we have shown that the extrapolation method provides second-order ε-uniform convergence in space and time. Numerical experiments are carried out to validate theoretical findings.

Chapter 5 deals with a singularly perturbed two-dimensional DPDE of the form (1.4.4). We discretized the temporal domain with the uniform mesh and the spatial domains with a special piecewise-uniform Shishkin mesh. To discretize the continuous problem, we used the implicit-Euler scheme and the classical upwind scheme for the temporal and spatial derivatives, respectively. The method converges uniformly with first-order (up to a logarithmic factor) in space and first-order in time. Numerical experiments are carried to validate the theoretical findings.

Chapter 6 contains the characterization of the Bakhvalov-Shishkin mesh, for discretization of the spatial domains while solving a singularly perturbed 2D delay parabolic convection-diffusion problem of the form (1.4.4). We formed the Bakhvalov-Shishkin mesh with the help of an appropriate mesh-generating function. To discretize the continuous problem, we applied the implicit-Euler scheme and the classical upwind scheme for the temporal and spatial derivatives, respectively. We proved theoretically and numerically that the proposed scheme applied on the Bakhvalov-Shishkin mesh provides first-order accuracy in space as well as in time.

Chapter 7 is devoted to solve the singularly perturbed 2D delay parabolic convection-diffusion problems of the form (1.4.4) with the fractional-step method on the uniform mesh in the temporal direction and a special piecewise-uniform Shishkin mesh in the spatial directions. With the help of the fractional-step method, we obtained two 1D stationary problems, which we discretized further by the classical upwind scheme. It is theoretically proved that the proposed scheme converges first-order (up to a logarithmic factor) in space and first-order in time. Along with the analysis, we provided numerical examples, which verify the theoretical findings.

Finally, **Chapter 8** contains the summary of the results highlighting the contributions made in this thesis and also provides possible future scopes of the present works.

Extensive numerical examples are given in support of the theoretical results and to show the accuracy of the numerical scheme. Those examples are presented at the end of each chapter of the thesis.

CHAPTER 2

Uniformly Convergent Hybrid Numerical Scheme for Singularly Perturbed 1D Delay Parabolic Convection-Diffusion Problems on Shishkin Mesh

This chapter studies the numerical solution of singularly perturbed one-dimensional delay parabolic convection-diffusion problems. Since the solutions of these problems exhibit regular boundary layers in the spatial variable, we use the piecewise-uniform Shishkin mesh for the discretization of the domain in the spatial direction and uniform mesh in the temporal direction. The time derivative is discretized by the implicit-Euler scheme and the spatial derivatives are discretized by the hybrid scheme. For the proposed scheme, the stability analysis is carried out and parameter-uniform error estimates are derived. Numerical examples are presented to show the accuracy and efficiency of the proposed scheme.

2.1 Introduction

Let $\Omega_x = (0,1)$, $\Lambda_t = (0,T]$, $D = \Omega_x \times \Lambda_t$ and $\Gamma = \Gamma_l \cup \Gamma_b \cup \Gamma_r$, where Γ_l and Γ_r are the left and the right sides of the rectangular domain D corresponding to $x = 0$ and $x = 1$, respectively, and $\Gamma_b = \overline{\Omega}_x \times [-\tau, 0]$, $\tau > 0$. In this chapter, we consider the following class of singularly perturbed DPDEs with Dirichlet boundary conditions:

$$\begin{cases} \left(\dfrac{\partial}{\partial t} + \mathscr{L}_\varepsilon\right) u(x,t) = -c(x,t)u(x,t-\tau) + f(x,t), & (x,t) \in D, \\ u(x,t) = \phi_b(x,t), & (x,t) \in \Gamma_b, \\ u(0,t) = \phi_l(t), & \text{on } \Gamma_l = \{(0,t) : 0 \le t \le T\}, \\ u(1,t) = \phi_r(t), & \text{on } \Gamma_r = \{(1,t) : 0 \le t \le T\}, \end{cases} \tag{2.1.1}$$

where

$$\mathscr{L}_\varepsilon u(x,t) = -\varepsilon u_{xx}(x,t) + a(x)u_x(x,t) + b(x,t)u(x,t),$$

$0 < \varepsilon \ll 1$ is the singular perturbation parameter and $\tau > 0$ is the delay parameter. The coefficients $a(x)$, $b(x,t)$, $c(x,t)$, $f(x,t)$ on $\overline{D}$ and the boundary, initial values $\phi_l(t)$, $\phi_r(t)$, $\phi_b(x,t)$ on Γ, are sufficiently smooth and bounded functions, such that $a(x) \geq \alpha > 0$, $b(x,t) \geq 0$ and $c(x,t)$ is nonzero on $\overline{D}$.

Under these assumptions, the solution of the IBVP (2.1.1) exhibits a regular boundary layer of width $O(\varepsilon)$ along $x = 1$. The terminal time T is assumed to satisfy the condition $T = k\tau$ for some positive integer k.

The classical finite difference methods applied on the uniform mesh fail to provide satisfactory numerical solution for SPPs, until we use unacceptably large number of mesh-points in comparison with the perturbation parameter ε. This drawback motivates to develop ε-uniform numerical methods for SPPs, *i.e.,* the order of convergence and the error constant are independent of ε.

The outline of this chapter is as follows: In Section 2.2, we obtain the bounds of the solution of the continuous problem. Section 2.3 deals with the piecewise-uniform Shishkin mesh and the hybrid numerical scheme. The main proof of convergence has been derived in Section 2.4. Section 2.5 deals with the singularly perturbed semilinear DPDE. Numerical results are presented in Section 2.6 and the chapter ends with Section 2.7 that summarizes the main conclusions.

2.2 Bounds for the Solution of the Continuous Problem

In this section, we study the analytical aspects of the solution of the IBVP (2.1.1) and its derivatives. The existence and uniqueness of the solution for our model problem (2.1.1) can be guaranteed by the sufficient smoothness of $\phi_l(t)$, $\phi_b(x,t)$ and $\phi_r(t)$ along with the compatibility condition at the corner points and delay terms as stated below:

$$\phi_b(0,0) = \phi_l(0), \ \phi_b(1,0) = \phi_r(0), \tag{2.2.1}$$

and

$$\begin{aligned}
&\frac{d\phi_l(t)}{dt} - \varepsilon\frac{\partial^2\phi_b(x,t)}{\partial x^2} + a(x)\frac{\partial\phi_b(x,t)}{\partial x} \quad + b(x,t)\phi_b(x,t) \\
&\qquad = -c(x,t)\phi_b(x,t-\tau) + f(x,t), \text{ at } (x,t) = (0,0), \\
&\frac{d\phi_r(t)}{dt} - \varepsilon\frac{\partial^2\phi_b(x,t)}{\partial x^2} + a(x)\frac{\partial\phi_b(x,t)}{\partial x} \quad + b(x,t)\phi_b(x,t) \\
&\qquad = -c(x,t)\phi_b(x,t-\tau) + f(x,t), \text{ at } (x,t) = (1,0).
\end{aligned} \tag{2.2.2}$$

The operator $\left(\frac{\partial}{\partial t}+\mathscr{L}_\varepsilon\right)$ defined in (2.1.1) satisfies the following maximum principle.

Lemma 2.2.1. *(***Maximum principle***) Suppose the function* $\psi(x,t)\in \mathfrak{C}^0(\overline{D})\cap\mathfrak{C}^2(D)$, *satisfies* $\left(\frac{\partial}{\partial t}+\mathscr{L}_\varepsilon\right)\psi(x,t)\geq 0$ *in* D *and* $\psi(x,t)\geq 0$ *on* Γ. *Then* $\psi(x,t)\geq 0$, *for all* $(x,t)\in\overline{D}$.

Proof. Let $(x^*,t^*)\in\overline{D}$, such that $\psi(x^*,t^*)=\min\limits_{(x,t)\in\overline{D}}\psi(x,t)$ and assume that $\psi(x^*,t^*)<0$. Clearly $(x^*,t^*)\notin\Gamma$ and $(x^*,t^*)\in D$.

As it attains minimum at (x^*,t^*), we have $\psi_x=0$, $\psi_t=0$ and $\psi_{xx}\geq 0$ at (x^*,t^*). Therefore, from (2.1.1), we have

$$\left(\frac{\partial}{\partial t}+\mathscr{L}_\varepsilon\right)\psi(x^*,t^*)\leq 0,$$

which is a contradiction as $\left(\frac{\partial}{\partial t}+\mathscr{L}_\varepsilon\right)\psi(x,t)\geq 0$. Hence $\psi(x,t)\geq 0$, for all $(x,t)\in\overline{D}$. ∎

The following lemma will help us to find the bound of the continuous solution u.

Lemma 2.2.2. *The solution of the DPDE (2.1.1) satisfies the following estimate:*

$$|u(x,t)-\phi_b(x,0)|\leq Ct \quad \textit{and} \quad |u(x,t)|\leq C, \quad (x,t)\in\overline{D},$$

where the constant C *is independent of* ε.

Proof. Let

$$q(x,t)=\begin{cases} u(x,t)-\phi_b(x,0), & \text{for } \ 0\leq t\leq T,\\ u(x,t)-\phi_b(x,t), & \text{for } \ -\tau\leq t\leq 0,\end{cases}$$

then $q(x,t)$ satisfies the following PDE

$$\left(\frac{\partial}{\partial t}+\mathscr{L}_\varepsilon\right)q(x,t)=h(x,t), \quad (x,t)\in D, \tag{2.2.3}$$

where

$$\begin{aligned} h(x,t) &= f(x,t)-c(x,t)u(x,t-\tau)-\left(\frac{\partial}{\partial t}+\mathscr{L}_\varepsilon\right)(\phi_b(x,0))\\ &= f(x,t)-c(x,t)u(x,t-\tau)+\varepsilon(\phi_b)_{xx}(x,0)-a(x)(\phi_b)_x(x,0)-b(x,t)\phi_b(x,0)\end{aligned}$$

and on the boundary Γ_b:

$$q(x,t)=u(x,t)-\phi_b(x,t)=\phi_b(x,t)-\phi_b(x,t)=0.$$

Then $q(0,t)=\phi_l(t)-\phi_b(0,0)$ and $q(1,t)=\phi_r(t)-\phi_b(1,0)$, where $t\in[0,T]$.

Now, by taking modulus on both the sides and by using the compatibility conditions at the corner points along with the smoothness of ϕ_l and ϕ_r, we get

$$|q(0,t)| = C_1 t, \quad |q(1,t)| = C_2 t, \ t \in [0,T],$$

for some constants C_1 and C_2. To prove the required bound, we will proceed step by step. When, the domain of definition of the PDE (2.2.3) is $\Omega_x \times (0,\tau)$, we consider a function $r(x,t)$ as follows:

$$r(x,t) = \begin{cases} Ct, & \text{for } \ 0 \le t \le \tau, \\ 0, & \text{for } \ -\tau \le t \le 0, \end{cases}$$

for any constant C, we have

$$\begin{cases} \left(\dfrac{\partial}{\partial t} + \mathscr{L}_\varepsilon\right) r(x,t) = (1 + tb(x,t))\, C, & (x,t) \in \Omega_x \times (0,\tau), \\ r(x,t) = 0, & \text{on } \Gamma_b, \\ r(0,t) = r(1,t) = Ct, & \text{for } 0 \le t \le \tau. \end{cases}$$

Now, for sufficiently large C, from the above PDE and (2.2.3), we get

$$\left|\left(\frac{\partial}{\partial t} + \mathscr{L}_\varepsilon\right) q(x,t)\right| \le \left(\frac{\partial}{\partial t} + \mathscr{L}_\varepsilon\right) r(x,t), \quad (x,t) \in \Omega_x \times (0,\tau),$$

and from the initial and boundary conditions, we have

$$|q(x,t)| \le r(x,t), \quad \text{on } \Gamma.$$

Therefore, by using the maximum principle (Lemma 2.2.1), we get

$$|q(x,t)| \le r(x,t), \quad (x,t) \in \overline{\Omega}_x \times [0,\tau],$$

which implies that

$$|q(x,t)| \le Ct, \quad (x,t) \in \overline{\Omega}_x \times [0,\tau].$$

Now, from the definition of $q(x,t)$, one can easily deduce that

$$|u(x,t)| \le C, \quad (x,t) \in \overline{\Omega}_x \times [0,\tau].$$

Next, we consider the PDE (2.2.3) in the domain $\Omega_x \times (0,2\tau)$. Now, by choosing $r(x,t) = Ct$, $0 \le t \le 2\tau$ and proceeding in a similar way along with the bound of the solution obtained in $[0,\tau]$, we can obtain

$$|q(x,t)| \le Ct, \quad (x,t) \in \overline{\Omega}_x \times [0,2\tau],$$

which immediately gives that

$$|u(x,t)| \leq C, \quad (x,t) \in \overline{\Omega}_x \times [0, 2\tau].$$

Analogously, we can prove the required bound for the entire domain $\overline{D}$. This completes the proof. ∎

To obtain the bounds of the derivatives of the solution $u(x,t)$ of (2.1.1), we follow the approach adapted in [77]. Further, without loss of generality we assume that the initial and boundary values of (2.1.1) are identically zero, *i.e.*, $\phi_b(x,t) = 0$, $\phi_l(t) = 0$ and $\phi_r(t) = 0$.

Theorem 2.2.3. *For all non-negative integers l, m, satisfying $0 \leq l + m \leq 5$, the derivatives of the exact solution $u(x,t)$ of the IBVP (2.1.1) satisfy the estimate*

$$\left| \frac{\partial^{l+m} u}{\partial x^l \partial t^m} \right| \leq C \left(1 + \varepsilon^{-l} \exp(-\alpha(1-x)/\varepsilon)\right), \qquad (x,t) \in D.$$

Proof. To prove the above bound, we will consider several cases.

Case 1. Here we consider the case, where $l = 0$ and $m = 0$. The required bound follows from Lemma 2.2.2.

Case 2. Let us take $l = 0$ and $m = 1$. On the sides $x = 0$ and $x = 1$ of $\overline{D}$, we have $u \equiv 0$, therefore $u_t = 0$ along $x = 0$ and $x = 1$. On the side $t = 0$, *i.e.*, along the x-axis, we have $u \equiv 0$, which implies that $u_x \equiv 0$, $u_{xx} \equiv 0$. Substituting these values in (2.1.1), we obtain that $u_t(x,0) = f(x,0)$. For $(x,t) \in \Gamma_b$, we have

$$u_t = \lim_{k \to 0} \frac{u(x,t+k) - u(x,t)}{k} = 0.$$

Thus for sufficiently large C on Γ, we can have $|u_t(x,t)| \leq C$.

Now, apply the differential operator $\left(\frac{\partial}{\partial t} + \mathscr{L}_\varepsilon\right)$ as defined in (2.1.1) to u_t, then we obtain

$$\begin{aligned} \left(\frac{\partial}{\partial t} + \mathscr{L}_\varepsilon\right)(u_t)(x,t) &= u_{tt} - \varepsilon u_{txx} + a(x) u_{tx} + b(x,t) u_t(x,t) \\ &= (u_t - \varepsilon u_{xx} + a(x) u_x + b(x,t) u)_t - b_t(x,t) u. \end{aligned} \tag{2.2.4}$$

First we consider the case, where $u(x, t-\tau)$ is a known function, *i.e.*, when $t \in [0, \tau]$. In (2.2.4), if we use the given initial condition, we get $\left(\frac{\partial}{\partial t} + \mathscr{L}_\varepsilon\right)(u_t) = f_t(x,t) - b_t(x,t)u$.

By using Lemma 2.2.2, we get

$$\left| \left(\frac{\partial}{\partial t} + \mathscr{L}_\varepsilon\right)(u_t)(x,t) \right| \leq C, \text{ for } (x,t) \in \Omega_x \times [0, \tau]. \tag{2.2.5}$$

Now applying the maximum principle (Lemma 2.2.1), we get $|u_t(x,t)| \leq C$, $(x,t) \in \overline{\Omega}_x \times [0, \tau]$.

Next, let us take $(x,t) \in \overline{\Omega}_x \times [0, 2\tau]$. For $t \in [\tau, 2\tau]$, from (2.2.4), we get

$$\left(\frac{\partial}{\partial t} + \mathscr{L}_\varepsilon\right)(u_t)(x,t) = f_t(x,t) - b_t(x,t)u - c_t u(x,t-\tau) - cu_t(x,t-\tau).$$

As we know $|u_t(x,t)| \leq C$, for all $(x,t) \in \overline{\Omega}_x \times [0,\tau]$, therefore, in this case also we have

$$\left|\left(\frac{\partial}{\partial t} + \mathscr{L}_\varepsilon\right)(u_t)(x,t)\right| \leq C, \quad \text{for } (x,t) \in \Omega_x \times [\tau, 2\tau]. \tag{2.2.6}$$

Therefore, by combining (2.2.5) and (2.2.6) and by applying the maximum principle (Lemma 2.2.1) over the domain $\Omega_x \times [0, 2\tau]$, we get $|u_t(x,t)| \leq C$. In a similar way, we can prove the required bound for the entire domain $\overline{D}$.

Case 3. Now consider the case, where $l = 1$ and $m = 0$. In the DPDE (2.1.1), the effect of delay occurs only in the time variable t, and there is no effect of delay in the spatial variable x, therefore, if we fix $t \in [0, T]$, the result can be obtained by using the argument of [77] and [41] on the line segment along with the bounds $|u(x,t)| \leq C$ and $|u_t(x,t)| \leq C$.

Case 4. Let $l = 0$ and $m = 2$. Along the sides $x = 0$ and $x = 1$ of $\overline{D}$, we have $u \equiv 0$ and hence $u_{tt} \equiv 0$. For $t \in [-\tau, 0]$, we have $u \equiv 0$, $u_x \equiv 0$ and $u_{xx} \equiv 0$, therefore, from (2.1.1), we have

$$u_t(x,t) = \begin{cases} 0, & \text{for } \ t \in [-\tau, 0), \\ f(x,0), & \text{for } \ t = 0. \end{cases}$$

Also, we have

$$u_{tx}(x,t) = \begin{cases} 0, & \text{for } \ t \in [-\tau, 0), \\ f_x(x,0), & \text{for } \ t = 0, \end{cases}$$

and

$$u_{txx}(x,t) = \begin{cases} 0, & \text{for } \ t \in [-\tau, 0), \\ f_{xx}(x,0), & \text{for } \ t = 0. \end{cases}$$

Therefore, one can show that

$$|u_{tx}(x,t)| \leq C \quad \text{and} \quad |u_{txx}(x,t)| \leq C, \quad \text{on } \Gamma.$$

Now, differentiating (2.1.1) with respect to t, we get

$$u_{tt} - \varepsilon u_{txx} + a(x)u_{tx} + b_t u(x,t) + bu_t(x,t) = f_t - c_t u(x,t-\tau) - cu_t(x,t-\tau).$$

Next, by proceeding in a similar way as we have done for u_t, we can obtain $|u_{tt}(x,t)| \leq C$, for $(x,t) \in \Gamma$.

Consider the operator defined in (2.1.1) and operating it on u_{tt}, we get

$$\begin{aligned}\left(\frac{\partial}{\partial t}+\mathscr{L}_{\varepsilon}\right)(u_{tt})(x,t) &= u_{ttt}-\varepsilon u_{ttxx}+a(x)u_{ttx}+b(x,t)u_{tt}\\ &= (u_t-\varepsilon u_{xx}+a(x)u_x+b(x,t)u)_{tt}-b_{tt}u-2b_tu_t.\end{aligned} \tag{2.2.7}$$

For $t\in[0,\tau]$, using the given initial condition, we get

$$\left(\frac{\partial}{\partial t}+\mathscr{L}_{\varepsilon}\right)(u_{tt})=f_{tt}(x,t)-b_{tt}(x,t)u-2b_tu_t,$$

which implies that $\left|\left(\frac{\partial}{\partial t}+\mathscr{L}_{\varepsilon}\right)(u_{tt})\right|\leq C$. As the operator $\left(\frac{\partial}{\partial t}+\mathscr{L}_{\varepsilon}\right)$ satisfies the maximum principle (Lemma 2.2.1), we have $|u_{tt}|\leq C$, $(x,t)\in\overline{\Omega}_x\times[0,\tau]$.

For $t\in[\tau,2\tau]$, from (2.2.7) we get that

$$\left(\frac{\partial}{\partial t}+\mathscr{L}_{\varepsilon}\right)(u_{tt})(x,t)=f_{tt}(x,t)-b_{tt}(x,t)u-2b_tu_t-(cu(x,t-\tau))_{tt}.$$

As $(x,t)\in\overline{\Omega}_x\times[\tau,2\tau]$, all the terms in the right hand side of the above equation are bounded, therefore, we have

$$\left|\left(\frac{\partial}{\partial t}+\mathscr{L}_{\varepsilon}\right)(u_{tt})\right|\leq C.$$

We already found that the above bound is valid for $(x,t)\in\overline{\Omega}_x\times[0,\tau]$. Therefore, by applying the maximum principle (Lemma 2.2.1), we get $|u_{tt}|\leq C$, $(x,t)\in\overline{\Omega}_x\times[0,2\tau]$. In an analogous way, we can prove the required bound for the entire domain $\overline{D}$.

Case 5. Here we consider the case, where $l=1$ and $m=1$. Differentiating (2.1.1) with respect to t on $\overline{D}$ and rearranging the terms, we get

$$\begin{aligned}-\varepsilon(u_{xt})_x+a(x)u_{xt} &+ b_t(x,t)u+b(x,t)u_t+u_{tt}\\ &= -c_t(x,t)u(x,t-\tau)-c(x,t)u_t(x,t-\tau)+f_t(x,t).\end{aligned}$$

Now using the argument as given in [77] and [41] along with the bounds $|u(x,t)|\leq C$, $|u_t(x,t)|\leq C$, $|u_{tt}(x,t)|\leq C$, we get the required bound.

By following the similar approach one can obtain the bound for the other derivatives as well, *i.e.*, for $0\leq l+m\leq 5$. ∎

2.2.1 Decomposition of the solution

To obtain the ε-uniform error estimate, we require some stronger bounds on the derivatives of the analytical solution $u(x,t)$ of the problem (2.1.1). For this, we decompose the analytical solution u as $u=v+w$, where v and w are the smooth and singular components.

We express the smooth component v as

$$v(x,t) = \sum_{j=0}^{4} \varepsilon^j v_j(x,t), \quad (x,t) \in \overline{D},$$

where $v_j(x,t)$, $j = 0,1,2,3$, are the solutions of the following first-order PDEs (2.2.8) and (2.2.9):

$$\begin{cases} (v_0)_t(x,t) + a(x)(v_0)_x(x,t) + b(x,t)v_0(x,t) = -c(x,t)v_0(x,t-\tau) + f(x,t), \\ \qquad\qquad\qquad\qquad\qquad\qquad\qquad\qquad\qquad\qquad (x,t) \in D, \\ v_0(x,t) = \phi_b(x,t), \qquad\qquad\qquad\qquad\qquad\qquad (x,t) \in \Gamma_b, \\ v_0(0,t) = \phi_l(t), \qquad\qquad\qquad\qquad\qquad\qquad 0 \le t \le T, \end{cases} \tag{2.2.8}$$

and

$$\begin{cases} (v_j)_t(x,t) + a(x)(v_j)_x(x,t) + b(x,t)v_j(x,t) = -c(x,t)v_j(x,t-\tau) + (v_{j-1})_{xx}(x,t), \\ \qquad\qquad\qquad\qquad\qquad\qquad\qquad\qquad\qquad\qquad (x,t) \in D, \quad j = 1,2,3, \\ v_j(x,t) = 0, \qquad\qquad\qquad\qquad\qquad\qquad (x,t) \in \Gamma_b, \\ v_j(0,t) = 0, \qquad\qquad\qquad\qquad\qquad\qquad 0 \le t \le T, \end{cases} \tag{2.2.9}$$

and lastly, the function v_4 satisfies

$$\begin{cases} (v_4)_t(x,t) + \mathscr{L}_\varepsilon v_4(x,t) = -c(x,t)v_4(x,t-\tau) + (v_3)_{xx}(x,t), \quad (x,t) \in D, \\ v_4(x,t) = 0, \qquad (x,t) \in \Gamma_b, \\ v_4(0,t) = 0 = v_4(1,t), \qquad 0 \le t \le T. \end{cases} \tag{2.2.10}$$

Therefore, the smooth component satisfies the following problem

$$\begin{cases} v_t(x,t) + \mathscr{L}_\varepsilon v(x,t) = -c(x,t)v(x,t-\tau) + f(x,t), \quad (x,t) \in D, \\ v(x,t) = \phi_b(x,t), \qquad\qquad\qquad\qquad (x,t) \in \Gamma_b, \\ v(0,t) = \phi_l(t), \qquad\qquad\qquad\qquad 0 \le t \le T, \\ v(1,t) = \displaystyle\sum_{i=0}^{4} \varepsilon^i v_i(1,t), \qquad\qquad 0 \le t \le T, \end{cases} \tag{2.2.11}$$

and the singular component satisfies the PDE

$$\begin{cases} w_t(x,t) + \mathscr{L}_\varepsilon w(x,t) = -c(x,t)w(x,t-\tau), & (x,t) \in D, \\ w(x,t) = 0, & (x,t) \in \Gamma_b, \\ w(0,t) = 0, & 0 \le t \le T, \\ w(1,t) = u(1,t) - v(1,t), & 0 \le t \le T. \end{cases} \tag{2.2.12}$$

The following theorem will provide the bounds for the derivatives of the smooth and singular components of the solution u of (2.1.1).

Theorem 2.2.4. *For all non-negative integers l, m, satisfying $0 \le l + m \le 5$, and with sufficient compatibility conditions at the corners, the smooth component v and the singular component w defined in (2.2.11) and (2.2.12), respectively, satisfy the following bounds:*

$$\left|\left| \frac{\partial^{l+m} v}{\partial x^l \partial t^m} \right|\right|_\infty \le C\left(1 + \varepsilon^{4-l}\right),$$

and

$$\left| \frac{\partial^{l+m} w}{\partial x^l \partial t^m} \right| \le C\varepsilon^{-l} \exp(-\alpha(1-x)/\varepsilon), \quad (x,t) \in D.$$

Proof. We can see that the PDEs (2.2.8) and (2.2.9) are independent of ε. Therefore, for the derivatives of v_j defined in (2.2.8) and (2.2.9), $j = 0, 1, 2, 3$ we can have the following ε-uniform bound

$$\left|\left| \frac{\partial^{l+m} v_j}{\partial x^l \partial t^m} \right|\right|_\infty \le C.$$

Now, the problem (2.2.10) is of the form (2.1.1). Hence, the solution v_4 of (2.2.10) will have the same bound as stated in Theorem 2.2.3. Thus, by summing up the bounds for the derivatives of v_j, $j = 0, 1, 2, 3, 4$, we get

$$\left|\left| \frac{\partial^{l+m} v}{\partial x^l \partial t^m} \right|\right|_\infty \le C(1 + \varepsilon^{4-l}).$$

To prove the bounds for the derivatives of the smooth component $w(x,t)$, we will use the following step by step procedure.

Since $w(x, t-\tau)$ mentioned in (2.2.12) is a known function when $t \in [0, \tau]$, we can use the derivative bound obtained in [66]. Hence, we can have

$$\left| \frac{\partial^{l+m} w}{\partial x^l \partial t^m} \right| \le C\varepsilon^{-l} \exp(-\alpha(1-x)/\varepsilon), \quad (x,t) \in \Omega_x \times [0,\tau]. \tag{2.2.13}$$

Now, we extend the domain of definition, *i.e.*, consider $(x,t) \in \Omega_x \times [0, 2\tau]$. To prove the required bound in $\Omega_x \times [0, 2\tau]$, we consider few cases depending on the values of l and m.

Case 1. Let $l = 0$ and $m = 0$. Consider the barrier functions

$$\psi^{\pm} = C\exp(-\alpha(1-x)/\varepsilon) \pm w(x,t).$$

We can show that for sufficiently large C, we have $\psi^{\pm} \geq 0$ on Γ. Now,

$$\begin{aligned}\left(\frac{\partial}{\partial t} + \mathscr{L}_{\varepsilon}\right)\psi^{\pm}(x,t) &= C\left(\frac{a(x)\alpha}{\varepsilon} + b(x,t) - \frac{\alpha^2}{\varepsilon}\right)\exp(-\alpha(1-x)/\varepsilon) \\ &\quad \pm \left(\frac{\partial}{\partial t} + \mathscr{L}_{\varepsilon}\right) w(x,t) \\ &= C\left(\frac{a(x)\alpha}{\varepsilon} + b(x,t) - \frac{\alpha^2}{\varepsilon}\right)\exp(-\alpha(1-x)/\varepsilon) \\ &\quad \pm \left(-c(x,t)w(x,t-\tau)\right),\end{aligned}$$

by using (2.2.12). From (2.2.13), we have the bound of $w(x,t)$ when $t \in [0,\tau]$. By using the bound given in (2.2.13) along with the condition $a(x) \geq \alpha$ and sufficiently large C, we have

$$\left(\frac{\partial}{\partial t} + \mathscr{L}_{\varepsilon}\right)\psi^{\pm}(x,t) \geq 0, \quad \text{for } (x,t) \in \Omega_x \times [0,2\tau].$$

Now applying the maximum principle (Lemma 2.2.1), we have

$$\psi^{\pm}(x,t) \geq 0, \quad (x,t) \in \Omega_x \times [0,2\tau].$$

which implies $|w(x,t)| \leq C\exp(-\alpha(1-x)/\varepsilon)$.

Case 2. Let $l = 0$ and $m = 1$. We apply the differential operator $\left(\frac{\partial}{\partial t} + \mathscr{L}_{\varepsilon}\right)$ to w_t, then we obtain

$$\begin{aligned}\left(\frac{\partial}{\partial t} + \mathscr{L}_{\varepsilon}\right)(w_t)(x,t) &= w_{tt} - \varepsilon w_{txx} + a(x)w_{tx} + b(x,t)w_t(x,t) \\ &= (w_t - \varepsilon w_{xx} + a(x)w_x + b(x,t)w)_t(x,t) - b_t(x,t)w(x,t), \\ &= -c_t(x,t)w(x,t-\tau) - c(x,t)w_t(x,t-\tau) - b_t(x,t)w(x,t),\end{aligned}$$

by using (2.2.12). Now, by using the barrier functions $\psi_1^{\pm} = C\exp(-\alpha(1-x)/\varepsilon) \pm w_t(x,t)$ and proceeding as in the previous case, we can obtain the required bound for $w_t(x,t)$, *i.e.*,

$$|w_t(x,t)| \leq C\exp(-\alpha(1-x)/\varepsilon), \quad (x,t) \in \Omega_x \times [0,2\tau].$$

Case 3. Next we consider the case for $l = 1$ and $m = 0$. We can write (2.2.12) as

$$\mathscr{L}_{\varepsilon}w(x,t) = -w_t(x,t) - c(x,t)w(x,t-\tau).$$

For a fixed $t \in [0,2\tau]$, the required bound for $w_x(x,t)$, when $(x,t) \in \Omega_x \times [0,2\tau]$, can be obtained by using the argument of [77] and [41] on the line segment along with

the bounds $|w(x,t)| \leq C\exp(-\alpha(1-x)/\varepsilon)$ and $|w_t(x,t)| \leq C\exp(-\alpha(1-x)/\varepsilon)$, when $(x,t) \in \Omega_x \times [0, 2\tau]$.

By following the similar approach as done in the above three cases, one can obtain the bound for the other derivatives, *i.e.*, for $0 \leq l+m \leq 5$. Hence, we can have

$$\left|\frac{\partial^{l+m} w}{\partial x^l \partial t^m}\right| \leq C\varepsilon^{-l}\exp(-\alpha(1-x)/\varepsilon), \quad (x,t) \in \Omega_x \times [0, 2\tau].$$

In a similar way, the required bound can be obtained for $t \geq 2\tau$, and hence the proof is completed. ∎

2.3 The Numerical Solution

Here, in this section, we describe the piecewise-uniform Shishkin mesh for the spatial discretization of the domain and study the behavior of the difference scheme used to discretize the DPDE (2.1.1).

2.3.1 The piecewise-uniform Shishkin mesh

Since the DPDE (2.1.1) has a boundary layer along the side $x = 1$, the mesh should be condensing in the neighborhood of $x = 1$. To define the piecewise-uniform mesh, we divide the domain $[0, 1]$ into two sub-domains, such that $[0, 1] = [0, 1-\rho] \cup (1-\rho, 1]$ and then divide each of the sub-domains into $N/2$ equal intervals and denote the spatial meshes by

$$\overline{\Omega}_x^N = \{0 = x_0, x_1, \cdots, x_{N/2} = 1-\rho, \cdots, x_N = 1\},$$

where

$$x_i = \begin{cases} i\dfrac{2(1-\rho)}{N}, & i = 0, \cdots, N/2, \\ (1-\rho) + \left(i - \dfrac{N}{2}\right)\dfrac{2\rho}{N}, & i = (N/2)+1, \cdots, N, \end{cases}$$

$N \geq 4$ be a positive even integer and $\Omega_x^N = \overline{\Omega}_x^N \cap \Omega_x$.

Here the transition point $1-\rho$, which separates the coarse and fine portions of the mesh, obtained by taking

$$\rho = \min\left\{\frac{1}{2}, \rho_0\varepsilon\ln N\right\}, \tag{2.3.1}$$

where $\rho_0 \geq 2/\alpha$. The analysis has been done by assuming that $\rho = \rho_0\varepsilon\ln N$, as otherwise N is exponentially large compared with ε.

The spatial mesh-sizes are denoted by

$$h_i = x_i - x_{i-1},\ i = 1, \cdots, N, \quad \widehat{h}_i = h_i + h_{i+1},\ i = 1, \cdots, N-1.$$

Now, by the definition of x_i's the spatial mesh-sizes can be written as

$$h_i = \begin{cases} H = \dfrac{2(1-\rho)}{N}, & i = 1, \cdots, N/2, \\ h = \dfrac{2\rho}{N}, & i = (N/2)+1, \cdots, N, \end{cases}$$

H and h are the spatial mesh-sizes in $[0, 1-\rho]$ and $(1-\rho, 1]$, respectively. It is clear from the above equation that $N^{-1} \leq H \leq 2N^{-1}$, $h = 2\rho_0 \varepsilon N^{-1} \ln N$, and the uniform mesh can be obtained by choosing $\rho = 1/2$.

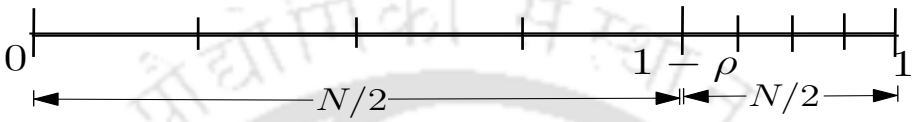

Figure 2.1: *Shishkin mesh in 1D.*

For the time domain $[0, T]$, we will use uniform mesh with mesh-size Δt, such that

$$\Lambda_t^M = \{t_n = n\Delta t, n = 0, \cdots, M, \Delta t = T/M\},$$

where M is the number of mesh-points in the t-direction on the interval $[0, T]$ and the temporal mesh-size Δt satisfies the constraint $p\Delta t = \tau$, where p is a positive integer, $t_n = n\Delta t$, $n \geq -p$.

We define the discrete domain by $D^{N,M} = \overline{D}^{N,M} \cap D$ where $\overline{D}^{N,M} = \overline{\Omega}_x^N \times \Lambda_t^M$ and $\Gamma_b^N = \overline{\Omega}_x^N \times \Lambda_t^p$, where Λ_t^p denotes the set of $p+1$ uniform mesh-points in $[-\tau, 0]$. The boundary points Γ^N of $\overline{D}^{N,M}$ are $\Gamma^N = \overline{D}^{N,M} \cap \Gamma$. Similarly, we define the left and right boundary points by $\Gamma_l^N = \overline{D}^{N,M} \cap \Gamma_l$ and $\Gamma_r^N = \overline{D}^{N,M} \cap \Gamma_r$, respectively. We further discretize $\overline{D}_j^{N,M} = \overline{\Omega}_x^N \times \Lambda_{j,t}^p$, where $\Lambda_{j,t}^p$ denotes the set of $p+1$ uniform mesh-points in $[(j-1)\tau, j\tau]$, for $j = 1, 2, \cdots, k$. From the above discretization we can observe that $\overline{D}^{N,M} = \bigcup_{j=1}^{k} \overline{D}_j^{N,M}$.

2.3.2 The finite difference scheme

Here, we propose a numerical scheme to solve the DPDE (2.1.1), which consists of the implicit-Euler scheme for the time derivative and the hybrid scheme for the spatial derivatives. The hybrid scheme is a proper combination of the midpoint upwind scheme and the central difference scheme. More precisely, for spatial derivatives, we apply the midpoint upwind scheme in the outer region $[0, 1-\rho]$ and the central difference scheme in the boundary layer region $(1-\rho, 1]$. Hence, the numerical scheme takes the following

form:

$$\begin{cases} (\tilde{\delta}_t^- + \mathscr{L}_{Hybrid})U_i^{n+1} = \widetilde{F}, & \text{for } i = 1, \cdots, N-1, \quad n = 0, \cdots, M-1, \\ U_0^{n+1} = \phi_l(t_{n+1}), \qquad U_N^{n+1} = \phi_r(t_{n+1}), & \text{for } n = 0, \cdots, M-1, \\ U_i^{-j} = \phi_b(x_i, -t_j), & \text{for } i = 0, \cdots, N, \text{ and } j = 0, \cdots, p, \end{cases} \tag{2.3.2}$$

where

$$\tilde{\delta}_t^- U_i^{n+1} = \begin{cases} \delta_t^- U_{i-\frac{1}{2}}^{n+1}, & \text{for } 1 \le i \le N/2, \\ \delta_t^- U_i^{n+1}, & \text{for } N/2 < i < N, \end{cases}$$

$$\mathscr{L}_{Hybrid}U_i^{n+1} = \begin{cases} \mathscr{L}_{mu}U_i^{n+1} = -\varepsilon\delta_x^2 U_i^{n+1} + a_{i-\frac{1}{2}}\delta_x^- U_i^{n+1} + b_{i-\frac{1}{2},n+1}U_{i-\frac{1}{2}}^{n+1}, \text{ for } 1 \le i \le N/2, \\ \mathscr{L}_{cen}U_i^{n+1} = -\varepsilon\delta_x^2 U_i^{n+1} + a_i\delta_x^0 U_i^{n+1} + b_{i,n+1}U_i^{n+1}, \quad \text{for } N/2 < i < N, \end{cases}$$

and

$$\widetilde{F} = \begin{cases} -c_{i-\frac{1}{2},n+1}U_{i-\frac{1}{2}}^{n-p+1} + f_{i-\frac{1}{2}}^{n+1}, & \text{for } 1 \le i \le N/2, \\ -c_{i,n+1}U_i^{n-p+1} + f_i^{n+1}, & \text{for } N/2 < i < N. \end{cases}$$

In the above equations $a_{i-1/2} = (a_{i-1} + a_i)/2$, $b_{i-\frac{1}{2},n+1} = (b_{i-1,n+1} + b_{i,n+1})/2$, $c_{i,n+1} = c(x_i, t_{n+1})$ and $a_i = a(x_i)$.

After rearranging the terms in (2.3.2), we obtain the following system of linear algebraic equations:

$$\begin{cases} r_i^- U_{i-1}^{n+1} + r_i^0 U_i^{n+1} + r_i^+ U_{i+1}^{n+1} = g_i^n, & \text{for } i = 1, \cdots, N-1, \quad n = 0, \cdots, M-1, \\ U_0^{n+1} = \phi_l(t_{n+1}), \qquad U_N^{n+1} = \phi_r(t_{n+1}), & \text{for } n = 0, \cdots, M-1, \\ U_i^{-j} = \phi_b(x_i, -t_j), & \text{for } i = 0, \cdots, N, \text{ and } j = 0, \cdots, p, \end{cases} \tag{2.3.3}$$

where the coefficients are given by

$$\begin{cases} r_i^- = \Delta t \left(-\dfrac{2\varepsilon}{\widehat{h}_i h_i} - \dfrac{a_{i-\frac{1}{2}}}{h_i} + \dfrac{b_{i-\frac{1}{2},n+1}}{2} \right) + \dfrac{1}{2}, \\ r_i^0 = \Delta t \left(\dfrac{2\varepsilon}{h_{i+1}h_i} + \dfrac{a_{i-\frac{1}{2}}}{h_i} + \dfrac{b_{i-\frac{1}{2},n+1}}{2} \right) + \dfrac{1}{2}, \\ r_i^+ = \Delta t \left(-\dfrac{2\varepsilon}{\widehat{h}_i h_{i+1}} \right), \end{cases} \tag{2.3.4}$$

for $i = 1, \cdots, N/2$, and

$$\begin{cases} r_i^- = \Delta t \left(-\dfrac{2\varepsilon}{\widehat{h}_i h_i} - \dfrac{a_i}{\widehat{h}_i} \right), \\ r_i^0 = \Delta t \left(\dfrac{2\varepsilon}{h_{i+1} h_i} + b_{i,n+1} \right) + 1, \\ r_i^+ = \Delta t \left(-\dfrac{2\varepsilon}{\widehat{h}_i h_{i+1}} + \dfrac{a_i}{\widehat{h}_i} \right), \end{cases} \tag{2.3.5}$$

for $i = N/2 + 1, \cdots, N-1$. Further, g_i^n defined in equation (2.3.3) is given by

$$g_i^n = \begin{cases} -\dfrac{1}{2}\Delta t \left(c_{i-1,n+1} U_{i-1}^{n-p+1} + c_{i,n+1} U_i^{n-p+1} \right) + \dfrac{1}{2}\left(U_{i-1}^n + \Delta t f_{i-1}^{n+1} \right) \\ \qquad + \dfrac{1}{2}\left(U_i^n + \Delta t f_i^{n+1} \right), \quad \text{for } \ 1 \le i \le N/2, \\ U_i^n + \Delta t \left(-c_{i,n+1} U_i^{n-p+1} + f_i^{n+1} \right), \qquad \text{for } \ N/2 < i < N. \end{cases}$$

The tridiagonal system of linear algebraic equations (2.3.3) can be solved by any existing codes.

2.4 Convergence Analysis

In this section, we shall discuss about the stability of the proposed scheme (2.3.2) and by using the truncation error, we shall obtain the ε-uniform error estimate.

The following lemma will help to study the stability of the proposed scheme.

Lemma 2.4.1. *Assume that*

$$\rho_0 \|a\|_\infty < \frac{N}{\ln N} \quad \textit{and} \quad \alpha N \ge (\|b\|_\infty + \Delta t^{-1}). \tag{2.4.1}$$

Then, we have

$$\begin{cases} r_i^- < 0, \ r_i^+ < 0, & \textit{for } \ 1 \le i \le N-1, \\ |r_1^0| - |r_1^+| \ge 0, \ |r_i^0| - |r_i^-| - |r_i^+| \ge 0, & \textit{for } \ 1 < i \le N/2, \\ |r_{N-1}^0| - |r_{N-1}^-| > 0, |r_i^0| - |r_i^-| - |r_i^+| > 0, & \textit{for } \ N/2 < i < N-1. \end{cases}$$

Proof. We divide the proof of this lemma into two cases depending on the location of the mesh.

Case 1. (For outer region) Consider the case $1 \le i \le N/2$. From equation (2.3.4), it is apparent that $r_i^+ < 0$. Now from (2.3.4), r_i^- is defined by

$$r_i^- = \Delta t \left(-\frac{2\varepsilon}{\widehat{h}_i h_i} - \frac{a_{i-\frac{1}{2}}}{h_i} + \frac{b_{i-\frac{1}{2},n+1}}{2} \right) + \frac{1}{2}.$$

For $1 \leq i \leq N/2$, the mesh-size $h_i = H$, therefore, from the above equation, we have

$$\begin{aligned} r_i^- &= \Delta t \left(-\frac{2\varepsilon}{2H^2} - \frac{a_{i-\frac{1}{2}}}{H} \right) + \frac{\Delta t}{2} \left(b_{i-\frac{1}{2},n+1} + \Delta t^{-1} \right) \\ &\leq -\frac{2\varepsilon \Delta t}{2H^2} - \frac{a_{i-\frac{1}{2}} \Delta t}{H} + \frac{\Delta t}{2} \left(||b||_\infty + \Delta t^{-1} \right) \\ &\leq -\frac{\varepsilon \Delta t N^2}{4} - \frac{\Delta t}{2} \left(a_{i-\frac{1}{2}} - \alpha \right) N, \quad \text{as } \alpha N \geq (\|b\|_\infty + \Delta t^{-1}) \quad \text{and} \quad H \leq 2N^{-1}. \end{aligned}$$

We know that $a(x) \geq \alpha$, therefore $r_i^- < 0$. Some simple calculation provides the results

$$|r_1^0| - |r_1^+| \geq 0, \ |r_i^0| - |r_i^-| - |r_i^+| \geq 0, \quad \text{for } \ 1 \leq i \leq N/2.$$

Case 2. (For inner region) Here, $N/2 < i \leq N-1$, we consider the equation (2.3.5). It is clear that $r_i^- < 0$. By using the given condition, we get

$$\begin{aligned} r_i^+ &= \Delta t \left(-\frac{2\varepsilon}{\widehat{h}_i h_{i+1}} + \frac{a_i}{\widehat{h}_i} \right) \\ &\leq \Delta t \left(-\frac{2\varepsilon}{\widehat{h}_i h_{i+1}} + \frac{||a||_\infty}{\widehat{h}_i} \right) \\ &= -\frac{\Delta t}{\widehat{h}_i} \left(\frac{2\varepsilon}{h_{i+1}} - ||a||_\infty \right) < 0, \quad \text{as} \quad \rho_0 \|a\|_\infty < \frac{N}{\ln N}. \end{aligned}$$

From (2.3.5), we deduce that

$$|r_i^-| + |r_i^+| = \Delta t \left(\frac{2\varepsilon}{\widehat{h}_i h_i} + \frac{a_i}{\widehat{h}_i} + \frac{2\varepsilon}{\widehat{h}_i h_{i+1}} - \frac{a_i}{\widehat{h}_i} \right) = \frac{2\varepsilon \Delta t}{h_i h_{i+1}} < |r_i^0|,$$

for $N/2 < i < N-1$ and

$$\begin{aligned} |r_{N-1}^-| &= \Delta t \left(\frac{2\varepsilon}{\widehat{h}_{N-1} h_{N-1}} + \frac{a_{N-1}}{\widehat{h}_{N-1}} \right) \\ &= \Delta t \left(\frac{2\varepsilon}{h_{N-1} h_N} - \left(\frac{2\varepsilon}{\widehat{h}_{N-1} h_N} - \frac{a_{N-1}}{\widehat{h}_{N-1}} \right) \right) \\ &< \frac{2\Delta t \varepsilon}{h_{N-1} h_N} < \Delta t \left(\frac{2\varepsilon}{h_{N-1} h_N} + b_{N-1,n+1} \right) + 1 = |r_{N-1}^0|. \end{aligned}$$

Hence the proof is completed. ∎

Remark 2.4.2. *Under the assumptions given in (2.4.1), Lemma 2.4.1 shows that the matrix associated with (2.3.3) at each time level is an M-matrix. Hence, the operator* $(\tilde{\delta}_t^- + \mathscr{L}_{Hybrid})$ *in (2.3.2) satisfies the* ***discrete maximum principle*** *on* $D^{N,M}$. *Therefore, the method is uniformly stable in the supremum norm.*

Lemma 2.4.3. *(***Discrete maximum principle***) Assume that the discrete function* Ψ_i^n *satisfies* $\Psi_i^n \geq 0$ *on* Γ^N. *Then* $(\tilde{\delta}_t^- + \mathscr{L}_{Hybrid})\Psi_i^n \geq 0$ *on* $D^{N,M}$ *implies that* $\Psi_i^n \geq 0$ *at each point of* $\overline{D}^{N,M}$.

Now we will provide our main result for the ε-uniform convergence of the numerical solution.

Theorem 2.4.4. *Let* u *and* U *be respectively the continuous and numerical solutions of the* IBVPs *(2.1.1) and (2.3.2) and satisfying the compatibility conditions at the corners. Then, we have the following error bound for* $(x_i, t_n) \in D^{N,M}$

$$\max_{i,n} |(u-U)(x_i,t_n)| \leq \begin{cases} C(N^{-1}(\varepsilon + N^{-1}) + \Delta t), & \text{for } \ 0 \leq i \leq N/2, \\ C(N^{-2}\ln^2 N + \Delta t), & \text{for } \ N/2 < i < N, \end{cases}$$

where $U(x_i, t_n) = U_i^n$.

Proof. Here, we divide the proof into various steps for different time levels. We can notice that on the first interval $[0, \tau]$, *i.e.,* where the time discretization parameter n varies from 0 to p, the initial conditions of *IBVPs* (2.1.1) and (2.3.2) will be same. So, the analysis can be carried out in the same way as one can do for a problem with out delay.

Therefore, for $(x_i, t_n) \in D_1^{N,M} = \Omega_x^N \times \Lambda_{1,t}^p$, by using the convergence result of [65], we can obtain

$$\max_{i,n} |(u-U)(x_i,t_n)| \leq \begin{cases} C(N^{-1}(\varepsilon + N^{-1}) + \Delta t), & \text{for } \ 0 \leq i \leq N/2, \\ C(N^{-2}\ln^2 N + \Delta t), & \text{for } \ N/2 < i < N. \end{cases} \tag{2.4.2}$$

On the second interval $(\tau, 2\tau]$, the approach of [65] is not applicable because, the value of the delay term involves in the right hand side of (2.3.2) will be the numerical solution obtained in previous time interval $[0, \tau]$. Therefore, we will do the detailed analysis to get the error over the interval $(\tau, 2\tau]$.

On the domain $D_2 = \Omega_x \times (\tau, 2\tau)$, we consider the following singularly perturbed delay parabolic equation:

$$\begin{cases} \left(\dfrac{\partial}{\partial t} + \mathscr{L}_\varepsilon\right) u(x,t) = -c(x,t)u(x,t-\tau) + f(x,t), \quad (x,t) \in D_2, \\ u(x,t) = u_\tau(x,t), \qquad (x,t) \in \overline{D}_1 = \overline{\Omega}_x \times [0,\tau], \\ u(0,t) = \phi_l(t), \quad u(1,t) = \phi_r(t), \quad t \in [\tau, 2\tau], \end{cases} \tag{2.4.3}$$

where u_τ is the exact solution on D_1.

We apply the proposed scheme to determine the numerical solution U of (2.4.3) at $(x_i, t_n) \in D_2^N$. The discrete problem corresponding to equation (2.4.3) becomes

$$\begin{cases} \begin{cases} \delta_t^- U_{i-\frac{1}{2}}^n - \varepsilon \delta_x^2 U_i^n + a_{i-\frac{1}{2}} \delta_x^- U_i^n + b_{i-\frac{1}{2},n} U_{i-\frac{1}{2}}^n & = -c_{i-\frac{1}{2},n} U_{i-\frac{1}{2}}^{n-p} + f(x_{i-\frac{1}{2}}, t_n), \\ & (x_i, t_n) \in [0, 1-\rho] \times [\tau, 2\tau], \\ \delta_t^- U_i^n - \varepsilon \delta_x^2 U_i^n + a_i \delta_x^0 U_i^n + b_{i,n} U_i^n = -c_{i,n} U_i^{n-p} & + f(x_i, t_n), \\ & (x_i, t_n) \in (1-\rho, 1] \times [\tau, 2\tau], \end{cases} \\ U_0^n = \phi_l(t_n), \qquad U_N^n = \phi_r(t_n), \qquad t_n \in \Lambda_{2,t}^p, \\ U_i^n = U_1(x_i, t_n), \qquad (x_i, t_n) \in \overline{D}_1^{N,M}, \end{cases} \tag{2.4.4}$$

where $U_1(\cdot, \cdot)$ is the numerical solution calculated on $D_1^{N,M}$. The solution u of (2.4.3) is decomposed into the smooth and singular components as $u = y + z$. Since $D_2 \subset D$, the estimates given in Theorem 2.2.4 can be used for both y and z. The smooth component y is further decomposed into $y = y_0 + \varepsilon y_1$, where y_0 and y_1 are the solutions of the following problems:

$$\begin{cases} \dfrac{\partial y_0}{\partial t}(x,t) + a(x)\dfrac{\partial y_0}{\partial x}(x,t) + b(x,t) y_0(x,t) = -c(x,t) y_0(x, t-\tau) + f(x,t), & (x,t) \in D_2, \\ y_0(x,t) = u_\tau(x,t), \qquad (x,t) \in \overline{D}_1, \\ y_0(0,t) = u(0,t), \qquad t \in [\tau, 2\tau], \end{cases}$$

and

$$\begin{cases} \left(\dfrac{\partial}{\partial t} + \mathscr{L}_\varepsilon\right) y_1(x,t) = -c(x,t) y_1(x, t-\tau) + \dfrac{\partial^2 y_0}{\partial x^2}(x,t), \qquad (x,t) \in D_2, \\ y_1(x,t) = 0, \qquad (x,t) \in \overline{D}_1, \\ y_1(0,t) = y_1(1,t) = 0, \qquad t \in [\tau, 2\tau]. \end{cases}$$

Therefore, y satisfies

$$\begin{cases} \left(\dfrac{\partial}{\partial t} + \mathscr{L}_\varepsilon\right) y(x,t) = -c(x,t) y(x, t-\tau) + f(x,t), \qquad (x,t) \in D_2, \\ y(x,t) = u_\tau(x,t), \qquad (x,t) \in \overline{D}_1, \\ y(0,t) = y_0(0,t), \qquad y(1,t) = y_0(1,t), \qquad t \in [\tau, 2\tau]. \end{cases} \tag{2.4.5}$$

Then, the singular component z satisfies the following IBVP:

$$\begin{cases} \left(\dfrac{\partial}{\partial t} + \mathscr{L}_\varepsilon\right) z(x,t) = -c(x,t) z(x, t-\tau), \qquad (x,t) \in D_2, \\ z(x,t) = 0, \qquad (x,t) \in \overline{D}_1, \\ z(0,t) = \phi_l(t) - y_0(0,t), \qquad z(1,t) = \phi_r(t) - y_0(1,t), \qquad t \in [\tau, 2\tau]. \end{cases} \tag{2.4.6}$$

In a similar way, the solution U of (2.4.4) can be decomposed into the smooth and singular components Y and Z, respectively. Thus,

$$U = Y + Z,$$

where Y is the solution of the following nonhomogeneous problem

$$\begin{cases} (\tilde{\delta}_t^- + \mathscr{L}_{Hybrid})Y_i^n = -c_{i,n}Y(x_i, t_{n-p}) + f(x_i, t_n), & (x_i, t_n) \in D_2^{N,M}, \\ Y_i^n = U_1(x_i, t_n), & (x_i, t_n) \in \overline{D}_1^{N,M}, \\ Y_0^n = y(0, t_n), \quad Y_1^n = y(1, t_n), & t_n \in \Lambda_{2,t}^p, \end{cases} \tag{2.4.7}$$

and therefore, Z satisfies

$$\begin{cases} (\tilde{\delta}_t^- + \mathscr{L}_{Hybrid})Z_i^n = -c_{i,n}Z(x_i, t_{n-p}), & (x_i, t_n) \in D_2^{N,M}, \\ Z_i^n = 0, & (x_i, t_n) \in \overline{D}_1^{N,M}, \\ Z_0^n = \phi_l(t_n) - y(0, t_n), \quad Z_1^n = \phi_r(t_n) - y(1, t_n), & t_n \in \Lambda_{2,t}^p. \end{cases} \tag{2.4.8}$$

Therefore, at (x_i, t_n) the error can be written in the form

$$(U - u)(x_i, t_n) = (Y - y)(x_i, t_n) + (Z - z)(x_i, t_n),$$

which implies that

$$|(U - u)(x_i, t_n)| \leq |(Y - y)(x_i, t_n)| + |(Z - z)(x_i, t_n)|, \tag{2.4.9}$$

so that the error for the smooth and singular components can be estimated separately.
Case I. For the smooth component, the truncation error at (x_i, t_n) can be written as

$$\left(\tilde{\delta}_t^- + \mathscr{L}_{Hybrid}\right)(Y - y) = \begin{cases} -c_{i-\frac{1}{2},n}Y(x_{i-\frac{1}{2}}, t_{n-p}) - \left(\tilde{\delta}_t^- + \mathscr{L}_{mu}\right) y(x_i, t_n) \\ \qquad + f(x_{i-\frac{1}{2}}, t_n), \text{ for } i \leq N/2, \\ -c_{i,n}Y(x_i, t_{n-p}) - \left(\tilde{\delta}_t^- + \mathscr{L}_{cen}\right) y(x_i, t_n) \\ \qquad + f(x_i, t_n), \text{ for } i > N/2. \end{cases} \tag{2.4.10}$$

Case (i). First, we consider the case, when $i > N/2$. From (2.4.10), at (x_i, t_n), we get

$$\begin{aligned} \left(\tilde{\delta}_t^- + \mathscr{L}_{Hybrid}\right)(Y - y) &= c_{i,n}\left(y(x_i, t_{n-p}) - Y(x_i, t_{n-p})\right) \\ &\quad + \left(\left(\frac{\partial}{\partial t} + \mathscr{L}_{\varepsilon}\right) - \left(\tilde{\delta}_t^- + \mathscr{L}_{cen}\right)\right) y. \end{aligned}$$

Using the initial conditions from equation (2.4.5) and (2.4.7), we get

$$\begin{aligned}(\tilde{\delta}_t^- + \mathscr{L}_{Hybrid})(Y-y) = \;& c_{i,n}(u_\tau(x_i,t_{n-p}) - U_1(x_i,t_{n-p})) \\ & + \left(\left(\frac{\partial}{\partial t} + \mathscr{L}_\varepsilon\right) - \left(\tilde{\delta}_t^- + \mathscr{L}_{cen}\right)\right) y,\end{aligned}$$

therefore,

$$\begin{aligned}(\tilde{\delta}_t^- + \mathscr{L}_{Hybrid})(Y-y) = \;& c_{i,n}\left(u_\tau(x_i,t_{n-p}) - U_1(x_i,t_{n-p})\right) + \left(\frac{\partial}{\partial t} - \tilde{\delta}_t^-\right) y \\ & + \left(\mathscr{L}_\varepsilon y(x_i,t_n) - \mathscr{L}_{cen} y(x_i,t_n)\right).\end{aligned}$$

Now, taking modulus on both sides and applying the triangle inequality and using (2.4.2), we obtain

$$\begin{aligned}\left|\left(\tilde{\delta}_t^- + \mathscr{L}_{Hybrid}\right)(Y-y)\right| \;\leq\; & C(N^{-2}\ln^2 N + \Delta t) + \left|\varepsilon\left(\frac{\partial^2}{\partial x^2} - \delta_x^2\right) y\right| \\ & + \left|a_i\left(\frac{\partial}{\partial x} - \delta_x^0\right) y\right| + \left|\left(\frac{\partial}{\partial t} - \tilde{\delta}_t^-\right) y\right|.\end{aligned}$$

From the Taylor series expansion, we get

$$\begin{aligned}|(\tilde{\delta}_t^- + \mathscr{L}_{Hybrid})(Y-y)| \leq C\Bigg[(N^{-2}\ln^2 N + \Delta t) \;& + \varepsilon h_i^2 \left|\left|\frac{\partial^4 y}{\partial x^4}\right|\right|_\infty + h_i^2 \left|\left|\frac{\partial^3 y}{\partial x^3}\right|\right|_\infty \\ & + \Delta t \left|\left|\frac{\partial^2 y}{\partial t^2}\right|\right|_\infty\Bigg].\end{aligned}$$

Using the estimates for the derivatives from Theorem 2.2.4, we obtain that

$$|(\tilde{\delta}_t^- + \mathscr{L}_{Hybrid})(Y-y)| \leq C(N^{-2}\ln^2 N + \Delta t). \tag{2.4.11}$$

Case (ii). Now we consider the case, when $i \leq N/2$. From (2.4.10), we obtain

$$\begin{aligned}&\left(\tilde{\delta}_t^- + \mathscr{L}_{Hybrid}\right)(Y-y) \\ &= c_{i-\frac{1}{2},n}\left(y(x_{i-\frac{1}{2}},t_{n-p}) - Y(x_{i-\frac{1}{2}},t_{n-p})\right) + \left(\frac{\partial}{\partial t} + \mathscr{L}_\varepsilon\right) y\left(x_{i-\frac{1}{2}},t_n\right) \\ &\qquad - \left(\tilde{\delta}_t^- + \mathscr{L}_{mu}\right) y(x_i,t_n), \\ &= c_{i-\frac{1}{2},n}\left(y(x_{i-\frac{1}{2}},t_{n-p}) - Y(x_{i-\frac{1}{2}},t_{n-p})\right) + \left(\frac{\partial}{\partial t} - \delta_t^-\right) y(x_{i-\frac{1}{2}},t_n) \\ &\qquad + \left((\mathscr{L}_\varepsilon y)(x_{i-\frac{1}{2}},t_n) - (\mathscr{L}_{mu} y(x_i,t_n))\right).\end{aligned} \tag{2.4.12}$$

Analyzing in the same way as done for $i > N/2$ and using (2.4.2), we can obtain

$$\begin{aligned}|(\tilde{\delta}_t^- + \mathscr{L}_{Hybrid})(Y-y)| \leq \;& C\Bigg[(N^{-1}(\varepsilon + N^{-1}) + \Delta t) + (\varepsilon + h_{i+1})(h_i + h_{i+1}) \left|\left|\frac{\partial^3 y}{\partial x^3}\right|\right|_\infty \\ & + h_{i+1}^2\left(\left|\left|\frac{\partial^2 y}{\partial x^2}\right|\right|_\infty + \left|\left|\frac{\partial y}{\partial x}\right|\right|_\infty\right) + \Delta t \left|\left|\frac{\partial^2 y}{\partial t^2}\right|\right|_\infty\Bigg].\end{aligned}$$

Now, using the estimates of the derivatives of the smooth component y given in Theorem 2.2.4 along with the inequality $h_i \leq 2N^{-1}$, $h_i + h_{i+1} \leq 4N^{-1}$, we obtain that

$$\left|(\delta_t^- + \mathscr{L}_{Hybrid})(Y-y)\right| \leq C\left(N^{-1}\left(\varepsilon + N^{-1}\right) + \Delta t\right).$$

As the discrete operator $(\tilde{\delta}_t^- + \mathscr{L}_{Hybrid})$ satisfies the discrete maximum principle (Lemma 2.4.3) and the inverse operator is uniformly bounded, the inequality given above and (2.4.11) can be reduced to

$$|(Y-y)(x_i,t_n)| \leq \begin{cases} C\left(N^{-1}(\varepsilon+N^{-1}) + \Delta t\right), & \text{for } \ 0 \leq i \leq N/2, \\ C\left(N^{-2}\ln^2 N + \Delta t\right), & \text{for } \ N/2 < i < N. \end{cases} \tag{2.4.13}$$

Case II. Here, we derive the error bound for the singular component $(Z-z)(\cdot,\cdot)$. From the IBVP (2.4.6) and the difference equation (2.4.8), we obtain the truncation error

$$\begin{aligned} &\left(\tilde{\delta}_t^- + \mathscr{L}_{Hybrid}\right)(Z-z) \\ &= \begin{cases} \left(\left(\dfrac{\partial}{\partial t} + \mathscr{L}_{\varepsilon}\right) z(x_{i-\frac{1}{2}},t_n) - \left(\tilde{\delta}_t^- + \mathscr{L}_{mu}\right) z(x_i,t_n)\right) \\ \qquad + \ c_{i-\frac{1}{2},n}\left(z(x_{i-\frac{1}{2}},t_{n-p}) - Z(x_{i-\frac{1}{2}},t_{n-p})\right), \quad \text{for } \ i \leq N/2, \\ \left(\left(\dfrac{\partial}{\partial t} + \mathscr{L}_{\varepsilon}\right) z(x_i,t_n) - \left(\tilde{\delta}_t^- + \mathscr{L}_{cen}\right) z(x_i,t_n)\right) \\ \qquad + \ c_{i,n}\left(z(x_i,t_{n-p}) - Z(x_i,t_{n-p})\right), \quad \text{for } \ i > N/2. \end{cases} \end{aligned} \tag{2.4.14}$$

Using the initial conditions from equation (2.4.6) and (2.4.8), we obtain

$$\left(\tilde{\delta}_t^- + \mathscr{L}_{Hybrid}\right)(Z-z) = \begin{cases} \left(\dfrac{\partial}{\partial t} - \delta_t^-\right) z(x_{i-\frac{1}{2}},t_n) + \left(\mathscr{L}_{\varepsilon} z(x_{i-\frac{1}{2}},t_n) - \mathscr{L}_{mu} z(x_i,t_n)\right), \\ \qquad \text{for } \ i \leq N/2, \\ \left(\dfrac{\partial}{\partial t} - \delta_t^-\right) z(x_i,t_n) + \left(\mathscr{L}_{\varepsilon} z(x_i,t_n) - \mathscr{L}_{cen} z(x_i,t_n)\right), \\ \qquad \text{for } \ i > N/2. \end{cases} \tag{2.4.15}$$

By fixing t, the right hand side of the above equation can be seen as the truncation error of the two-point BVP as done in [89]. Hence, we obtain for $(x_i,t_n) \in D_2^{N,M}$,

$$\left|(\tilde{\delta}_t^- + \mathscr{L}_{Hybrid})(Z-z)\right| \leq \begin{cases} C\left(N^{-1}(\varepsilon+N^{-1}) + \Delta t\right), & \text{for } \ 0 \leq i \leq N/2, \\ C\left(N^{-2}\ln^2 N + \Delta t\right), & \text{for } \ N/2 < i < N. \end{cases} \tag{2.4.16}$$

Now, using the fact that the discrete operator $(\tilde{\delta}_t^- + \mathscr{L}_{Hybrid})$ satisfies the discrete maximum principle (Lemma 2.4.3) and the inverse operator is uniformly bounded, from the

above inequality we obtain

$$|(Z-z)(x_i,t_n)| \leq \begin{cases} C\left(N^{-1}(\varepsilon+N^{-1})+\Delta t\right), & \text{for } 0 \leq i \leq N/2, \\ C\left(N^{-2}\ln^2 N+\Delta t\right), & \text{for } N/2 < i < N. \end{cases} \tag{2.4.17}$$

Combining (2.4.13), (2.4.17), and using it on (2.4.9), we complete the proof on the interval $[\tau, 2\tau]$. We can prove the theorem in an analogous way for the successive intervals in temporal direction. ∎

2.5 Semilinear Delay Parabolic Problem

In this section, we consider the following class of singularly perturbed semilinear DPDEs of the form:

$$\begin{cases} u_t - \varepsilon u_{xx} + a(x)u_x = r(x,t,u(x,t),u(x,t-\tau)), & (x,t) \in D, \\ u(x,t) = \phi_b(x,t), & (x,t) \in \Gamma_b, \\ u(0,t) = \phi_l(t), & \text{on } \Gamma_l = \{(0,t) : 0 \leq t \leq T\}, \\ u(1,t) = \phi_r(t), & \text{on } \Gamma_r = \{(1,t) : 0 \leq t \leq T\}, \end{cases} \tag{2.5.1}$$

$0 < \varepsilon \ll 1$ is the singular perturbation parameter and $\tau > 0$ is the delay parameter. The functions $a(x)$, $r(x,t,s,s_\tau)$, ϕ_b, ϕ_l and ϕ_r are sufficiently smooth with

$$\gamma \leq \frac{\partial r}{\partial s} \leq \overline{\gamma} < 0, \quad \text{and} \quad 0 < \gamma_\tau \leq \left|\frac{\partial r}{\partial s_\tau}\right| \leq \overline{\gamma}_\tau, \quad \text{for } (x,t,s,s_\tau) \in \overline{D} \times \mathbb{R}^2.$$

Under suitable continuity and compatibility conditions imposed on the data, the existence and uniqueness of the solution of the semilinear DPDE can be shown by using the result given in [48] along with the method of steps. For the first time interval, when $t \in (0, \tau]$, the delay term $u(x,t-\tau) = \phi_b$. Now, the resultant equation can be considered as a non-delay problem, hence by using [48], we can guarantee the existence and uniqueness for $t \in (0,\tau]$. Now, on the second time interval $(\tau, 2\tau]$ the delay term $u(x,t-\tau) = u_\tau$, where u_τ is the exact solution of (2.5.1) in the previous time interval, *i.e.*, for $t \in (0,\tau]$. Repeating the same argument we can show that the problem (2.5.1) admits a unique solution for all $t \in (0, T]$.

To solve the semilinear problem (2.5.1), first, we linearize the problem (2.5.1) with the help of Newton's linearization method, then we obtain the sequence $\{u^m\}$ for the initial guess u^0 satisfying the initial and boundary conditions of the problem. In this way, we define u^{m+1} for each fixed m, to be the solution of the following linear delay

parabolic IBVP:

$$\begin{cases} u_t^{m+1} - \varepsilon u_{xx}^{m+1} + a(x)u_x^{m+1} - b^m(x,t)u^{m+1} = & c^m(x,t)u^{m+1}(x,t-\tau) + g^m(x,t), \\ & (x,t) \in D, \\ u^{m+1}(x,t) = \phi_b(x,t), & (x,t) \in \Gamma_b, \\ u^{m+1}(0,t) = \phi_l(t), & \text{on } \Gamma_l = \{(0,t) : 0 \le t \le T\}, \\ u^{m+1}(1,t) = \phi_r(t), & \text{on } \Gamma_r = \{(1,t) : 0 \le t \le T\}, \end{cases} \tag{2.5.2}$$

where $m \geq 0$ and $b^m(x,t)$, $c^m(x,t)$, and $g^m(x,t)$ are given by

$$\begin{cases} b^m(x,t) = \dfrac{\partial r}{\partial u}(x,t,u^m(x,t),s_\tau^m(x,t)), \\ c^m(x,t) = \dfrac{\partial r}{\partial s_\tau}(x,t,u^m(x,t),s_\tau^m(x,t)), \\ g^m(x,t) = r(x,t,u^m(x,t),s_\tau^m(x,t)) - b^m(x,t)u^m - s_\tau^m(x,t)c^m(x,t), \end{cases} \tag{2.5.3}$$

where $s_\tau^m(x,t) = u^m(x,t-\tau)$.

Now, we solve (2.5.2) by using the computational method proposed in Section 2.3.

Numerical results of the delay IBVPs of the form (2.1.1) and (2.5.2) are provided in the following section.

2.6 Numerical Results

In this section, we shall present the numerical results obtained by the proposed numerical scheme (2.3.2) for three test problems on the piecewise-uniform rectangular mesh $D^{N,M} = \Omega_x^N \times \Lambda_t^M$. In all the cases we perform the numerical experiments by choosing the constant $\rho_0 = 4.2$, $\Delta t = 0.8/N$ and $p = 1/\Delta t$.

Example 2.6.1. *Consider the following singularly perturbed 1D linear delay parabolic IBVP:*

$$\begin{cases} u_t - \varepsilon u_{xx} + (1 + x(1-x))u_x = u(x,t-1) + f(x,t), & (x,t) \in \Omega_x \times (0,2], \\ u(x,t) = \phi_b(x,t), & (x,t) \in \overline{\Omega}_x \times [-1,0], \\ u(0,t) = 0,\ u(1,t) = 0, & t \in [0,2]. \end{cases} \tag{2.6.1}$$

We choose the initial data $\phi_b(x,t)$ and the source function $f(x,t)$ to fit with the exact solution

$$u(x,t) = \exp(-t)\left(C_1 + C_2 x - \exp\left(-(1-x)/\varepsilon\right)\right),$$

where $C_1 = \exp(-1/\varepsilon)$ and $C_2 = 1 - \exp(-1/\varepsilon)$.

As the exact solution of the problem (2.6.1) is known, we calculate the maximum pointwise error by

$$e_\varepsilon^{N,\Delta t} = \max_{(x_i,t_n)\in D^{N,M}} \left| u(x_i,t_n) - U^{N,\Delta t}(x_i,t_n) \right|,$$

for each ε, where $u(x_i,t_n)$ and $U^{N,\Delta t}(x_i,t_n)$ denote the exact and numerical solutions obtained on the mesh $D^{N,M}$ with N mesh-intervals in the spatial direction and M mesh-intervals in the t-direction, such that $\Delta t = T/M$ is the uniform mesh-size. We determine the corresponding order of convergence by

$$p_\varepsilon^{N,\Delta t} = \log_2 \left(\frac{e_\varepsilon^{N,\Delta t}}{e_\varepsilon^{2N,\Delta t/2}} \right).$$

Now, for each N and Δt, we define the ε-uniform maximum pointwise error by $e^{N,\Delta t} = \max_\varepsilon e_\varepsilon^{N,\Delta t}$ and the corresponding ε-uniform order of convergence by

$$p^{N,\Delta t} = \log_2 \left(\frac{e^{N,\Delta t}}{e^{2N,\Delta t/2}} \right).$$

The calculated maximum pointwise errors $e_\varepsilon^{N,\Delta t}$ and the corresponding order of convergence $p_\varepsilon^{N,\Delta t}$ for Example 2.6.1 by using the hybrid scheme are presented in Table 2.1, for various values of ε and N. From the result, given in Table 2.1, one can observe the ε-uniform convergence of the scheme. We can observe that the numerical order of convergence does not clearly reflect the actual theoretical order of convergence of the proposed scheme (2.3.2) in space as proved in Theorem 2.4.4. The reason behind this, is the error consists of two parts due to spatial and temporal discretizations. The order of convergence observed in Table 2.1 is due to the effect of time error, which is first-order. In order to justify the spatial order of convergence precisely, we have done the numerical experiments by taking $M = N^2$ and displayed the maximum pointwise errors and the corresponding order of convergence in Table 2.2 for both inner and outer regions. Also one can observe from this table that the order of convergence in nearly two in the outer region and close to 1.5 in the inner region, this is because of the logarithmic factor appears in the error estimate in the inner region.

Example 2.6.2. *Consider the following singularly perturbed 1D linear delay parabolic IBVP:*

$$\begin{cases} u_t - \varepsilon u_{xx} + (2-x^2)u_x + xu = u(x,t-1) + 10t^2\exp(-t)x(1-x), & \\ & (x,t) \in \Omega_x \times (0,2], \\ u(x,t) = 0, & (x,t) \in \overline{\Omega}_x \times [-1,0], \\ u(0,t) = 0,\ u(1,t) = 0, & t \in [0,2]. \end{cases} \tag{2.6.2}$$

As the exact solution $u(x,t)$ of the DPDE (2.6.2) is unknown, to obtain the pointwise errors and to verify the ε-uniform convergence of the proposed scheme, we use the double mesh principle which is described as follows:

Let $\widetilde{U}(x_i,t_n)$ be the numerical solution obtained on the fine mesh $\widetilde{D}^{2N,2M} = \widetilde{\Omega}_x^{2N} \times \Lambda_t^{2M}$ with $2N$ mesh-intervals in the spatial direction and $2M$ mesh-intervals in the temporal direction, where $\widetilde{\Omega}_x^{2N}$ is a piecewise-uniform Shishkin mesh as like Ω_x^N with transition parameter $\widetilde{\rho}$ given by

$$\widetilde{\rho} = \min\left\{\frac{1}{2}, \rho_0 \varepsilon \ln\left(\frac{N}{2}\right)\right\},$$

such that for $i = 0, 1, \cdots, N$, the i-th point of the mesh Ω_x^N coincides with $2i$-th point of the mesh $\widetilde{\Omega}_x^{2N}$. Then for each ε, we calculate the maximum pointwise error by

$$E_\varepsilon^{N,\Delta t} = \max_{(x_i,t_n)\in D^{N,M}} \left|U(x_i,t_n) - \widetilde{U}(x_i,t_n)\right|,$$

and the corresponding order of convergence by

$$P_\varepsilon^{N,\Delta t} = \log_2\left(\frac{E_\varepsilon^{N,\Delta t}}{E_\varepsilon^{2N,\Delta t/2}}\right).$$

For each N and Δt, the quantities $E^{N,\Delta t}$ and $P^{N,\Delta t}$ are defined like $e^{N,\Delta t}$ and $p^{N,\Delta t}$ based on the error $E_\varepsilon^{N,\Delta t}$ as in the previous example.

In Table 2.4, we have displayed the computed maximum pointwise errors $E_\varepsilon^{N,\Delta t}$ and the corresponding order of convergence $P_\varepsilon^{N,\Delta t}$ for Example 2.6.2. The ε-uniform convergence of the scheme can also be seen from Table 2.4. Further, we have computed the maximum pointwise errors and the corresponding order of convergence in Table 2.5 by considering $M = N^2$, to justify the spatial order of convergence properly for Example 2.6.2.

Example 2.6.3. *Consider the following singularly perturbed semilinear delay parabolic IBVP:*

$$\begin{cases} u_t - \varepsilon u_{xx} + (1 + x(1-x))u_x + \exp(u) = u(x,t-1) + f(x,t), & (x,t) \in \Omega_x \times (0,2], \\ u(x,t) = \phi_b(x,t), & (x,t) \in \overline{\Omega}_x \times [-1,0], \\ u(0,t) = 0,\ u(1,t) = 0, & t \in [0,2]. \end{cases} \tag{2.6.3}$$

We choose the initial data $\phi_b(x,t)$ and the source function $f(x,t)$ to fit with the exact solution

$$u(x,t) = \exp(-t)\left(C_1 + C_2 x - \exp\left(-(1-x)/\varepsilon\right)\right),$$

where $C_1 = \exp(-1/\varepsilon)$ and $C_2 = 1 - \exp(-1/\varepsilon)$.

By using the Newton's linearization process (2.5.2) on (2.6.3), we obtain the following singularly perturbed linear system of delay IBVPs:

$$\begin{cases} u_t^{m+1} - \varepsilon u_{xx}^{m+1} + (1 + x(1-x))u_x^{m+1} + \exp(u^m)u^{m+1} = u^{m+1}(x, t-1) - \exp(u^m)(1-u^m) \\ \qquad\qquad\qquad\qquad\qquad\qquad\qquad\qquad\qquad\qquad\qquad\qquad + f(x,t), \quad (x,t) \in \Omega_x \times (0,2], \\ u^{m+1}(x,t) = \phi_b(x,t), \qquad\qquad\qquad\qquad\qquad\qquad\qquad\qquad (x,t) \in \overline{\Omega}_x \times [-1,0], \\ u^{m+1}(0,t) = 0, \ u^{m+1}(1,t) = 0, \qquad\qquad\qquad\qquad\qquad\qquad\qquad\qquad t \in [0,2]. \end{cases} \tag{2.6.4}$$

Now, for a fixed m, we solve (2.6.4) by using the numerical method discussed in Section 2.3. As a convergence criterion for the Newton's linearization process, we use

$$\max_{(x_i,t_n)\in D^{N,M}} \left| U^{m+1}(x_i,t_n) - U^m(x_i,t_n) \right| \leq \delta, \quad m \geq 0,$$

where $U^m(x_i,t_n)$ is the m-th iteration solution at the mesh-point (x_i,t_n) and δ is the tolerance value. Here, we used the tolerance value $\delta = 10^{-7}$.

As the exact solution of the problem (2.6.3) is known, for each ε, we calculate the maximum pointwise error by

$$\hat{e}_\varepsilon^{N,\Delta t} = \max_{(x_i,t_n)\in D^{N,M}} \left| u(x_i,t_n) - U^{N,\Delta t}(x_i,t_n) \right|,$$

where $u(x_i,t_n)$ and $U^{N,\Delta t}(x_i,t_n)$ denote the exact and numerical solutions obtained on the mesh $D^{N,M}$ with N mesh-intervals in the spatial direction and M mesh-intervals in the t-direction, such that $\Delta t = T/M$ is the uniform mesh-size. We determine the corresponding order of convergence by

$$\hat{p}_\varepsilon^{N,\Delta t} = \log_2 \left(\frac{\hat{e}_\varepsilon^{N,\Delta t}}{\hat{e}_\varepsilon^{2N,\Delta t/2}} \right).$$

Now, for each N and Δt, we define the ε-uniform maximum pointwise error by $\hat{e}^{N,\Delta t} = \max_\varepsilon \hat{e}_\varepsilon^{N,\Delta t}$ and the corresponding ε-uniform order of convergence by

$$\hat{p}^{N,\Delta t} = \log_2 \left(\frac{\hat{e}^{N,\Delta t}}{\hat{e}^{2N,\Delta t/2}} \right).$$

The calculated maximum pointwise errors $\hat{e}_\varepsilon^{N,\Delta t}$ and the corresponding order of convergence $\hat{p}_\varepsilon^{N,\Delta t}$ for Example 2.6.3 by using the hybrid scheme are presented in Table 2.7, for various values of ε and N. The ε-uniform convergence of the scheme can be seen from Table 2.7. To justify the spatial order of convergence properly for Example 2.6.3, we have computed the maximum pointwise errors and the corresponding order of convergence in Table 2.8 by considering $M = N^2$.

In order to show that the proposed method performs better than the earlier methods available in the literature, we have solved the problems given in Examples 2.6.1, 2.6.2 and 2.6.3 by using the first-order upwind scheme given in [32]. The corresponding numerical results are given in Tables 2.3, 2.6 and 2.9. One can compare the errors and the order of convergence given in Tables 2.1 and 2.3 for Example 2.6.1 and Tables 2.4 and 2.6 for Example 2.6.2 and Tables 2.7 and 2.9 for Example 2.6.3 and easily conclude that the proposed scheme performs better than the scheme used in [32].

To show the effect of some Shishkin-type meshes, we have computed the maximum pointwise errors and the corresponding order of convergence for the Shishkin mesh, the Bakhvalov-Shishkin mesh and the modified Bakhvalov-Shishkin mesh in Table 2.10 by taking $M = N^2$.

To visualize the appearance of the boundary layers in the solutions of Examples 2.6.1, 2.6.2 and 2.6.3, we have plotted the surface plots for $N = 64$ in Figure 2.2 for $\varepsilon = 10^{-4}$.

In order to reveal the numerical order of convergence, we have plotted the maximum pointwise errors in loglog scale, obtained by applying both the hybrid and upwind schemes for Examples 2.6.1, 2.6.2 and 2.6.3 in Figure 2.3, which again ensure the effectiveness of the proposed hybrid scheme in comparison with the upwind scheme.

Further, we have plotted the maximum pointwise errors in Figures 2.4 for all the examples by taking $M = N^2$. From these figures one can easily observe the second-order convergence of the hybrid scheme, for the spatial variable.

2.7 Conclusion

In this chapter, we proposed a numerical method to solve the one-dimensional singularly perturbed delay parabolic convection-diffusion problem of the form (2.1.1). To discretize the domain, we used the uniform mesh in the temporal direction and the piecewise-uniform Shishkin mesh for the spatial direction. The numerical scheme consists of the implicit-Euler scheme for the time derivative and the hybrid numerical scheme, which is a combination of the midpoint upwind scheme (for the outer region) and the central difference scheme (for the inner region) for the spatial derivatives. We have derived the ε-uniform error estimate for the proposed scheme, which is almost second-order in space and first-order in time. The proposed scheme is also applied numerically on the semilinear DPDEs by using the Newton's linearization method. Numerical results are provided for some examples to show the efficiency and accuracy of the method.

Table 2.1: *Maximum pointwise errors $e^{N,\Delta t}$ and the corresponding order of convergence $p^{N,\Delta t}$ for Example 2.6.1 by using the hybrid scheme.*

ε	Number of mesh-intervals N/temporal mesh-size Δt					
	$16/\frac{1}{20}$	$32/\frac{1}{40}$	$64/\frac{1}{80}$	$128/\frac{1}{160}$	$256/\frac{1}{320}$	$512/\frac{1}{640}$
10^{-1}	1.1626e-2	3.5451e-3	1.2302e-3	4.8808e-4	2.1444e-4	1.0023e-4
	1.7134	1.5269	1.3337	1.1866	1.0972	
10^{-2}	6.8405e-2	2.5940e-2	8.9480e-3	3.0529e-3	1.0271e-3	3.5498e-4
	1.3989	1.5355	1.5514	1.5715	1.5328	
10^{-3}	7.0493e-2	2.6902e-2	9.2019e-3	3.1079e-3	1.0171e-3	3.5176e-4
	1.3898	1.5477	1.5660	1.6115	1.5318	
10^{-4}	7.2726e-2	2.7273e-2	9.2643e-3	3.1235e-3	1.0149e-3	3.5151e-4
	1.4150	1.5577	1.5685	1.6218	1.5298	
10^{-5}	7.2960e-2	2.7418e-2	9.3171e-3	3.1252e-3	1.0147e-3	3.5148e-4
	1.4120	1.5572	1.5759	1.6229	1.5295	
10^{-6}	7.2983e-2	2.7432e-2	9.3275e-3	3.1319e-3	1.0147e-3	3.5148e-4
	1.4117	1.5563	1.5745	1.6260	1.5295	
10^{-7}	7.2985e-2	2.7434e-2	9.3285e-3	3.1325e-3	1.0147e-3	3.5149e-4
	1.4117	1.5562	1.5743	1.6263	1.5295	
10^{-8}	7.2986e-2	2.7434e-2	9.3286e-3	3.1326e-3	1.0146e-3	3.5135e-4
	1.4117	1.5562	1.5743	1.6265	1.5299	
10^{-9}	7.2986e-2	2.7434e-2	9.3284e-3	3.1331e-3	1.0146e-3	3.5016e-4
	1.4116	1.5563	1.5740	1.6267	1.5348	
10^{-10}	7.2985e-2	2.7434e-2	9.3283e-3	3.1275e-3	1.0143e-3	3.3857e-4
	1.4117	1.5563	1.5766	1.6245	1.5830	
$e^{N,\Delta t}$	**7.2986e-2**	**2.7434e-2**	**9.3286e-3**	**3.1331e-3**	**1.0271e-3**	**3.5498e-4**
$p^{N,\Delta t}$	**1.4116**	**1.5562**	**1.5741**	**1.6089**	**1.5328**	

Table 2.2: *Maximum pointwise errors and the corresponding order of convergence for Example 2.6.1 by taking $M = N^2$.*

N	$\varepsilon = 1e-4$		$\varepsilon = 1e-8$	
	outer region $[0, 1-\rho]$	inner region $(1-\rho, 1]$	outer region $[0, 1-\rho]$	inner region $(1-\rho, 1]$
16	1.0810e-3	7.4569e-2	1.0835e-3	7.5149e-2
	1.9904	1.4253	1.9897	1.4304
32	2.7206e-4	2.7765e-2	2.7282e-4	2.7883e-2
	1.9990	1.5684	1.9982	1.5703
64	6.8061e-5	9.3620e-3	6.8292e-5	9.3890e-3
	1.9999	1.5795	1.9991	1.5805
128	1.7016e-5	3.1326e-3	1.7084e-5	3.1394e-3
	2.0006	1.6299	1.9999	1.6300

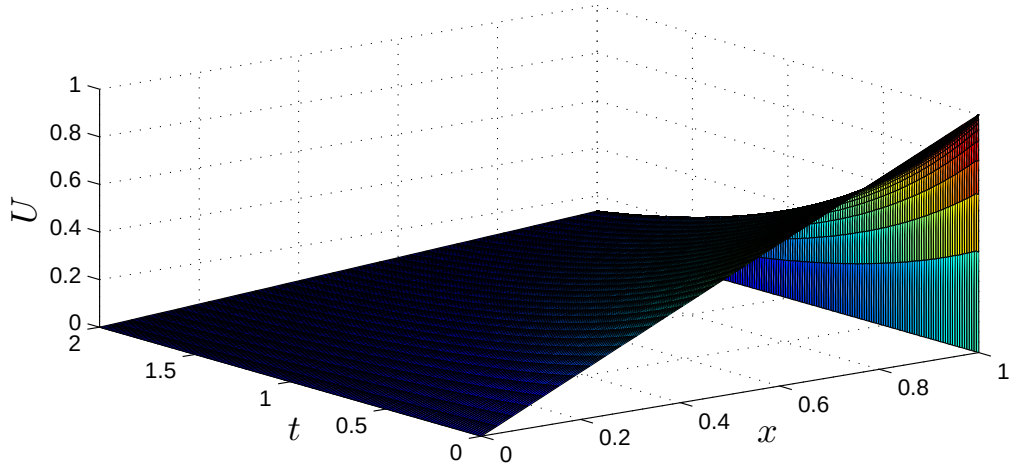

(a) Example 2.6.1.

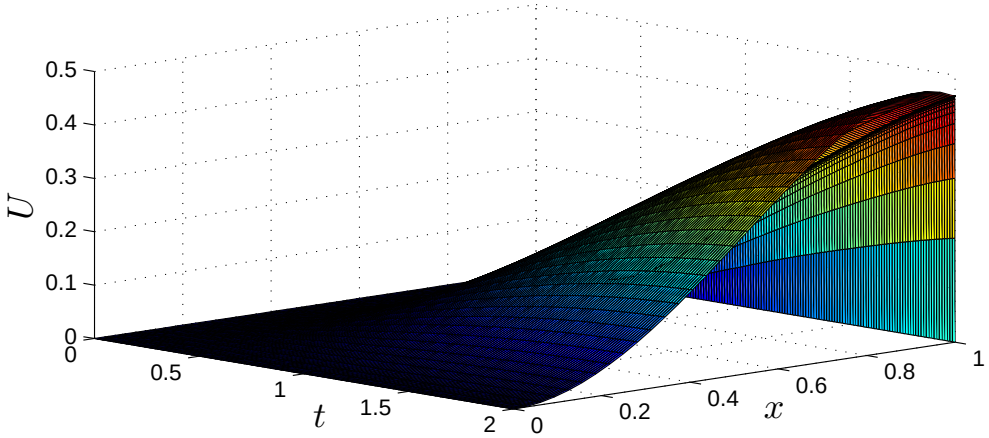

(b) Example 2.6.2.

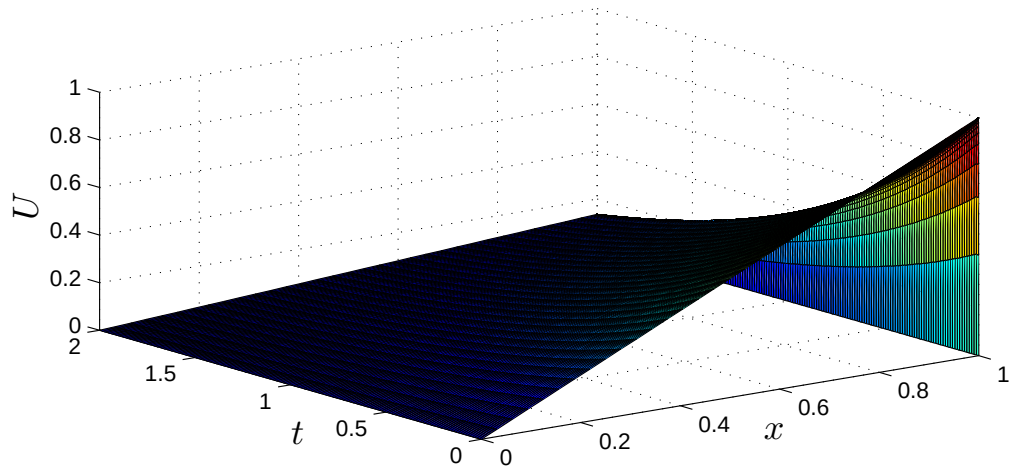

(c) Example 2.6.3.

Figure 2.2: *Surface plots of the numerical solutions for* $\varepsilon = 1e-4$, $N = 64$.

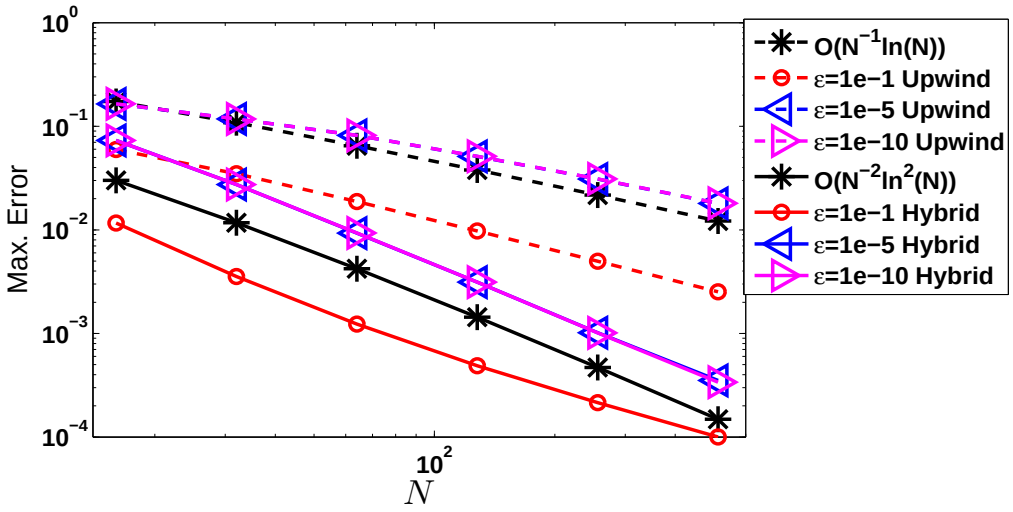

(a) Example 2.6.1.

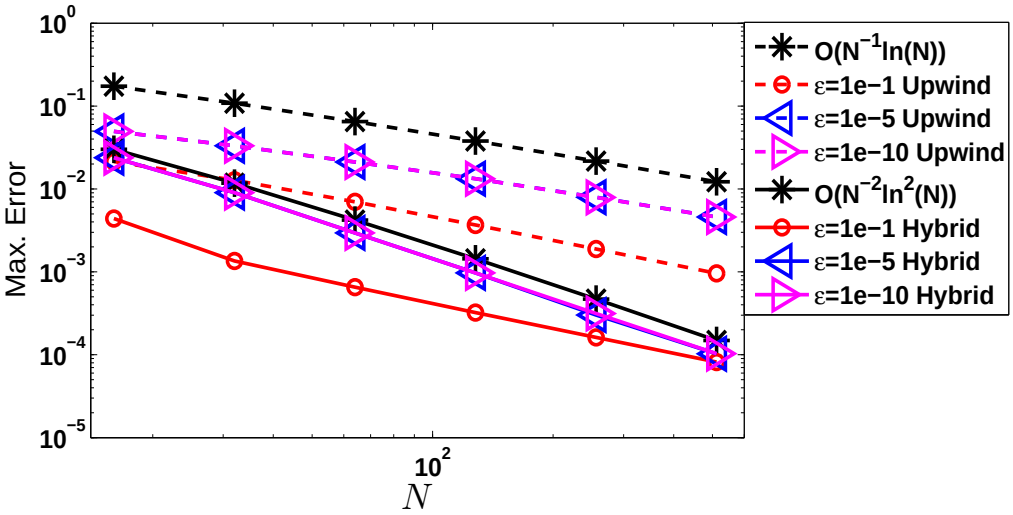

(b) Example 2.6.2.

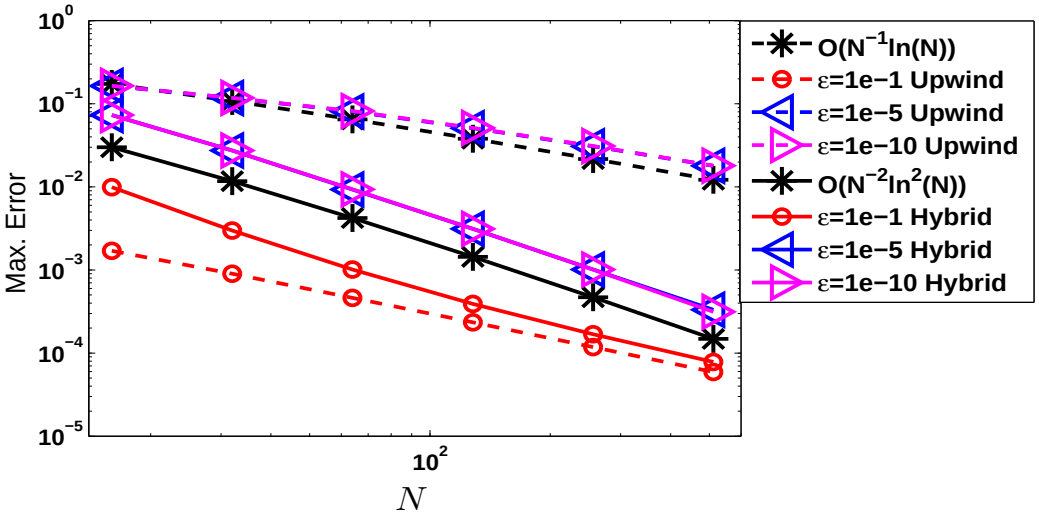

(c) Example 2.6.3.

Figure 2.3: *Visualization of the order of convergence through loglog plot.*

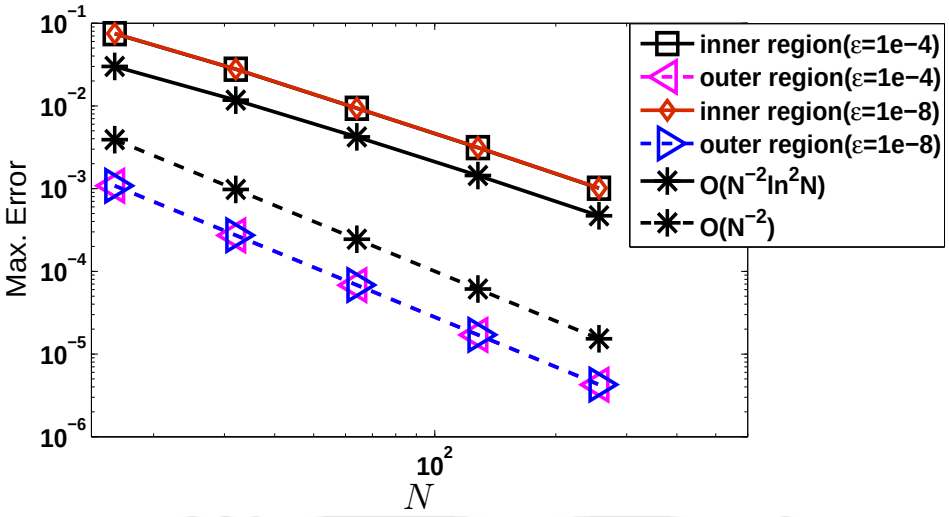

(a) *Example* 2.6.1.

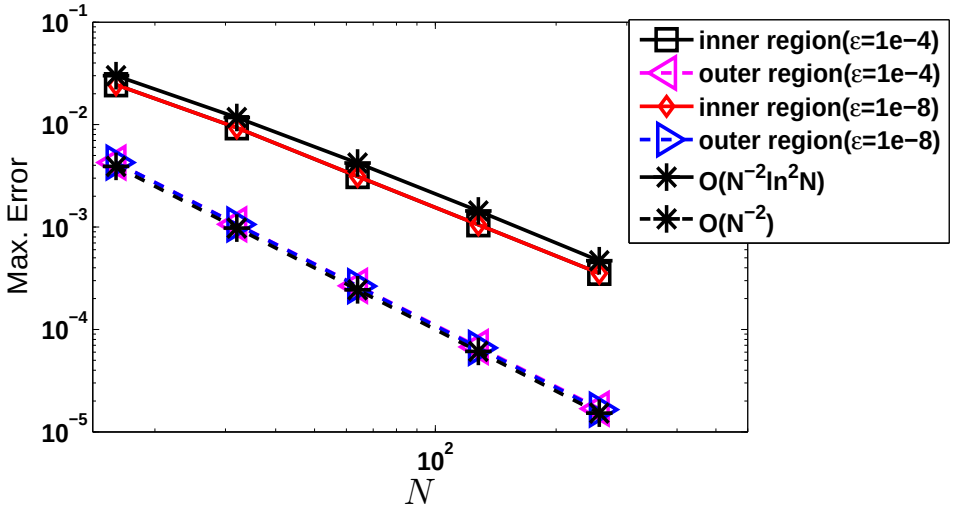

(b) *Example* 2.6.2.

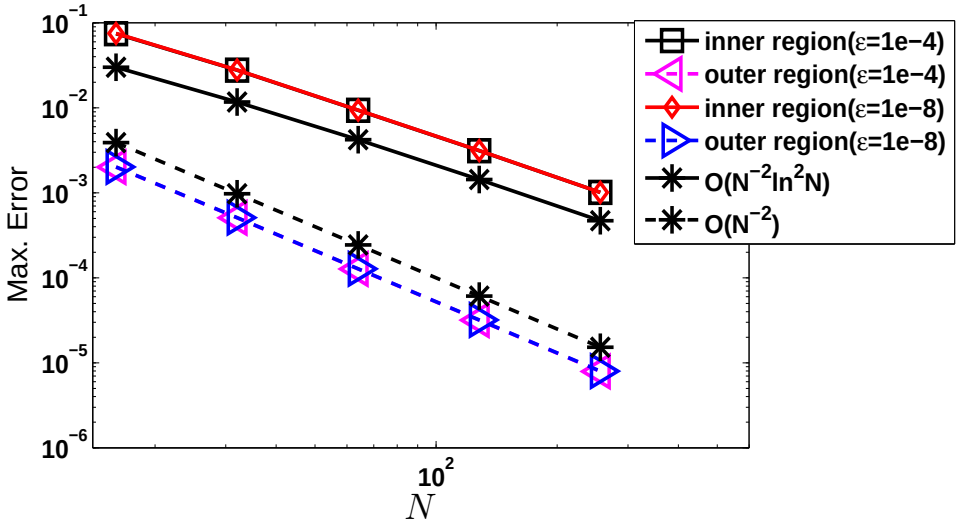

(c) *Example* 2.6.3.

Figure 2.4: *Visualization for the spatial order of convergence (for* $M = N^2$*).*

Table 2.3: *Maximum pointwise errors $e^{N,\Delta t}$ and the corresponding order of convergence $p^{N,\Delta t}$ for Example 2.6.1 by using the upwind scheme [32].*

ε	Number of mesh-intervals N/temporal mesh-size Δt					
	$16/\frac{1}{20}$	$32/\frac{1}{40}$	$64/\frac{1}{80}$	$128/\frac{1}{160}$	$256/\frac{1}{320}$	$512/\frac{1}{640}$
10^{-1}	5.9627e-2	3.4842e-2	1.8779e-2	9.7731e-3	4.9886e-3	2.5210e-3
	0.7751	0.8917	0.9422	0.9702	0.9846	
10^{-2}	1.4533e-1	1.0654e-1	7.4088e-2	4.6809e-2	2.8342e-2	1.6521e-2
	0.4480	0.5240	0.6625	0.7239	0.7786	
10^{-3}	1.5869e-1	1.1439e-1	7.9507e-2	5.0194e-2	3.0437e-2	1.7723e-2
	0.4723	0.5248	0.6636	0.7217	0.7802	
10^{-4}	1.6401e-1	1.1715e-1	8.0732e-2	5.0943e-2	3.0845e-2	1.7958e-2
	0.4853	0.5372	0.6643	0.7239	0.7804	
10^{-5}	1.6457e-1	1.1780e-1	8.1649e-2	5.1186e-2	3.0934e-2	1.8007e-2
	0.4824	0.5288	0.6737	0.7266	0.7806	
10^{-6}	1.6462e-1	1.1786e-1	8.1742e-2	5.1296e-2	3.1019e-2	1.8021e-2
	0.4821	0.5279	0.6722	0.7257	0.7835	
10^{-7}	1.6463e-1	1.1787e-1	8.1751e-2	5.1307e-2	3.1033e-2	1.8036e-2
	0.4821	0.5279	0.6721	0.7254	0.7829	
10^{-8}	1.6463e-1	1.1787e-1	8.1752e-2	5.1308e-2	3.1034e-2	1.8038e-2
	0.4821	0.5278	0.6721	0.7253	0.7828	
10^{-9}	1.6463e-1	1.1787e-1	8.1753e-2	5.1308e-2	3.1034e-2	1.8041e-2
	0.4821	0.5278	0.6721	0.7253	0.7826	
10^{-10}	1.6463e-1	1.1787e-1	8.1753e-2	5.1313e-2	3.1035e-2	1.8063e-2
	0.4821	0.5278	0.6719	0.7254	0.7808	
$e^{N,\Delta t}$	**1.6463e-1**	**1.1787e-1**	**8.1753e-2**	**5.1313e-2**	**3.1035e-2**	**1.8063e-2**
$p^{N,\Delta t}$	**0.4821**	**0.5278**	**0.6719**	**0.7254**	**0.7808**	

Table 2.4: *Maximum pointwise errors $E^{N,\Delta t}$ and the corresponding order of convergence $P^{N,\Delta t}$ for Example 2.6.2 by using the hybrid scheme.*

ε	Number of mesh-intervals N/temporal mesh-size Δt					
	$16/\frac{1}{20}$	$32/\frac{1}{40}$	$64/\frac{1}{80}$	$128/\frac{1}{160}$	$256/\frac{1}{320}$	$512/\frac{1}{640}$
10^{-1}	4.3906e-3	1.3510e-3	6.5408e-4	3.2242e-4	1.6185e-4	8.1519e-5
	1.7004	1.0465	1.0205	0.9943	0.9895	
10^{-2}	2.4637e-2	9.2843e-3	2.9695e-3	9.6870e-4	2.9557e-4	9.0157e-5
	1.4080	1.6446	1.6161	1.7126	1.7130	
10^{-3}	2.3812e-2	9.0139e-3	2.9292e-3	9.6140e-4	2.9658e-4	1.0119e-4
	1.4015	1.6217	1.6073	1.6967	1.5514	
10^{-4}	2.3796e-2	9.0165e-3	2.9429e-3	9.6933e-4	3.0104e-4	1.0275e-4
	1.4001	1.6153	1.6022	1.6870	1.5508	
10^{-5}	2.3795e-2	9.0172e-3	2.9446e-3	9.7029e-4	3.0158e-4	1.0292e-4
	1.3999	1.6146	1.6016	1.6859	1.5510	
10^{-6}	2.3795e-2	9.0173e-3	2.9447e-3	9.7038e-4	3.0163e-4	1.0294e-4
	1.3999	1.6145	1.6015	1.6858	1.5510	
10^{-7}	2.3795e-2	9.0173e-3	2.9448e-3	9.7040e-4	3.0162e-4	1.0294e-4
	1.3999	1.6145	1.6015	1.6858	1.5510	
10^{-8}	2.3795e-2	9.0173e-3	2.9448e-3	9.7046e-4	3.0179e-4	1.0294e-4
	1.3999	1.6145	1.6014	1.6851	1.5518	
10^{-9}	2.3795e-2	9.0171e-3	2.9448e-3	9.6970e-4	3.0166e-4	1.0294e-4
	1.3999	1.6145	1.6026	1.6846	1.5511	
10^{-10}	2.3795e-2	9.0190e-3	2.9474e-3	9.7161e-4	3.1402e-4	1.0295e-4
	1.3996	1.6135	1.6010	1.6295	1.6089	
$E^{N,\Delta t}$	**2.4637e-2**	**9.2843e-3**	**2.9695e-3**	**9.7161e-4**	**3.1402e-4**	**1.0295e-4**
$P^{N,\Delta t}$	**1.4080**	**1.6446**	**1.6118**	**1.6295**	**1.6089**	

Table 2.5: *Maximum pointwise errors and the corresponding order of convergence for Example 2.6.2 by taking $M = N^2$.*

N	$\varepsilon = 1e-4$		$\varepsilon = 1e-8$	
	outer region $[0, 1-\rho]$	inner region $(1-\rho, 1]$	outer region $[0, 1-\rho]$	inner region $(1-\rho, 1]$
16	4.2580e-3	2.4494e-2	4.2539e-3	2.4494e-2
	2.0019	1.3934	2.0055	1.3932
32	1.0631e-3	9.3241e-3	1.0594e-3	9.3251e-3
	1.9936	1.5798	2.0014	1.5791
64	2.6697e-4	3.1191e-3	2.6459e-4	3.1211e-3
	1.9840	1.5672	1.9996	1.5665
128	6.7484e-5	1.0526e-3	6.6163e-5	1.0538e-3
	1.9999	1.5751	2.0008	1.5743

Table 2.6: *Maximum pointwise errors $E^{N,\Delta t}$ and the corresponding order of convergence $P^{N,\Delta t}$ for Example 2.6.2 by using the upwind scheme [32].*

ε	Number of mesh-intervals N/temporal mesh-size Δt					
	$16/\frac{1}{20}$	$32/\frac{1}{40}$	$64/\frac{1}{80}$	$128/\frac{1}{160}$	$256/\frac{1}{320}$	$512/\frac{1}{640}$
10^{-1}	2.1370e-2	1.2716e-2	6.9955e-3	3.6793e-3	1.8883e-3	9.5709e-4
	0.7490	0.8621	0.9270	0.9624	0.9804	
10^{-2}	3.8385e-2	2.5033e-2	1.7683e-2	1.1260e-2	6.9364e-3	4.0793e-3
	0.6167	0.5015	0.6511	0.6990	0.7658	
10^{-3}	4.7904e-2	3.1897e-2	2.0434e-2	1.2904e-2	7.7134e-3	4.4579e-3
	0.5867	0.6424	0.6631	0.7424	0.7910	
10^{-4}	4.9321e-2	3.3066e-2	2.1081e-2	1.3275e-2	7.9104e-3	4.5722e-3
	0.5769	0.6494	0.6673	0.7469	0.7908	
10^{-5}	4.9469e-2	3.3189e-2	2.1157e-2	1.3315e-2	7.9321e-3	4.5850e-3
	0.5758	0.6496	0.6681	0.7473	0.7908	
10^{-6}	4.9484e-2	3.3202e-2	2.1164e-2	1.3319e-2	7.9342e-3	4.5863e-3
	0.5757	0.6496	0.6681	0.7473	0.7908	
10^{-7}	4.9485e-2	3.3203e-2	2.1165e-2	1.3319e-2	7.9345e-3	4.5865e-3
	0.5757	0.6496	0.6681	0.7473	0.7908	
10^{-8}	4.9485e-2	3.3203e-2	2.1165e-2	1.3319e-2	7.9344e-3	4.5864e-3
	0.5757	0.6496	0.6682	0.7473	0.7908	
10^{-9}	4.9485e-2	3.3203e-2	2.1165e-2	1.3320e-2	7.9345e-3	4.5859e-3
	0.5757	0.6496	0.6681	0.7474	0.7909	
10^{-10}	4.9485e-2	3.3202e-2	2.1164e-2	1.3319e-2	7.9243e-3	4.5813e-3
	0.5757	0.6497	0.6681	0.7491	0.7905	
$E^{N,\Delta t}$	**4.9485e-2**	**3.3203e-2**	**2.1165e-2**	**1.3320e-2**	**7.9345e-3**	**4.5865e-3**
$P^{N,\Delta t}$	**0.5757**	**0.6496**	**0.6681**	**0.7474**	**0.7908**	

Table 2.7: *Maximum pointwise errors $\hat{e}^{N,\Delta t}$ and the corresponding order of convergence $\hat{p}^{N,\Delta t}$ for Example 2.6.3 by using the hybrid scheme.*

ε	Number of mesh-intervals N/temporal mesh-size Δt					
	$16/\frac{1}{20}$	$32/\frac{1}{40}$	$64/\frac{1}{80}$	$128/\frac{1}{160}$	$256/\frac{1}{320}$	$512/\frac{1}{640}$
10^{-1}	9.9061e-3	2.9824e-3	1.0125e-3	3.9061e-4	1.6856e-4	7.8043e-5
	1.7319	1.5586	1.3741	1.2125	1.1109	
10^{-2}	6.5871e-2	2.5202e-2	8.6651e-3	2.9591e-3	9.8819e-4	3.2970e-4
	1.3861	1.5403	1.55	1.5823	1.5836	
10^{-3}	7.0412e-2	2.6832e-2	9.1700e-3	3.0970e-3	1.0126e-3	3.3195e-4
	1.3919	1.5489	1.5661	1.6129	1.6090	
10^{-4}	7.2914e-2	2.7287e-2	9.2655e-3	3.1229e-3	1.0145e-3	3.3223e-4
	1.4180	1.5582	1.5690	1.6221	1.6106	
10^{-5}	7.3184e-2	2.7441e-2	9.3203e-3	3.1255e-3	1.0147e-3	3.3226e-4
	1.4152	1.5579	1.5763	1.6231	1.6106	
10^{-6}	7.3211e-2	2.7456e-2	9.3310e-3	3.1323e-3	1.0147e-3	3.3226e-4
	1.4149	1.5570	1.5748	1.6262	1.6107	
10^{-7}	7.3213e-2	2.7458e-2	9.3321e-3	3.1329e-3	1.0147e-3	3.3228e-4
	1.4149	1.5570	1.5747	1.6265	1.6106	
10^{-8}	7.3214e-2	2.7458e-2	9.3322e-3	3.1330e-3	1.0146e-3	3.3206e-4
	1.4149	1.5570	1.5747	1.6266	1.6114	
10^{-9}	7.3214e-2	2.7458e-2	9.3319e-3	3.1335e-3	1.0146e-3	3.3029e-4
	1.4149	1.5570	1.5744	1.6268	1.6191	
10^{-10}	7.3213e-2	2.7458e-2	9.3318e-3	3.1279e-3	1.0143e-3	3.1337e-4
	1.4149	1.5570	1.5770	1.6247	1.6946	
$\hat{e}^{N,\Delta t}$	**7.3214e-2**	**2.7458e-2**	**9.3322e-3**	**3.1335e-3**	**1.0147e-3**	**3.3228e-4**
$\hat{p}^{N,\Delta t}$	**1.4149**	**1.5570**	**1.5744**	**1.6267**	**1.6106**	

Table 2.8: *Maximum pointwise errors and the corresponding order of convergence for Example 2.6.3 by taking $M = N^2$.*

N	$\varepsilon = 1e-4$		$\varepsilon = 1e-8$	
	outer region $[0, 1-\rho]$	inner region $(1-\rho, 1]$	outer region $[0, 1-\rho]$	inner region $(1-\rho, 1]$
16	2.0084e-3	7.4655e-2	2.0148e-3	7.5206e-2
	1.9787	1.4270	1.9785	1.4313
32	5.0957e-4	2.7764e-2	5.1126e-4	2.7886e-2
	2.0037	1.5687	2.0021	1.5705
64	1.2707e-4	9.3595e-3	1.2763e-4	9.3892e-3
	2.0007	1.5795	2.0003	1.5805
128	3.1751e-5	3.1316e-3	3.1901e-5	3.1395e-3
	2.0013	1.6299	2.0001	1.6301

Table 2.9: *Maximum pointwise errors* $\hat{e}^{N,\Delta t}$ *and the corresponding order of convergence* $\hat{p}^{N,\Delta t}$ *for Example 2.6.3 by using the upwind scheme [32].*

ε	Number of mesh-intervals N/temporal mesh-size Δt					
	$16/\frac{1}{20}$	$32/\frac{1}{40}$	$64/\frac{1}{80}$	$128/\frac{1}{160}$	$256/\frac{1}{320}$	$512/\frac{1}{640}$
10^{-1}	1.7004e-3	9.0004e-4	4.6216e-4	2.3426e-4	1.1794e-4	5.9178e-5
	0.9178	0.9616	0.9803	0.9900	0.9949	
10^{-2}	5.2574e-2	3.1177e-2	1.6776e-2	8.7265e-3	4.4560e-3	2.2517e-3
	0.7539	0.8941	0.9429	0.9697	0.9847	
10^{-3}	1.4104e-1	1.0400e-1	7.2175e-2	4.5672e-2	2.7603e-2	1.6101e-2
	0.4394	0.5271	0.6602	0.7265	0.7777	
10^{-4}	1.5815e-1	1.1405e-1	7.9245e-2	5.0036e-2	3.0336e-2	1.7666e-2
	0.4716	0.5253	0.6634	0.7219	0.7801	
10^{-5}	1.6399e-1	1.1712e-1	8.0705e-2	5.0926e-2	3.0834e-2	1.7952e-2
	0.4856	0.5373	0.6642	0.7239	0.7804	
10^{-6}	1.6461e-1	1.1780e-1	8.1647e-2	5.1184e-2	3.0933e-2	1.8007e-2
	0.4827	0.5289	0.6737	0.7266	0.7806	
10^{-7}	1.6468e-1	1.1787e-1	8.1743e-2	5.1296e-2	3.1019e-2	1.8021e-2
	0.4824	0.5280	0.6723	0.7257	0.7835	
10^{-8}	1.6468e-1	1.1788e-1	8.1753e-2	5.1307e-2	3.1033e-2	1.8036e-2
	0.4824	0.5279	0.6721	0.7254	0.7829	
10^{-9}	1.6468e-1	1.1788e-1	8.1754e-2	5.1308e-2	3.1034e-2	1.8038e-2
	0.4824	0.5279	0.6721	0.7253	0.7828	
10^{-10}	1.6468e-1	1.1788e-1	8.1754e-2	5.1308e-2	3.1034e-2	1.8038e-2
	0.4824	0.5279	0.6721	0.7253	0.7828	
$\hat{e}^{N,\Delta t}$	**1.6468e-1**	**1.1788e-1**	**8.1754e-2**	**5.1308e-2**	**3.1034e-2**	**1.8038e-2**
$\hat{p}^{N,\Delta t}$	**0.4824**	**0.5279**	**0.6721**	**0.7253**	**0.7828**	

Table 2.10: *Maximum pointwise errors and corresponding order of convergence for Example 2.6.1 by taking* $M = N^2$.

	$\varepsilon = 10^{-2}$			$\varepsilon = 10^{-6}$		
N	**S** mesh	**B–S** mesh	**Modified B–S** mesh	**S** mesh	**B–S** mesh	**Modified B–S** mesh
16	7.0551e-2	9.0812e-3	7.8444e-3	7.5388e-2	1.0027e-2	8.6568e-3
	1.4323	1.9144	1.8557	1.4350	1.9213	1.8605
32	2.6141e-2	2.4091e-3	2.1674e-3	2.7883e-2	2.6473e-3	2.3839e-3
	1.5762	1.9503	1.8956	1.5704	1.9523	1.8932
64	8.7667e-3	6.2336e-4	5.8251e-4	9.3888e-3	6.8408e-4	6.4179e-4
	1.5800	1.9791	1.9220	1.5804	1.9791	1.9201
128	2.9322e-3	1.5812e-4	1.5372e-4	3.1395e-3	1.7352e-4	1.6958e-4
	1.6303	1.9891	1.9391	1.6300	1.9892	1.9380
256	9.4719e-4	3.9829e-5	4.0086e-5	1.0143e-3	4.3707e-5	4.4259e-5

CHAPTER 3

Second-Order Uniformly Convergent Numerical Method for Singularly Perturbed 1D Delay Parabolic Partial Differential Equations

This chapter is devoted to the study of a post-processing technique for singularly perturbed 1D delay parabolic convection-diffusion problem having a regular boundary layer. To handle this layer phenomenon, the problem is solved on an *apriori* special mesh by using the implicit-Euler scheme for the discretization of the time derivative and the upwind scheme for the discretization of the spatial derivatives which results in almost first-order convergence, *i.e.*, $O(N^{-1}\ln N + \Delta t)$. Then, the Richardson extrapolation technique is applied on the computed solution fixing the transition parameter of the Shishkin mesh in order to improve the accuracy. We show that the Richardson extrapolation technique improves the order of convergence to $O(N^{-2}\ln^2 N + \Delta t^2)$. To support the theoretical results, numerical experiments are carried out.

3.1 Introduction

We consider the following class of singularly perturbed delay parabolic IBVPs with Dirichlet boundary conditions. Let $\Omega_x = (0,1)$, $\Lambda_t = (0,T]$, $D = \Omega_x \times \Lambda_t$ and $\Gamma = \Gamma_l \cup \Gamma_b \cup \Gamma_r$, where Γ_l and Γ_r are the left and the right sides of the rectangular domain D corresponding to $x = 0$ and $x = 1$, respectively, and $\Gamma_b = \overline{\Omega}_x \times [-\tau, 0]$.

$$\begin{cases} \left(\dfrac{\partial}{\partial t} + \mathscr{L}_\varepsilon\right) u(x,t) = -c(x,t)u(x,t-\tau) + f(x,t), & (x,t) \in D, \\ u(x,t) = \phi_b(x,t), & (x,t) \in \Gamma_b, \\ u(0,t) = \phi_l(t), & \text{on } \Gamma_l = \{(0,t) : 0 \le t \le T\}, \\ u(1,t) = \phi_r(t), & \text{on } \Gamma_r = \{(1,t) : 0 \le t \le T\}, \end{cases} \tag{3.1.1}$$

where

$$\mathscr{L}_\varepsilon u(x,t) = -\varepsilon u_{xx}(x,t) + a(x)u_x(x,t) + b(x,t)u(x,t),$$

$0 < \varepsilon \ll 1$ is the singular perturbation parameter and $\tau > 0$ is the delay parameter. The coefficients $a(x)$, $b(x,t)$, $c(x,t)$, $f(x,t)$ on $\overline{D}$ and the boundary, initial values $\phi_l(t)$, $\phi_r(t)$, $\phi_b(x,t)$ on Γ, are sufficiently smooth and bounded functions, such that $a(x) \geq \alpha > 0$, $b(x,t) \geq 0$ and $c(x,t)$ is nonzero on $\overline{D}$. The solution of the IBVP (3.1.1) exhibits a regular boundary layer of width $O(\varepsilon)$ along $x = 1$. The existence and uniqueness of the solution for our model problem (3.1.1) can be guaranteed by the sufficient smoothness and compatibility conditions (2.2.1) and (2.2.2) as given in Chapter 2, imposed on $\phi_l(t)$, $\phi_b(x,t)$ and $\phi_r(t)$. The terminal time T is assumed to satisfy the condition $T = k\tau$ for some positive integer k.

Here, first we discretize the domain with the uniform mesh in the time direction and by the piecewise-uniform Shishkin mesh in the spatial direction. Then the time derivative is replaced by the implicit-Euler scheme and the spatial derivatives are approximated by the upwind finite difference scheme. First, we solve the DPDE by this numerical scheme on $N+1$ and $M+1$ number of spatial and temporal mesh-points, respectively, after that we solve the DPDE by the same numerical scheme on $2N+1$ (by fixing the transition parameter) and $2M+1$ number of mesh-points. Then we combine these two solutions properly to obtain a better approximate numerical solution. This method enhances the order of convergence from first-order to second-order. ε-uniform error estimates are derived separately for the smooth and singular components. Numerical experiments are carried out to show the accuracy and efficiency of the proposed method.

The outline of this chapter is as follows: Section 3.2 deals with the upwind scheme. The Richardson extrapolation technique has been described in Section 3.3. The main proof of convergence after extrapolation has been given in Section 3.3.1. Numerical results are presented in Section 3.4 and the chapter ends with Section 3.5 that summarizes the main conclusions.

3.2 The Numerical Solution

This section describes the difference scheme used to discretize the DPDE (3.1.1).

3.2.1 Discretization of the domain

Since the solution of the DPDE (3.1.1) exhibits a regular boundary layer only in the spatial variable, we discretize the domain with the piecewise-uniform Shishkin mesh in the spatial direction and the uniform mesh in the temporal direction.

Here, we construct the piecewise-uniform mesh in such a way that the density of the mesh-points is more in the boundary layer region than the outer region. Since the DPDE (3.1.1) has a boundary layer along the side $x = 1$, the mesh should be condensing in the neighborhood of $x = 1$. To define the piecewise-uniform mesh, we divide the domain $[0, 1]$ into two sub-domains $[0, 1-\rho]$ and $(1-\rho, 1]$, where the transition parameter $1-\rho$, which separates the coarse and fine portion of the mesh is obtained by taking

$$\rho = \min\left\{\frac{1}{2}, \rho_0 \varepsilon \ln N\right\}, \tag{3.2.1}$$

provided $\rho_0 \geq 2/\alpha$. We denote the spatial meshes by

$$\overline{\Omega}_x^N = \{0 = x_0, x_1, \cdots, x_{N/2} = 1-\rho, \cdots, x_N = 1\},$$

where

$$x_i = \begin{cases} i\dfrac{2(1-\rho)}{N}, & i = 0, \cdots, N/2, \\ 1-\rho+\left(i-\dfrac{N}{2}\right)\dfrac{2\rho}{N}, & i = (N/2)+1, \cdots, N, \end{cases}$$

$N \geq 4$ be a positive even integer and $\Omega_x^N = \overline{\Omega}_x^N \cap \Omega_x$. The analysis has been carried out by assuming that $\rho = \rho_0 \varepsilon \ln N$, as otherwise N is exponentially large in comparison with ε. The spatial mesh-sizes are denoted by

$$h_i = x_i - x_{i-1},\ i = 1, \cdots, N, \quad \widehat{h}_i = h_i + h_{i+1},\ i = 1, \cdots, N-1.$$

Further, let $H = 2(1-\rho)/N$ and $h = 2\rho/N$ be the spatial mesh-sizes in $[0,\ 1-\rho]$ and $[1-\rho,\ 1]$, respectively. It is clear that $N^{-1} \leq H \leq 2N^{-1}$, $h = 2\rho_0 \varepsilon N^{-1} \ln N$, and the uniform mesh can be obtained by choosing $\rho = 1/2$. For the time domain $\overline{\Lambda}_t$, we will use a uniform mesh with mesh-size Δt, such that

$$\Lambda_t^M = \{t_n = n\Delta t, n = 0, \cdots, M, \Delta t = T/M\},$$

where M is the number of mesh-intervals in the t-direction on the interval $[0, T]$ and the temporal mesh-size Δt satisfies the constraint $p\Delta t = \tau$, where p is a positive integer, $t_n = n\Delta t$, $n \geq -p$.

We define the discrete domain by $D^{N,M} = \overline{D}^{N,M} \cap D$ where $\overline{D}^{N,M} = \overline{\Omega}_x^N \times \Lambda_t^M$ and $\Gamma_b^N = \overline{\Omega}_x^N \times \Lambda_t^p$, where Λ_t^p denotes the set of $p+1$ uniform mesh-points in $[-\tau, 0]$. The boundary points of $\overline{D}^{N,M}$ are $\Gamma^N = \overline{D}^{N,M} \cap \Gamma$. Similarly, we define the left and right boundary points by $\Gamma_l^N = \overline{D}^{N,M} \cap \Gamma_l$ and $\Gamma_r^N = \overline{D}^{N,M} \cap \Gamma_r$, respectively. We further discretize $\overline{D}_j^{N,M} = \overline{\Omega}_x^N \times \Lambda_{j,t}^p$, where $\Lambda_{j,t}^p$ denotes the set of $p+1$ uniform mesh-points in $[(j-1)\tau, j\tau]$, for $j = 1, 2, \cdots, k$. From the above discretization we can observe that $\overline{D}^{N,M} = \bigcup_{j=1}^{k} \overline{D}_j^{N,M}$.

3.2.2 Numerical scheme

In this section, we approximate the continuous problem (3.1.1) by means of the implicit-Euler scheme for the time derivative and the upwind scheme for the spatial derivatives.

Hence the discretization of the IBVP (3.1.1) takes the form

$$\begin{cases} (\delta_t^- + \mathscr{L}_\varepsilon^N)U_i^{n+1} = -c_{i,n+1}U_i^{n-p+1} + f_i^{n+1}, \quad \text{for} \quad i = 1, \cdots, N-1, \quad n = 0, \cdots, M-1, \\ U_0^{n+1} = \phi_l(t_{n+1}), \qquad U_N^{n+1} = \phi_r(t_{n+1}), \qquad \text{for} \quad n = 0, \cdots, M-1, \\ U_i^{-j} = \phi_b(x_i, -t_j), \qquad \text{for} \quad i = 0, \cdots, N, \ \text{and} \ \ j = 0, \cdots, p, \end{cases} \tag{3.2.2}$$

where

$$\mathscr{L}_\varepsilon^N U_i^{n+1} = -\varepsilon\delta_x^2 U_i^{n+1} + a_i\delta_x^- U_i^{n+1} + b_{i,n+1}U_i^{n+1}.$$

After rearranging the terms in (3.2.2), we obtain the following system of linear algebraic equations:

$$\begin{cases} r_i^- U_{i-1}^{n+1} + r_i^0 U_i^{n+1} + r_i^+ U_{i+1}^{n+1} = g_i^n, \qquad \text{for} \quad i = 1, \cdots, N-1, \quad n = 0, \cdots, M-1, \\ U_0^{n+1} = \phi_l(t_{n+1}), \qquad U_N^{n+1} = \phi_r(t_{n+1}), \qquad \text{for} \quad n = 0, \cdots, M-1, \\ U_i^{-j} = \phi_b(x_i, -t_j), \qquad \text{for} \quad i = 0, \cdots, N, \ \text{and} \ j = 0, \cdots, p, \end{cases}$$

where

$$\begin{cases} r_i^- = \Delta t\left(-\dfrac{2\varepsilon}{\widehat{h}_i h_i} - \dfrac{a_i}{h_i}\right), \quad r_i^+ = \Delta t\left(-\dfrac{2\varepsilon}{\widehat{h}_i h_{i+1}}\right), \quad r_i^0 = 1 + \Delta t b_{i,n+1} - r_i^- - r_i^+, \\ c_{i,n+1} = c(x_i, t_{n+1}), \quad a_i = a(x_i), \quad g_i^n = U_i^n + \Delta t\left(-c_{i,n+1}U_i^{n-p+1} + f_i^{n+1}\right). \end{cases}$$

The finite difference operator $(\delta_t^- + \mathscr{L}_\varepsilon^N)$ defined in (3.2.2) satisfies the following discrete maximum principle on $D^{N,M}$, which provides the ε-uniform stability of the difference operator $(\delta_t^- + \mathscr{L}_\varepsilon^N)$.

Lemma 3.2.1. *(***Discrete maximum principle***) Assume that the discrete function* Ψ_i^n *satisfies* $\Psi_i^n \geq 0$ *on* Γ^N. *Then* $(\delta_t^- + \mathscr{L}_\varepsilon^N)\Psi_i^n \geq 0$ *on* $D^{N,M}$ *implies that* $\Psi_i^n \geq 0$ *at each point of* $\overline{D}^{N,M}$.

Proof. Assume that there exist a point $(x_i^*, t_n^*) \in \overline{D}^{N,M}$, such that

$$\Psi(x_i^*, t_n^*) = \min_{(x_i,t_n)\in\overline{D}^{N,M}} \Psi(x_i, t_n) < 0.$$

Clearly $(x_i^*, t_n^*) \notin \Gamma^N$, which implies $(x_i^*, t_n^*) \in D^{N,M}$.

Now, by applying the operator $(\delta_t^- + \mathscr{L}_\varepsilon^N)$ on $\Psi(x_i^*, t_n^*)$, we get

$$(\delta_t^- + \mathscr{L}_\varepsilon^N)\Psi(x_i^*, t_n^*) = \delta_t^-\Psi(x_i^*, t_n^*) - \varepsilon\delta_x^2\Psi(x_i^*, t_n^*) + a(x_i^*)\delta_x^-\Psi(x_i^*, t_n^*) + b(x_i^*, t_n^*)\Psi(x_i^*, t_n^*).$$

Since, we have $\Psi(x_i^*, t_n^*) - \Psi(x_i^*, t_{n-1}^*) < 0$, $\Psi(x_i^*, t_n^*) - \Psi(x_{i-1}^*, t_n^*) < 0$ and $\Psi(x_{i+1}^*, t_n^*) - \Psi(x_i^*, t_n^*) > 0$, therefore

$$(\delta_t^- + \mathscr{L}_\varepsilon^N)\Psi(x_i^*, t_n^*) < 0,$$

which is a contradiction as $(\delta_t^- + \mathscr{L}_\varepsilon^N)\Psi(x_i, t_n) \geq 0$, for all $(x_i, t_n) \in D^{N,M}$. Hence $\Psi(x_i, t_n) \geq 0$, for all $(x_i, t_n) \in \overline{D}^{N,M}$. ∎

3.2.3 Error estimate for the difference scheme (3.2.2)

The following theorem explains that the upwind scheme defined in (3.2.2), converges ε-uniformly on the Shishkin mesh $D^{N,M}$, with almost first-order accuracy.

Theorem 3.2.2. *Let u and U be respectively the continuous and the numerical solutions of (3.1.1) and (3.2.2). Then, we have the following error bound for $(x_i, t_n) \in D^{N,M}$*

$$\max_{i,n} |(u - U)(x_i, t_n)| \leq C(N^{-1}\ln N + \Delta t), \quad \text{for} \quad 1 \leq i \leq N-1,$$

where $U(x_i, t_n) = U_i^n$.

Proof. The proof of the theorem is given in [32]. ∎

From the theorem stated above, one can see that the spatial order of convergence is almost one (up to a logarithmic factor) and the temporal order of convergence is one. In this chapter, our main goal is to apply the Richardson extrapolation technique on the discrete solution U_i^n of the problem (3.2.2) to attain second-order ε-uniform convergence with respect to both the spatial and temporal variables of the DPDE (3.1.1).

3.3 Richardson Extrapolation Technique

We now describe the Richardson extrapolation technique, which is used to increase the accuracy of the computed solutions of the basic scheme. To apply this technique, we will solve the discrete problem (3.2.2) on the fine mesh $\overline{D}^{2N,2M} = \overline{\Omega}_x^{2N} \times \Lambda_t^{2M}$ with $2N$ mesh-intervals in the spatial direction and $2M$ mesh-intervals in the temporal direction, where $\overline{\Omega}_x^{2N}$ is the piecewise-uniform Shishkin mesh having the same transition point $1-\rho$ as used in $\overline{\Omega}_x^N$. In fact, the discrete domain $\overline{\Omega}_x^{2N}$ can be obtained through bisecting each mesh-interval of $\overline{\Omega}_x^N$. From such construction, it is clear that $\overline{D}^{N,M} = \{(x_i, t_n)\} \subset \overline{D}^{2N,2M} = \{(\widetilde{x}_i, \widetilde{t}_n)\}$. Hence the corresponding spatial mesh-sizes in $\overline{D}^{2N,2M}$ can be given by

$$\widetilde{x}_i - \widetilde{x}_{i-1} = \begin{cases} H/2, & \text{for} \quad \widetilde{x}_i \in \overline{\Omega}_x^{2N} \cap [0, 1-\rho], \\ h/2, & \text{for} \quad \widetilde{x}_i \in \overline{\Omega}_x^{2N} \cap [1-\rho, 1], \end{cases}$$

and $\widetilde{t}_n - \widetilde{t}_{n-1} = \Delta t/2$, for $\widetilde{t}_n \in \Lambda_t^{2M}$.

Let $U(x_i, t_n)$ be the numerical solution of the discrete problem (3.2.2) on $\overline{D}^{N,M}$. Therefore, from Theorem 3.2.2, one can express the error as

$$\begin{aligned} U(x_i,t_n) - u(x_i,t_n) &= C\left(N^{-1}\ln N + \Delta t\right) + o(N^{-1}\ln N + \Delta t) \\ &= C(N^{-1}\left(\rho/\rho_0\varepsilon\right) + \Delta t\big) + o(N^{-1}\ln N + \Delta t), \quad (x_i,t_n) \in \overline{D}^{N,M}, \end{aligned} \tag{3.3.1}$$

where C is a fixed constant. Similarly, if $\widetilde{U}(\widetilde{x}_i, \widetilde{t}_n)$ is the solution of the discrete problem (3.2.2) on $\overline{D}^{2N,2M}$, then

$$\widetilde{U}(\widetilde{x}_i,\widetilde{t}_n) - u(\widetilde{x}_i,\widetilde{t}_n) = C\left((2N)^{-1}(\rho/\rho_0\varepsilon) + (\Delta t/2)\right) + o(N^{-1}\ln N + \Delta t), \ (\widetilde{x}_i,\widetilde{t}_n) \in \overline{D}^{2N,2M}, \tag{3.3.2}$$

by considering the fact that $\widetilde{U}(\widetilde{x}_i, \widetilde{t}_n)$ is obtained by using the same transition point $1-\rho$. Now from (3.3.1) and (3.3.2), eliminating the terms of $O(N^{-1})$ and $O(\Delta t)$, we get

$$u(x_i,t_n) - \left(2\widetilde{U}(x_i,t_n) - U(x_i,t_n)\right) = o(N^{-1}\ln N + \Delta t), \quad (x_i,t_n) \in \overline{D}^{N,M}.$$

We shall therefore use the following extrapolation formula

$$U_{extp}(x_i,t_n) = 2\widetilde{U}(x_i,t_n) - U(x_i,t_n), \quad (x_i,t_n) \in \overline{D}^{N,M}, \tag{3.3.3}$$

to obtain a better approximate numerical solution to the DPDE (3.1.1).

3.3.1 Error estimate for the extrapolated solution (3.3.3)

The section provides the ε-uniform error estimate of the numerical solution after the extrapolation technique. The main result of this chapter for the ε-uniform convergence of the numerical solution is given at the end of this section.

The following theorem provides the error bounds, when $t \in [0, \tau]$.

Theorem 3.3.1. *(Error after extrapolation in $D_1^{N,M}$) Assume that $\varepsilon \le N^{-1}$. Let u be the solution of the continuous problem (3.1.1) and U_{extp} be the solution obtained via the Richardson extrapolation technique (3.3.3) by solving the discrete problem (3.2.2) on two nested meshes $D_1^{N,M}$ and $D_1^{2N,2M}$. Then, we have the following error bound associated with U_{extp}:*

$$\|u(x_i,t_n) - U_{extp}(x_i,t_n)\|_\infty \le C\left(N^{-2}\ln^2 N + \Delta t^2\right), \quad \text{for } (x_i,t_n) \in D_1^{N,M}.$$

Proof. We know in the first interval $[0, \tau]$, *i.e.,* where the time discretization parameter n varies from 0 to p, the initial conditions of *IBVPs* (3.1.1) and (3.2.2) will be same.

So, the analysis can be carried out in the same way as one can do for a non-delay problem. Therefore, for $(x_i, t_n) \in D_1^{N,M}$, we can adapt the proof of convergence of the extrapolation technique as given in [66], that is, we can have the following error bound:

$$\|u(x_i,t_n) - U_{extp}(x_i,t_n)\|_\infty \leq C\left(N^{-2}\ln^2 N + \Delta t^2\right), \quad \text{for } (x_i,t_n) \in D_1^{N,M}. \qquad \blacksquare$$

On the second interval $[\tau, 2\tau]$, the approach of [66] is not applicable due to the fact that the value of the delay term present in the right hand side of (3.2.2) will be the numerical solution obtained in previous time interval $[0, \tau]$. Therefore, we will do the detailed analysis to get the error over the interval $[\tau, 2\tau]$.

On the domain $D_2 = \Omega_x \times (\tau, 2\tau)$, we consider the following singularly perturbed delay parabolic PDE:

$$\begin{cases} \left(\dfrac{\partial}{\partial t} + \mathscr{L}_\varepsilon\right) u(x,t) = -c(x,t)u(x,t-\tau) + f(x,t), & (x,t) \in D_2, \\ u(x,t) = u_\tau(x,t), \qquad (x,t) \in \overline{D}_1 = \overline{\Omega}_x \times [0,\tau], \\ u(0,t) = \phi_l(t), \quad u(1,t) = \phi_r(t), \quad t \in [\tau, 2\tau], \end{cases} \tag{3.3.4}$$

where $u_\tau(x,t)$ is the exact solution on D_1.

To discretize the DPDE (3.3.4), we apply the difference scheme as given in (3.2.2). Hence in the domain $(x_i, t_n) \in D_2^{N,M}$, the discrete problem corresponding to (3.3.4) becomes

$$\begin{cases} \delta_t^- U_i^n - \varepsilon\delta_x^2 U_i^n + a_i\delta_x^- U_i^n + b_{i,n}U_i^n = -c_{i,n}U_i^{n-p} + f(x_i,t_n), & (x_i,t_n) \in D_2^{N,M}, \\ U_0^n = \phi_l(t_n), \qquad U_N^n = \phi_r(t_n), \qquad t_n \in \Lambda_{2,t}^p, \\ U_i^n = U_1(x_i,t_n), \qquad (x_i,t_n) \in \overline{D}_1^{N,M}, \end{cases} \tag{3.3.5}$$

where $U_1(\cdot,\cdot)$ is the numerical solution calculated on $D_1^{N,M}$.

The solution u of (3.3.4) is decomposed into the smooth and singular components as $u = y + z$. Since $D_2 \subset D$, the estimates given in Theorem 2.2.4, can be used for both y and z. The smooth component y is further decomposed into $y = y_0 + \varepsilon y_1$, where y_0 and y_1 are the solutions of the following problems:

$$\begin{cases} \dfrac{\partial y_0}{\partial t}(x,t) + a(x)\dfrac{\partial y_0}{\partial x}(x,t) + b(x,t)y_0(x,t) = -c(x,t)y_0(x,t-\tau) + f(x,t), & (x,t) \in D_2, \\ y_0(x,t) = u_\tau(x,t), \qquad (x,t) \in \overline{D}_1, \\ y_0(0,t) = u(0,t), \qquad t \in [\tau, 2\tau], \end{cases}$$

and

$$\begin{cases} \left(\dfrac{\partial}{\partial t}+\mathscr{L}_\varepsilon\right) y_1(x,t) = -c(x,t)y_1(x,t-\tau)+\dfrac{\partial^2 y_0}{\partial x^2}(x,t), & (x,t)\in D_2,\\ y_1(x,t)=0, \qquad (x,t)\in \overline{D}_1,\\ y_1(0,t)=y_1(1,t)=0, \qquad t\in[\tau,2\tau]. \end{cases}$$

Therefore, y satisfies the following problem:

$$\begin{cases} \left(\dfrac{\partial}{\partial t}+\mathscr{L}_\varepsilon\right) y(x,t) = -c(x,t)y(x,t-\tau)+f(x,t), & (x,t)\in D_2,\\ y(x,t)=u_\tau(x,t), \qquad (x,t)\in \overline{D}_1,\\ y(0,t)=y_0(0,t), \qquad y(1,t)=y_0(1,t), \qquad t\in[\tau,2\tau]. \end{cases} \tag{3.3.6}$$

Then, the singular component z satisfies

$$\begin{cases} \left(\dfrac{\partial}{\partial t}+\mathscr{L}_\varepsilon\right) z(x,t) = -c(x,t)z(x,t-\tau), & (x,t)\in D_2,\\ z(x,t)=0, \qquad (x,t)\in \overline{D}_1,\\ z(0,t)=\phi_l(t)-y_0(0,t), \qquad z(1,t)=\phi_r(t)-y_0(1,t), \qquad t\in[\tau,2\tau]. \end{cases} \tag{3.3.7}$$

In a similar way, the numerical solution U of (3.3.5) can be decomposed into the smooth and singular components Y and Z, respectively. Thus,

$$U = Y + Z,$$

where Y is the solution of the following nonhomogeneous problem:

$$\begin{cases} (\delta_t^- + \mathscr{L}_\varepsilon^N)Y_i^n = -c_{i,n}Y(x_i,t_{n-p})+f(x_i,t_n), & (x_i,t_n)\in D_2^{N,M},\\ Y_i^n = U_1(x_i,t_n), \qquad (x_i,t_n)\in \overline{D}_1^{N,M},\\ Y_0^n = y(0,t_n), \qquad Y_N^n = y(1,t_n), \qquad t_n\in\Lambda_{2,t}^p, \end{cases} \tag{3.3.8}$$

and therefore, Z satisfies

$$\begin{cases} (\delta_t^- + \mathscr{L}_\varepsilon^N)Z_i^n = -c_{i,n}Z(x_i,t_{n-p}), & (x_i,t_n)\in D_2^{N,M},\\ Z_i^n = 0, \qquad (x_i,t_n)\in \overline{D}_1^{N,M},\\ Z_0^n = \phi_l(t_n)-y(0,t_n), \qquad Z_N^n = \phi_r(t_n)-y(1,t_n), \qquad t_n\in\Lambda_{2,t}^p. \end{cases} \tag{3.3.9}$$

Similarly, the solution $\widetilde{U}$, can be decomposed into the smooth and singular components $\widetilde{Y}$ and $\widetilde{Z}$, respectively, on the fine mesh $D^{2N,2M}$, *i.e.*,

$$\widetilde{U} = \widetilde{Y} + \widetilde{Z}.$$

Therefore at the node (x_i,t_n) the errors can be written in the form $(U-u)(x_i,t_n) = (Y-y)(x_i,t_n)+(Z-z)(x_i,t_n)$ and $(\widetilde{U}-u)(x_i,t_n) = (\widetilde{Y}-y)(x_i,t_n)+(\widetilde{Z}-z)(x_i,t_n)$.

3.3.2 Error estimate for the smooth component Y

Lemma 3.3.2. *Assume that $\varepsilon \leq N^{-1}$. Then the local truncation error in $D_2^{N,M}$ associated to the smooth component satisfies*

$$(\delta_t^- + \mathscr{L}_\varepsilon^N)(Y-y)(x_i,t_n) = C(N^{-1}\ln N + \Delta t) + h_i \frac{1}{2}a(x_i)\frac{\partial^2 y}{\partial x^2}(x_i,t_n) + \Delta t \frac{1}{2}\frac{\partial^2 y}{\partial t^2}(x_i,t_n) + O(H^2+\Delta t^2).$$

Proof. The local truncation error of the smooth component can be written as

$$\left(\delta_t^- + \mathscr{L}_\varepsilon^N\right)(Y-y) = c_{i,n}\left(y(x_i,t_{n-p}) - Y(x_i,t_{n-p})\right) + \left(\left(\frac{\partial}{\partial t} + \mathscr{L}_\varepsilon\right) - \left(\delta_t^- + \mathscr{L}_\varepsilon^N\right)\right) y.$$

Using the initial conditions from (3.3.6) and (3.3.8), we get

$$(\delta_t^- + \mathscr{L}_\varepsilon^N)(Y-y) = \ c_{i,n}(u_\tau(x_i,t_{n-p}) - U_1(x_i,t_{n-p})) + \left(\left(\frac{\partial}{\partial t} + \mathscr{L}_\varepsilon\right) - \left(\delta_t^- + \mathscr{L}_\varepsilon^N\right)\right) y.$$

Now, by using the error estimates given in Theorem 3.2.2 and the Taylor's expansion, we obtain

$$\begin{aligned}(\delta_t^- + \mathscr{L}_\varepsilon^N)(Y-y) = \ & C(N^{-1}\ln N + \Delta t) + \frac{\varepsilon}{3\widehat{h}_i}\left[h_{i+1}^2\frac{\partial^3 y}{\partial x^3}(\kappa_1,\, t_n) - h_i^2\frac{\partial^3 y}{\partial x^3}(\kappa_2,\, t_n)\right] \\ & + \frac{h_i}{2}a(x_i)\frac{\partial^2 y}{\partial x^2}(x_i,\, t_n) - \frac{h_i^2}{3!}a(x_i)\frac{\partial^3 y}{\partial x^3}(\kappa_3,\, t_n) + \frac{\Delta t}{2}\frac{\partial^2 y}{\partial t^2}(x_i,\, t_n) \\ & - \frac{\Delta t^2}{3!}\frac{\partial^3 y}{\partial t^3}(x_i,\, \widetilde{t}),\end{aligned}$$

where $\kappa_1 \in (x_i,\, x_{i+1})$, $\kappa_2,\, \kappa_3 \in (x_{i-1},\, x_i)$ and $\widetilde{t} \in (t_{n-1},\, t_n)$.

Finally, applying the bounds on the derivatives of y given in Theorem 2.2.4, along with the fact $\varepsilon \leq N^{-1} \leq H$, one can get the required result. ∎

Following the classical approach of Keller [40], define the functions ξ_k, $k = 1, 2$, to be the solutions of the following IBVPs:

$$\begin{cases} \left(\dfrac{\partial}{\partial t} + \mathscr{L}_\varepsilon\right)\xi_1 = \dfrac{1}{2}a(x)\dfrac{\partial^2 y}{\partial x^2}(x,t), \text{ in } D, \\ \xi_1(x,t) = 0, \quad (x,t) \in \Gamma_b, \\ \xi_1(0,t) = \xi_1(1,t) = 0, \quad t \in \Lambda_t, \end{cases} \quad \text{and} \quad \begin{cases} \left(\dfrac{\partial}{\partial t} + \mathscr{L}_\varepsilon\right)\xi_2 = \dfrac{1}{2}\dfrac{\partial^2 y}{\partial t^2}(x,t), \text{ in } D, \\ \xi_2(x,t) = 0, \quad (x,t) \in \Gamma_b, \\ \xi_2(0,t) = \xi_2(1,t) = 0, \quad t \in \Lambda_t. \end{cases} \tag{3.3.10}$$

From Theorem 2.2.4, we obtain that the right hand side terms of the above equations are ε-uniformly bounded. Therefore the above equations are similar to (3.1.1).

We again decompose ξ_k as $\xi_k = \phi_k + \psi_k$, $k = 1, 2$, where ϕ_k is the smooth component and ψ_k is the singular component satisfying the following bounds:

$$\left\| \frac{\partial^{l+m}\phi_k}{\partial x^l \partial t^m} \right\|_\infty \leq C\left(1 + \varepsilon^{2-l}\right), \quad \left| \frac{\partial^{l+m}\psi_k}{\partial x^l \partial t^m} \right| \leq C\varepsilon^{-l}\exp(-\alpha(1-x)/\varepsilon),$$

on D, for $0 \leq l + m \leq 3$, which can be obtained in an analogous way, as discussed in Theorem 2.2.4.

Since, in this context, we are considering $(x, t) \in D_2$, therefore (3.3.10) reduces to the following IBVPs:

$$\begin{cases} \left(\dfrac{\partial}{\partial t} + \mathscr{L}_\varepsilon\right)\xi_1 = \dfrac{1}{2}a(x)\dfrac{\partial^2 y}{\partial x^2}(x,t), \text{ in } D_2, \\ \xi_1(x,t) = \xi_{1_\tau}(x,t), \quad (x,t) \in \overline{D}_1, \\ \xi_1(0,t) = \xi_1(1,t) = 0, \quad t \in [\tau, 2\tau], \end{cases} \text{ and } \begin{cases} \left(\dfrac{\partial}{\partial t} + \mathscr{L}_\varepsilon\right)\xi_2 = \dfrac{1}{2}\dfrac{\partial^2 y}{\partial t^2}(x,t), \text{ in } D_2, \\ \xi_2(x,t) = \xi_{2_\tau}(x,t), \quad (x,t) \in \overline{D}_1, \\ \xi_2(0,t) = \xi_2(1,t) = 0, \quad t \in [\tau, 2\tau], \end{cases}$$

where $\xi_{1_\tau}(\cdot,\cdot)$ and $\xi_{2_\tau}(\cdot,\cdot)$ are the respective exact solutions in D_1.

Therefore, the components ϕ_k and ψ_k, $k = 1, 2$, satisfy the following IBVPs

$$\begin{cases} \left(\dfrac{\partial}{\partial t} + \mathscr{L}_\varepsilon\right)\phi_1 = \dfrac{1}{2}a(x)\dfrac{\partial^2 y}{\partial x^2}(x,t), \left(\dfrac{\partial}{\partial t} + \mathscr{L}_\varepsilon\right)\phi_2 = \dfrac{1}{2}\dfrac{\partial^2 y}{\partial t^2}(x,t), \quad (x,t) \in D_2, \\ \left(\dfrac{\partial}{\partial t} + \mathscr{L}_\varepsilon\right)\psi_k = 0, \\ \phi_1(x,t) = \xi_{1_\tau}(x,t),\ \psi_1(x,t) = 0,\ \phi_2(x,t) = \xi_{2_\tau}(x,t),\ \psi_2(x,t) = 0, \quad (x,t) \in \overline{D}_1, \\ \phi_k(0,t) = \psi_k(0,t) = 0, \quad t \in [\tau, 2\tau], \\ \phi_k(1,t) = -\psi_k(1,t), \quad t \in [\tau, 2\tau]. \end{cases} \tag{3.3.11}$$

Lemma 3.3.3. *Assume that $\varepsilon \leq N^{-1}$. Then, for all $(x_i, t_n) \in D_2^{N,M}$, we have*

$$(Y - y)(x_i, t_n) = C\left(N^{-1}\ln N + \Delta t\right) + h_i\phi_1(x_i, t_n) + \Delta t\phi_2(x_i,\, t_n) + \ O\left(H^2 + \Delta t^2\right).$$

Proof. From Lemma 3.3.2 and (3.3.11), one can easily obtain that

$$\begin{aligned} &(\delta_t^- + \mathscr{L}_\varepsilon^N)(Y - y)(x_i, t_n) \\ &= C\left(N^{-1}\ln N + \Delta t\right) + h_i\left(\left(\frac{\partial}{\partial t} + \mathscr{L}_\varepsilon\right) - \left(\delta_t^- + \mathscr{L}_\varepsilon^N\right)\right)\phi_1(x_i, t_n) \\ &\quad + h_i\left(\delta_t^- + \mathscr{L}_\varepsilon^N\right)\phi_1(x_i, t_n) + \Delta t\left(\left(\frac{\partial}{\partial t} + \mathscr{L}_\varepsilon\right) - \left(\delta_t^- + \mathscr{L}_\varepsilon^N\right)\right)\phi_2(x_i,\, t_n) \\ &\quad + \Delta t\left(\delta_t^- + \mathscr{L}_\varepsilon^N\right)\phi_2(x_i,\, t_n) + O\left(H^2 + \Delta t^2\right). \end{aligned} \tag{3.3.12}$$

From the Taylor's expansion it follows that for $k = 1,\ 2$, we have

$$\left|\left(\left(\frac{\partial}{\partial t} + \mathscr{L}_\varepsilon\right) - \left(\delta_t^- + \mathscr{L}_\varepsilon^N\right)\right)\phi_k(x_i, t_n)\right|$$
$$\leq \left[\frac{\varepsilon}{3}\,(h_i + h_{i+1})\,\left\|\frac{\partial^3\phi_k}{\partial x^3}\right\|_\infty + \frac{h_i}{2}\,a(x_i)\,\left\|\frac{\partial^2\phi_k}{\partial x^2}\right\|_\infty + \frac{\Delta t}{2}\,\left\|\frac{\partial^2\phi_k}{\partial t^2}\right\|_\infty\right].$$

Again, by using the bounds for the derivatives of ϕ_k and the inequality $h_i \leq H$ for all i, we have

$$\left|h_i\left(\left(\frac{\partial}{\partial t} + \mathscr{L}_\varepsilon\right) - \left(\delta_t^- + \mathscr{L}_\varepsilon^N\right)\right)\phi_1(x_i,\, t_n) + \Delta t\left(\left(\frac{\partial}{\partial t} + \mathscr{L}_\varepsilon\right) - \left(\delta_t^- + \mathscr{L}_\varepsilon^N\right)\right)\phi_2(x_i,\, t_n)\right|$$

$$\leq C\left(H^2 + H\Delta t + \Delta t^2\right)$$

$$\leq C\left(H^2 + \Delta t^2\right). \tag{3.3.13}$$

Therefore, from (3.3.12) and (3.3.13), we get

$$\left|(\delta_t^- + \mathscr{L}_\varepsilon^N)(Y - y - h_i\phi_1 - \Delta t\phi_2)(x_i, t_n)\right| \leq C\left(N^{-1}\ln N + \Delta t + H^2 + \Delta t^2\right).$$

Now, we define two discrete functions $\theta^\pm$ as

$$\theta^\pm(x_i,\, t_n) = C\left(N^{-2} + \Delta t^2\right)(1 + x_i) \pm \varrho(x_i,\, t_n), \quad \text{for } 0 \leq i \leq N,$$

where

$$\varrho(x_i,\, t_n) = \begin{cases} \left(Y - y - h_i\phi_1 - \Delta t\phi_2\right)(x_i,\, t_n), & \text{for } 1 \leq i \leq N-1, \\ 0, & \text{for } i = 0,\ N. \end{cases}$$

Now, by applying the discrete maximum principle (Lemma 3.2.1), we obtain

$$\left|\left(Y - y - h_i\phi_1 - \Delta t\phi_2\right)(x_i,\, t_n)\right| \leq C(N^{-1}\ln N + \Delta t + N^{-2} + \Delta t^2), \quad \text{for } 1 \leq i \leq N-1,$$

and hence the required result follows. ∎

Lemma 3.3.4. *The error associated to the smooth component Y after extrapolation satisfies the following bound:*

$$\left|(y - Y_{extp})(x_i,\, t_n)\right| \leq C(N^{-2} + \Delta t^2), \quad \textit{for } (x_i, t_n) \in D_2^{N,M}.$$

Proof. By using $\rho = \rho_0\varepsilon\ln N$ in Lemma 3.3.3, we get

$$(Y - y)(x_i, t_n) = C\left(N^{-1}\left(\rho/\rho_0\varepsilon\right) + \Delta t\right) + h_i\phi_1(x_i, t_n) + \Delta t\phi_2(x_i,\, t_n) + \ O\left(H^2 + \Delta t^2\right). \tag{3.3.14}$$

Therefore, on the fine mesh $\overline{D}_2^{2N,2M}$, we have

$$\left(\widetilde{Y}-y\right)(x_i,\,t_n)=\begin{cases} C\left((2N)^{-1}\left(\rho/\rho_0\varepsilon\right)+(\Delta t/2)\right)+(H/2)\phi_1(x_i,\,t_n) \\ \qquad +(\Delta t/2)\phi_2(x_i,\,t_n)+O\left(N^{-2}+\Delta t^2\right), \quad \text{for } \ 1\le i\le N/2, \\ C\left((2N)^{-1}\left(\rho/\rho_0\varepsilon\right)+(\Delta t/2)\right)+(h/2)\phi_1(x_i,\,t_n) \\ \qquad +(\Delta t/2)\phi_2(x_i,\,t_n)+O\left(N^{-2}+\Delta t^2\right), \\ \qquad\qquad \text{for } \ N/2+1\le i\le N-1. \end{cases} \tag{3.3.15}$$

From the extrapolation formula (3.3.3), one can write

$$\begin{aligned} y(x_i,t_n)-Y_{extp}(x_i,t_n) &= y(x_i,t_n)-\left(2\widetilde{Y}(x_i,t_n)-Y(x_i,t_n)\right) \\ &= -2\left(\widetilde{Y}-y\right)(x_i,t_n)+(Y-y)(x_i,t_n). \end{aligned}$$

For $1\le i\le N/2$, by using (3.3.14) and (3.3.15), we get

$$\begin{aligned} -2\left(\widetilde{Y}-y\right)(x_i,t_n)+(Y-y)(x_i,t_n) &= -C\left(N^{-1}\left(\rho/\rho_0\varepsilon\right)+\Delta t\right)-H\phi_1(x_i,t_n) \\ &\quad -\Delta t\phi_2(x_i,t_n)+C\left(N^{-1}\left(\rho/\rho_0\varepsilon\right)+\Delta t\right) \\ &\quad +H\phi_1(x_i,t_n)+\Delta t\phi_2(x_i,t_n)+O(N^{-2}+\Delta t^2) \\ &= O(N^{-2}+\Delta t^2). \end{aligned}$$

Therefore, we have $y(x_i,t_n)-Y_{extp}(x_i,t_n)=O(N^{-2}+\Delta t^2)$. For $N/2+1\le i\le N-1$, approaching in the similar way as done above, we will get $y(x_i,t_n)-Y_{extp}(x_i,t_n)=O(N^{-2}+\Delta t^2)$. Hence, the desired result follows. ∎

3.3.3 Error estimate for the singular component Z

Lemma 3.3.5. *The local truncation error associated to the singular component satisfies*

$$|Z_{extp}(x_i,\,t_n)-z(x_i,\,t_n)|\le CN^{-2}, \quad \textit{for } \ 1\le i\le N/2.$$

Proof. From the bound given in Theorem 2.2.4, we get

$$\begin{aligned} |z(x_i,\,t_n)| &\le C\exp(-\alpha(1-x_i)/\varepsilon) \\ &\le C\exp(-\alpha(1-(1-\rho))/\varepsilon) \\ &= C\exp(-\alpha\rho/\varepsilon). \end{aligned}$$

Since, $\rho\ge(2\varepsilon/\alpha)\ln N$, we get $|z(x_i,\,t_n)|\le CN^{-2}$.

To find the bound of $Z(x_i,\, t_n)$, for a fixed time level t_n, we consider a barrier function

$$\wp(x_i) = C\left[\prod_{j=1}^{N}\left(1+\frac{\alpha h_j}{\varepsilon}\right)^{-1}\right]\prod_{j=1}^{i}\left(1+\frac{\alpha h_j}{\varepsilon}\right).$$

Now, by following the similar approach as used in [89], we can obtain $|Z(x_i,\, t_n)| \le CN^{-2}$.

Therefore, we have $|Z(x_i,\, t_n) - z(x_i,\, t_n)| \le CN^{-2}$.

In a similar way, we can get $\left|\widetilde{Z}(x_i,\, t_n) - z(x_i,\, t_n)\right| \le CN^{-2}$. Hence, from the extrapolation formula (3.3.3), we can obtain the required bound. ∎

To analyze the effect of the extrapolation technique in the boundary layer region $[1-\rho, 1]$, we define the function λ_k, $k = 1,\, 2$, on $[1-\rho, 1]$ by the following IBVPs:

$$\begin{cases} \left(\dfrac{\partial}{\partial t} + \mathscr{L}_\varepsilon\right)\lambda_1 = \rho_0\varepsilon a(x)\dfrac{\partial^2 z}{\partial x^2}(x,\, t), & \left(\dfrac{\partial}{\partial t} + \mathscr{L}_\varepsilon\right)\lambda_2 = \dfrac{1}{2}\dfrac{\partial^2 z}{\partial t^2}(x,\, t), \\ & (x,t) \in D_r = (1-\rho, 1)\times\Lambda_t, \\ \lambda_k(x,\, t) = 0, \quad (x,\, t) \in [1-\rho, 1]\times[-\tau, 0], \\ \lambda_k(1-\rho,\, t) = \lambda_k(1,\, t) = 0, \quad t \in \Lambda_t. \end{cases} \tag{3.3.16}$$

Lemma 3.3.6. *The solutions λ_k, $k = 1,\, 2$, of (3.3.16) satisfy the following bounds:*

$$\left|\frac{\partial^{l+m}\lambda_k}{\partial x^l \partial t^m}\right| \le C\varepsilon^{-l}\exp(-\alpha(1-x)/\varepsilon), \quad (x,t) \in D,$$

for all non-negative integers l, m, where $0 \le l+m \le 3$.

Proof. Employing the similar idea used in the proof of Theorem 2.2.4, along with the bounds of the derivatives of the singular component given there, one can get the required bound. ∎

Here, we are considering $t \in (\tau,\, 2\tau)$, therefore (3.3.16) reduces to the following IBVPs:

$$\begin{cases} \left(\dfrac{\partial}{\partial t} + \mathscr{L}_\varepsilon\right)\lambda_1 = \rho_0\varepsilon a(x)\dfrac{\partial^2 z}{\partial x^2}(x,\, t), & \left(\dfrac{\partial}{\partial t} + \mathscr{L}_\varepsilon\right)\lambda_2 = \dfrac{1}{2}\dfrac{\partial^2 z}{\partial t^2}(x,\, t), \\ & (x,\, t) \in D_{r_2} = (1-\rho, 1)\times(\tau,\, 2\tau), \\ \lambda_k(x,\, t) = \lambda_{k_\tau}(x,t), & (x,\, t) \in \overline{D}_{r_1} = [1-\rho, 1]\times[0, \tau], \\ \lambda_k(1-\rho,\, t) = \lambda_k(1,\, t) = 0, & t \in (\tau,\, 2\tau), \end{cases} \tag{3.3.17}$$

where $\lambda_{k_\tau}(\cdot,\cdot)$, $k = 1,\, 2$, are the exact solutions in D_{r_1}.

Lemma 3.3.7. *For $N/2+1 \le i \le N-1$ and $t_n \in \Lambda^p_{2,t}$, the error associated to the singular component Z satisfies*

$$(Z-z)(x_i,\, t_n) = \; (N^{-1}\ln N)\,\lambda_1(x_i, t_n) + \Delta t\lambda_2(x_i,\, t_n) + O\left(N^{-2}\ln^2 N + \Delta t^2\right).$$

Proof. From the IBVP (3.3.7) and the difference equation (3.3.9), we obtain the truncation error as

$$(\delta_t^- + \mathscr{L}_\varepsilon^N)(Z-z)(x_i,\, t_n) = \; c_{i,n}\,(z(x_i,t_{n-p}) - Z(x_i,t_{n-p})) + \left(\left(\frac{\partial}{\partial t} + \mathscr{L}_\varepsilon\right) - \left(\delta_t^- + \mathscr{L}_\varepsilon^N\right)\right) z.$$

Using the initial conditions from the equations (3.3.7) and (3.3.9), we get that

$$(\delta_t^- + \mathscr{L}_\varepsilon^N)(Z-z)(x_i,\, t_n) = \left(\left(\frac{\partial}{\partial t} + \mathscr{L}_\varepsilon\right) - \left(\delta_t^- + \mathscr{L}_\varepsilon^N\right)\right) z.$$

Therefore, from the Taylor's expansion, for some $\kappa_1 \in (x_i,\, x_{i+1})$, $\kappa_2,\, \kappa_3 \in (x_{i-1},\, x_i)$ and $\widetilde{t} \in (t_{n-1},\, t_n)$, one can have

$$\begin{aligned}(\delta_t^- + \mathscr{L}_\varepsilon^N)(Z-z)(x_i,\, t_n) \;&= \frac{\varepsilon h^2}{4!}\left[\frac{\partial^4 z}{\partial x^4}(\kappa_1,\, t_n) + \frac{\partial^4 z}{\partial x^4}(\kappa_2,\, t_n)\right] + \frac{h}{2}a(x_i)\frac{\partial^2 z}{\partial x^2}(x_i,\, t_n)\\ &\quad - \frac{h^2}{3!}a(x_i)\frac{\partial^3 z}{\partial x^3}(\kappa_3,\, t_n) + \frac{\Delta t}{2}\frac{\partial^2 z}{\partial t^2}(x_i,\, t_n) - \frac{\Delta t^2}{3!}\frac{\partial^3 z}{\partial t^3}(x_i,\, \widetilde{t}).\end{aligned}$$

Now, using the result of Theorem 2.2.4, we get that

$$\begin{aligned}(\delta_t^- + \mathscr{L}_\varepsilon^N)(Z-z)(x_i,\, t_n) \;&= \rho_0 \varepsilon N^{-1}\ln N a(x_i)\frac{\partial^2 z}{\partial x^2}(x_i,\, t_n) + \frac{\Delta t}{2}\frac{\partial^2 z}{\partial t^2}(x_i,\, t_n)\\ &\quad + O\left(\varepsilon^{-1}\exp(-\alpha(1-x_{i+1})/\varepsilon)N^{-2}\ln^2 N\right.\\ &\quad \left. + \exp(-\alpha(1-x_i)/\varepsilon)\Delta t^2\right).\end{aligned}$$

Therefore, from (3.3.17) one can write the above equation as follows:

$$\begin{aligned}(\delta_t^- + \mathscr{L}_\varepsilon^N)(Z-z)(x_i,\, t_n) \;&= N^{-1}\ln N\left(\frac{\partial}{\partial t} + \mathscr{L}_\varepsilon\right)\lambda_1 + \Delta t\left(\frac{\partial}{\partial t} + \mathscr{L}_\varepsilon\right)\lambda_2\\ &\quad + O\left(\varepsilon^{-1}\exp(-\alpha(1-x_{i+1})/\varepsilon)N^{-2}\ln^2 N\right.\\ &\quad \left. + \exp(-\alpha(1-x_i)/\varepsilon)\Delta t^2\right).\end{aligned} \tag{3.3.18}$$

Now, from the Taylor's expansion and Lemma 3.3.6, we obtain that

$$\begin{aligned}\left(\left(\frac{\partial}{\partial t} + \mathscr{L}_\varepsilon\right) - \left(\delta_t^- + \mathscr{L}_\varepsilon^N\right)\right)\lambda_k(x_i,t_n) = \; &O(\varepsilon^{-1}\exp(-\alpha(1-x_{i+1})/\varepsilon)N^{-1}\ln N\\ &+ \exp(-\alpha(1-x_i)/\varepsilon)\Delta t).\end{aligned} \tag{3.3.19}$$

Therefore, using (3.3.19), we get that

$$\begin{aligned}&\left|N^{-1}\ln N\left(\left(\frac{\partial}{\partial t} + \mathscr{L}_\varepsilon\right) - \left(\delta_t^- + \mathscr{L}_\varepsilon^N\right)\right)\lambda_1 + \Delta t\left(\left(\frac{\partial}{\partial t} + \mathscr{L}_\varepsilon\right) - \left(\delta_t^- + \mathscr{L}_\varepsilon^N\right)\right)\lambda_2\right|\\ &\leq C\varepsilon^{-1}\exp(-\alpha(1-x_{i+1})/\varepsilon)\left(N^{-2}\ln^2 N + \Delta t^2\right).\end{aligned} \tag{3.3.20}$$

Hence, from (3.3.18) and (3.3.20), we have

$$\left|(\delta_t^- + \mathscr{L}_\varepsilon^N)(Z - z - (N^{-1}\ln N)\lambda_1 - \Delta t\lambda_2)(x_i, t_n)\right| \leq C\varepsilon^{-1}\exp(-\alpha(1-x_{i+1})/\varepsilon)\left(N^{-2}\ln^2 N + \Delta t^2\right).$$

Now by choosing an appropriate barrier function and applying the discrete maximum principle (Lemma 3.2.1), one can obtain the required result. ∎

Lemma 3.3.8. *The error after extrapolation associated to the singular component Z satisfies the following bound:*

$$|(z - Z_{extp})(x_i, t_n)| \leq C\left(N^{-2}\ln^2 N + \Delta t^2\right), \quad \text{for } N/2+1 \leq i \leq N-1, \text{ and } t_n \in \Lambda_{2,t}^p.$$

Proof. Using the fact $\rho = \rho_0\varepsilon\ln N$ and from Lemma 3.3.7, we get

$$(z - Z)(x_i, t_n) = \left(N^{-1}(\rho/\rho_0\varepsilon)\right)\lambda_1(x_i, t_n) + \Delta t\lambda_2(x_i, t_n) + O\left(N^{-2}\ln^2 N + \Delta t^2\right). \tag{3.3.21}$$

Again, the transition point for the fine mesh $D_2^{2N,2M}$, will remain same as that of $D_2^{N,M}$. So, from Lemma 3.3.7, we get

$$\left(z - \widetilde{Z}\right)(x_i, t_n) = \left((2N)^{-1}(\rho/\rho_0\varepsilon)\right)\lambda_1(x_i, t_n) + (\Delta t/2)\lambda_2(x_i, t_n) + O\left(N^{-2}\ln^2 N + \Delta t^2\right). \tag{3.3.22}$$

Here-after elimination of the terms $O(N^{-1})$ and $O(\Delta t)$ from (3.3.21) and (3.3.22) provides the required result. ∎

Theorem 3.3.9. *(Error after extrapolation in $D_2^{N,M}$) Assume that $\varepsilon \leq N^{-1}$. Let u be the solution of the continuous problem (3.1.1) and U_{extp} be the solution obtained via the Richardson extrapolation technique (3.3.3) by solving the discrete problem (3.2.2) on two meshes $D_2^{N,M}$ and $D_2^{2N,2M}$. Then, we have the following error bound associated with U_{extp}:*

$$\|u(x_i, t_n) - U_{extp}(x_i, t_n)\|_\infty \leq C\left(N^{-2}\ln^2 N + \Delta t^2\right), \quad \text{for } (x_i, t_n) \in D_2^{N,M}.$$

Proof. For each $(x_i, t_n) \in D_2^{N,M}$, we have

$$u(x_i, t_n) - U_{extp}(x_i, t_n) = (y(x_i, t_n) - Y_{extp}(x_i, t_n)) + (z(x_i, t_n) - Z_{extp}(x_i, t_n)).$$

Now, combining the result of Lemma 3.3.4 for the smooth component and Lemmas 3.3.5 and 3.3.8 for the singular component, we can get the required result. ∎

The above theorem provides the convergence result on the interval $[\tau, 2\tau]$. If we proceed in an analogous way, we can achieve the same convergence result for $t > 2\tau$.

The following theorem provides the main result of this chapter, that is, the second-order ε-uniform convergent error estimate for the extrapolated solution (3.3.3).

Theorem 3.3.10. *(Error after extrapolation) Assume that $\varepsilon \leq N^{-1}$. Let u be the solution of the continuous problem (3.1.1) and U_{extp} be the solution obtained via the Richardson extrapolation technique (3.3.3) by solving the discrete problem (3.2.2) on two meshes $D^{N,M}$ and $D^{2N,2M}$. Then we have the following error bound associated with U_{extp}:*

$$\|u(x_i,t_n) - U_{extp}(x_i,t_n)\|_{\infty} \leq C\left(N^{-2}\ln^2 N + \Delta t^2\right), \quad for\,(x_i,t_n) \in D^{N,M}.$$

3.4 Numerical Results

To validate the theoretical result proved in the previous section, here we present the numerical result obtained by the Richardson extrapolation technique for three test problems on the piecewise-uniform rectangular mesh $D^{N,M}$. In all the cases, we perform the numerical experiments by choosing $\rho_0 = 2.2$ and $T = 2$. Moreover in all the tables we begin the computation with $N = 16$, $\Delta t = 0.1$ and $p = 1/\Delta t$ and we multiply N by two and divide Δt by two.

Example 3.4.1. *Consider the following singularly perturbed 1D linear delay parabolic IBVP:*

$$\begin{cases} u_t - \varepsilon u_{xx} + (1 + x(1-x))u_x + (1+\exp(x))u = u(x,t-1) & +f(x,t), \\ & (x,t) \in \Omega_x \times (0,2], \\ u(x,t) = \phi_b(x,t), & (x,t) \in \overline{\Omega}_x \times [-1,0], \\ u(0,t) = 2t/3,\ u(1,t) = t, & t \in [0,2]. \end{cases} \tag{3.4.1}$$

We choose the initial data $\phi_b(x,t)$ and the source function $f(x,t)$ to fit with the exact solution

$$u(x,t) = \exp(-t)\left(C_1 + C_2 x - \exp\left(-(1-x)/\varepsilon\right)\right) + (2x+4)t/6,$$

where $C_1 = \exp(-1/\varepsilon)$ and $C_2 = 1 - \exp(-1/\varepsilon)$.

As the exact solution of the problem (3.4.1) is known, we calculate the maximum pointwise error for each ε by

$$e_{\varepsilon}^{N,\Delta t} = \max_{(x_i,t_n)\in D^{N,M}} |u(x_i,t_n) - U(x_i,t_n)|, \quad (\text{before extrapolation}),$$

and

$$e_{\varepsilon,extp}^{N,\Delta t} = \max_{(x_i,t_n)\in D^{N,M}} |u(x_i,t_n) - U_{extp}(x_i,t_n)|, \quad (\text{after extrapolation}),$$

where $u(x_i, t_n)$, $U(x_i, t_n)$ and $U_{extp}(x_i, t_n)$ denote the exact solution, the numerical solution obtained before extrapolation and the numerical solution obtained after extrapolation in $D^{N,M}$ with N mesh-intervals in the spatial direction and M mesh-intervals in the temporal direction, such that $\Delta t = T/M$ is the uniform mesh-size. We determine the corresponding order of convergence for each ε by

$$p_{\varepsilon}^{N,\Delta t} = \log_2 \left(\frac{e_{\varepsilon}^{N,\Delta t}}{e_{\varepsilon}^{2N,\Delta t/2}} \right), \quad \text{(before extrapolation)},$$

and

$$p_{\varepsilon,\,extp}^{N,\Delta t} = \log_2 \left(\frac{e_{\varepsilon,\,extp}^{N,\Delta t}}{e_{\varepsilon,\,extp}^{2N,\Delta t/2}} \right), \quad \text{(after extrapolation)}.$$

Now, for each N and Δt, we define the ε-uniform maximum pointwise error by

$$e^{N,\Delta t} = \max_{\varepsilon} e_{\varepsilon}^{N,\Delta t}, \quad \text{(before extrapolation)},$$

and

$$e_{extp}^{N,\Delta t} = \max_{\varepsilon} e_{\varepsilon,\,extp}^{N,\Delta t}, \quad \text{(after extrapolation)},$$

and the corresponding ε-uniform order of convergence by

$$p^{N,\Delta t} = \log_2 \left(\frac{e^{N,\Delta t}}{e^{2N,\Delta t/2}} \right), \quad \text{(before extrapolation)},$$

and

$$p_{extp}^{N,\Delta t} = \log_2 \left(\frac{e_{extp}^{N,\Delta t}}{e_{extp}^{2N,\Delta t/2}} \right), \quad \text{(after extrapolation)}.$$

The calculated maximum pointwise errors and the corresponding order of convergence for Example 3.4.1 are presented in Table 3.1 for various values of ε and N. From Table 3.1, we can observe that for fixed ε the maximum pointwise errors computed before and after extrapolation decrease monotonically as N increases, which confirm that the implicit upwind scheme (3.2.2) is ε-uniform convergent. Moreover, one can observe that the maximum pointwise errors and the corresponding order of convergence have been improved after the extrapolation technique.

In order to show the influence of the parameter ρ_0 (appears in the transition point (3.2.1)) in the order of convergence, we have performed some numerical experiments for Example 3.4.1 with different values of ρ_0. These results are given in Table 3.2. From these values, one can notice that when $\rho_0 < 2.2$, the order of convergence is either negative or not reflecting the theoretical estimate given in Theorem 3.3.10. But, only when $\rho_0 \geq 2.2$, we are getting the expected order of convergence. In fact, ρ_0 should satisfy the condition $\rho_0 > 2/\alpha$ as stated in (3.2.1). Since in this case, $\alpha = 1$, therefore, we have chosen $\rho_0 = 2.2$.

Example 3.4.2. *Consider the following singularly perturbed 1D linear delay parabolic IBVP:*

$$\begin{cases} u_t - \varepsilon u_{xx} + (2-x^2)u_x + (x+1)(t+1)u = u(x,t-1) & +10t^2\exp(-t)x(1-x), \\ & (x,t) \in \Omega_x \times (0,2], \\ u(x,t) = 0, & (x,t) \in \overline{\Omega}_x \times [-1,0], \\ u(0,t) = 0,\ u(1,t) = 0, & t \in [0,2]. \end{cases} \tag{3.4.2}$$

As the exact solution of the IBVP (3.4.2) is not known, we have presented the numerical results for Example 3.4.2 by using the double mesh principle, as described in Chapter 2. For each N and Δt, the quantities $E^{N,\Delta t}$, $P^{N,\Delta t}$, $E^{N,\Delta t}_{extp}$ and $P^{N,\Delta t}_{extp}$ are defined in a similar way as done in the previous example. In Table 3.3, we have displayed the maximum pointwise errors (before and after extrapolation) and the corresponding order of convergence for Example 3.4.2. The numerical results presented in Table 3.3 reflect the fact that the extrapolation doubles the order of convergence. The ε-uniform convergence of the scheme can also be seen from Table 3.3.

Example 3.4.3. *Consider the following singularly perturbed semilinear delay parabolic IBVP:*

$$\begin{cases} u_t - \varepsilon u_{xx} + (1 + x(1-x))u_x + \exp(u) = u(x,t-1) + f(x,t), & (x,t) \in \Omega_x \times (0,2], \\ u(x,t) = \phi_b(x,t), & (x,t) \in \overline{\Omega}_x \times [-1,0], \\ u(0,t) = 0,\ u(1,t) = 0, & t \in [0,2]. \end{cases} \tag{3.4.3}$$

We choose the initial data $\phi_b(x,t)$ and the source function $f(x,t)$ to fit with the exact solution

$$u(x,t) = \exp(-t)\left(C_1 + C_2 x - \exp\left(-(1-x)/\varepsilon\right)\right),$$

where $C_1 = \exp(-1/\varepsilon)$ and $C_2 = 1 - \exp(-1/\varepsilon)$.

By using the Newton's linearization process (2.5.2) on (3.4.3), we obtain the following singularly perturbed linear system of delay IBVPs:

$$\begin{cases} u_t^{m+1} - \varepsilon u_{xx}^{m+1} + (1 + x(1-x))u_x^{m+1} + \exp(u^m)u^{m+1} = & u^{m+1}(x,t-1) + f(x,t) \\ & -\exp(u^m)(1-u^m), \\ & (x,t) \in \Omega_x \times (0,2], \\ u^{m+1}(x,t) = \phi_b(x,t), & (x,t) \in \overline{\Omega}_x \times [-1,0], \\ u^{m+1}(0,t) = 0,\ u^{m+1}(1,t) = 0, & t \in [0,2]. \end{cases} \tag{3.4.4}$$

Now, for a fixed m, we solve (3.4.4) by using the numerical method discussed in Section 3.2 and we apply the Richardson extrapolation technique. As a convergence criterion for the Newton's linearization process, we use

$$\max_{(x_i,t_n)\in D^{N,M}} \left|U^{m+1}(x_i,t_n) - U^m(x_i,t_n)\right| \leq \delta, \quad m \geq 0,$$

where $U^m(x_i,t_n)$ is the m-th iteration solution at the mesh-point (x_i,t_n) and δ is the tolerance value. Here, we used the tolerance value $\delta = 10^{-7}$.

As the exact solution of the problem (3.4.3) is known, we calculate the maximum pointwise error for each ε by

$$\hat{e}_{\varepsilon}^{N,\Delta t} = \max_{(x_i,t_n)\in D^{N,M}} \left|u(x_i,t_n) - U(x_i,t_n)\right|, \quad \text{(before extrapolation)},$$

and

$$\hat{e}_{\varepsilon,\,extp}^{N,\Delta t} = \max_{(x_i,t_n)\in D^{N,M}} \left|u(x_i,t_n) - U_{extp}(x_i,t_n)\right|, \quad \text{(after extrapolation)},$$

where $u(x_i,t_n)$, $U(x_i,t_n)$ and $U_{extp}(x_i,t_n)$ denote the exact solution, the numerical solution obtained before extrapolation and the numerical solution obtained after extrapolation in $D^{N,M}$ with N mesh-intervals in the spatial direction and M mesh-intervals in the temporal direction, such that $\Delta t = T/M$ is the uniform mesh-size. We determine the corresponding order of convergence for each ε by

$$\hat{p}_{\varepsilon}^{N,\Delta t} = \log_2\left(\frac{\hat{e}_{\varepsilon}^{N,\Delta t}}{\hat{e}_{\varepsilon}^{2N,\Delta t/2}}\right), \quad \text{(before extrapolation)},$$

and

$$\hat{p}_{\varepsilon,\,extp}^{N,\Delta t} = \log_2\left(\frac{\hat{e}_{\varepsilon,\,extp}^{N,\Delta t}}{\hat{e}_{\varepsilon,\,extp}^{2N,\Delta t/2}}\right), \quad \text{(after extrapolation)}.$$

Now, for each N and Δt, we define the ε-uniform maximum pointwise error by

$$\hat{e}^{N,\Delta t} = \max_{\varepsilon} \hat{e}_{\varepsilon}^{N,\Delta t}, \quad \text{(before extrapolation)},$$

and

$$\hat{e}_{extp}^{N,\Delta t} = \max_{\varepsilon} \hat{e}_{\varepsilon,\,extp}^{N,\Delta t}, \quad \text{(after extrapolation)},$$

and the corresponding ε-uniform order of convergence by

$$\hat{p}^{N,\Delta t} = \log_2\left(\frac{\hat{e}^{N,\Delta t}}{\hat{e}^{2N,\Delta t/2}}\right), \quad \text{(before extrapolation)},$$

and

$$\hat{p}_{extp}^{N,\Delta t} = \log_2\left(\frac{\hat{e}_{extp}^{N,\Delta t}}{\hat{e}_{extp}^{2N,\Delta t/2}}\right), \quad \text{(after extrapolation)}.$$

The calculated maximum pointwise errors and the corresponding order of convergence for Example 3.4.3 are presented in Table 3.4 for various values of ε and N. From Table 3.4, we can observe that for fixed ε, the maximum pointwise errors computed before and after extrapolation, decrease monotonically as N increases, which confirm that the implicit upwind scheme (3.2.2) is ε-uniform convergent. Moreover, one can observe that the maximum pointwise errors and the corresponding order of convergence have been improved after the extrapolation technique.

To visualize the appearance of the boundary layers in the solutions of Examples 3.4.1, 3.4.2 and 3.4.3, we have provided the surface plots for $\varepsilon = 10^{-8}$ and $N = 64$ in Figure 3.1.

In order to reveal the numerical order of convergence, we have plotted the maximum pointwise errors (before and after extrapolation) in loglog scale for Examples 3.4.1, 3.4.2 and 3.4.3 in the Figure 3.2, which again confirms the effectiveness of the extrapolation technique.

3.5 Conclusion

To obtain second-order uniformly convergent numerical solution of singularly perturbed 1D delay convection-diffusion problem of the form (3.1.1), we have applied the Richardson extrapolation technique in this chapter. For this, first we discretized the domain with the uniform mesh in the temporal direction and the piecewise-uniform Shishkin mesh in the spatial direction, then we replaced the continuous PDE by the implicit-Euler scheme for the time derivative and the upwind finite difference for the spatial derivatives. We obtained the numerical solution of this discrete problem on two embedded meshes, first with $N+1$ and $M+1$ number of spatial and temporal mesh-points, respectively, then with $2N+1$ (here we fix the transition parameter as given in (3.2.1)) and $2M+1$ number of mesh-points. After that, we calculated the extrapolated solution by using these two numerical results. Theoretically we have proved that the extrapolation provides second-order ε-uniformly convergent results. The proposed scheme is also applied numerically on the semilinear DPDEs. Numerical experiments are carried out to validate the theoretical findings.

Table 3.1: *Maximum pointwise errors and the corresponding order of convergence for Example 3.4.1.*

ε	Extrp.	Number of mesh-intervals N/temporal mesh-size Δt					
		$16/\frac{1}{10}$	$32/\frac{1}{20}$	$64/\frac{1}{40}$	$128/\frac{1}{80}$	$256/\frac{1}{160}$	$512/\frac{1}{320}$
10^{-2}	Before	7.6591e-2	5.9336e-2	3.9153e-2	2.4519e-2	1.4558e-2	8.3846e-3
		0.3683	0.5998	0.6752	0.7521	0.7960	
	After	2.1076e-2	1.0446e-2	5.1551e-3	2.1496e-3	7.7455e-4	2.6466e-4
		1.0126	1.0189	1.2619	1.4727	1.5492	
10^{-4}	Before	9.1503e-2	6.8788e-2	4.5433e-2	2.7962e-2	1.6615e-2	9.5501e-3
		0.4117	0.5984	0.7003	0.7510	0.7989	
	After	1.5517e-2	6.8853e-3	2.9875e-3	1.1578e-3	4.1096e-4	1.3973e-4
		1.1723	1.2046	1.3675	1.4943	1.5564	
10^{-6}	Before	9.1726e-2	6.9031e-2	4.5748e-2	2.8311e-2	1.6746e-2	9.6097e-3
		0.4101	0.5936	0.6924	0.7576	0.8012	
	After	1.5433e-2	6.7009e-3	2.7455e-3	1.0388e-3	3.6193e-4	1.2139e-4
		1.2036	1.2873	1.4022	1.5211	1.5760	
10^{-8}	Before	9.1728e-2	6.9034e-2	4.5751e-2	2.8314e-2	1.6750e-2	9.6144e-3
		0.4101	0.5935	0.6923	0.7574	0.8009	
	After	1.5433e-2	6.6992e-3	2.7431e-3	1.0360e-3	3.5861e-4	1.1746e-4
		1.2039	1.2882	1.4047	1.5306	1.6102	
$e^{N,\Delta t}$	Before	**9.1728e-2**	**6.9034e-2**	**4.5751e-2**	**2.8314e-2**	**1.6750e-2**	**9.6144e-3**
$p^{N,\Delta t}$		**0.4101**	**0.5935**	**0.6923**	**0.7574**	**0.8009**	
$e^{N,\Delta t}_{extp}$	After	**2.1076e-2**	**1.0446e-2**	**5.1551e-3**	**2.1496e-3**	**7.7455e-4**	**2.6466e-4**
$p^{N,\Delta t}_{extp}$		**1.0126**	**1.0189**	**1.2619**	**1.4727**	**1.5492**	

Table 3.2: *Maximum pointwise errors and the corresponding order of convergence for Example 3.4.1 for* $\varepsilon = 1e-6$ *and different values of* ρ_0.

ρ_0	Extrp.	Number of mesh-intervals N/temporal mesh-size Δt				
		$32/\frac{1}{20}$	$64/\frac{1}{40}$	$128/\frac{1}{80}$	$256/\frac{1}{160}$	$512/\frac{1}{320}$
0.2	Before	1.4270e-1	1.5593e-1	1.6162e-1	1.6105e-1	1.5614e-1
		-0.1280	-0.0517	0.0051	0.0446	
	After	1.7837e-1	1.8627e-1	1.8585e-1	1.8127e-1	1.7545e-1
		-0.0626	0.0033	0.0360	0.0470	
0.3	Before	1.4497e-1	1.4561e-1	1.3803e-1	1.2565e-1	1.1118e-1
		-0.0063	0.0771	0.1355	0.1766	
	After	1.7773e-1	1.6846e-1	1.5841e-1	1.4322e-1	1.2605e-1
		0.0773	0.0887	0.1455	0.1842	
0.6	Before	9.1494e-2	7.0029e-2	5.0018e-2	3.4346e-2	2.3109e-2
		0.3857	0.4855	0.5423	0.5717	
	After	1.0270e-1	7.7027e-2	5.4628e-2	3.7560e-2	2.5374e-2
		0.4150	0.4957	0.5405	0.5658	
1.2	Before	4.5982e-2	2.9064e-2	1.7299e-2	9.9415e-3	5.5927e-3
		0.6618	0.7486	0.7991	0.8299	
	After	1.8468e-2	8.1858e-3	3.5331e-3	1.5134e-3	6.4833e-4
		1.1738	1.2122	1.2231	1.223	
2.2	Before	6.9031e-2	4.5748e-2	2.8311e-2	1.6746e-2	9.6097e-3
		0.5935	0.6923	0.7576	0.8012	
	After	6.7009e-3	2.7455e-3	1.0388e-3	3.6193e-4	1.2139e-4
		1.2873	1.4022	1.5211	1.576	
3.2	Before	9.3348e-2	6.3334e-2	3.9963e-2	2.3920e-2	1.3844e-2
		0.5596	0.6643	0.7404	0.7890	
	After	1.1746e-2	5.1538e-3	2.0389e-3	7.3106e-4	2.4789e-4
		1.1884	1.3378	1.4797	1.5603	

Table 3.3: *Maximum pointwise errors and the corresponding order of convergence for Example 3.4.2.*

ε	Extrp.	Number of mesh-intervals N/temporal mesh-size Δt					
		$16/\frac{1}{10}$	$32/\frac{1}{20}$	$64/\frac{1}{40}$	$128/\frac{1}{80}$	$256/\frac{1}{160}$	$512/\frac{1}{320}$
10^{-2}	Before	1.1720e-2	6.9383e-3	4.0380e-3	2.3371e-3	1.3195e-3	7.3362e-4
		0.7564	0.7810	0.7889	0.8248	0.8469	
	After	1.9337e-3	8.1351e-4	3.2470e-4	1.1992e-4	4.0881e-5	1.3174e-5
		1.2491	1.3251	1.4370	1.5526	1.6337	
10^{-4}	Before	1.4962e-2	9.2070e-3	5.4334e-3	3.1252e-3	1.7548e-3	9.6682e-4
		0.7005	0.7609	0.7979	0.8326	0.8600	
	After	2.6219e-3	1.1273e-3	4.2622e-4	1.4991e-4	4.9878e-5	1.5842e-5
		1.2178	1.4032	1.5075	1.5876	1.6547	
10^{-6}	Before	1.4999e-2	9.2386e-3	5.4551e-3	3.1383e-3	1.7623e-3	9.7104e-4
		0.6991	0.7601	0.7976	0.8325	0.8598	
	After	2.6309e-3	1.1320e-3	4.2789e-4	1.5047e-4	5.0049e-5	1.5890e-5
		1.2167	1.4035	1.5078	1.5881	1.6552	
10^{-8}	Before	1.5000e-2	9.2390e-3	5.4553e-3	3.1384e-3	1.7623e-3	9.7108e-4
		0.6991	0.7601	0.7976	0.8325	0.8598	
	After	2.6310e-3	1.1321e-3	4.2796e-4	1.5048e-4	5.0213e-5	1.6227e-5
		1.2166	1.4034	1.5079	1.5834	1.6297	
$E^{N,\Delta t}$	Before	**1.5000e-2**	**9.2390e-3**	**5.4553e-3**	**3.1384e-3**	**1.7623e-3**	**9.7108e-4**
$P^{N,\Delta t}$		**0.6991**	**0.7601**	**0.7976**	**0.8325**	**0.8598**	
$E^{N,\Delta t}_{extp}$	After	**2.6310e-3**	**1.1321e-3**	**4.2796e-4**	**1.5048e-4**	**5.0213e-5**	**1.6227e-5**
$P^{N,\Delta t}_{extp}$		**1.2166**	**1.4034**	**1.5079**	**1.5834**	**1.6297**	

Table 3.4: *Maximum pointwise errors and the corresponding order of convergence for Example 3.4.3.*

ε	Extrp.	Number of mesh-intervals N/temporal mesh-size Δt					
		$16/\frac{1}{10}$	$32/\frac{1}{20}$	$64/\frac{1}{40}$	$128/\frac{1}{80}$	$256/\frac{1}{160}$	$512/\frac{1}{320}$
10^{-2}	Before	4.8294e-2	2.9540e-2	1.6110e-2	8.4545e-3	4.3326e-3	2.1935e-3
		0.7092	0.8747	0.9302	0.9645	0.9820	
	After	9.8703e-3	3.2054e-3	9.3662e-4	2.5562e-4	6.6821e-5	1.7094e-5
		1.6226	1.7750	1.8735	1.9356	1.9668	
10^{-4}	Before	8.9849e-2	6.6830e-2	4.4182e-2	2.7454e-2	1.6312e-2	9.3934e-3
		0.4270	0.5970	0.6864	0.7511	0.7962	
	After	1.9124e-2	8.7214e-3	3.8613e-3	1.6255e-3	6.1803e-4	2.2807e-4
		1.1328	1.1755	1.2482	1.3951	1.4382	
10^{-6}	Before	9.1805e-2	6.98e-2	4.5718e-2	2.8279e-2	1.6708e-2	9.5812e-3
		0.4118	0.5940	0.6930	0.7592	0.8023	
	After	1.5485e-2	6.7243e-3	2.7694e-3	1.0638e-3	3.9158e-4	1.3682e-4
		1.2034	1.2798	1.3803	1.4419	1.5170	
10^{-8}	Before	9.1825e-2	6.9031e-2	4.5749e-2	2.8314e-2	1.6749e-2	9.6139e-3
		0.4117	0.5935	0.6922	0.7574	0.8009	
	After	1.5476e-2	6.7053e-3	2.7441e-3	1.0364e-3	3.5897e-4	1.1788e-4
		1.2067	1.2889	1.4048	1.5296	1.6066	
$\hat{e}^{N,\Delta t}$	Before	**9.1825e-2**	**6.9031e-2**	**4.5749e-2**	**2.8314e-2**	**1.6749e-2**	**9.6139e-3**
$\hat{p}^{N,\Delta t}$		**0.4117**	**0.5935**	**0.6922**	**0.7574**	**0.8009**	
$\hat{e}^{N,\Delta t}_{extp}$	After	**1.9124e-2**	**8.7214e-3**	**3.8613e-3**	**1.6255e-3**	**6.1803e-4**	**2.2807e-4**
$\hat{p}^{N,\Delta t}_{extp}$		**1.1328**	**1.1755**	**1.2482**	**1.3951**	**1.4382**	

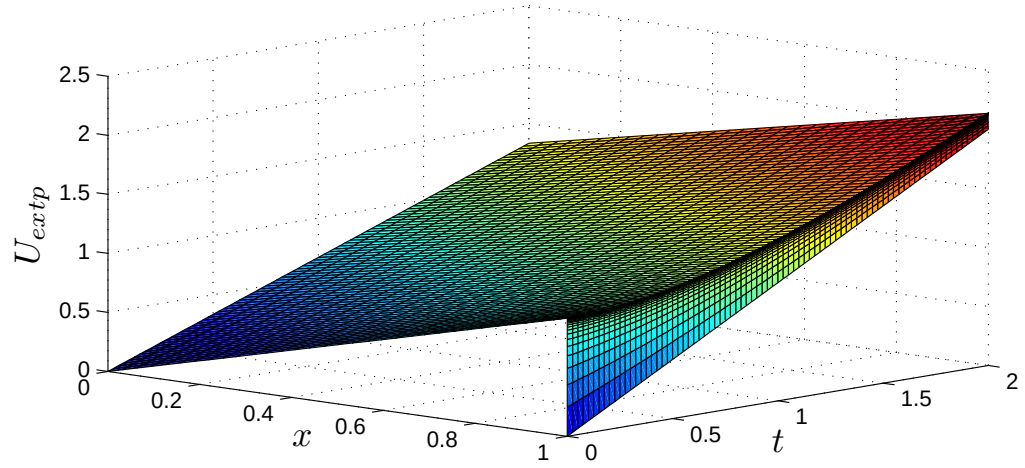

(a) Example 3.4.1.

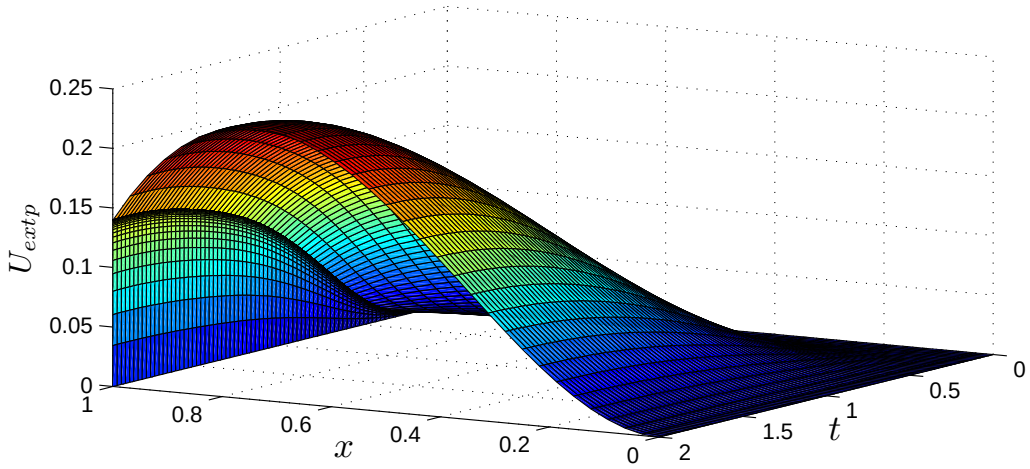

(b) Example 3.4.2.

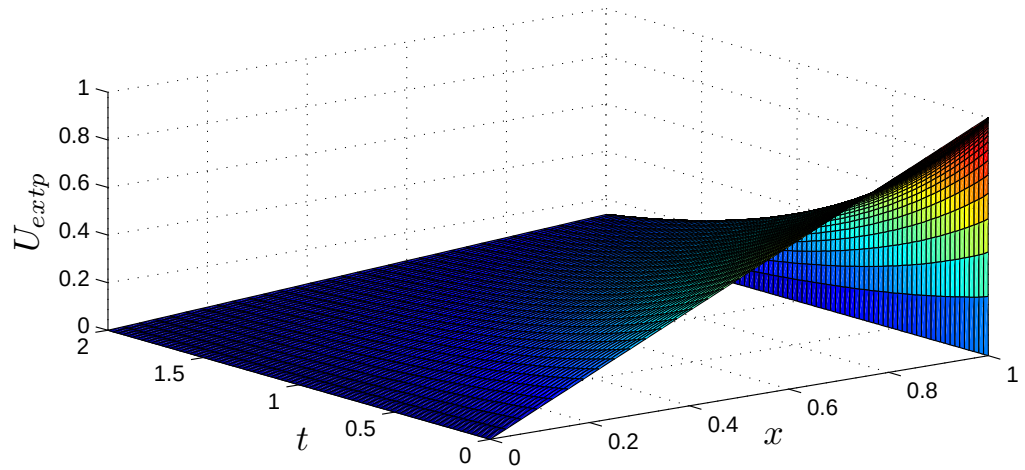

(c) Example 3.4.3.

Figure 3.1: *Surface plots of the numerical solutions for* $\varepsilon = 1e-8$, $N = 64$.

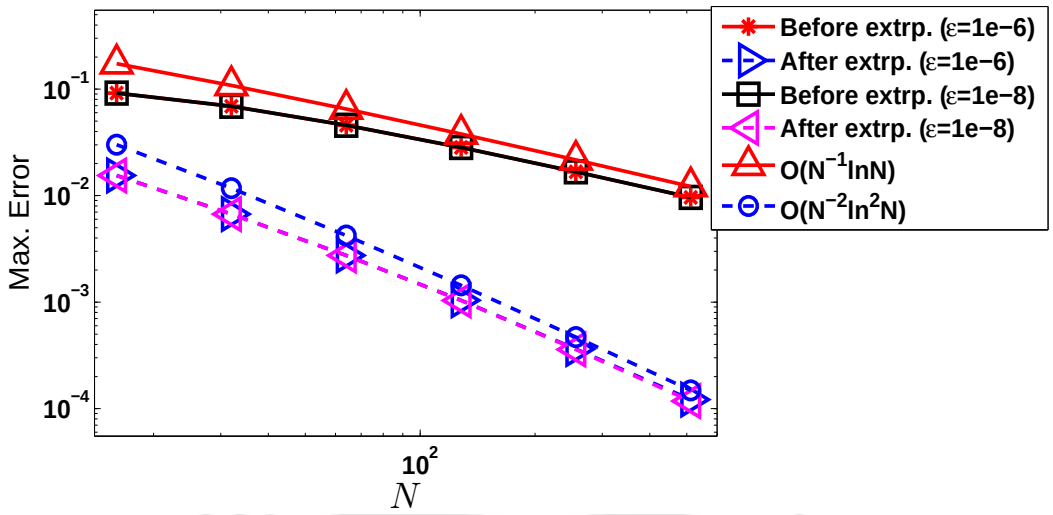

(a) Example 3.4.1.

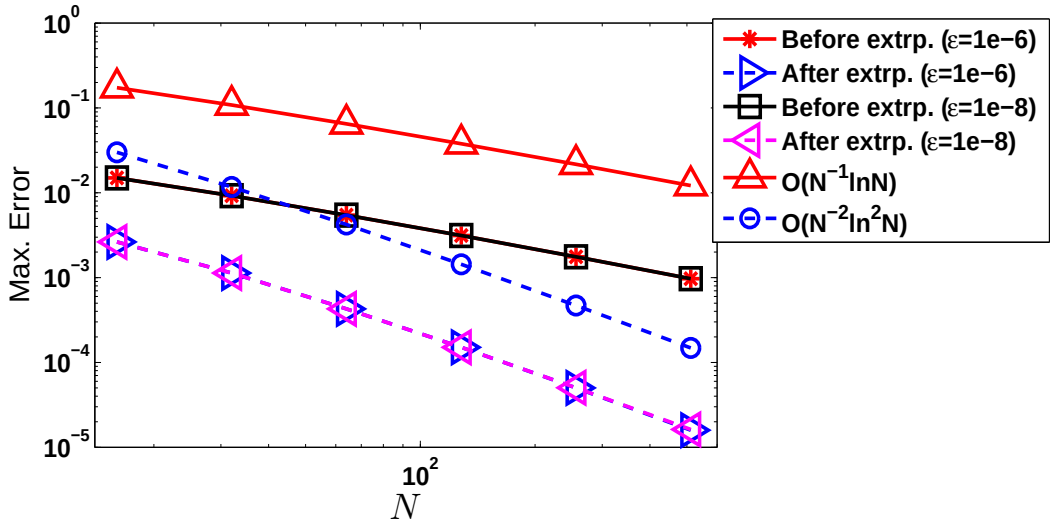

(b) Example 3.4.2.

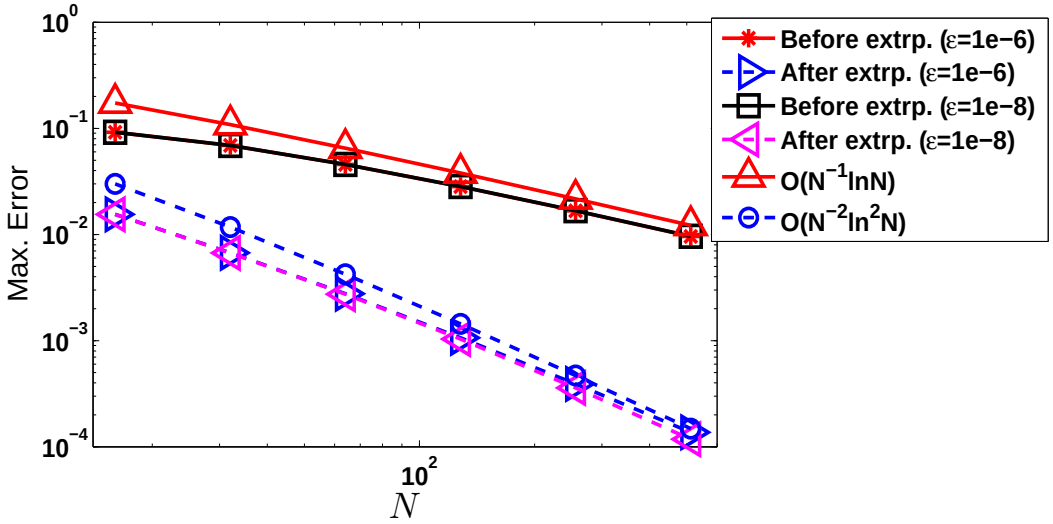

(c) Example 3.4.3.

Figure 3.2: *Visualization of the order of convergence through loglog plot.*

CHAPTER 4

Higher-Order Convergence with Fractional-Step Method for Singularly Perturbed 2D Parabolic Convection-Diffusion Problems on Shishkin Mesh

So far, we have dealt with singularly perturbed 1D delay parabolic PDE of convection-diffusion type. But, in reality, modeling of physical phenomena becomes more appropriate in higher-dimensions. By considering this fact, in this chapter, we propose a second-order uniformly convergent numerical method for a singularly perturbed 2D parabolic convection-diffusion IBVP. First, we use a fractional-step method to discretize the time derivative of the continuous problem on the uniform mesh in the temporal direction, which gives a set of two 1D problems. Then, we use the classical finite difference scheme to discretize those 1D problems on a special mesh, which results almost first-order convergence, *i.e.*, $O(N^{-1+q}\ln N + \Delta t)$. The special mesh is used to capture the boundary layers and the fractional-step method permits a low computational cost algorithm. To enhance the order of convergence to $O(N^{-2+q}\ln^2 N + \Delta t^2)$, we use the Richardson extrapolation technique. In support of the theoretical results, numerical experiments are performed by employing the proposed technique.

4.1 Introduction

Here, we consider the following singularly perturbed 2D parabolic convection-diffusion IBVP posed on the domain $\mathfrak{G} = \mathfrak{D} \times \Lambda_t$, where $\mathfrak{D} = \Omega_x \times \Omega_y = (0,1)^2$ and $\Lambda_t = (0,T]$:

$$\begin{cases} u_t + \mathcal{L}_\varepsilon u(x,y,t) = f(x,y,t), & (x,y,t) \in \mathfrak{G}, \\ u(x,y,0) = s(x,y), & (x,y) \in \overline{\mathfrak{D}}, \\ u(x,y,t) = 0, & (x,y,t) \in \partial\mathfrak{D} \times \overline{\Lambda}_t, \end{cases} \tag{4.1.1}$$

where

$$\mathcal{L}_\varepsilon u = -\varepsilon\Delta u + \mathbf{a}(x,y).\nabla u + b(x,y)u,$$

$0 < \varepsilon \ll 1$ is the singular perturbation parameter. The coefficients $\mathbf{a} = (a_1, a_2)$ and b are sufficiently smooth and bounded functions such that $a_1(x, y) \geq \alpha_x > 0$, $a_2(x, y) \geq \alpha_y > 0$ and $b(x, y) \geq 0$, on $\overline{\mathfrak{D}}$. Under the sufficient smoothness and necessary compatibility conditions imposed on the functions f and s, the parabolic IBVP (4.1.1) admits a unique solution $u(x, y, t)$, which exhibits a regular boundary layer of width $O(\varepsilon)$ along the sides $x = 1$ and $y = 1$, and a corner layer at $(x, y) = (1, 1)$.

In this work, first, by using the fractional-step method, we obtain two 1D problems. Then we discretize the spatial domains by the piecewise-uniform Shishkin mesh and we use the upwind finite difference scheme to discretize the spatial derivatives. We solve those two 1D problems by the upwind scheme, then we double the number of mesh-intervals (by fixing the transition parameter) and solve the same 1D problems. Then, to obtain a better approximate numerical solution, we combine those two solutions according to the technique. This method enhances the order of convergence from first-order to second-order.

The rest of this chapter is organized as follows: In Section 4.2, the time semidiscretization process through fractional-step method has been discussed. Section 4.3 contains the extrapolation technique of the semidiscrete solution. Section 4.4 deals with the piecewise-uniform Shishkin mesh and the classical upwind scheme. The main proof of convergence of the extrapolated numerical solution has been provided in Section 4.5. Numerical results are presented in Section 4.6 and the chapter ends with Section 4.7, that summarizes the main conclusions.

4.2 Time Semidiscretization

Here, we describe the time semidiscretization of the singularly perturbed 2D parabolic IBVP (4.1.1). Time semidiscretization is required to do the analysis of the fully discrete scheme.

4.2.1 The semidiscrete problem

First, we discretize the time domain $\overline{\Lambda}_t$ by uniform mesh with mesh-size Δt, such that

$$\Lambda_t^M = \{t_n = n\Delta t,\ n = 0, \cdots, M,\ \Delta t = T/M\},$$

where M is the number of mesh-points in the t-direction.

Now, we split the differential operator $\mathcal{L}_\varepsilon$ as $\mathcal{L}_\varepsilon = \mathcal{L}_{x,\varepsilon} + \mathcal{L}_{y,\varepsilon}$, where

$$\mathcal{L}_{x,\varepsilon} \equiv -\varepsilon \frac{\partial^2}{\partial x^2} + a_1(x, y)\frac{\partial}{\partial x} + b_1(x, y),$$
$$\mathcal{L}_{y,\varepsilon} \equiv -\varepsilon \frac{\partial^2}{\partial y^2} + a_2(x, y)\frac{\partial}{\partial y} + b_2(x, y),$$

with $b(x,y) = b_1(x,y) + b_2(x,y)$. We split the source term into two smooth terms as $f(x,y,t) = f_1(x,y,t) + f_2(x,y,t)$, such that

$$f_1(x,0,t) = f_1(x,1,t) = f_2(0,y,t) = f_2(1,y,t) = 0. \tag{4.2.1}$$

The operator $\mathcal{L}_{x,\varepsilon}$ can be considered as a family of one-dimensional differential operators with one parameter $y \in (0,1)$ (similarly for $\mathcal{L}_{y,\varepsilon}$).

Now, we introduce a time semidiscretization process by means of the following fractional-step scheme:

$$u^0 = s(x,y), \quad (x,y) \in \overline{\mathfrak{D}},$$

$$\begin{cases} (I + \Delta t \mathcal{L}_{x,\varepsilon}) u^{n+1/2} = u^n + \Delta t f_1(x,y,t_{n+1}), & y \in (0,1), \\ u^{n+1/2}(0,y) = u^{n+1/2}(1,y) = 0, \end{cases} \tag{4.2.2}$$

$$\begin{cases} (I + \Delta t \mathcal{L}_{y,\varepsilon}) u^{n+1} = u^{n+1/2} + \Delta t f_2(x,y,t_{n+1}), & x \in (0,1), \\ u^{n+1}(x,0) = u^{n+1}(x,1) = 0. \end{cases} \tag{4.2.3}$$

The above scheme provides the approximation $u^n(x,y)$ to the solution $u(x,y,t)$ of (4.1.1) at the time level $t_n = n\Delta t$.

The operators $(I + \Delta t \mathcal{L}_{i,\varepsilon})$, $i = x, y$, satisfy the following maximum principle, which ensures the stability of the semidiscrete scheme (4.2.2)-(4.2.3).

Lemma 4.2.1. *(***Maximum principle***) Let $\Psi(x,y) \geq 0$ on the boundary $\partial\mathfrak{D}$ and $(I + \Delta t \mathcal{L}_{i,\varepsilon})\Psi(x,y) \geq 0$, $i = x, y$ on $\mathfrak{D}$. Then $\Psi(x,y) \geq 0$ on $\overline{\mathfrak{D}}$.*

Proof. First we prove the maximum principle for the operator $(I + \Delta t \mathcal{L}_{x,\varepsilon})$. Let $(x^*, y^*) \in \overline{\mathfrak{D}}$ be such that $\Psi(x^*, y^*) = \min_{\overline{\mathfrak{D}}} \Psi(x,y) < 0$. It is clear that the point $(x^*, y^*) \notin \partial\mathfrak{D}$, which implies $(x^*, y^*) \in \mathfrak{D}$. Since $\Psi_x(x^*, y^*) = 0$ and $\Psi_{xx}(x^*, y^*) \geq 0$, we get

$$\begin{aligned} (I + \Delta t \mathcal{L}_{x,\varepsilon})\Psi(x^*, y^*) \; &= \Psi(x^*, y^*) - \varepsilon \Delta t \Psi_{xx}(x^*, y^*) + \Delta t a_1(x^*, y^*)\Psi_x(x^*, y^*) \\ &+ \Delta t b_1(x^*, y^*)\Psi(x^*, y^*) < 0, \end{aligned}$$

which is a contradiction. Hence the required result follows for the operator $(I + \Delta t \mathcal{L}_{x,\varepsilon})$. Similarly, we can prove the maximum principle for the operator $(I + \Delta t \mathcal{L}_{y,\varepsilon})$. ∎

In order to analyze the convergence of the semidiscrete scheme (4.2.2)-(4.2.3), let $\widehat{u}^{n+1}$ be the solution of the following system:

$$\begin{cases} (I + \Delta t \mathcal{L}_{x,\varepsilon})\widehat{u}^{n+1/2} = u(x, y, t_n) + \Delta t f_1(x, y, t_{n+1}), \quad y \in (0, 1), \\ \widehat{u}^{n+1/2}(0, y) = \widehat{u}^{n+1/2}(1, y) = 0, \end{cases} \tag{4.2.4}$$

$$\begin{cases} (I + \Delta t \mathcal{L}_{y,\varepsilon})\widehat{u}^{n+1} = \widehat{u}^{n+1/2} + \Delta t f_2(x, y, t_{n+1}), \quad x \in (0, 1), \\ \widehat{u}^{n+1}(x, 0) = \widehat{u}^{n+1}(x, 1) = 0. \end{cases} \tag{4.2.5}$$

4.3 Extrapolation of $\widehat{u}$

This section introduces the extrapolation of the time semidiscrete solution $\widehat{u}$. The error estimate after extrapolation technique associated to $\widehat{u}$ is given in this section.

For the improvement of the semidiscrete solution $\widehat{u}(t_n)$, we need to solve the semidiscrete problem (4.2.4)-(4.2.5) on the fine mesh Λ_t^{2M}, with $2M$ number of mesh-intervals in the temporal direction. From such construction, it is clear that $\Lambda_t^M = \{t_n\} \subset \Lambda_t^{2M} = \{\widetilde{t}_n\}$. Clearly Λ_t^{2M} is obtained from Λ_t^M by bisecting each mesh-interval of Λ_t^M. Therefore $\widetilde{t}_n - \widetilde{t}_{n-1} = \Delta t/2$, for $\widetilde{t}_n \in \Lambda_t^{2M}$. Let $\widehat{z}$ be the solution of the semidiscrete problem (4.2.4)-(4.2.5) on the mesh Λ_t^{2M}. Now, we know that

$$\widehat{u}(t_n) - u(t_n) = \Delta t + o(\Delta t), \quad t_n \in \Lambda_t^M. \tag{4.3.1}$$

Similarly, we have

$$\widehat{z}(\widetilde{t}_n) - u(\widetilde{t}_n) = \Delta t/2 + o(\Delta t), \quad \widetilde{t}_n \in \Lambda_t^{2M}. \tag{4.3.2}$$

Now, from (4.3.1) and (4.3.2), we get

$$u(t_n) - (2\widehat{z}(t_n) - \widehat{u}(t_n)) = o(\Delta t), \quad t_n \in \Lambda_t^M.$$

We shall therefore use the following extrapolation formula

$$\widehat{u}_{extp^t}(t_n) = 2\widehat{z}(t_n) - \widehat{u}(t_n), \quad t_n \in \Lambda_t^M, \tag{4.3.3}$$

to obtain a better semidiscrete solution of the problem (4.1.1).

4.3.1 Error estimate for $\widehat{u}_{extp^t}$

To obtain the error $|u(t_{n+1}) - \widehat{u}_{extp^t}(t_{n+1})|$, first by combining (4.2.4) and (4.2.5), we get

$$(I + \Delta t \mathcal{L}_{x,\varepsilon})\left((I + \Delta t \mathcal{L}_{y,\varepsilon})\widehat{u}^{n+1} - \Delta t f_2(x, y, t_{n+1})\right) = u(t_n) + \Delta t f_1(x, y, t_{n+1}),$$

therefore, we obtain

$$u(t_n) = (I + \Delta t\mathcal{L}_{x,\varepsilon})(I + \Delta t\mathcal{L}_{y,\varepsilon})\widehat{u}^{n+1} - \Delta t f_1(t_{n+1}) - \Delta t(I + \Delta t\mathcal{L}_{x,\varepsilon})f_2(t_{n+1}).$$

On the other hand, since the solution of (4.1.1) is smooth enough, we have

$$\begin{aligned} u(t_n) &= u(t_{n+1} - \Delta t) = u(t_{n+1}) - \Delta t\frac{\partial u}{\partial t}\Big|_{t_{n+1}} + \frac{(\Delta t)^2}{2}\frac{\partial^2 u}{\partial t^2}\Big|_{t_{n+1}} + O(\Delta t^3) \\ &= u(t_{n+1}) + \Delta t\left[(\mathcal{L}_{x,\varepsilon} + \mathcal{L}_{y,\varepsilon})u(t_{n+1}) - (f_1(t_{n+1}) + f_2(t_{n+1}))\right] \\ &\quad + \frac{(\Delta t)^2}{2}\frac{\partial^2 u}{\partial t^2}\Big|_{t_{n+1}} + O(\Delta t^3) \\ &= (I + \Delta t\mathcal{L}_{x,\varepsilon})\left[(I + \Delta t\mathcal{L}_{y,\varepsilon})u(t_{n+1}) - \Delta t f_2(t_{n+1})\right] - \Delta t f_1(t_{n+1}) \\ &\quad -(\Delta t)^2\mathcal{L}_{x,\varepsilon}\mathcal{L}_{y,\varepsilon}u(x,y,t_{n+1}) + (\Delta t)^2\mathcal{L}_{x,\varepsilon}f_2(t_{n+1}) + \frac{(\Delta t)^2}{2}\frac{\partial^2 u}{\partial t^2}\Big|_{t_{n+1}} + O(\Delta t^3). \end{aligned}$$

So, we have

$$\begin{aligned} &(I + \Delta t\mathcal{L}_{x,\varepsilon})(I + \Delta t\mathcal{L}_{y,\varepsilon})(\widehat{u}^{n+1} - u(t_{n+1})) \\ &= -(\Delta t)^2\mathcal{L}_{x,\varepsilon}\mathcal{L}_{y,\varepsilon}u(x,y,t_{n+1}) + (\Delta t)^2\mathcal{L}_{x,\varepsilon}f_2(t_{n+1}) + \frac{(\Delta t)^2}{2}\frac{\partial^2 u}{\partial t^2}\Big|_{t_{n+1}} + O(\Delta t^3). \end{aligned} \tag{4.3.4}$$

Let us denote $\chi = -\mathcal{L}_{x,\varepsilon}\mathcal{L}_{y,\varepsilon}u(x,y,t_{n+1}) + \mathcal{L}_{x,\varepsilon}f_2(t_{n+1}) + (1/2)u_{tt}(t_{n+1})$. We define the function $\lambda(x,y,t_{n+1})$, to be the solution of the following BVP:

$$\begin{cases} (I + \Delta t\mathcal{L}_{x,\varepsilon})(I + \Delta t\mathcal{L}_{y,\varepsilon})\lambda(x,y,t_{n+1}) = \chi\Delta t, & \text{in } \mathfrak{D}, \\ \lambda(x,y,t_{n+1}) = 0, \qquad (x,y) \in \partial\mathfrak{D}. \end{cases} \tag{4.3.5}$$

By subtracting $\lambda(x,y,t_n)$ from both the sides of (4.3.5), we get

$$(I + \Delta t\mathcal{L}_{x,\varepsilon})(I + \Delta t\mathcal{L}_{y,\varepsilon})\lambda(x,y,t_{n+1}) - \lambda(x,y,t_n) = \chi\Delta t - \lambda(x,y,t_n),$$

which implies that

$$\lambda(x,y,t_{n+1}) - \lambda(x,y,t_n) + \Delta t\mathcal{L}_{\varepsilon}\lambda(x,y,t_{n+1}) = \chi\Delta t - \lambda(x,y,t_n) + O(\Delta t^2).$$

Now, if we divide both the sides by Δt, we obtain an equation of λ, which is similar to (4.1.1). Let $\widehat{\lambda}$ be the time semidiscrete approximation of λ. Hence, by following the same approach given in [15, Lemma 1], we get that

$$(I + \Delta t\mathcal{L}_{x,\varepsilon})(I + \Delta t\mathcal{L}_{y,\varepsilon})(\widehat{\lambda} - \lambda)(x,y,t_{n+1}) \leq C(\Delta t)^2. \tag{4.3.6}$$

Now, (4.3.4), (4.3.5) and (4.3.6), together imply that

$$(I + \Delta t\mathcal{L}_{x,\varepsilon})(I + \Delta t\mathcal{L}_{y,\varepsilon})(\widehat{u} - u - \Delta t\widehat{\lambda})(t_{n+1}) = O(\Delta t^3).$$

Now, by using the maximum principle (Lemma 4.2.1) for the operators $(I+\Delta t\mathcal{L}_{i,\varepsilon})$, $i = x,\, y$, we obtain that

$$[\widehat{u} - u - \Delta t\widehat{\lambda}](x, y, t_{n+1}) \leq C(\Delta t^3),$$

which implies that

$$(\widehat{u} - u)\,(x, y, t_{n+1}) = \Delta t\widehat{\lambda} + O(\Delta t^3).$$

For the Richardson extrapolation, we consider the finer mesh in the temporal direction, *i.e.*, we use the temporal mesh-size $\Delta t/2$. Then, one can have

$$(\widehat{z} - u)\,(x, y, t_{n+1}) = \frac{\Delta t}{2}\widehat{\lambda} + O(\Delta t^3).$$

Therefore, by using the formula given in (4.3.3) for the Richardson extrapolation technique, we obtain that

$$\begin{aligned}(u - \widehat{u}_{extp^t})\,(x, y, t_{n+1}) &= (u - 2\widehat{z} + \widehat{u})\,(x, y, t_{n+1}) \\ &= (-2(\widehat{z} - u) + (\widehat{u} - u))\,(x, y, t_{n+1}) \\ &= O(\Delta t^3). \end{aligned} \tag{4.3.7}$$

Lemma 4.3.1. *The solution of (4.2.4) satisfies the following bound:*

$$\left|\frac{\partial^i \widehat{u}^{n+1/2}}{\partial x^i}\right| \leq C\left(1 + \varepsilon^{-i}\exp\left(-\alpha_{_x}(1-x)/\varepsilon\right)\right), \quad 0 \leq i \leq 4.$$

Proof. One can see [14, Appendix A] for the proof. ∎

Here, we decompose the solution $\widehat{u}^{n+1/2}$ of (4.2.4) as $\widehat{u}^{n+1/2} = \widehat{v}^{n+1/2} + \widehat{w}^{n+1/2}$, for the purpose of convergence analysis done in Section 4.5, where $\widehat{v}^{n+1/2}$ is the smooth component and $\widehat{w}^{n+1/2}$ is the singular component. In a similar way, we decompose u in right hand side of (4.2.4) into the smooth and singular components as $u = v + w$. We decompose $\widehat{z}^{n+1/2}$ as $\widehat{z}^{n+1/2} = \widehat{\psi}_v^{n+1/2} + \widehat{\psi}_w^{n+1/2}$. The smooth components $\widehat{v}$ and v are further decomposed into $\widehat{v}^{n+1/2} = \sum_{k=0}^{3}\varepsilon^k\widehat{v}_k^{n+1/2}$ and $v = \sum_{k=0}^{3}\varepsilon^k v_k$, so that $\widehat{v}^{n+1/2}$ and v satisfy the following problem:

$$\begin{cases} (I + \Delta t\mathcal{L}_{x,\varepsilon})\widehat{v}^{n+1/2} = v(x, y, t_n) + \Delta t f_1(x, y, t_{n+1}), \quad y \in (0, 1), \\ \widehat{v}^{n+1/2}(0) = 0, \quad \widehat{v}^{n+1/2}(1) = \displaystyle\sum_{i=0}^{3}\varepsilon^i\,\widehat{v}_i^{n+1/2}(1), \end{cases}$$

and the singular components $\widehat{w}^{n+1/2}$ and w satisfy the following problem:

$$\begin{cases} (I + \Delta t\mathcal{L}_{x,\varepsilon})\widehat{w}^{n+1/2} = w(x, y, t_n), \quad y \in (0, 1), \\ \widehat{w}^{n+1/2}(0) = 0, \quad \widehat{w}^{n+1/2}(1) = \widehat{u}^{n+1/2}|_{x=1} - \widehat{v}^{n+1/2}(1). \end{cases}$$

Note that, since, we have the bounds of the derivatives of $\widehat{u}^{n+1/2}$, one can easily obtain the following bounds:

$$\left|\left|\frac{\partial^i \widehat{v}^{n+1/2}}{\partial x^i}\right|\right|_\infty \leq C\left(1+\varepsilon^{3-i}\right), \tag{4.3.8}$$

and

$$\left|\frac{\partial^i \widehat{w}^{n+1/2}}{\partial x^i}\right| \leq C\varepsilon^{-i}\exp(-\alpha_{_x}(1-x)/\varepsilon), \quad 0 \leq i \leq 4, \tag{4.3.9}$$

by following the similar idea used in Theorem 2.2.4.

4.4 The Discrete Problem

In this section, we describe the layer-adapted Shishkin meshes for the spatial directions, then we discretize the spatial derivatives of the semidiscrete scheme (4.2.4)-(4.2.5) by using the upwind scheme.

4.4.1 Discretization of the domain

Let the rectangular mesh $\overline{\mathfrak{D}}^N$ be defined by the tensor product of the 1D Shishkin meshes, *i.e.*, $\overline{\mathfrak{D}}^N = \overline{\Omega}_x^N \times \overline{\Omega}_y^N$, which is constructed as follows:

First, define the transition parameters

$$\rho_{_l} = \min\left\{\frac{1}{2},\, \rho_{l,0}\varepsilon \ln N\right\},\ l = x,\, y,$$

where $\rho_{l,0} \geq 2/\alpha_{_l}$. In the analysis, we shall assume that $\rho_{_l} = \rho_{l,0}\varepsilon \ln N$. Note that, if $\rho_{_l} = 1/2$, $l = x,\, y$, then the mesh is uniform and in this case the error estimates can be obtained in the classical way.

To obtain the piecewise-uniform Shishkin mesh, we divide the domain $\overline{\Omega}_x^N$ into two sub-domains $[0, 1-\rho_{_x}]$ and $(1-\rho_{_x}, 1]$ and each sub-domain will have $N/2$ uniform mesh-intervals and denote it by

$$\overline{\Omega}_x^N = \left\{0 = x_0,\, x_1,\, \cdots,\, x_{N/2} = 1-\rho_{_x},\, \cdots,\, x_N = 1\right\}.$$

Similarly, we define $\overline{\Omega}_y^N = \left\{0 = y_0,\, y_1,\, \cdots,\, y_{N/2} = 1-\rho_{_y},\, \cdots,\, y_N = 1\right\}$.

We denote the mesh-sizes in both the spatial directions by

$$h_{x,i} = x_i - x_{i-1},\ i = 1, \cdots, N, \quad \widehat{h}_{x,i} = h_{x,i} + h_{x,i+1},\ i = 1, \cdots, N-1,$$

$$h_{y,j} = y_j - y_{j-1},\ j = 1, \cdots, N, \quad \widehat{h}_{y,j} = h_{y,j} + h_{y,j+1},\ j = 1, \cdots, N-1,$$

and let $H_l = 2(1-\rho_l)/N$ and $h_l = 2\rho_l/N$, $l = x, y$, be the mesh-sizes in $[0, 1-\rho_l]$ and $[1-\rho_l, 1]$ respectively. Then it is easy to see that

$$N^{-1} \leq H_l \leq 2N^{-1}, \quad h_l = 2\rho_{l,0}\varepsilon N^{-1}\ln N, \quad l = x,\, y.$$

Let us denote $\Omega_x^N = \overline{\Omega}_x^N \cap \Omega_x$, $\Omega_y^N = \overline{\Omega}_y^N \cap \Omega_y$. We define the discrete domain by $\mathfrak{G}^{N,M} = \overline{\mathfrak{G}}^{N,M} \cap \mathfrak{G}$ where $\overline{\mathfrak{G}}^{N,M} = \overline{\Omega}_x^N \times \overline{\Omega}_y^N \times \Lambda_t^M$.

4.4.2 Numerical scheme

Let $\mathcal{L}_{x,\varepsilon}^N$ be the discretization of the differential operator $\mathcal{L}_{x,\varepsilon}$ after replacing the spatial derivatives by the upwind finite difference scheme on Ω_x^N. Then the discretized equation can be written as follows: For $y \in \Omega_y^N$,

$$\begin{cases} (I + \Delta t\mathcal{L}_{x,\varepsilon}^N)\widehat{U}_{x_i,y}^{n+1/2} & = (I + \Delta t(-\varepsilon\delta_x^2 + a_1(x_i,y)\delta_x^- + b_1(x_i,y)))\widehat{U}_{x_i,y}^{n+1/2} \\ & = u(x_i,y,t_n) + \Delta t f_1(x_i,y,t_{n+1}), \quad i = 1,\cdots,N-1, \\ \widehat{U}_{0,y}^{n+1/2} = \widehat{U}_{1,y}^{n+1/2} = 0. \end{cases} \tag{4.4.1}$$

Similarly, for $x \in \Omega_x^N$,

$$\begin{cases} (I + \Delta t\mathcal{L}_{y,\varepsilon}^N)\widehat{U}_{x,y_j}^{n+1} & = (I + \Delta t(-\varepsilon\delta_y^2 + a_2(x,y_j)\delta_y^- + b_2(x,y_j)))\widehat{U}_{x,y_j}^{n+1} \\ & = \widehat{U}_{x,y_j}^{n+1/2} + \Delta t f_2(x,y_j,t_{n+1}), \quad j = 1,\cdots,N-1, \\ \widehat{U}_{x,0}^{n+1} = \widehat{U}_{x,1}^{n+1} = 0. \end{cases} \tag{4.4.2}$$

After rearranging the terms in (4.4.1) and (4.4.2), we get

$$\begin{cases} (I + \Delta t\mathcal{L}_{x,\varepsilon}^N)\widehat{U}_{x_i,y}^{n+1/2} \equiv r_i^{1,-}\widehat{U}_{x_{i-1},y}^{n+1/2} + r_i^{1,0}\widehat{U}_{x_i,y}^{n+1/2} + r_i^{1,+}\widehat{U}_{x_{i+1},y}^{n+1/2} = F_{1x_i,y}, \; i = 1,\cdots,N-1, \\ \widehat{U}_{0,y}^{n+1/2} = \widehat{U}_{1,y}^{n+1/2} = 0, \end{cases} \tag{4.4.3}$$

and

$$\begin{cases} (I + \Delta t\mathcal{L}_{y,\varepsilon}^N)\widehat{U}_{x,y_j}^{n+1} \equiv r_j^{2,-}\widehat{U}_{x,y_{j-1}}^{n+1} + r_j^{2,0}\widehat{U}_{x,y_j}^{n+1} + r_j^{2,+}\widehat{U}_{x,y_{j+1}}^{n+1} = F_{2x,y_j}, \quad j = 1,\cdots,N-1, \\ \widehat{U}_{x,0}^{n+1} = \widehat{U}_{x,1}^{n+1} = 0, \end{cases} \tag{4.4.4}$$

respectively, where

$$\begin{cases} r_i^{1,-} = \Delta t\left(-\dfrac{2\varepsilon}{\widehat{h}_{x,i}h_{x,i}} - \dfrac{a_1(x_i,y)}{h_{x,i}}\right), \quad r_i^{1,+} = \Delta t\left(-\dfrac{2\varepsilon}{\widehat{h}_{x,i}h_{x,i+1}}\right), \\ r_i^{1,0} = 1 + \Delta t b_1(x_i,y) - r_i^{1,-} - r_i^{1,+}, \quad F_{1x_i,y} = u(x_i,y,t_n) + \Delta t f_1(x_i,y,t_{n+1}), \end{cases} \tag{4.4.5}$$

and

$$\begin{cases} r_j^{2,-} = \Delta t \left(-\dfrac{2\varepsilon}{\widehat{h}_{y,j} h_{y,j}} - \dfrac{a_2(x,y_j)}{h_{y,j}} \right), \quad r_j^{2,+} = \Delta t \left(-\dfrac{2\varepsilon}{\widehat{h}_{y,j} h_{y,j+1}} \right), \\ r_j^{2,0} = 1 + \Delta t b_2(x,y_j) - r_j^{2,-} - r_j^{2,+}, \quad F_{2x,y_j} = \widehat{U}_{x,y_j}^{n+1/2} + \Delta t f_2(x,y_j,t_{n+1}). \end{cases} \tag{4.4.6}$$

Lemma 4.4.1. *The matrices associated with the finite difference schemes (4.4.1) and (4.4.2) are M-matrices.*

Proof. It is clear from the above equations (4.4.3)-(4.4.6) that, for $\ell = 1, 2$, we have

$$r_l^{\ell,-} < 0,\ r_l^{\ell,+} < 0 \,\text{and}\, r_l^{\ell,0} > 0$$

along with

$$|r_1^{\ell,0}| - |r_1^{\ell,+}| > 0,\ |r_{N-1}^{\ell,0}| - |r_{N-1}^{\ell,-}| > 0 \text{ and } |r_l^{\ell,0}| - |r_l^{\ell,+}| - |r_l^{\ell,-}| > 0, \text{ for } l = 1, \cdots, N-1.$$

Therefore, the matrices associated with the finite difference schemes are M-matrices. ∎

As a consequence, the difference operator given in (4.4.1) satisfies the following discrete maximum principle.

Lemma 4.4.2. *(***Discrete maximum principle***) Assume that the discrete function Ψ_i satisfies $\Psi_i \geq 0$ on $i = 0, N$. Then $(I + \Delta t \mathcal{L}_{x,\varepsilon}^N)\Psi_i \geq 0$ on Ω_x^N implies that $\Psi_i \geq 0$ at each point of $\overline{\Omega}_x^N$.*

Hence the method is uniformly stable in the supremum norm. Similar property holds for the difference operator defined in (4.4.2).

4.4.3 Error estimate for the fully discrete solution

Let us define the fully discrete scheme on $\overline{\mathfrak{G}}^{N,M}$ as follows:

$$U_{i,j}^0 = s(x_i, y_j), \quad i,\, j = 0, \cdots, N,$$

$$\begin{cases} (I + \Delta t \mathcal{L}_{x,\varepsilon}^N) U_{i,j}^{n+1/2} = U_{i,j}^n + \Delta t f_1(x_i, y_j, t_{n+1}),\ 1 \leq i \leq N-1, \\ U_{0,j}^{n+1/2} = U_{N,j}^{n+1/2} = 0, \quad 0 \leq j \leq N, \end{cases} \tag{4.4.7}$$

$$\begin{cases} (I + \Delta t \mathcal{L}_{y,\varepsilon}^N) U_{i,j}^{n+1} = U_{i,j}^{n+1/2} + \Delta t f_2(x_i, y_j, t_{n+1}),\ 1 \leq j \leq N-1, \\ U_{i,0}^{n+1} = U_{i,N}^{n+1} = 0, \quad 0 \leq i \leq N. \end{cases} \tag{4.4.8}$$

The following theorem explains that the upwind scheme defined in (4.4.7)-(4.4.8), converges ε-uniformly on $\mathfrak{G}^{N,M}$, with almost first-order accuracy.

Theorem 4.4.3. *Let u be the exact solution of (4.1.1) and $\{U^n\}$ be the numerical solution of the fully discrete scheme (4.4.7)-(4.4.8) at time level $t_n = n\Delta t$. Then there exists a positive constant C, independent of ε, N, with $0 < q < 1$ such that*

$$\left\|u(x_i, y_j, t_n) - U^n_{i,j}\right\|_\infty \leq C(\Delta t + N^{-1+q} \ln N),$$

for $(x_i, y_j, t_n) \in \mathfrak{G}^{N,M}$.

Proof. The proof can be found in [14]. ∎

One can observe from the above theorem that the temporal order of convergence is one and the spatial order of convergence is almost one (up to a logarithmic factor). To enhance the order of convergence, we apply the Richardson extrapolation technique on the discrete solution $U^n_{i,j}$ of the fully discrete scheme (4.4.7)-(4.4.8).

4.5 Extrapolation of $\widehat{U}$

In this section, we describe the Richardson extrapolation technique in the spatial directions, which is used to increase the accuracy of the computed solutions of the basic scheme. The main result of this chapter for the ε-uniform convergence of the extrapolated numerical solution is given at the end of this section.

To apply the technique, we will solve the discrete problem (4.4.1)-(4.4.2) on the fine mesh $\overline{\mathfrak{D}}^{2N} = \overline{\Omega}_x^{2N} \times \overline{\Omega}_y^{2N}$ with $2N$ mesh-intervals in the spatial direction, where $\overline{\Omega}_x^{2N}$ and $\overline{\Omega}_y^{2N}$ are the piecewise-uniform Shishkin meshes having the same transition points $1-\rho_x$ and $1-\rho_y$, respectively, as used in $\overline{\Omega}_x^{N}$ and $\overline{\Omega}_y^{N}$. The discrete domain $\overline{\Omega}_x^{2N}$ (similarly $\overline{\Omega}_y^{2N}$) can be obtained through bisecting each mesh-interval of $\overline{\Omega}_x^{N}$. From such construction, it is clear that $\overline{\mathfrak{D}}^{N} = \{(x_i, y_j)\} \subset \overline{\mathfrak{D}}^{2N} = \{(\widetilde{x}_i, \widetilde{y}_j)\}$. Hence the corresponding mesh-sizes in $\overline{\mathfrak{D}}^{2N}$ can be given by

$$\widetilde{x}_i - \widetilde{x}_{i-1} = \begin{cases} H_x/2, & \text{for} \quad \widetilde{x}_i \in \overline{\Omega}_x^{2N} \cap [0, 1-\rho_x], \\ h_x/2, & \text{for} \quad \widetilde{x}_i \in \overline{\Omega}_x^{2N} \cap [1-\rho_x, 1]. \end{cases}$$

Let $\widehat{U}^n_{x_i,y_j}$ be the solution of (4.4.1)-(4.4.2) on $\overline{\mathfrak{D}}^{N}$. Therefore, from [14], one can express the error as

$$\begin{aligned} (\widehat{U}^n - \widehat{u}^n)(x_i, y_j) &= C\left(N^{-1}\ln N\right) + o(N^{-1}\ln N) \\ &= C_1\left(N^{-1}\ln N\right) + C_2\left(N^{-1}\ln N\right) + o(N^{-1}\ln N) \\ &= C_1\left(N^{-1}(\rho_x/\rho_{x,0}\varepsilon)\right) + C_2\left(N^{-1}(\rho_y/\rho_{y,0}\varepsilon)\right) \\ &\quad + o(N^{-1}\ln N), \quad (x_i, y_j) \in \overline{\mathfrak{D}}^{N}, \end{aligned} \tag{4.5.1}$$

where C_1 and C_2 are some fixed constants. Similarly, if $\widetilde{U}^n_{\widetilde{x}_i,\widetilde{y}_j}$ is the solution of the discrete problem (4.4.1)-(4.4.2) on $\overline{\mathfrak{D}}^{2N}$, then we have

$$(\widetilde{U}^n - \widehat{u}^n)(\widetilde{x}_i,\widetilde{y}_j) = C_1\left((2N)^{-1}(\rho_x/\rho_{x,0}\varepsilon)\right) + C_2\left((2N)^{-1}(\rho_y/\rho_{y,0}\varepsilon)\right) + o(N^{-1}\ln N), \quad (\widetilde{x}_i,\widetilde{y}_j)\in\overline{\mathfrak{D}}^{2N}. \tag{4.5.2}$$

Now, from (4.5.1) and (4.5.2), eliminating $O(N^{-1})$, we get

$$\left(\widehat{u}^n - \left(2\widetilde{U}^n - \widehat{U}^n\right)\right)(x_i,y_j) = o(N^{-1}\ln N), \quad (x_i,y_j)\in\overline{\mathfrak{D}}^N.$$

We shall therefore use the following extrapolation formula

$$\widehat{U}^n_{extp}(x_i,y_j) = (2\widetilde{U}^n - \widehat{U}^n)(x_i,y_j), \quad (x_i,y_j)\in\overline{\mathfrak{D}}^N, \tag{4.5.3}$$

to obtain a better approximate solution of the problem (4.4.1)-(4.4.2).

To proceed further, we decompose the discrete solution $\widehat{U}^{n+1/2}_{x_i,y}$ of (4.4.1) into the smooth and singular components as $\widehat{V}^{n+1/2} + \widehat{W}^{n+1/2}$ in $\mathfrak{G}^{N,M}$, $\widehat{\mathcal{V}}^{n+1/2} + \widehat{\mathcal{W}}^{n+1/2}$ in $\mathfrak{G}^{N,2M}$.

The smooth component $\widehat{V}^{n+1/2}$ satisfies the following discrete equation:

$$\begin{cases} (I+\Delta t\mathcal{L}^N_{x,\varepsilon})\widehat{V}^{n+1/2} &= (I+\Delta t(-\varepsilon\delta_x^2 + a_1(x_i,y)\delta_x^- + b_1(x_i,y)))\widehat{V}^{n+1/2} \\ &= v(x_i,y,t_n) + \Delta t f_1(x_i,y,t_{n+1}), \quad i=1,\cdots,N-1, \\ \widehat{V}^{n+1/2}_0 = \widehat{v}^{n+1/2}(0), & \widehat{V}^{n+1/2}_1 = \widehat{v}^{n+1/2}(1), \end{cases}$$

and the singular component $\widehat{W}^{n+1/2}$ satisfies

$$\begin{cases} (I+\Delta t\mathcal{L}^N_{x,\varepsilon})\widehat{W}^{n+1/2} &= (I+\Delta t(-\varepsilon\delta_x^2 + a_1(x_i,y)\delta_x^- + b_1(x_i,y)))\widehat{W}^{n+1/2} \\ &= w(x_i,y,t_n), \quad i=1,\cdots,N-1, \\ \widehat{W}^{n+1/2}_0 = \widehat{w}^{n+1/2}(0), & \widehat{W}^{n+1/2}_1 = \widehat{w}^{n+1/2}(1). \end{cases} \tag{4.5.4}$$

At the node $(x_i,y,t_{n+1/2})$ the errors can be written in the form

$$(\widehat{U}-\widehat{u})(x_i,y,t_{n+1/2}) = (\widehat{V}-\widehat{v})(x_i,y,t_{n+1/2}) + (\widehat{W}-\widehat{w})(x_i,y,t_{n+1/2}).$$

4.5.1 Extrapolation of the smooth component

Lemma 4.5.1. *Assume that $\varepsilon \le N^{-1}$. Then, the local truncation error associated to the smooth component satisfies*

$$(I+\Delta t\mathcal{L}^N_{x,\varepsilon})(\widehat{V}-\widehat{v})(x_i,y,t_{n+1/2}) = \Delta t\frac{h_{x,i}}{2}a_1(x_i,y)\frac{\partial^2\widehat{v}}{\partial x^2}(x_i,y,t_{n+1/2}) + O(H_x^2).$$

Proof. By using (4.3.8) and $\varepsilon < N^{-1} < H_x$ along with the following Taylor's expansion,

$$\begin{aligned}
&(I + \Delta t\mathcal{L}^N_{x,\varepsilon})(\widehat{V} - \widehat{v})(x_i, y, t_{n+1/2}) \\
&= \frac{\varepsilon\Delta t}{3(h_{x,i} + h_{x,i+1})}\left[h^2_{x,i+1}\frac{\partial^3\widehat{v}}{\partial x^3}(\zeta_1, y, t_{n+1/2}) - h^2_{x,i}\frac{\partial^3\widehat{v}}{\partial x^3}(\zeta_2, y, t_{n+1/2})\right] \\
&\quad + \Delta t\frac{h_{x,i}}{2}a_1(x_i, y)\frac{\partial^2\widehat{v}}{\partial x^2}(x_i, y, t_{n+1/2}) - \Delta t\frac{h^2_{x,i}}{6}a_1(x_i, y)\frac{\partial^3\widehat{v}}{\partial x^3}(\zeta_3, y, t_{n+1/2}),
\end{aligned}$$

for some $\zeta_1 \in (x_i, x_{i+1})$, ζ_2, $\zeta_3 \in (x_{i-1}, x_i)$, it is easy to obtain the required result. ∎

Let us assume Θ be the solution of the following BVP:

$$\begin{cases}
(I + \Delta t\mathcal{L}_{x,\varepsilon})\Theta = \dfrac{\Delta t}{2}a_1(x, y)\dfrac{\partial^2\widehat{v}}{\partial x^2}(x, y, t_{n+1/2}), \quad y \in (0, 1), \\
\Theta(0) = \Theta(1) = 0.
\end{cases}$$

Now, we decompose Θ as $\Theta = \eta + \nu$, where η is the smooth component and ν is the singular component, which satisfy the following equations for $y \in (0, 1)$:

$$\begin{cases}
(I + \Delta t\mathcal{L}_{x,\varepsilon})\eta = \dfrac{\Delta t}{2}a_1(x, y)\dfrac{\partial^2\widehat{v}}{\partial x^2}(x, y, t_{n+1/2}), \\
(I + \Delta t\mathcal{L}_{x,\varepsilon})\nu = 0, \\
\eta(0) = 0 = \nu(0), \\
\eta(1) = -\nu(1).
\end{cases} \tag{4.5.5}$$

Therefore, by following [73], we can have the theorem stated below.

Theorem 4.5.2. *The smooth component η defined in (4.5.5) satisfies the following bounds:*

$$\left\|\frac{\partial^k\eta}{\partial x^k}\right\|_\infty \le C, \quad k = 0,\ 1,\ 2, \text{ and } \quad \left\|\frac{\partial^3\eta}{\partial x^3}\right\|_\infty \le C\varepsilon^{-1}.$$

Lemma 4.5.3. *Assume that $\varepsilon \le N^{-1}$. Then, for $1 \le i \le N-1$, the error in the smooth component satisfies*

$$(\widehat{V} - \widehat{v})(x_i, y, t_{n+1/2}) = h_{x,i}\eta(x_i) + O(N^{-2}).$$

Proof. By using Lemma 4.5.1 and (4.5.5), we get

$$(I + \Delta t\mathcal{L}^N_{x,\varepsilon})(\widehat{V} - \widehat{v})(x_i, y, t_{n+1/2}) = h_{x,i}(I + \Delta t\mathcal{L}_{x,\varepsilon})\eta(x_i) + O(H_x^2). \tag{4.5.6}$$

Now, by using the Taylor's expansion, it can be obtained easily that

$$\begin{aligned}
&\left|\left((I + \Delta t\mathcal{L}^N_{x,\varepsilon}) - (I + \Delta t\mathcal{L}_{x,\varepsilon})\right)\eta(x_i)\right| \\
&\le \left[\Delta t\frac{\varepsilon(h_{x,i} + h_{x,i+1})}{3}\left\|\frac{\partial^3\eta}{\partial x^3}\right\|_\infty + \Delta t\frac{h_{x,i}}{2}a_1(x, y)\left\|\frac{\partial^2\eta}{\partial x^2}\right\|_\infty\right]
\end{aligned} \tag{4.5.7}$$

and by using Theorem 4.5.2 along with the inequality $h_{x,i} \leq H_x$, we obtain

$$\left|h_{x,i}\left((I+\Delta t\mathcal{L}^N_{x,\varepsilon})-(I+\Delta t\mathcal{L}_{x,\varepsilon})\right)\eta(x_i)\right| \leq C\left(H_x^2\Delta t\right) \leq CH_x^2. \tag{4.5.8}$$

Therefore, (4.5.6) and (4.5.8) together imply that

$$(I+\Delta t\mathcal{L}^N_{x,\varepsilon})[(\widehat{V}-\widehat{v})(x_i,y,t_{n+1/2})-h_{x,i}\eta(x_i)] \leq CH_x^2.$$

From the discrete maximum principle (Lemma 4.4.2), we get that

$$(\widehat{V}-\widehat{v})(x_i,y,t_{n+1/2}) = h_{x,i}\eta(x_i)+O(N^{-2}), \tag{4.5.9}$$

which reflects the required result. ∎

Similarly, in the finer mesh of temporal direction, we get that

$$(\widehat{\mathcal{V}}-\widehat{\psi}_v)(x_i,y,t_{n+1/2}) = h_{x,i}\eta(x_i)+O(N^{-2}).$$

Therefore, we have

$$(\widehat{V}_{extp^t}-\widehat{v}_{extp^t})(x_i,y,t_{n+1/2}) = h_{x,i}\eta(x_i)+O(N^{-2}),$$

where $\widehat{V}^{n+1/2}_{extp^t}$ and $\widehat{v}^{n+1/2}_{extp^t}$ are the time extrapolated solutions of $\widehat{V}^{n+1/2}$ and $\widehat{v}^{n+1/2}$, respectively.

Lemma 4.5.4. *Assume that $\varepsilon \leq N^{-1}$. Then, the error after extrapolation associated to the smooth component $\widehat{V}^{n+1/2}$ satisfies*

$$\left(\widehat{V}_{extp}-\widehat{v}_{extp^t}\right)(x_i,y,t_{n+1/2}) \leq CN^{-2}.$$

Proof. Due to the construction of $\overline{\mathfrak{G}}^{2N,2M}$ and $\overline{\mathfrak{G}}^{N,M}$, we have

$$\left(\widehat{\mathcal{V}}_{extp^t}-\widehat{v}_{extp^t}\right)(x_i,y,t_{n+1/2}) = \begin{cases} (H_x/2)\eta(x_i)+O\left(N^{-2}\right), & \text{for } 1 \leq i \leq N/2, \\ (h_x/2)\eta(x_i)+O\left(N^{-2}\right), & \text{for } N/2+1 \leq i \leq N-1, \end{cases}$$

where $\widehat{\mathcal{V}}^{n+1/2}_{extp^t}$ is the time extrapolated solution in $\overline{\mathfrak{G}}^{2N,M}$.

Therefore, we have

$$\begin{aligned}\left(\widehat{V}_{extp}-\widehat{v}_{extp^t}\right)(x_i,y,t_{n+1/2}) &= \left(\left(2\widehat{\mathcal{V}}_{extp^t}-\widehat{V}_{extp^t}\right)-\widehat{v}_{extp^t}\right)(x_i,y,t_{n+1/2}) \\ &= \left(2\left(\widehat{\mathcal{V}}_{extp^t}-\widehat{v}_{extp^t}\right)-\left(\widehat{V}_{extp^t}-\widehat{v}_{extp^t}\right)\right)(x_i,y,t_{n+1/2}) \\ &= O(N^{-2}),\end{aligned}$$

which is the required result. ∎

4.5.2 Extrapolation of the singular component

Lemma 4.5.5. *The singular component $\widehat{W}^{n+1/2}$ satisfies*

$$|\widehat{W}^{n+1/2}| \leq \prod_{j=i+1}^{N} \left(1 + \frac{\alpha_x h_{x,j}}{\varepsilon}\right)^{-1}, \text{ for } i = 0,\, 1, \cdots,\, N-1.$$

Proof. Let us define $S_i = \prod_{j=1}^{i} \left(1 + \frac{\alpha_x h_{x,j}}{\varepsilon}\right)$, with $S_0 = 1$.

Therefore,

$$\begin{aligned} \frac{S_i}{S_N} &= \prod_{j=i+1}^{N} \left(1 + \frac{\alpha_x h_{x,j}}{\varepsilon}\right)^{-1} \\ &\geq \prod_{j=i+1}^{N} \exp\left(-\alpha_x h_{x,j}/\varepsilon\right) \\ &= \exp\left(-\alpha_x (1 - x_i)/\varepsilon\right). \end{aligned}$$

Let, $Y_i = CS_i/S_N$, for $i = 0,\, 1, \cdots,\, N-1$. Applying the difference operator on Y_i we get

$$(I + \Delta t \mathcal{L}^N_{x,\varepsilon}) Y_i = \frac{C}{S_N} (I + \Delta t \mathcal{L}^N_{x,\varepsilon}) S_i.$$

Now, we have

$$\begin{aligned} (I + \Delta t \mathcal{L}^N_{x,\varepsilon}) S_i &= \left(I + \Delta t(-\varepsilon \delta_x^2 + a_1(x_i, y)\delta_x^- + b_1(x_i, y))\right) S_i \\ &= (1 + \Delta t b_1(x_i, y)) S_i - \Delta t \varepsilon \delta_x^2 S_i + \Delta t a_1(x_i, y) \delta_x^- S_i. \quad (4.5.10) \end{aligned}$$

It is easy to derive that

$$\delta_x^- S_i = \frac{\alpha_x}{(\varepsilon + \alpha_x h_{x,i})} S_i, \quad \delta_x^+ S_i = \frac{\alpha_x}{\varepsilon} S_i, \quad \text{and} \quad \varepsilon \delta_x^2 S_i = \frac{-\alpha_x^2 h_{x,i}}{\widehat{h}_{x,i}(\varepsilon + \alpha_x h_{x,i})} S_i.$$

Therefore, from (4.5.10), we get

$$(I + \Delta t \mathcal{L}^N_{x,\varepsilon}) S_i \geq \frac{C}{\max\{\varepsilon,\, h_{x,i}\}} S_i.$$

Now, by using the bound for the singular component (4.5.4) can be written as

$$(I + \Delta t \mathcal{L}^N_{x,\varepsilon}) \widehat{W}^{n+1/2} \leq C \exp\left(-\alpha_x (1 - x_i)/\varepsilon\right) \leq C \frac{S_i}{S_N} \leq (I + \Delta t \mathcal{L}^N_{x,\varepsilon}) Y_i.$$

By using the discrete maximum principle (Lemma 4.4.2), we obtain $\widehat{W}^{n+1/2} \leq CY_i$. With the same argument, we can have $-\widehat{W}^{n+1/2} \leq CY_i$.

Hence, we have $|\widehat{W}^{n+1/2}| \leq CY_i$, which is the required bound. ∎

Lemma 4.5.6. *Assume that $\varepsilon \leq N^{-1}$. Then, the error after extrapolation associated to the singular component $\widehat{W}^{n+1/2}$ satisfies*

$$\left|\left(\widehat{W}_{extp} - \widehat{w}_{extp^t}\right)(x_i, y, t_{n+1/2})\right| \leq CN^{-2}, \quad \text{for} \quad 1 \leq i \leq N/2.$$

Proof. By using (4.3.9), one can get

$$\widehat{w}(x_i, y, t_{n+1/2}) \leq C \exp(-\alpha_{_x}\rho_{_x}/\varepsilon).$$

Since, $\rho_{_x} \geq (2\varepsilon/\alpha_{_x}) \ln N$, we can easily obtain $\left|\widehat{w}(x_i, y, t_{n+1/2})\right| \leq CN^{-2}$.

Again, by using the similar approach used in [89] on the result obtained in Lemma 4.5.5, we obtain $\left|\widehat{W}^{n+1/2}\right| \leq CN^{-2}$.

Therefore,

$$\left|\left(\widehat{W} - \widehat{w}\right)(x_i, y, t_{n+1/2})\right| \leq CN^{-2}. \tag{4.5.11}$$

Similarly, in the finer mesh of temporal direction, we get

$$\left|\left(\widehat{\mathcal{W}} - \widehat{\psi}_w\right)(x_i, y, t_{n+1/2})\right|(x_i, y, t_{n+1/2}) \leq CN^{-2}.$$

So, we have

$$\left|\left(\widehat{W}_{extp^t} - \widehat{w}_{extp^t}\right)(x_i, y, t_{n+1/2})\right| \leq CN^{-2},$$

where $\widehat{W}^{n+1/2}_{extp^t}$ and $\widehat{w}^{n+1/2}_{extp^t}$ are the time extrapolated solutions of $\widehat{W}^{n+1/2}$ and $\widehat{w}^{n+1/2}$, respectively.

Let $\widehat{\mathcal{W}}^{n+1/2}_{extp^t}$ be the time extrapolated solution in $\overline{\mathfrak{G}}^{2N,M}$. Thus, we have

$$\begin{aligned}
&\left|\left(\widehat{W}_{extp} - \widehat{w}_{extp^t}\right)(x_i, y, t_{n+1/2})\right| \\
&= \left|\left(2\widehat{\mathcal{W}}_{extp^t} - \widehat{W}_{extp^t} - \widehat{w}_{extp^t}\right)(x_i, y, t_{n+1/2})\right| \\
&= \left|\left(2\left(\widehat{\mathcal{W}}_{extp^t} - \widehat{w}_{extp^t}\right) - \left(\widehat{W}_{extp^t} - \widehat{w}_{extp^t}\right)\right)(x_i, y, t_{n+1/2})\right| \\
&\leq CN^{-2},
\end{aligned}$$

which is the required result. ∎

To analyze the effect of the extrapolation on $x_i \in (1-\rho_{_x}, 1]$, we use the Taylor series expansion, *i.e.*,

$$\begin{aligned}
&\left(I + \Delta t\mathcal{L}^N_{x,\varepsilon}\right)\left(\widehat{W} - \widehat{w}\right)(x_i, y, t_{n+1/2}) \\
&= \left((I + \Delta t\mathcal{L}_{x,\varepsilon}) - \left(I + \Delta t\mathcal{L}^N_{x,\varepsilon}\right)\right)\widehat{w}(x_i, y, t_{n+1/2}) \\
&= -\frac{\varepsilon\Delta t h_x^2}{4!}\left[\frac{\partial^4\widehat{w}}{\partial x^4}(\xi_1, y, t_{n+1/2}) + \frac{\partial^4\widehat{w}}{\partial x^4}(\xi_2, y, t_{n+1/2})\right] + \frac{h_x\Delta t}{2}a_1(x_i, y)\frac{\partial^2\widehat{w}}{\partial x^2}(x_i, y, t_{n+1/2}) \\
&\quad -\frac{h_x^2\Delta t}{3!}a_1(x_i, y)\frac{\partial^3\widehat{w}}{\partial x^3}(\xi_3, y, t_{n+1/2}),
\end{aligned}$$

where $\xi_1 \in (x_i, x_{i+1})$ and $\xi_2,\ \xi_3 \in (x_{i-1}, x_i)$.

Now, by using (4.3.9), we can write

$$\left(I + \Delta t \mathcal{L}^N_{x,\varepsilon}\right)\left(\widehat{W} - \widehat{w}\right)(x_i, y, t_{n+1/2}) = \frac{2\varepsilon\Delta t}{\alpha_{_x}}\left(N^{-1}\ln N\right) a_1(x_i, y)\frac{\partial^2 \widehat{w}}{\partial x^2}(x_i, y, t_{n+1/2}) + O(\varepsilon^{-1}\exp(-\alpha_{_x}(1 - x_{i+1})/\varepsilon)N^{-2}\ln^2 N).$$

We consider a BVP, when $x \in (1 - \rho_{_x}, 1)$,

$$\begin{cases} (I + \Delta t \mathcal{L}_{x,\varepsilon})\,\mathcal{F} = \dfrac{2\varepsilon}{\alpha_{_x}}\Delta t a_1(x, y)\dfrac{\partial^2 \widehat{w}}{\partial x^2}(x, y, t_{n+1/2}), \quad y \in (0, 1), \\ \mathcal{F}(1 - \rho_{_x}) = \mathcal{F}(1) = 0. \end{cases}$$

Since, this is an ODE, we can obtain

$$(\widehat{W} - \widehat{w})(x_i, y, t_{n+1/2}) = (N^{-1}\ln N)\mathcal{F}(x_i, y) + O(N^{-2}\ln^2 N), \tag{4.5.12}$$

by following the idea of [73].

Similarly, in the finer mesh of the temporal direction, we get that

$$(\widehat{\mathcal{W}} - \widehat{\psi}_w)(x_i, y, t_{n+1/2}) = (N^{-1}\ln N)\mathcal{F}(x_i, y) + O(N^{-2}\ln^2 N).$$

Now, one can easily obtain, that

$$\left(\widehat{W}_{extp^t} - \widehat{w}_{extp^t}\right)(x_i, y, t_{n+1/2}) = (N^{-1}\ln N)\mathcal{F}(x_i, y) + O(N^{-2}\ln^2 N).$$

So,

$$\begin{aligned} &\left|\left(\widehat{W}_{extp} - \widehat{w}_{extp^t}\right)(x_i, y, t_{n+1/2})\right| \\ &= \left|\left(2\widehat{\mathcal{W}}_{extp^t} - \widehat{W}_{extp^t} - \widehat{w}_{extp^t}\right)(x_i, y, t_{n+1/2})\right| \\ &= \left|\left(2\left(\widehat{\mathcal{W}}_{extp^t} - \widehat{w}_{extp^t}\right) - \left(\widehat{W}_{extp^t} - \widehat{w}_{extp^t}\right)\right)(x_i, y, t_{n+1/2})\right| \\ &\leq CN^{-2}\ln^2 N. \end{aligned}$$

Therefore, we can state the following lemma.

Lemma 4.5.7. *The error after extrapolation associated to the singular component $\widehat{W}$ satisfies*

$$\left|\left(\widehat{W}_{extp} - \widehat{w}_{extp^t}\right)(x_i, y, t_{n+1/2})\right| \leq C\left(N^{-2}\ln^2 N\right), \quad \textit{for} \quad N/2 + 1 \leq i \leq N - 1.$$

Now, by combining the results of Lemmas 4.5.4, 4.5.6 and 4.5.7, we obtain that

$$\left|\left(\widehat{u}^{n+1/2}_{extp^t} - \widehat{U}^{n+1/2}_{extp}\right)(x_i, y)\right| \leq CN^{-2}\ln^2 N. \tag{4.5.13}$$

The following theorem provides the error bound for the solution of (4.4.2).

Theorem 4.5.8. *Let $\widehat{u}^{n+1}$ and $\widehat{U}^{n+1}_{x,y_j}$ be the solutions of (4.2.5) and (4.4.2), respectively, defined on the special mesh Ω^N_y. Then, we have the following error bound:*

$$\left|\left(\widehat{u}^{n+1}_{extp^t} - \widehat{U}^{n+1}_{extp}\right)(x, y_j)\right| \leq CN^{-2}\ln^2 N, \quad \text{for } 1 \leq j \leq N-1. \tag{4.5.14}$$

Proof. The semidiscrete problems (4.2.4) and (4.2.5) are almost of the same type except the first term in the right hand side of both the equations, *i.e.*, the right hand side of (4.2.5) contains $\widehat{u}^{n+1/2}$ instead of $u(x, y, t_n)$ as in (4.2.4). So, by decomposing $\widehat{u}^{n+1/2}$, $\widehat{u}^{n+1}$, $\widehat{U}^{n+1/2}$ and $\widehat{U}^{n+1}$ of (4.2.5) and (4.4.2) into the smooth and singular components and using (4.5.9), (4.5.11), (4.5.12) and proceeding in a similar way as done before, we can obtain the required bound. ∎

The main result of this chapter is stated in the following theorem.

Theorem 4.5.9. *(Error after extrapolation) Assume that $\varepsilon \leq N^{-1}$. Let u be the solution of the continuous problem (4.1.1) and U_{extp} be the solution obtained via the Richardson extrapolation technique, by solving the fully discrete scheme (4.4.7)-(4.4.8) at time level $t_n = n\Delta t$ on two meshes $\mathfrak{G}^{N,M}$ and $\mathfrak{G}^{2N,2M}$. Then, for $0 < q < 1$, we have the following error bound associated with U_{extp}:*

$$\|u(x_i, y_j, t_n) - U_{extp}(x_i, y_j, t_n)\|_\infty \leq C\left(N^{-2+q}\ln^2 N + \Delta t^2\right), \quad (x_i, y_j, t_n) \in \mathfrak{G}^{N,M}.$$

Proof.

$$\begin{aligned}
\|(u - U_{extp})(x_i, y_j, t_n)\|_\infty &= \left\|\left(u - \widehat{u}_{extp^t} + \widehat{u}_{extp^t} - \widehat{U}_{extp} + \widehat{U}_{extp} - U_{extp}\right)(x_i, y_j, t_n)\right\|_\infty \\
&\leq \|(u - \widehat{u}_{extp^t})(x_i, y_j, t_n)\|_\infty + \left\|\left(\widehat{u}_{extp^t} - \widehat{U}_{extp}\right)(x_i, y_j, t_n)\right\|_\infty \\
&\quad + \left\|\left(\widehat{U}_{extp} - U_{extp}\right)(x_i, y_j, t_n)\right\|_\infty \\
&\leq C\left(\Delta t^3 + N^{-2}\ln^2 N\right) + \left\|\left(\widehat{U}_{extp} - U_{extp}\right)(x_i, y_j, t_n)\right\|_\infty, \\
&\qquad \text{(by using (4.3.7) and (4.5.14)).}
\end{aligned}$$

Note that, if we take $N^{-q} \leq C\Delta t$ with $0 < q < 1$, we can deduce that

$$\begin{aligned}
\|(u - U_{extp})(x_i, y_j, t_n)\|_\infty &= C\Delta t\left(\Delta t^2 + N^{-2+q}\ln^2 N\right) \\
&\quad + \left\|\left(\widehat{U}_{extp} - U_{extp}\right)(x_i, y_j, t_n)\right\|_\infty.
\end{aligned} \tag{4.5.15}$$

Then, by using the stability of the fully discrete scheme, it can be obtained that

$$\left\|\left(\widehat{U}_{extp} - U_{extp}\right)(x_i, y_j, t_n)\right\|_\infty \leq \left\|u(x_i, y_j, t_{n-1}) - U^{n-1}_{extp_{x_i,y_j}}\right\|_\infty.$$

Hence, (4.5.15) can be written as

$$\|u(x_i, y_j, t_n) - U_{extp}(x_i, y_j, t_n)\|_\infty \leq C\left(N^{-2+q}\ln^2 N + \Delta t^2\right).$$

Hereby, the proof is complete. ∎

4.6 Numerical Results

This section computationally verifies the theoretical results obtained in the previous section. We apply the proposed higher-order method on two 2D test problems by choosing the transition parameter $\rho_{l,0} = 2.1$, $l = x, y$. Note that in the following examples, we decompose the source term $f(x, y, t)$ in the form

$$f_2(x, y, t) = f(x, 0, t) + y\left(f(x, 1, t) - f(x, 0, t)\right), \quad f_1(x, y, t) = f(x, y, t) - f_2(x, y, t),$$

so that the property (4.2.1) is satisfied under the following compatibility condition:

$$f(0, 0, t) = f(0, 1, t) = f(1, 0, t) = f(1, 1, t) = 0, \quad \text{for } t \in [0, T].$$

Example 4.6.1. *Consider the following singularly perturbed 2D parabolic IBVP with constant coefficients:*

$$\begin{cases} u_t - \varepsilon\Delta u + u_x + u_y = f(x, y, t), & (x, y, t) \in \mathfrak{D} \times (0, 1], \\ u(x, y, 0) = s(x, y), & (x, y) \in \overline{\mathfrak{D}}, \\ u(x, y, t) = 0, & (x, y, t) \in \partial\mathfrak{D} \times [0, 1]. \end{cases} \tag{4.6.1}$$

We choose the initial data $s(x, y)$ and the source function $f(x, y, t)$ to fit with the exact solution

$$u(x, y, t) = (1-\exp(-t))\left(m_1 + m_2 x + \exp(-(1-x)/\varepsilon)\right)\left(m_1 + m_2 y + \exp(-(1-y)/\varepsilon)\right),$$

where $m_1 = -\exp(-1/\varepsilon)$, $m_2 = -1 - m_1$. We calculate the maximum pointwise error for each ε by

$$e_\varepsilon^{N,\Delta t} = \max_{(x_i, y_j, t_n) \in \mathfrak{G}^{N,M}} \left|u(x_i, y_j, t_n) - U(x_i, y_j, t_n)\right|, \quad (\text{before extrapolation}),$$

and

$$e_{\varepsilon,\, extp}^{N,\Delta t} = \max_{(x_i, y_j, t_n) \in \mathfrak{G}^{N,M}} \left|u(x_i, y_j, t_n) - U_{extp}(x_i, y_j, t_n)\right|, \quad (\text{after extrapolation}),$$

where $u(x_i, y_j, t_n)$, $U(x_i, y_j, t_n)$ and $U_{extp}(x_i, y_j, t_n)$ denote the exact solution, the numerical solution obtained before extrapolation and the numerical solution obtained after extrapolation in $\mathfrak{G}^{N,M}$ with N mesh-intervals in the spatial direction and M mesh-intervals in the temporal direction, such that $\Delta t = T/M$ is the uniform mesh-size. We determine the corresponding order of convergence for each ε by

$$p_\varepsilon^{N,\Delta t} = \log_2\left(\frac{e_\varepsilon^{N,\Delta t}}{e_\varepsilon^{2N,\Delta t/2}}\right), \quad (\text{before extrapolation}),$$

and

$$p^{N,\Delta t}_{\varepsilon,\,extp} = \log_2\left(\frac{e^{N,\Delta t}_{\varepsilon,\,extp}}{e^{2N,\Delta t/2}_{\varepsilon,\,extp}}\right), \quad \text{(after extrapolation)}.$$

Now, for each N and Δt, we define the ε-uniform maximum pointwise error by

$$e^{N,\Delta t} = \max_{\varepsilon} e^{N,\Delta t}_{\varepsilon}, \quad \text{(before extrapolation)},$$

and

$$e^{N,\Delta t}_{extp} = \max_{\varepsilon} e^{N,\Delta t}_{\varepsilon,\,extp}, \quad \text{(after extrapolation)},$$

and the corresponding ε-uniform order of convergence by

$$p^{N,\Delta t} = \log_2\left(\frac{e^{N,\Delta t}}{e^{2N,\Delta t/2}}\right), \quad \text{(before extrapolation)},$$

and

$$p^{N,\Delta t}_{extp} = \log_2\left(\frac{e^{N,\Delta t}_{extp}}{e^{2N,\Delta t/2}_{extp}}\right), \quad \text{(after extrapolation)}.$$

Next, we consider an example with variable coefficients.

Example 4.6.2. *Consider the following singularly perturbed 2D parabolic IBVP:*

$$\begin{cases} u_t - \varepsilon\Delta u + (1+x)u_x + (2-y)u_y + (x^2+y^2+1)u = f(x,y,t), & (x,y,t) \in \mathfrak{D} \times (0,1], \\ u(x,y,0) = s(x,y), & (x,y) \in \overline{\mathfrak{D}}, \\ u(x,y,t) = 0, & (x,y,t) \in \partial\mathfrak{D} \times [0,1]. \end{cases} \tag{4.6.2}$$

We choose the initial data $s(x,y)$ and the source function $f(x,y,t)$ to fit with the exact solution

$$u(x,y,t) = \exp(-t)xy(\gamma_1(x)-1)(\gamma_2(y)-1),$$

with

$$\gamma_1(x) = \exp(-(3-2x-x^2)/(2\varepsilon)) \quad \text{and} \quad \gamma_2(y) = \exp(-(3-4y+y^2)/(2\varepsilon)).$$

We calculate the maximum pointwise error and the corresponding order of convergence in a similar way as discussed earlier. The calculated maximum pointwise errors and the corresponding order of convergence for the Examples 4.6.1 and 4.6.2 are presented in the Tables 4.1 and 4.2, respectively, for various values of ε and N. From both the Tables 4.1 and 4.2, we can observe that for fixed ε, the maximum pointwise errors computed before and after extrapolation, decrease monotonically as N increases, which confirms that the proposed method is ε-uniform convergent. One can observe that the maximum

pointwise errors and the corresponding order of convergence have been improved after the extrapolation technique. To visualize the appearance of the boundary layer and its behavior for different ε, we have given the surface plots of the solutions of the Examples 4.6.1 and 4.6.2 for $\varepsilon = 10^{-2}, 10^{-8}$ and $N = 32$ in the Figures 4.1 and 4.3, respectively. Moreover, the maximum pointwise errors (before and after extrapolation) for Examples 4.6.1 and 4.6.2 are plotted in loglog scale in the Figures 4.2 and 4.4, respectively. These figures clearly show that the Richardson extrapolation technique increases the order of convergence from first-order to second-order, which supports the theoretical results obtained in the previous section.

4.7 Conclusions

In this chapter, we have solved the singularly perturbed 2D parabolic convection-diffusion problem of the form (4.1.1), using the uniform mesh for the temporal domain and the piecewise-uniform Shishkin mesh for the spatial domains. To discretize the time derivative, we have used the fractional-step method then to solve the 1D stationary problems resulting of the first step, we have used the classical upwind scheme. To obtain second-order uniformly convergent numerical solution of (4.1.1), we have applied the Richardson extrapolation technique. For that, we have obtained the numerical solution of the discrete problems on two embedded meshes, first with $N + 1$ and $M + 1$ number of mesh-points in the spatial (both x and y) and temporal directions, respectively, then with $2N + 1$ and $2M + 1$ number of mesh-points (by fixing the transition parameter), then we have calculated the extrapolated solution by using these two numerical results. Theoretically we have proved that the extrapolation provides almost second-order ε-uniform convergence. Numerical experiments are carried out to validate the theoretical findings.

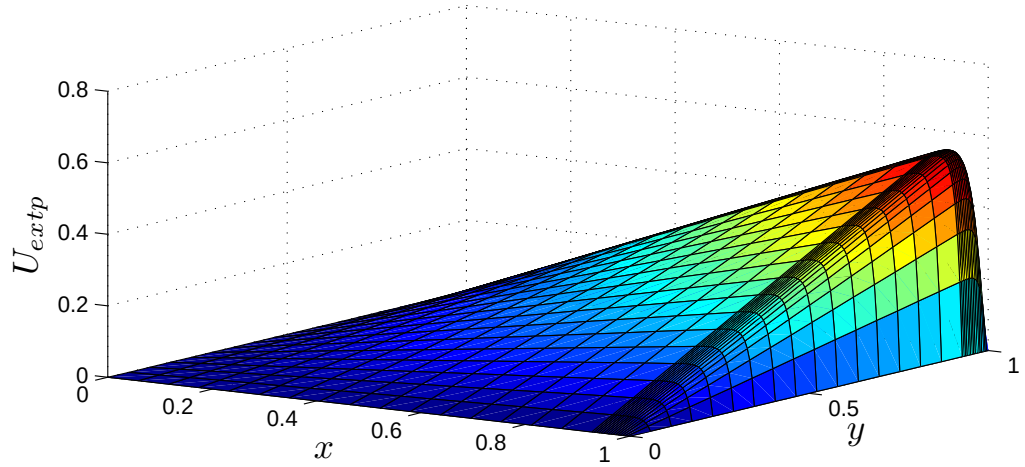

(a) $\varepsilon = 1e-2$.

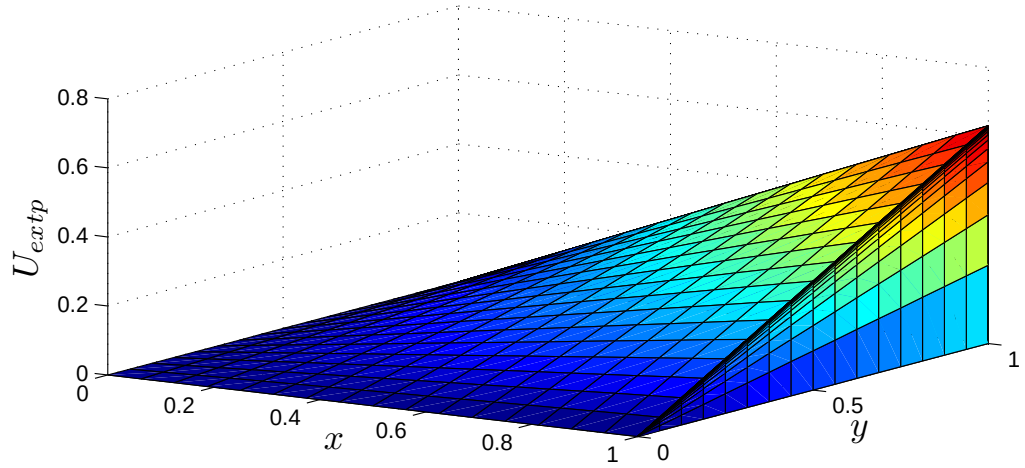

(b) $\varepsilon = 1e-8$.

Figure 4.1: *Surface plots of the numerical solutions at* $t = 1$ *and* $N = 32$ *for Example 4.6.1.*

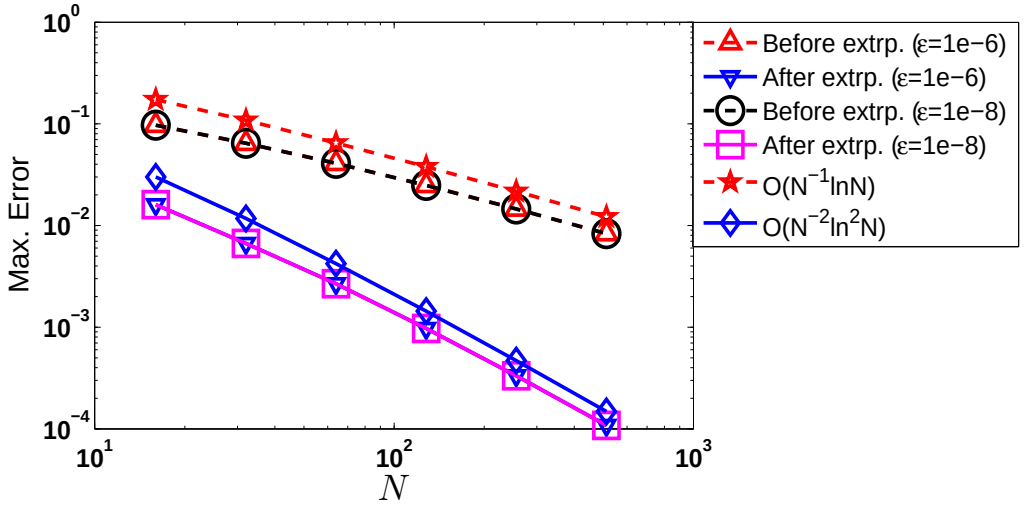

Figure 4.2: *Visualization of the order of convergence through loglog plot for Example 4.6.1.*

Table 4.1: *Maximum pointwise errors and the corresponding order of convergence for Example 4.6.1.*

ε	Extrapolation	Number of mesh-intervals N/temporal mesh-size Δt				
		$32/\frac{1}{40}$	$64/\frac{1}{80}$	$128/\frac{1}{160}$	$256/\frac{1}{320}$	$512/\frac{1}{640}$
10^{-2}	Before	6.0581e-2	3.8660e-2	2.3563e-2	1.3843e-2	7.9089e-3
		0.6480	0.7143	0.7674	0.8076	
	After	6.1159e-3	2.4952e-3	9.1768e-4	3.1554e-4	1.0285e-4
		1.2934	1.4431	1.5402	1.6173	
10^{-4}	Before	6.4451e-2	4.0922e-2	2.4817e-2	1.4550e-2	8.3103e-3
		0.6553	0.7216	0.7703	0.8081	
	After	6.6600e-3	2.6722e-3	9.7208e-4	3.3234e-4	1.0791e-4
		1.3175	1.4589	1.5484	1.6229	
10^{-6}	Before	6.4493e-2	4.0947e-2	2.4830e-2	1.4557e-2	8.3144e-3
		0.6554	0.7217	0.7703	0.8081	
	After	6.6688e-3	2.6757e-3	9.7341e-4	3.3287e-4	1.0811e-4
		1.3175	1.4588	1.5481	1.6225	
10^{-8}	Before	6.4493e-2	4.0947e-2	2.4830e-2	1.4557e-2	8.3145e-3
		0.6554	0.7217	0.7703	0.8080	
	After	6.6689e-3	2.6758e-3	9.7337e-4	3.3286e-4	1.0816e-4
		1.3175	1.4589	1.5481	1.6217	
$e^{N,\Delta t}$	Before	**6.4493e-2**	**4.0947e-2**	**2.4830e-2**	**1.4557e-2**	**8.3145e-3**
$p^{N,\Delta t}$		**0.6554**	**0.7217**	**0.7703**	**0.8080**	
$e^{N,\Delta t}_{extp}$	After	**6.6689e-3**	**2.6758e-3**	**9.7341e-4**	**3.3287e-4**	**1.0816e-4**
$p^{N,\Delta t}_{extp}$		**1.3175**	**1.4588**	**1.5481**	**1.6217**	

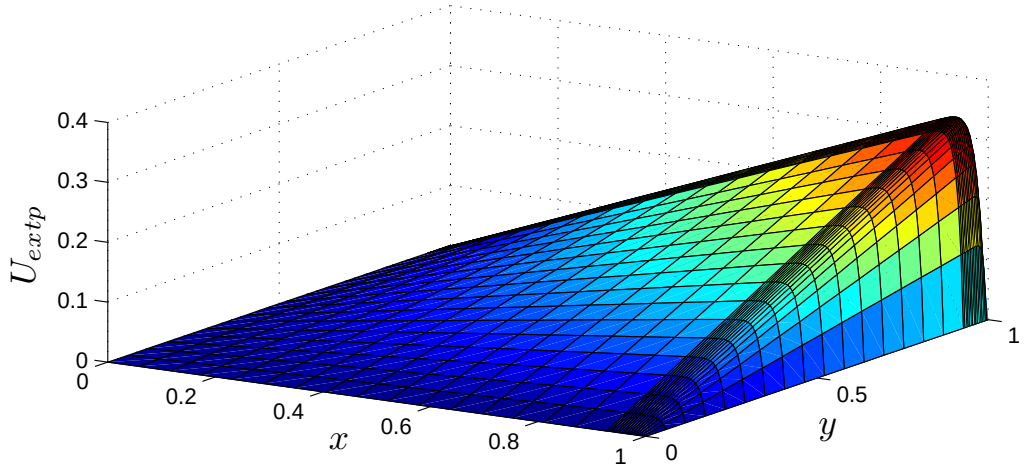

(a) $\varepsilon = 1e-2$.

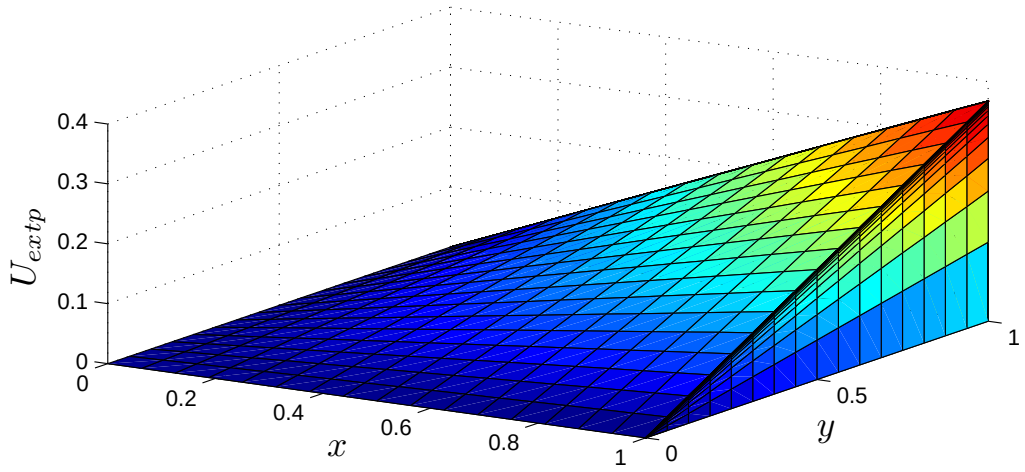

(b) $\varepsilon = 1e-8$.

Figure 4.3: *Surface plots of the numerical solutions at* $t = 1$ *and* $N = 32$ *for Example 4.6.2.*

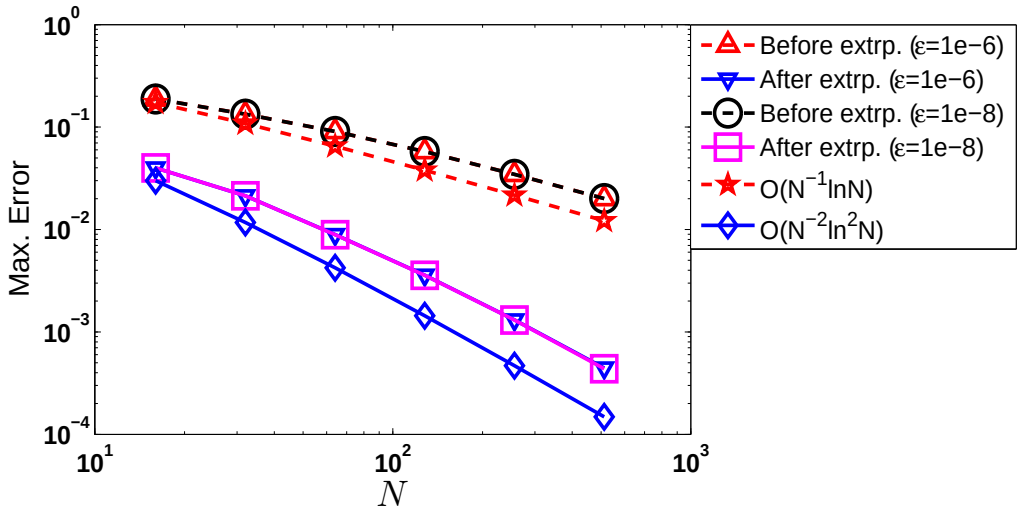

Figure 4.4: *Visualization of the order of convergence through loglog plot for Example 4.6.2.*

Table 4.2: *Maximum pointwise errors and the corresponding order of convergence for Example 4.6.2.*

ε	Extrapolation	Number of mesh-intervals N/temporal mesh-size Δt				
		$32/\frac{1}{40}$	$64/\frac{1}{80}$	$128/\frac{1}{160}$	$256/\frac{1}{320}$	$512/\frac{1}{640}$
10^{-2}	Before	1.2074e-1	8.2246e-2	5.2326e-2	3.1338e-2	1.8177e-2
		0.5539	0.6524	0.7396	0.7858	
	After	2.5458e-2	1.2441e-2	5.6588e-3	2.2416e-3	7.8676e-4
		1.0330	1.1365	1.3359	1.5106	
10^{-4}	Before	1.3323e-1	9.0067e-2	5.7453e-2	3.4445e-02	1.9972e-02
		0.5649	0.6486	0.7381	0.7863	
	After	2.1589e-2	9.3819e-3	3.8133e-3	1.4696e-3	5.5284e-4
		1.2023	1.2988	1.3756	1.4105	
10^{-6}	Before	1.3376e-1	9.0614e-2	5.7744e-2	3.4572e-2	2.0030e-2
		0.5618	0.6501	0.7401	0.7875	
	After	2.1305e-2	8.9155e-3	3.5800e-3	1.3122e-3	4.4522e-4
		1.2568	1.3164	1.4479	1.5594	
10^{-8}	Before	1.3376e-1	9.0620e-2	5.7751e-2	3.4580e-2	2.0040e-2
		0.5618	0.6500	0.7399	0.7871	
	After	2.1302e-2	8.9105e-3	3.5751e-3	1.3057e-3	4.3800e-4
		1.2574	1.3175	1.4532	1.5758	
$e^{N,\Delta t}$	Before	**1.3376e-1**	**9.0620e-2**	**5.7751e-2**	**3.4580e-2**	**2.0040e-2**
$p^{N,\Delta t}$		**0.5618**	**0.6500**	**0.7399**	**0.7871**	
$e^{N,\Delta t}_{extp}$	After	**2.5458e-2**	**1.2441e-2**	**5.6588e-3**	**2.2416e-3**	**7.8676e-4**
$p^{N,\Delta t}_{extp}$		**1.0330**	**1.1365**	**1.3359**	**1.5106**	

CHAPTER 5

Parameter-Uniform Numerical Method for Singularly Perturbed 2D Delay Parabolic Convection-Diffusion Problems on Shishkin Mesh

This chapter is devoted to develop and analyze an efficient numerical scheme for solving singularly perturbed 2D delay parabolic convection-diffusion problems. First, we discretize the domain with the uniform mesh in the temporal direction and the piecewise-uniform Shishkin mesh in the spatial directions. The numerical scheme used to discretize the continuous problem, consists of the implicit-Euler scheme for the time derivative and the classical upwind scheme for the spatial derivatives. Stability analysis is carried out and parameter-uniform error estimates are derived. The proposed scheme is of almost first-order (up to a logarithmic factor) in space and first-order in time. Numerical examples are carried out to verify the theoretical results.

5.1 Introduction

Here, we consider the following singularly perturbed 2D delay parabolic convection-diffusion IBVP posed on the domain $\mathfrak{G} = \mathfrak{D} \times \Lambda_t$, $\mathfrak{D} = (0,1)^2$, $\Lambda_t = (0,T]$ and $\Upsilon = \partial\mathfrak{D} \cup \Upsilon_b$, where $\Upsilon_b = \overline{\mathfrak{D}} \times [-\tau, 0]$:

$$\begin{cases} u_t + \mathcal{L}_\varepsilon u(x,y,t) = -c(x,y)u(x,y,t-\tau) + f(x,y,t), & (x,y,t) \in \mathfrak{G}, \\ u(x,y,t) = \varphi_b(x,y,t), & (x,y,t) \in \Upsilon_b, \\ u(x,y,t) = 0, & (x,y,t) \in \partial\mathfrak{D} \times \overline{\Lambda}_t, \end{cases} \tag{5.1.1}$$

where

$$\mathcal{L}_\varepsilon u = -\varepsilon\Delta u + \mathbf{a}(x,y).\nabla u + b(x,y)u,$$

$0 < \varepsilon \ll 1$ is the singular perturbation parameter and $\tau > 0$ is the delay parameter. The coefficients $\mathbf{a} = (a_1, a_2)$, b and c are sufficiently smooth and bounded functions such

that $a_1(x,y) \geq \alpha_{_x} > 0$, $a_2(x,y) \geq \alpha_{_y} > 0$, $b(x,y) \geq 0$ and $c(x,y)$ is nonzero on $\overline{\mathfrak{D}}$.

Under sufficient smoothness and necessary compatibility conditions imposed on the functions f and φ_b (which is given in the next section), the delay parabolic IBVP (5.1.1) admits a unique solution $u(x,y,t)$, which exhibits a regular boundary layer of width $O(\varepsilon)$ along the sides $x=1$ and $y=1$, and a corner layer at $(x,y)=(1,1)$.

The main aim of this chapter is to devise an ε-uniform numerical scheme to solve the delay parabolic PDE (5.1.1). Because of the presence of boundary layers, we discretize the spatial domains with a special piecewise-uniform Shishkin mesh and the temporal domain by the uniform mesh. Then, to obtain the discrete problem, we apply the implicit-Euler scheme for the time derivative and the classical upwind scheme for the spatial derivatives. Numerical stability of the proposed scheme is studied. The proposed method is of almost first-order accurate in spatial variables and first-order accurate in temporal variable. Numerical experiments are carried out to show the accuracy and efficiency of the proposed method.

The outline of this chapter is as follows: In Section 5.2, the bounds for the components of the solution of (5.1.1) have been discussed. Section 5.3 deals with the piecewise-uniform Shishkin mesh and the upwind scheme. The main result of ε-uniform convergence has been given in Section 5.4. Numerical results are presented in Section 5.5 and the chapter ends with Section 5.6, that summarizes the main conclusions.

5.2 Decomposition of the Solution and their Bounds

In this section, we present the analytical aspects of the solution of (5.1.1), which will be required for the proof of ε-uniform error estimate. The existence and uniqueness of the solution of (5.1.1) can be guaranteed under the assumption that the data are Hölder continuous and also satisfy the following compatibility conditions [48]:

$$f(0,0,t) = f(0,1,t) = f(1,0,t) = f(1,1,t) = 0, \quad t \in \overline{\Lambda}_t,$$

$$\varphi_b(x,y,0) = 0, \quad \text{in} \quad \partial\mathfrak{D},$$

$$\mathcal{L}_\varepsilon \varphi_b(x,y,0) = -c(x,y)\varphi_b(x,y,-\tau) + f(x,y,0), \quad \text{in} \quad \partial\mathfrak{D}.$$

Along with the above conditions, we assume that data of the problem are sufficiently smooth and satisfy stronger compatibility conditions in order to have $u(x,y,t) \in \mathcal{C}^{4,2}(\mathfrak{G})$. The additional sufficient higher-order compatibility conditions for (5.1.1) can be obtained as follows:

For $0 < \mu < 1$, if $f \in \mathcal{C}^{2+2\mu,1+\mu}(\overline{\mathfrak{G}})$ and $\varphi_b \in \mathcal{C}^{4,2}(\mathfrak{D} \times \{0\})$, then differentiating (5.1.1) with respect to t, we get

$$\frac{\partial^2 u}{\partial t^2} - \mathcal{L}_\varepsilon(\mathcal{L}_\varepsilon u) = \frac{\partial F}{\partial t} - \mathcal{L}_\varepsilon F,$$

where $F = f - cu(x, y, t - \tau)$. Now, by using the boundary condition given in (5.1.1), we obtain the second-order compatibility condition

$$\mathcal{L}_\varepsilon(\mathcal{L}_\varepsilon\varphi_b(x, y, 0)) = \mathcal{L}_\varepsilon F(x, y, 0) - \frac{\partial F}{\partial t}(x, y, 0), \quad \text{in} \quad \partial\mathfrak{D}.$$

Now, in order to obtain the ε-uniform error estimate, we decompose the solution of problem (5.1.1) as $u = G + E$, where G and E are the smooth and singular components, respectively, which are defined as solutions of the following problems, *i.e.*, E is the solution of

$$\begin{cases} E_t + \mathcal{L}_\varepsilon E(x, y, t) = -c(x, y)E(x, y, t - \tau), & (x, y, t) \in \mathfrak{G}, \\ E(x, y, t) = 0, & (x, y, t) \in \Upsilon_b, \\ E(x, y, t) = -G(x, y, t), & (x, y, t) \in \partial\mathfrak{D} \times \overline{\Lambda}_t, \end{cases} \tag{5.2.1}$$

and G is the restriction of G^* to $\mathfrak{G}$, where G^* is the solution of

$$\begin{cases} G^*_t + \mathcal{L}^*_\varepsilon G^*(x, y, t) = -c^*(x, y)G^*(x, y, t - \tau) + f^*(x, y, t), & (x, y, t) \in \mathfrak{G}^* = \mathfrak{D}^* \times \Lambda_t, \\ G^*(x, y, t) = \varphi^*_b(x, y, t), & (x, y, t) \in \Upsilon^*_b = \overline{\mathfrak{D}}^* \times [-\tau, 0], \\ G^*(x, y, t) = \varphi^*(x, y, t), & (x, y, t) \in \partial\mathfrak{D}^* \times \overline{\Lambda}_t. \end{cases} \tag{5.2.2}$$

The domain $\mathfrak{D}^*$ is a smooth extension of $\mathfrak{D}$, c^*, f^* are smooth extensions of c, f to $\mathfrak{G}^*$, φ^*_b is smooth extension of φ_b to Υ^*_b, φ^* is a smooth and compatible function and $\mathcal{L}^*_\varepsilon$ corresponds to the current extensions of the data.

Moreover, the singular component E can be decomposed into the sum $E = E_1 + E_2 + E_{12}$, where E_1 (similarly E_2) is the restriction of E^{**}_1 to $\mathfrak{G}$, where E^{**}_1 is the solution of

$$\begin{cases} (E^{**}_1)_t + \mathcal{L}^{**}_\varepsilon E^{**}_1(x, y, t) = -c^{**}(x, y)E^{**}_1(x, y, t - \tau), & (x, y, t) \in \mathfrak{G}^{**} = \mathfrak{D}^{**} \times \Lambda_t, \\ E^{**}_1(x, y, t) = 0, & (x, y, t) \in \Upsilon^{**}_b = \overline{\mathfrak{D}}^{**} \times [-\tau, 0], \\ E^{**}_1(x, y, t) = -G^{**}(x, y, t), & (x, y, t) \in \partial\mathfrak{D}^{**}_1 \times \overline{\Lambda}_t, \\ E^{**}_1(x, y, t) = 0, & (x, y, t) \in \partial\mathfrak{D}^{**}_2 \times \overline{\Lambda}_t. \end{cases} \tag{5.2.3}$$

The domain $\mathfrak{D}^{**}$ is the smooth extension of $\mathfrak{D}$ near the vertex $(1, 1)$. Along the boundary side $x = 1$, $\partial\mathfrak{D}^{**}_1$ is an extension beyond the vertex $(1, 1)$ and $\partial\mathfrak{D}^{**}_2 = \partial\mathfrak{D}^{**} \backslash \partial\mathfrak{D}^{**}_1$. G^{**} is a smooth and compatible extension of G to $\partial\mathfrak{D}^{**}_1$.

Finally, E_{12} is defined as the solution of the problem

$$\begin{cases} (E_{12})_t + \mathcal{L}_\varepsilon E_{12}(x, y, t) = -c(x, y)E_{12}(x, y, t - \tau), & (x, y, t) \in \mathfrak{G}, \\ E_{12}(x, y, t) = 0, & (x, y, t) \in \Upsilon_b, \\ E_{12}(x, y, t) = -(G + E_1 + E_2), & (x, y, t) \in \partial\mathfrak{D} \times \overline{\Lambda}_t. \end{cases} \tag{5.2.4}$$

Here, E_1 and E_2 are the singular components associated with the sides $x = 1$ and $y = 1$, respectively, and E_{12} is a corner layer function associated with the corner $(1, 1)$.

The following theorem provides the bounds for the derivative of the components of the solution of problem (5.1.1). This theorem will be used to estimate the truncation error associated with the proposed technique. Before stating the theorem, with out loss of generality, we assume the initial condition of (5.1.1) is zero, *i.e.*, $\varphi_b(x, y, t) = 0,\ (x, y, t) \in \Upsilon_b$.

Theorem 5.2.1. *For all non-negative integers k_1, k_2, k_t such that $k_s = k_1+k_2$, $k_s+2k_t \leq 4$, and for $(x, y, t) \in \mathfrak{G}$, the components of u satisfy the following bounds:*

$$\begin{aligned}
&\left|\frac{\partial^{k_s+k_t} G}{\partial x^{k_1}\partial y^{k_2}\partial t^{k_t}}\right| \leq C,\\
&\left|\frac{\partial^{k_s+k_t} E_1}{\partial x^{k_1}\partial y^{k_2}\partial t^{k_t}}\right| \leq C\varepsilon^{-k_1}\exp(-\alpha_{_x}(1-x)/\varepsilon),\\
&\left|\frac{\partial^{k_s+k_t} E_2}{\partial x^{k_1}\partial y^{k_2}\partial t^{k_t}}\right| \leq C\varepsilon^{-k_2}\exp(-\alpha_{_y}(1-y)/\varepsilon),\\
&\left|\frac{\partial^{k_s+k_t} E_{12}}{\partial x^{k_1}\partial y^{k_2}\partial t^{k_t}}\right| \leq C\varepsilon^{-k_s}\min\{\exp(-\alpha_{_x}(1-x)/\varepsilon), \exp(-\alpha_{_y}(1-y)/\varepsilon)\}.
\end{aligned}$$

Proof. First, we consider the case, when $t \in (0, \tau]$. Then, the DPDE (5.1.1), can be written as

$$\begin{cases}
u_t + \mathcal{L}_\varepsilon u(x, y, t) = -c(x, y)u(x, y, t-\tau) + f(x, y, t), & (x, y, t) \in \mathfrak{D} \times (0, \tau),\\
u(x, y, t) = 0, & (x, y, t) \in \Upsilon_b,\\
u(x, y, t) = 0, & (x, y, t) \in \partial\mathfrak{D} \times [0, \tau].
\end{cases} \tag{5.2.5}$$

Now, by using the initial condition, the above equation can be reduced to

$$u_t + \mathcal{L}_\varepsilon u(x, y, t) = f(x, y, t), \quad (x, y, t) \in \mathfrak{D} \times (0, \tau). \tag{5.2.6}$$

According to the result given in [13], one can decompose the solution of (5.2.6) as $u = G+E_1+E_2+E_{12}$, which will satisfy the required bounds, when $(x, y, t) \in \mathfrak{D}\times(0, \tau)$.

Now, we proceed to the next time level, *i.e.*, $t \in (\tau, 2\tau]$. In that case, (5.1.1) can be written as

$$\begin{cases}
u_t + \mathcal{L}_\varepsilon u(x, y, t) = -c(x, y)u(x, y, t-\tau) + f(x, y, t), & (x, y, t) \in \mathfrak{D} \times (\tau, 2\tau),\\
u(x, y, t) = u_\tau(x, y, t), & (x, y, t) \in \mathfrak{D} \times [0, \tau],\\
u(x, y, t) = 0, & (x, y, t) \in \partial\mathfrak{D} \times [\tau, 2\tau],
\end{cases} \tag{5.2.7}$$

where u_τ is the solution of (5.2.5).

One can verify that, the above equation satisfies the required compatibility conditions and the right hand side term of (5.2.7) has sufficient smoothness. Therefore, by using the result given in [14, Appendix A] and [86], one can obtain the required bounds for G, E_1, E_2 and E_{12}, when $t \in [\tau, 2\tau]$.

By proceeding in a similar way, we can obtain the required bounds for $t \geq 2\tau$. ∎

5.3 Domain Discretization

Let the rectangular mesh $\overline{\mathfrak{D}}^N$ be defined to be tensor product of the 1D Shishkin meshes, *i.e.*, $\overline{\mathfrak{D}}^N = \overline{\Omega}_x^N \times \overline{\Omega}_y^N$, which is constructed as follows:

First, define the transition parameters

$$\rho_l = \min\left\{\frac{1}{2}, \rho_{l,0}\varepsilon \ln N\right\},\ l = x,\ y,$$

where $\rho_{l,0} \geq 1/\alpha_l$.

In the analysis, we shall assume that $\rho_l = \rho_{l,0}\varepsilon \ln N$. Note that if $\rho_l = 1/2$, then mesh is uniform and in such cases the method can be analyzed in the classical way. To define the piecewise-uniform mesh, we define the mesh on $\overline{\Omega}_x^N$ by dividing the domain $[0, 1]$ into two sub-domains $[0, 1-\rho_x]$ and $(1-\rho_x, 1]$ and each sub-domain will have $N/2$ uniform mesh-intervals, *i.e.*, $\overline{\Omega}_x^N = \{0 = x_0, x_1, \cdots, x_{N/2} = 1-\rho_x, \cdots, x_N = 1\}$. Similarly, we define $\overline{\Omega}_y^N = \{0 = y_0, y_1, \cdots, y_{N/2} = 1-\rho_y, \cdots, y_N = 1\}$.

We denote the mesh-sizes in both the spatial directions by

$$h_{x,i} = x_i - x_{i-1},\ i = 1, \cdots, N, \quad \widehat{h}_{x,i} = h_{x,i} + h_{x,i+1},\ i = 1, \cdots, N-1,$$

$$h_{y,j} = y_j - y_{j-1},\ j = 1, \cdots, N, \quad \widehat{h}_{y,j} = h_{y,j} + h_{y,j+1},\ j = 1, \cdots, N-1,$$

and let $H_l = 2(1-\rho_l)/N$ and $h_l = 2\rho_l/N$, $l = x, y$, be the mesh-sizes in $[0, 1-\rho_l]$ and $[1-\rho_l, 1]$ respectively. Then it is easy to see that

$$N^{-1} \leq H_l \leq 2N^{-1}, \quad h_l = 2\rho_{l,0}\varepsilon N^{-1} \ln N, \quad l = x,\ y.$$

For the time domain $\overline{\Lambda}_t$, we will use uniform mesh with mesh-size Δt, such that

$$\Lambda_t^M = \{t_n = n\Delta t, n = 0, \cdots, M, \Delta t = T/M\},$$

where M is the number of mesh-points in the t-direction on the interval $[0, T]$ and the temporal mesh-size Δt satisfies the constraint $p\Delta t = \tau$, where p is a positive integer, $t_n = n\Delta t$, $n \geq -p$.

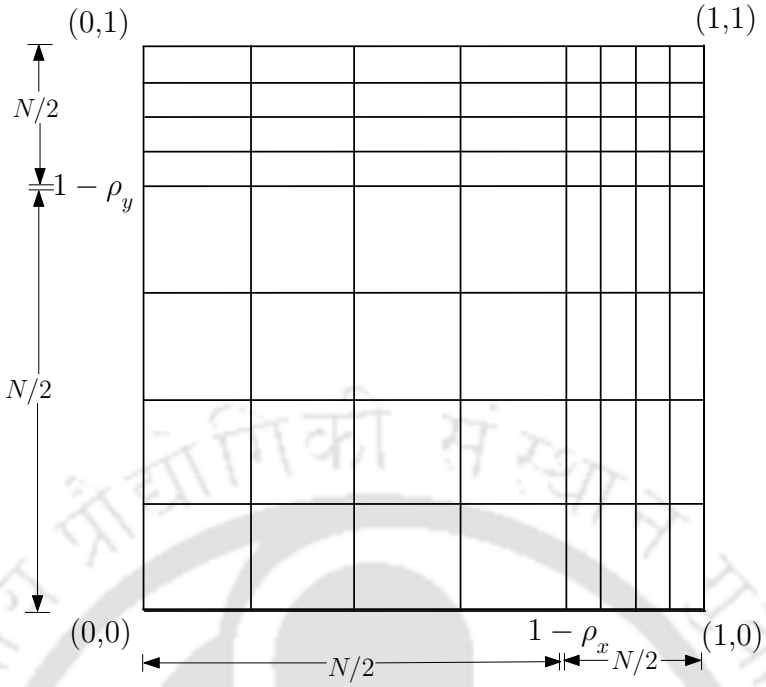

Figure 5.1: *Shishkin mesh in the unit square.*

We define the discrete domain by $\mathfrak{G}^{N,M} = \overline{\mathfrak{G}}^{N,M} \cap \mathfrak{G}$ where $\overline{\mathfrak{G}}^{N,M} = \overline{\Omega}_x^N \times \overline{\Omega}_y^N \times \Lambda_t^M$, and $\Upsilon_b^N = \overline{\Omega}_x^N \times \overline{\Omega}_y^N \times \Lambda_t^p$, where Λ_t^p denotes the set of $p+1$ uniform mesh-points in $[-\tau, 0]$ and $\Omega_x^N = \overline{\Omega}_x^N \cap \Omega_x$, $\Omega_y^N = \overline{\Omega}_y^N \cap \Omega_y$. The boundary points of $\overline{\mathfrak{G}}^{N,M}$ are $\Upsilon^N = \{\overline{\mathfrak{G}}^{N,M} \cap \Upsilon\} \cup \Upsilon_b^N$. We further discretize $\overline{\mathfrak{G}}_s{}^{N,M} = \mathfrak{D}^N \times \Lambda_{s,t}^p$, where $\Lambda_{s,t}^p$ denotes the set of $p+1$ uniform mesh-points in $[(s-1)\tau, s\tau]$, for $s = 1, 2, \cdots, k$. From the above discretization we can observe that $\overline{\mathfrak{G}}^{N,M} = \bigcup_{s=1}^{k} \overline{\mathfrak{G}}_s{}^{N,M}$.

5.3.1 Numerical scheme

We replace the time derivative by the implicit-Euler scheme and the spatial derivatives by the upwind scheme in (5.1.1), and obtain the following discrete problem:

$$\begin{cases} (\delta_t^- + \mathcal{L}_\varepsilon^N) U_{i,j}^{n+1} = -c_{i,j} U_{i,j}^{n+1-p} + f_{i,j}^{n+1}, \quad \text{on} \quad \mathfrak{G}^{N,M}, \\ U_{i,j}^{-s} = \varphi_b(x_i, y_j, -t_s), \quad i, j = 0, \cdots, N, \text{ and } s = 0, \cdots, p, \\ U_{i,j}^{n+1} = 0, \quad i = 0,\ N \text{ or } j = 0,\ N, \text{ and } n = 0, \cdots, M-1, \end{cases} \tag{5.3.1}$$

where

$$\mathcal{L}_\varepsilon^N U_{i,j}^{n+1} = -\varepsilon(\delta_x^2 + \delta_y^2) U_{i,j}^{n+1} + a_{1;i,j} \delta_x^- U_{i,j}^{n+1} + a_{2;i,j} \delta_y^- U_{i,j}^{n+1} + b_{i,j} U_{i,j}^{n+1}.$$

After rearranging the terms in (5.3.1), we obtain the following system of linear algebraic equations:

$$\begin{cases} r_{i,j-}U^{n+1}_{i,j-1} + r_{i-,j}U^{n+1}_{i-1,j} + r_{i,j}U^{n+1}_{i,j} + r_{i+,j}U^{n+1}_{i+1,j} + r_{i,j+}U^{n+1}_{i,j+1} = g^{n+1}_{i,j}, \\ \qquad\qquad \text{for } \ i,j = 1,\cdots,N-1, \text{ and } n = 0,\cdots,M-1, \\ U^{-s}_{i,j} = \varphi_b(x_i, y_j, -t_s), \quad i,j = 0,\cdots,N, \text{ and } s = 0,\cdots,p, \\ U^{n+1}_{i,j} = 0, \quad i = 0,\ N \text{ or } j = 0,\ N, \text{ and } n = 0,\cdots,M-1, \end{cases} \tag{5.3.2}$$

where

$$\begin{cases} r_{i-,j} = \left(-\dfrac{2\varepsilon}{\widehat{h}_{x,i}h_{x,i}} - \dfrac{a_{1;i,j}}{h_{x,i}}\right), & r_{i+,j} = \left(-\dfrac{2\varepsilon}{\widehat{h}_{x,i}h_{x,i+1}}\right), \\ r_{i,j-} = \left(-\dfrac{2\varepsilon}{\widehat{h}_{y,j}h_{y,j}} - \dfrac{a_{2;i,j}}{h_{y,j}}\right), & r_{i,j+} = \left(-\dfrac{2\varepsilon}{\widehat{h}_{y,j}h_{y,j+1}}\right), \\ r_{i,j} = \dfrac{1}{\Delta t} - r_{i-,j} - r_{i+,j} - r_{i,j-} - r_{i,j+} + b_{i,j}, & g^{n+1}_{i,j} = \dfrac{U^n_{i,j}}{\Delta t} - c_{i,j}U^{n-p+1}_{i,j} + f^{n+1}_{i,j}. \end{cases}$$

The finite difference operator $(\delta_t^- + \mathcal{L}_\varepsilon^N)$ defined in (5.3.1) satisfies the following discrete maximum principle on $\mathfrak{G}^{N,M}$, which provides the ε-uniform stability of the difference operator $(\delta_t^- + \mathcal{L}_\varepsilon^N)$.

Lemma 5.3.1. *(***Discrete maximum principle***) Assume that the discrete function* $\Psi^n_{i,j}$ *satisfies* $\Psi^n_{i,j} \geq 0$ *on* Υ^N*. Then* $(\delta_t^- + \mathcal{L}_\varepsilon^N)\Psi^n_{i,j} \geq 0$ *on* $\mathfrak{G}^{N,M}$ *implies that* $\Psi^n_{i,j} \geq 0$ *at each point of* $\overline{\mathfrak{G}}^{N,M}$*.*

Proof. Assume that there exist a point $(x_i^*, y_j^*, t_n^*) \in \overline{\mathfrak{G}}^{N,M}$, such that

$$\Psi(x_i^*, y_j^*, t_n^*) = \min_{(x_i,y_j,t_n)\in\overline{\mathfrak{G}}^{N,M}} \Psi(x_i, y_j, t_n) < 0.$$

Clearly $(x_i^*, y_j^*, t_n^*) \notin \Upsilon^N$, which implies $(x_i^*, y_j^*, t_n^*) \in \mathfrak{G}^{N,M}$.

Now, by applying the operator $(\delta_t^- + \mathcal{L}_\varepsilon^N)$ on $\Psi(x_i^*, y_j^*, t_n^*)$, we get

$$\begin{aligned} (\delta_t^- + \mathcal{L}_\varepsilon^N)\Psi(x_i^*, y_j^*, t_n^*) &= \delta_t^-\Psi(x_i^*, y_j^*, t_n^*) - \varepsilon\delta_x^2\Psi(x_i^*, y_j^*, t_n^*) - \varepsilon\delta_x^2\Psi(x_i^*, y_j^*, t_n^*) \\ &\quad + a_1(x_i^*, y_j^*)\delta_x^-\Psi(x_i^*, y_j^*, t_n^*) + a_2(x_i^*, y_j^*)\delta_y^-\Psi(x_i^*, y_j^*, t_n^*) \\ &\quad + b(x_i^*, y_j^*)\Psi(x_i^*, y_j^*, t_n^*). \end{aligned}$$

Since we have, $\Psi(x_i^*, y_j^*, t_n^*) - \Psi(x_i^*, y_j^*, t_{n-1}^*) < 0$, $\Psi(x_i^*, y_j^*, t_n^*) - \Psi(x_{i-1}^*, y_j^*, t_n^*) < 0$, $\Psi(x_i^*, y_j^*, t_n^*) - \Psi(x_i^*, y_{j-1}^*, t_n^*) < 0$, $\Psi(x_{i+1}^*, y_j^*, t_n^*) - \Psi(x_i^*, y_j^*, t_n^*) > 0$ and $\Psi(x_i^*, y_{j+1}^*, t_n^*) - \Psi(x_i^*, y_j^*, t_n^*) > 0$, therefore

$$(\delta_t^- + \mathscr{L}_\varepsilon^N)\Psi(x_i^*, y_j^*, t_n^*) < 0,$$

which is a contradiction as $(\delta_t^- + \mathscr{L}_\varepsilon^N)\Psi(x_i, y_j, t_n) \geq 0$, for all $(x_i, y_j, t_n) \in \mathfrak{G}^{N,M}$. Hence $\Psi(x_i, y_j, t_n) \geq 0$, for all $(x_i, y_j, t_n) \in \overline{\mathfrak{G}}^{N,M}$. ∎

5.4 Error Analysis

In this section, we provide the important theorem for the ε-uniform convergence of the numerical solution in the discrete maximum norm.

Theorem 5.4.1. *Let u and U be the solutions of the continuous problem (5.1.1) and the discrete problem (5.3.1), respectively. Then, we have the following error bound*

$$||u(x_i, y_j, t_n) - U^n_{i,j}||_\infty \leq C(N^{-1} \ln N + \Delta t), \quad (x_i, y_j, t_n) \in \mathfrak{G}^{N,M}.$$

Proof. We can notice that on the first interval $[0, \tau]$, *i.e.,* where the time discretization parameter n varies from 0 to p, the initial conditions of the continuous problem (5.1.1) and the discrete problem (5.3.1) will be same. So, the analysis can be carried out in the same way as one can do for a problem with out delay. Hence, by using the convergence result of [13], we can obtain

$$||u(x_i, y_j, t_n) - U^n_{i,j}||_\infty \leq C(N^{-1} \ln N + \Delta t), \quad (x_i, y_j, t_n) \in \mathfrak{G}_1^{N,M}. \tag{5.4.1}$$

For the second interval $(\tau, 2\tau]$, the approach of [13] is not applicable because, the value of the delay term involves in the right hand side of (5.3.1) will be the numerical solution obtained in previous time interval $[0, \tau]$. So, we will provide the detailed proof to get the error over the interval $(\tau, 2\tau]$.

On the domain $\mathfrak{G}_2 = \mathfrak{D} \times (\tau, 2\tau)$, we consider the following singularly perturbed delay parabolic equation:

$$\begin{cases} u_t + \mathcal{L}_\varepsilon u(x, y, t) = -c(x, y)u(x, y, t - \tau) + f(x, y, t), & (x, y, t) \in \mathfrak{G}_2, \\ u(x, y, t) = u_\tau(x, y, t), & (x, y, t) \in \overline{\mathfrak{G}}_1 = \overline{\mathfrak{D}} \times [0, \tau], \\ u(x, y, t) = 0, & (x, y, t) \in \partial\mathfrak{D} \times (\tau, 2\tau), \end{cases} \tag{5.4.2}$$

where u_τ is the exact solution on $\mathfrak{G}_1$.

We apply the implicit-Euler scheme for the time derivative and the upwind scheme for the spatial derivatives to determine the numerical solution U of (5.4.2) at $\mathfrak{G}_2^{N,M}$. The discrete problem corresponding to (5.4.2) is given by

$$\begin{cases} \delta_t^- U^n_{i,j} - \varepsilon(\delta_x^2 + \delta_y^2)U^n_{i,j} + a_{1;i,j}\delta_x^- U^n_{i,j} + a_{2;i,j}\delta_y^- U^n_{i,j} + b_{i,j}U^n_{i,j} = -c_{i,j}U^{n-p}_{i,j} + f^n_{i,j}, \text{ on } \mathfrak{G}_2^{N,M}, \\ U(x_i, y_j, t_n) = U_1(x_i, y_j, t_n), \quad (x_i, y_j, t_n) \in \overline{\mathfrak{G}}_1^{N,M}, \\ U(x_i, y_j, t_n) = 0, \quad i = 0,\ N \text{ or } j = 0,\ N, \text{ and } t_n \in \Lambda^p_{2,t}, \end{cases} \tag{5.4.3}$$

where $U_1(\cdot, \cdot, \cdot)$ is the numerical solution calculated on $\mathfrak{G}_1^{N,M}$.

Now, we split the solution of (5.4.2) as $u = G + E_1 + E_2 + E_{12}$, where the initial conditions in $\mathfrak{G}_1$ are $G = u_\tau(x, y, t)$, $E_1 = 0$, $E_2 = 0$ and $E_{12} = 0$. Following the continuous problem, we decompose the solution of the discrete problem (5.4.3), as

$$U^n_{i,j} = G^n_{i,j} + {E_1}^n_{i,j} + {E_2}^n_{i,j} + {E_{12}}^n_{i,j},$$

where $G^n_{i,j}$ is the solution of

$$\begin{cases} \delta_t^- G^n_{i,j} - \varepsilon(\delta_x^2 + \delta_y^2) G^n_{i,j} + a_{1;i,j}\delta_x^- G^n_{i,j} + a_{2;i,j}\delta_y^- G^n_{i,j} + b_{i,j} G^n_{i,j} = -c_{i,j} G^{n-p}_{i,j} + f^n_{i,j}, \text{ on } \mathfrak{G}_2^{N,M}, \\ G^n_{i,j} = U_1(x_i, y_j, t_n), \quad \text{on } \overline{\mathfrak{G}}_1^{N,M}, \\ G^n_{i,j} = G(x_i, y_j, t_n), \quad i = 0,\ N \text{ or } j = 0,\ N, \text{ and } t_n \in \Lambda^p_{2,t}, \end{cases} \tag{5.4.4}$$

and $E^n_{\ell i,j}$, $\ell = 1,\ 2,\ 12$, satisfy

$$\begin{cases} \delta_t^- E^n_{\ell i,j} - \varepsilon(\delta_x^2 + \delta_y^2) E^n_{\ell i,j} + a_{1;i,j}\delta_x^- E^n_{\ell i,j} + a_{2;i,j}\delta_y^- E^n_{\ell i,j} + b_{i,j} E^n_{\ell i,j} = -c_{i,j} E^{n-p}_{\ell i,j}, \text{ on } \mathfrak{G}_2^{N,M}, \\ E^n_{\ell i,j} = E_\ell(x_i, y_j, t_n), \quad \text{on } \overline{\mathfrak{G}}_1^{N,M}, \\ E^n_{\ell i,j} = E_\ell(x_i, y_j, t_n), \quad i = 0,\ N \text{ or } j = 0,\ N, \text{ and } t_n \in \Lambda^p_{2,t}. \end{cases} \tag{5.4.5}$$

The error can be splitted as

$$\begin{aligned} \|u(x_i, y_j, t_n) - U^n_{i,j}\|_\infty \ &\le \|G(x_i, y_j, t_n) - G^n_{i,j}\|_\infty + \|E_1(x_i, y_j, t_n) - {E_1}^n_{i,j}\|_\infty + \\ &\quad \|E_2(x_i, y_j, t_n) - {E_2}^n_{i,j}\|_\infty + \|E_{12}(x_i, y_j, t_n) - {E_{12}}^n_{i,j}\|_\infty. \end{aligned} \tag{5.4.6}$$

We will find the error separately for each term in the above equation.

Error estimate for the smooth part

By using the initial condition for the smooth part of the solution and the error estimate given in (5.4.1) along with the Taylor's expansions, we obtain the truncation error for the difference equation (5.4.4), as

$$\begin{aligned} \|(\delta_t^- + \mathcal{L}_\varepsilon^N)(G(x_i, y_j, t_n) - G^n_{i,j})\|_\infty \ &\le \Bigg[C\left(N^{-1}\ln N + \Delta t\right) + \frac{\varepsilon}{3}(h_{x,i} + h_{x,i+1}) \left\| \frac{\partial^3 G}{\partial x^3} \right\|_\infty \\ &\quad + \Delta t \left\| \frac{\partial^2 G}{\partial t^2} \right\|_\infty + a_{1;i,j}\frac{h_{x,i}}{2} \left\| \frac{\partial^2 G}{\partial x^2} \right\|_\infty \\ &\quad + \frac{\varepsilon}{3}(h_{y,j} + h_{y,j+1}) \left\| \frac{\partial^3 G}{\partial y^3} \right\|_\infty + a_{2;i,j}\frac{h_{y,j}}{2} \left\| \frac{\partial^2 G}{\partial y^2} \right\|_\infty \Bigg]. \end{aligned}$$

Now $h_{x,i} \le 2N^{-1}$, $h_{y,j} \le 2N^{-1}$ and by using the bounds of the derivatives of G given in Theorem 5.2.1, we obtain

$$\|(\delta_t^- + \mathcal{L}_\varepsilon^N)(G(x_i, y_j, t_n) - G^n_{i,j})\|_\infty \le C(N^{-1}\ln N + \Delta t),$$

for $1 \leq i, j \leq N-1$. Now, by choosing appropriate barrier function and applying the discrete maximum principle (Lemma 5.3.1), we can get

$$\|(G(x_i, y_j, t_n) - G^n_{i,j})\|_\infty \leq C(N^{-1} \ln N + \Delta t). \tag{5.4.7}$$

Next we shall estimate the error associated to the layer component E_1 by separately providing the proofs in two spatial subregions depending on the location of mesh-point x_i.

Error estimate for the boundary layer components

First, we consider the outer region in the x-direction, *i.e*, $x \in [0, 1-\rho_x]$. For $0 \leq i \leq N/2$ and $0 \leq j \leq N$, by following the proof of bound for E_1 in fixed time level t_n from [57], we get

$$|E_1(x_i, y_j, t_n) - E_{1}{}^n_{i,j}| \leq CN^{-1}. \tag{5.4.8}$$

Now, we shall estimate $|E_1(x_i, y_j, t_n) - E_{1}{}^n_{i,j}|$ for $N/2 < i < N$ and $0 < j < N$, by means of consistency and barrier function argument. For the difference equation (5.4.5), the truncation error can be written as

$$\begin{aligned}(\delta_t^- + \mathcal{L}_\varepsilon^N)\left(E_1(x_i, y_j, t_n) - E_{1}{}^n_{i,j}\right) = \;& c_{i,j}\left(E_1(x_i, y_j, t_{n-p}) - E_{1}{}_{i,j}{}^{n-p}\right) \\ &+ \left(\left(\frac{\partial}{\partial t} + \mathcal{L}_\varepsilon\right) - \left(\delta_t^- + \mathcal{L}_\varepsilon^N\right)\right) E_1.\end{aligned}$$

Now, by using the initial condition of (5.4.5) in the above equation, we get

$$(\delta_t^- + \mathcal{L}_\varepsilon^N)\left(E_1(x_i, y_j, t_n) - E_{1}{}^n_{i,j}\right) = \left(\left(\frac{\partial}{\partial t} + \mathcal{L}_\varepsilon\right) - \left(\delta_t^- + \mathcal{L}_\varepsilon^N\right)\right) E_1.$$

Therefore, the Taylor's expansions yield

$$\begin{aligned}\left\|(\delta_t^- + \mathcal{L}_\varepsilon^N)\left(E_1(x_i, y_j, t_n) - E_{1}{}^n_{i,j}\right)\right\|_\infty \leq \;& \left[\frac{\varepsilon}{3}(h_{x,i} + h_{x,i+1})\left\|\frac{\partial^3 E_1}{\partial x^3}\right\|_\infty\right. \\ &+ \frac{\varepsilon}{3}(h_{y,j} + h_{y,j+1})\left\|\frac{\partial^3 E_1}{\partial y^3}\right\|_\infty \\ &+ \frac{h_{x,i}}{2} a_{1;i,j}\left\|\frac{\partial^2 E_1}{\partial x^2}\right\|_\infty + \frac{h_{y,j}}{2} a_{2;i,j}\left\|\frac{\partial^2 E_1}{\partial y^2}\right\|_\infty \\ &\left.+ \Delta t\left\|\frac{\partial^2 E_1}{\partial t^2}\right\|_\infty\right].\end{aligned}$$

Since $h_{x,i} = 2\rho_{x,0}\varepsilon N^{-1} \ln N$, for $N/2 < i < N$, along with the bounds of the derivatives

of E_1 given in Theorem 5.2.1, the truncation error becomes

$$\begin{aligned}\|(\delta_t^- + \mathcal{L}_\varepsilon^N)\left(E_1(x_i,y_j,t_n) - E_{1_{i,j}}^n\right)\|_\infty \leq\ & C\left[\frac{\varepsilon^{-1}}{\alpha_{_x}}N^{-1}\ln N\exp\left(\frac{-\alpha_{_x}(1-x_i)}{\varepsilon}\right)\right.\\ &+\frac{\varepsilon}{3}(h_{y,j}+h_{y,j+1})\exp\left(\frac{-\alpha_{_x}(1-x_i)}{\varepsilon}\right)\\ &+\frac{h_{y,j}}{2}a_{2;i,j}\exp\left(\frac{-\alpha_{_x}(1-x_i)}{\varepsilon}\right)\\ &\left.+\Delta t\exp\left(\frac{-\alpha_{_x}(1-x_i)}{\varepsilon}\right)\right],\end{aligned}$$

after simplification, we obtain that

$$\begin{aligned}\|(\delta_t^- + \mathcal{L}_\varepsilon^N)\left(E_1(x_i,y_j,t_n) - E_{1_{i,j}}^n\right)\|_\infty \leq\ & C\left[\frac{\varepsilon^{-1}}{\alpha_{_x}}N^{-1}\ln N\exp\left(\frac{-\alpha_{_x}(1-x_i)}{\varepsilon}\right)\right.\\ &\left.+\Delta t\exp\left(\frac{-\alpha_{_x}(1-x_i)}{\varepsilon}\right)\right].\end{aligned}$$

Let us choose a barrier function $\phi_{i,j}^n = C\left(N^{-1}\ln N\left[\prod_{k=i+1}^{N}\left(1+\frac{\alpha_{_x}h_{x,k}}{\varepsilon}\right)^{-1}\right]+\Delta t\right)$, and by applying the discrete maximum principle (Lemma 5.3.1), we get

$$\|\left(E_1(x_i,y_j,t_n) - E_{1_{i,j}}^n\right)\|_\infty \leq C(N^{-1}\ln N + \Delta t). \tag{5.4.9}$$

We can get the bound for the other boundary layer part E_2 in an analogous way. Therefore, for $0 \leq i,j \leq N$, we can have

$$\|\left(E_2(x_i,y_j,t_n) - E_{2_{i,j}}^n\right)\|_\infty \leq C(N^{-1}\ln N + \Delta t). \tag{5.4.10}$$

Error estimate for the corner layer part

For $0 \leq i+j \leq 3N/2$, by following the proof of bound for E_{12} in fixed time level t_n from [57], we get

$$\left|E_{12}(x_i,y_j,t_n) - E_{12_{i,j}}^n\right| \leq CN^{-1}. \tag{5.4.11}$$

Now to estimate the truncation error for $i+j > 3N/2$, we will use the Taylor series approach. The local truncation error for the difference equation (5.4.5) of the corner layer part E_{12} can be written as

$$\begin{aligned}(\delta_t^- + \mathcal{L}_\varepsilon^N)\left(E_{12}(x_i,y_j,t_n) - E_{12_{i,j}}^n\right) =\ & c_{i,j}\left(E_{12}(x_i,y_j,t_{n-p}) - {E_{12_{i,j}}}^{n-p}\right)\\ &+\left(\left(\frac{\partial}{\partial t}+\mathcal{L}_\varepsilon\right)-\left(\delta_t^- + \mathcal{L}_\varepsilon^N\right)\right)E_{12}.\end{aligned}$$

Using the initial condition in the above equation, we get

$$(\delta_t^- + \mathcal{L}_\varepsilon^N)\left(E_{12}(x_i, y_j, t_n) - {E_{12}}_{i,j}^n\right) = \left(\left(\frac{\partial}{\partial t} + \mathcal{L}_\varepsilon\right) - (\delta_t^- + \mathcal{L}_\varepsilon^N)\right) E_{12}.$$

By using the Taylor's expansions, we obtain

$$\begin{aligned}\left\|(\delta_t^- + \mathcal{L}_\varepsilon^N)\left(E_{12}(x_i, y_j, t_n) - {E_{12}}_{i,j}^n\right)\right\|_\infty \leq \Bigg[&\frac{\varepsilon}{3}(h_{x,i} + h_{x,i+1})\left\|\frac{\partial^3 E_{12}}{\partial x^3}\right\|_\infty \\ &+\frac{\varepsilon}{3}(h_{y,j} + h_{y,j+1})\left\|\frac{\partial^3 E_{12}}{\partial y^3}\right\|_\infty \\ &+\frac{h_{y,j}}{2}a_{2;i,j}\left\|\frac{\partial^2 E_{12}}{\partial y^2}\right\|_\infty + \frac{h_{x,i}}{2}a_{1;i,j}\left\|\frac{\partial^2 E_{12}}{\partial x^2}\right\|_\infty \\ &+\Delta t\left\|\frac{\partial^2 E_{12}}{\partial t^2}\right\|_\infty\Bigg].\end{aligned}$$

Since $h_{x,i} = 2\rho_{x,0}\varepsilon N^{-1}\ln N$ and $h_{y,j} = 2\rho_{y,0}\varepsilon N^{-1}\ln N$, for $i + j > 3N/2$ along with the bounds of the derivatives of E_{12}, we get the truncation error as

$$\begin{aligned}&\|(\delta_t^- + \mathcal{L}_\varepsilon^N)\left(E_{12}(x_i, y_j, t_n) - {E_{12}}_{i,j}^n\right)\|_\infty \\ &\leq C\left[\frac{\varepsilon^{-1}}{\alpha_x}N^{-1}\ln N\min\left\{\exp\left(\frac{-\alpha_x(1-x_i)}{\varepsilon}\right), \exp\left(\frac{-\alpha_y(1-y_i)}{\varepsilon}\right)\right\}\right. \\ &+\frac{\varepsilon^{-1}}{\alpha_y}N^{-1}\ln N\min\left\{\exp\left(\frac{-\alpha_x(1-x_i)}{\varepsilon}\right), \exp\left(\frac{-\alpha_y(1-y_i)}{\varepsilon}\right)\right\} \\ &\left.+\Delta t\min\left\{\exp\left(\frac{-\alpha_x(1-x_i)}{\varepsilon}\right), \exp\left(\frac{-\alpha_y(1-y_i)}{\varepsilon}\right)\right\}\right].\end{aligned}$$

Now, by choosing a barrier function

$$\phi_{i,j}^n = C\left(N^{-1}\ln N\left[\prod_{k=i+1}^{N}\left(1 + \frac{\alpha_x h_{x,k}}{\varepsilon}\right)^{-1}\right] + N^{-1}\ln N\left[\prod_{k=j+1}^{N}\left(1 + \frac{\alpha_y h_{y,k}}{\varepsilon}\right)^{-1}\right] + \Delta t\right)$$

and by using the discrete maximum principle (Lemma 5.3.1), we get

$$\|\left(E_{12}(x_i, y_j, t_n) - {E_{12}}_{i,j}^n\right)\|_\infty \leq C(N^{-1}\ln N + \Delta t). \tag{5.4.12}$$

Hence, by collecting all the bounds from (5.4.7), (5.4.8), (5.4.9), (5.4.10), (5.4.11) and (5.4.12), then imposing on (5.4.6), we can get the desired bound.

For $t \geq 2\tau$, we can obtain the error bound in a similar way as done above. ∎

5.5 Numerical Results

To validate the error estimate obtained in Theorem 5.4.1, here we carry out some numerical experiments for the following 2D test problems by choosing $T = 2$ and

$\rho_{l,0} = 2.2$, $l = x, y$. In the tables, we begin with $N = 8$, $\Delta t = 0.2$ and $p = 1/\Delta t$ and we multiply N by two and divide Δt by two.

Example 5.5.1. *Consider the following singularly perturbed 2D delay parabolic IBVP with constant coefficients:*

$$\begin{cases} u_t - \varepsilon\Delta u + u_x + u_y = u(x,y,t-1) + f(x,y,t), & (x,y,t) \in \mathfrak{D} \times (0,2], \\ u(x,y,t) = \varphi_b(x,y,t), & (x,y,t) \in \overline{\mathfrak{D}} \times [-1,0], \\ u(x,y,t) = 0, & (x,y,t) \in \partial\mathfrak{D} \times [0,2]. \end{cases} \tag{5.5.1}$$

We choose the initial data $\varphi_b(x,y,t)$ and the source function $f(x,y,t)$ to fit with the exact solution

$$u(x,y,t) = (1-\exp(-t))\left(m_1 + m_2 x + \exp(-(1-x)/\varepsilon)\right)\left(m_1 + m_2 y + \exp(-(1-y)/\varepsilon)\right),$$

where $m_1 = -\exp(-1/\varepsilon)$, $m_2 = -1 - m_1$.

We calculate the maximum pointwise error for each ε by

$$e_\varepsilon^{N,\Delta t} = \max_{(x_i,y_j,t_n)\in\mathfrak{G}^{N,M}} \left|u(x_i,y_j,t_n) - U(x_i,y_j,t_n)\right|,$$

where $u(x_i,y_j,t_n)$ and $U(x_i,y_j,t_n)$ denote the exact solution and the numerical solution obtained in $\mathfrak{G}^{N,M}$ with N mesh-intervals in the spatial directions and M mesh-intervals in the temporal direction, such that $\Delta t = T/M$ is the uniform mesh-size. We determine the corresponding order of convergence for each ε by

$$p_\varepsilon^{N,\Delta t} = \log_2\left(\frac{e_\varepsilon^{N,\Delta t}}{e_\varepsilon^{2N,\Delta t/2}}\right).$$

Now, for each N and Δt, we define the ε-uniform maximum pointwise error by

$$e^{N,\Delta t} = \max_\varepsilon e_\varepsilon^{N,\Delta t},$$

and the corresponding ε-uniform order of convergence by

$$p^{N,\Delta t} = \log_2\left(\frac{e^{N,\Delta t}}{e^{2N,\Delta t/2}}\right).$$

Next, we consider an example where the convection coefficients are function of x and y.

Example 5.5.2. *Consider the following singularly perturbed 2D delay parabolic IBVP:*

$$\begin{cases} u_t - \varepsilon\Delta u + (1+x(1-x))u_x + (1+y(1-y))u_y = u(x,y,t-1) + f(x,y,t), \\ \qquad\qquad (x,y,t) \in \mathfrak{D} \times (0,2], \\ u(x,y,t) = \varphi_b(x,y,t), & (x,y,t) \in \overline{\mathfrak{D}} \times [-1,0], \\ u(x,y,t) = 0, & (x,y,t) \in \partial\mathfrak{D} \times [0,2]. \end{cases} \tag{5.5.2}$$

Here also, we choose the initial data $\varphi_b(x, y, t)$ and the source function $f(x, y, t)$ in such a way, so that they fit with the same exact solution as mentioned in the previous example.

The calculated maximum pointwise errors and the corresponding order of convergence for Examples 5.5.1 and 5.5.2 are presented in Tables 5.1 and 5.2, respectively, for various values of ε and N. In both the tables, we can observe that for a fixed ε, the maximum pointwise errors decrease monotonically as N increases, which confirm that the implicit upwind scheme (5.3.1) is ε-uniform convergent. It also reflects the fact that the classical upwind scheme applied on this class of problem results almost first-order convergence. To visualize the appearance of the boundary layer and its behavior for different ε, we have given the surface plots for $\varepsilon = 10^{-2}, 10^{-4}$ and $N = 32$ in Figures 5.2 and 5.4, for Examples 5.5.1 and 5.5.2, respectively.

In order to reveal the numerical order of convergence, we have plotted the maximum pointwise errors (in loglog scale) in Figures 5.3 and 5.5, for Examples 5.5.1 and 5.5.2, respectively, which again confirm the almost first-order convergence of the scheme.

5.6 Conclusions

In this chapter, we have analyzed an efficient numerical scheme for the singularly perturbed 2D delay parabolic convection-diffusion problem of the form (5.1.1), using the uniform mesh for the temporal domain and a special piecewise-uniform Shishkin mesh for the spatial domains. To discretize the continuous problem, we have applied the implicit-Euler scheme and the classical upwind scheme for the temporal and spatial derivatives, respectively. For the proposed scheme, the stability and error analysis have been carried out, which shows that the method converges uniformly with first-order (up to a logarithmic factor) in space and first-order in time. Along with the analysis, we have presented some numerical examples to verify the theoretical findings.

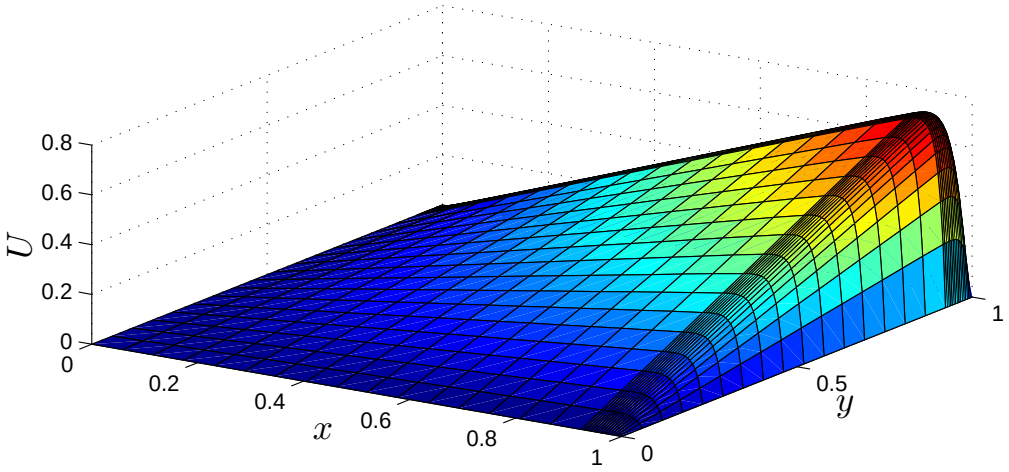

(a) $\varepsilon = 1e-2$.

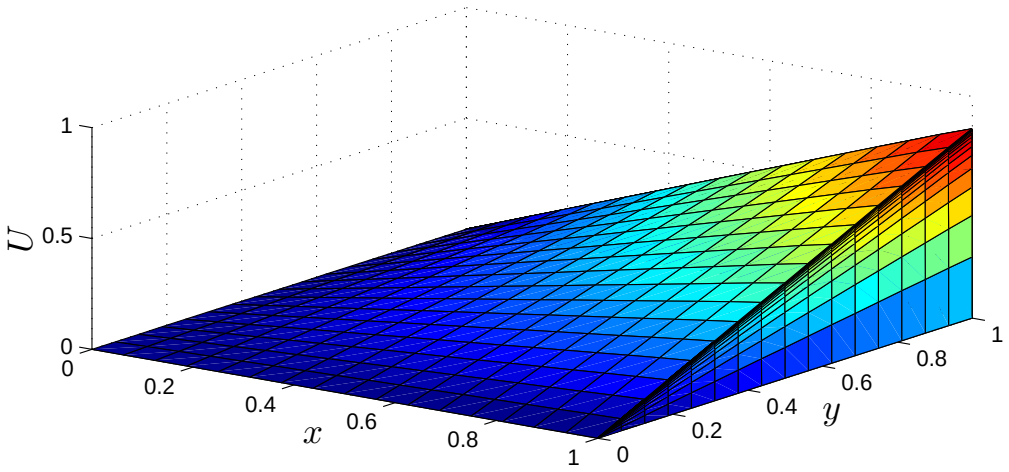

(b) $\varepsilon = 1e-4$.

Figure 5.2: *Surface plots of the numerical solutions U at $t = 2$ and $N = 32$ for Example 5.5.1.*

Table 5.1: *Maximum pointwise errors and the corresponding order of convergence for Example 5.5.1.*

ε	Number of mesh-intervals N/temporal mesh-size Δt					
	$8/\frac{1}{5}$	$16/\frac{1}{10}$	$32/\frac{1}{20}$	$64/\frac{1}{40}$	$128/\frac{1}{80}$	$256/\frac{1}{160}$
10^{-1}	1.0562e-1	7.1832e-2	4.0928e-2	2.2042e-2	1.1445e-2	5.8295e-3
	0.5562	0.8116	0.8928	0.9456	0.9732	
10^{-2}	1.9181e-1	1.3457e-1	8.8636e-2	5.6470e-2	3.4444e-2	2.0190e-2
	0.5114	0.6024	0.6504	0.7132	0.7706	
10^{-3}	2.0568e-1	1.4074e-1	9.2071e-2	5.8304e-2	3.5466e-2	2.0768e-2
	0.5473	0.6123	0.6592	0.7172	0.7720	
10^{-4}	2.0713e-1	1.4139e-1	9.2427e-2	5.8491e-2	3.5568e-2	2.0826e-2
	0.5509	0.6133	0.6601	0.7176	0.7722	
10^{-5}	2.0727e-1	1.4145e-1	9.2463e-2	5.8509e-2	3.5579e-2	2.0831e-2
	0.5512	0.6134	0.6602	0.7177	0.7723	
10^{-6}	2.0729e-1	1.4146e-1	9.2467e-2	5.8511e-2	3.5580e-2	2.0832e-2
	0.5512	0.6134	0.6602	0.7177	0.7723	
10^{-7}	2.0729e-1	1.4146e-1	9.2467e-2	5.8511e-2	3.5580e-2	2.0832e-2
	0.5513	0.6134	0.6602	0.7177	0.7723	
10^{-8}	2.0729e-1	1.4146e-1	9.2467e-2	5.8511e-2	3.5580e-2	2.0832e-2
	0.5513	0.6134	0.6602	0.7177	0.7723	
$e^{N,\Delta t}$	**2.0729e-1**	**1.4146e-1**	**9.2467e-2**	**5.8511e-2**	**3.5580e-2**	**2.0832e-2**
$p^{N,\Delta t}$	**0.5513**	**0.6134**	**0.6602**	**0.7177**	**0.7723**	

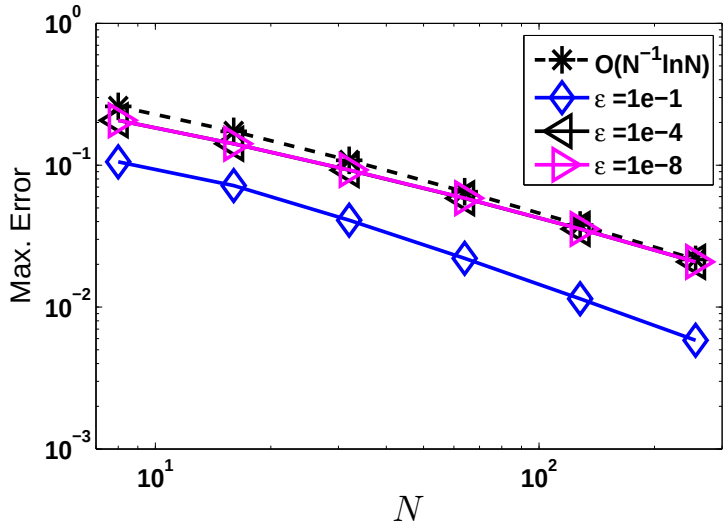

Figure 5.3: *Visualization of the order of convergence through loglog plot for Example 5.5.1.*

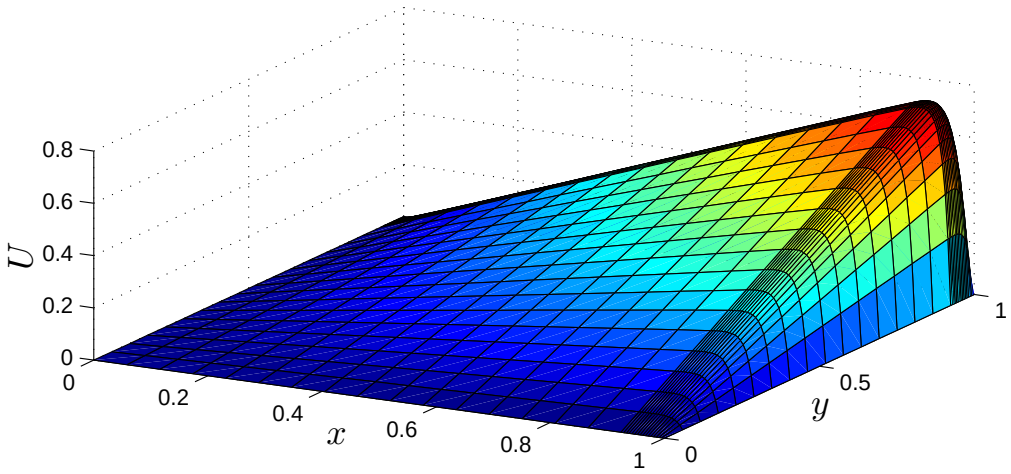

(a) $\varepsilon = 1e-2$.

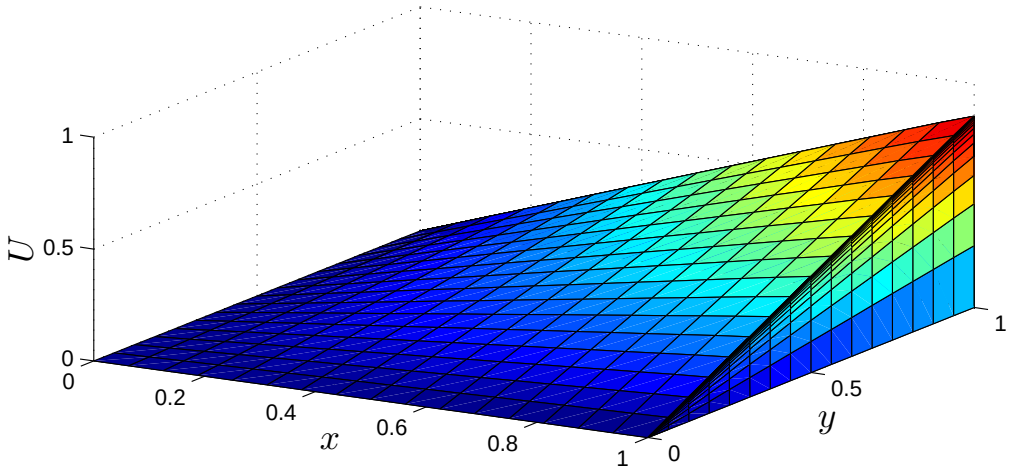

(b) $\varepsilon = 1e-4$.

Figure 5.4: *Surface plots of the numerical solutions U at $t = 2$ and $N = 32$ for Example 5.5.2.*

Table 5.2: *Maximum pointwise errors and the corresponding order of convergence for Example 5.5.2.*

ε	Number of mesh-intervals N/temporal mesh-size Δt					
	$8/\frac{1}{5}$	$16/\frac{1}{10}$	$32/\frac{1}{20}$	$64/\frac{1}{40}$	$128/\frac{1}{80}$	$256/\frac{1}{160}$
10^{-1}	1.0894e-1	7.3729e-2	4.1932e-2	2.2514e-2	1.1689e-2	5.9596e-3
	0.5632	0.8142	0.8972	0.9457	0.9718	
10^{-2}	1.9526e-1	1.3425e-1	8.8205e-2	5.6181e-2	3.4258e-2	2.0092e-2
	0.5405	0.6060	0.6508	0.7137	0.7698	
10^{-3}	2.1242e-1	1.4122e-1	9.1897e-2	5.8141e-2	3.5373e-2	2.0719e-2
	0.5890	0.6198	0.6605	0.7169	0.7717	
10^{-4}	2.1427e-1	1.4198e-1	9.2318e-2	5.8355e-2	3.5488e-2	2.0783e-2
	0.5938	0.6210	0.6618	0.7175	0.7719	
10^{-5}	2.1446e-1	1.4205e-1	9.2361e-2	5.8377e-2	3.5499e-2	2.0789e-2
	0.5942	0.6211	0.6619	0.7176	0.7719	
10^{-6}	2.1448e-1	1.4206e-1	9.2365e-2	5.8379e-2	3.5500e-2	2.0790e-2
	0.5943	0.6211	0.6619	0.7176	0.7720	
10^{-7}	2.1448e-1	1.4206e-1	9.2366e-2	5.8379e-2	3.5501e-2	2.0790e-2
	0.5943	0.6211	0.6619	0.7176	0.7720	
10^{-8}	2.1448e-1	1.4206e-1	9.2366e-2	5.8379e-2	3.5501e-2	2.0790e-2
	0.5943	0.6211	0.6619	0.7176	0.7720	
$e^{N,\Delta t}$	**2.1448e-1**	**1.4206e-1**	**9.2366e-2**	**5.8379e-2**	**3.5501e-2**	**2.0790e-2**
$p^{N,\Delta t}$	**0.5943**	**0.6211**	**0.6619**	**0.7176**	**0.7720**	

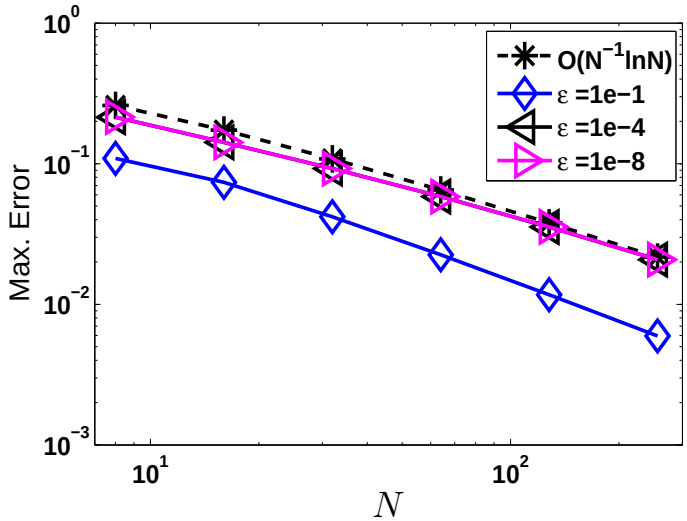

Figure 5.5: *Visualization of the order of convergence through loglog plot Example 5.5.2.*

CHAPTER 6

Uniformly Convergent Numerical Method for Singularly Perturbed 2D Delay Parabolic Convection-Diffusion Problems on Bakhvalov-Shishkin Mesh

In Chapter 5, we have seen that the upwind finite difference scheme on the Shishkin mesh for solving singularly perturbed 2D delay parabolic convection-diffusion IBVPs is almost first-order (up to a logarithmic factor) convergent, which is not optimal. To prevent this reduction of order due to the logarithmic factor, in this chapter, we use the upwind finite difference scheme on a modified Shishkin mesh (*i.e.*, on the Bakhvalov-Shishkin mesh) to discretize the domain in the spatial directions and we apply the implicit-Euler scheme for the time derivative on the uniform mesh in the temporal direction. We derive some conditions on the mesh-generating functions which are useful to prove the convergence of the method, uniformly with respect to the perturbation parameter ε. We prove that the numerical scheme applied on the Bakhvalov-Shishkin mesh is first-order convergent in the discrete supremum norm, which is optimal and does not require any extra computational effort compare to the standard Shishkin mesh. Numerical experiments verify the theoretical results.

6.1 Introduction

In this chapter, we consider the following singularly perturbed 2D delay parabolic convection-diffusion IBVP posed on the domain $\mathfrak{G} = \mathfrak{D} \times \Lambda_t$, $\mathfrak{D} = (0,1)^2$, $\Lambda_t = (0,T]$

and $\Upsilon = \partial\mathfrak{D} \cup \Upsilon_b$, where $\Upsilon_b = \overline{\mathfrak{D}} \times [-\tau, 0]$:

$$\begin{cases} u_t + \mathcal{L}_\varepsilon u(x,y,t) = -c(x,y)u(x,y,t-\tau) + f(x,y,t), & (x,y,t) \in \mathfrak{G}, \\ u(x,y,t) = \varphi_b(x,y,t), & (x,y,t) \in \Upsilon_b, \\ u(x,y,t) = 0, & (x,y,t) \in \partial\mathfrak{D} \times \overline{\Lambda}_t, \end{cases} \tag{6.1.1}$$

where

$$\mathcal{L}_\varepsilon u = -\varepsilon\Delta u + \mathbf{a}(x,y).\nabla u + b(x,y)u,$$

$0 < \varepsilon \ll 1$ is the singular perturbation parameter and $\tau > 0$ is the delay parameter. The coefficients $\mathbf{a} = (a_1, a_2)$, b and c are sufficiently smooth and bounded functions such that $a_1(x,y) \geq \alpha_{_x} > 0$, $a_2(x,y) \geq \alpha_{_y} > 0$, $b(x,y) \geq 0$ and $c(x,y)$ is nonzero on $\overline{\mathfrak{D}}$.

Under sufficient smoothness and necessary compatibility conditions given in Chapter 5, imposed on the functions f and φ_b the delay parabolic IBVP (6.1.1), admits a unique solution $u(x,y,t)$, which exhibits a regular boundary layer of width $O(\varepsilon)$ at the sides $x = 1$ and $y = 1$, along with a corner layer at $(x,y) = (1,1)$.

The main objective of this chapter is to use a modified Shishkin mesh, *i.e.*, the Bakhvalov-Shishkin mesh to solve the delay parabolic PDE (6.1.1). First, we discretize the spatial domain by the Bakhvalov-Shishkin mesh and the temporal domain by the uniform mesh. Then, we apply the implicit-Euler scheme for the time derivative and the classical upwind scheme for the spatial derivatives to obtain the discrete problem. We show theoretically and numerically that it gives more accurate results than on the standard Shishkin meshes. One can see that, the Bakhvalov-Shishkin meshes are easier to handle than the Bakhvalov meshes, moreover it can be used whenever the Shishkin meshes are applicable.

The outline of this chapter is as follows: Section 6.2 deals with the Bakhvalov-Shishkin mesh and the upwind scheme. The main proof of convergence has been derived in Section 6.3. Numerical results are presented in Section 6.4 and the chapter ends with Section 6.5, that summarizes the main conclusions.

6.2 Domain Discretization

Let the rectangular mesh $\overline{\mathfrak{D}}^N$ be defined to be tensor product of the 1D Bakhvalov-Shishkin meshes, *i.e.*, $\overline{\mathfrak{D}}^N = \overline{\Omega}_x^N \times \overline{\Omega}_y^N$, which is constructed as follows:

First, define the transition parameters

$$\rho_l = \min\left\{\frac{1}{2}, \rho_{l,0}\varepsilon \ln N\right\}, \; l = x, \, y,$$

where $\rho_{l,0} = 2/\alpha_l$. In the analysis, we shall assume that $\rho_l = \rho_{l,0}\varepsilon \ln N$. Note that if $\rho_l = 1/2$, then mesh is uniform and in such cases the method can be analyzed in the classical way.

Now, we define the mesh on $\overline{\Omega}_x^N$ by dividing the domain $[0,1]$ into two sub-domains $[0, 1-\rho_x]$ and $[1-\rho_x, 1]$ and each sub-domain will have $N/2$ mesh-intervals such that $x_0 = 0$, $x_{N/2} = 1-\rho_x$ and $x_N = 1$. The boundary layer region $[1-\rho_x, 1]$ is partitioned by the mesh-generating functions $\varphi(\sigma)$, $\sigma \in [1/2, 1]$, such that $\varphi(1/2) = -\ln N$ and $\varphi(1) = 0$, where $\varphi(\sigma)$ is a monotonically increasing and piecewise continuously differentiable function. Then, the mesh-points are defined by

$$x_i = \begin{cases} \dfrac{2(1-\rho_x)i}{N}, & \text{for } i = 0, \cdots, N/2-1, \\ 1 + \rho_{x,0}\varepsilon\varphi(\sigma_i), & \text{for } \sigma_i = i/N,\ i = N/2, \cdots, N, \end{cases}$$

and similarly for y_j.

We denote the mesh-sizes in both the spatial directions by

$$h_{x,i} = x_i - x_{i-1},\ i = 1, \cdots, N, \quad \widehat{h}_{x,i} = h_{x,i} + h_{x,i+1},\ i = 1, \cdots, N-1,$$

$$h_{y,j} = y_j - y_{j-1},\ j = 1, \cdots, N, \quad \widehat{h}_{y,j} = h_{y,j} + h_{y,j+1},\ j = 1, \cdots, N-1.$$

One can notice that $H_l = 2(1-\rho_l)/N$, $l = x, y$, be the mesh-sizes in $[0, 1-\rho_l]$ and on the fine mesh, *i.e.,* when, $i, j = N/2+1, \cdots, N-1$, $h_{x,i}$, $h_{y,j}$ are decreasing functions.

We now define a function ψ, which is closely related to φ, such that $\varphi = \ln\psi$, where ψ is a monotonically increasing function which satisfies $\psi(1/2) = N^{-1}$ and $\psi(1) = 1$. Here, we consider the mesh-generating function ψ as

$$\psi(\sigma) = 1 - 2(1-N^{-1})(1-\sigma).$$

Now, we give some properties of the Bakhvalov-Shishkin mesh only in the x-direction, since similar results can be obtained for the y-direction as well. These properties will be used in the error analysis.

Assumption 6.2.1. *The mesh-generating function φ satisfies*

$$\max_{\sigma\in[1/2,1]} |\varphi'(\sigma)| \le CN \quad \text{and} \quad \int_{1/2}^{1} \{\varphi'(\sigma)\}^2\, d\sigma \le CN. \tag{6.2.1}$$

Lemma 6.2.2. *The spatial mesh-size $h_{x,i}$ on the boundary layer region satisfies*

$$h_{x,i} \le CN^{-1} \quad \text{and} \quad \frac{h_{x,i}}{\varepsilon} \le C, \quad \text{for } i = N/2+1, \cdots, N,$$

provided the above assumption holds true.

Proof. For $i = N/2+1, \cdots, N$, we have

$$\begin{aligned} h_{x,i} &= \rho_{x,0}\varepsilon(\varphi(\sigma_i) - \varphi(\sigma_{i-1})) \\ &= \rho_{x,0}\varepsilon \int_{\sigma_{i-1}}^{\sigma_i} \varphi'(z)dz \\ &\leq \rho_{x,0}\varepsilon N^{-1} \max_{\sigma\in[\sigma_{i-1},\sigma_i]} |\varphi'(\sigma)|\,. \end{aligned}$$

Now, using (6.2.1) and $\varepsilon \leq N^{-1}$, we get the required results. ∎

For the time domain $\overline{\Lambda}_t$, we will use uniform mesh with mesh-size Δt, such that

$$\Lambda_t^M = \{t_n = n\Delta t, n = 0, \cdots, M, \Delta t = T/M\},$$

where M is the number of mesh-points in the t-direction on the interval $[0, T]$ and the temporal mesh-size Δt satisfies the constraint $p\Delta t = \tau$, where p is a positive integer, $t_n = n\Delta t$, $n \geq -p$.

We define the discrete domain by $\mathfrak{G}^{N,M} = \overline{\mathfrak{G}}^{N,M} \cap \mathfrak{G}$ where $\overline{\mathfrak{G}}^{N,M} = \overline{\Omega}_x^N \times \overline{\Omega}_y^N \times \Lambda_t^M$, and $\Upsilon_b^N = \overline{\Omega}_x^N \times \overline{\Omega}_y^N \times \Lambda_t^p$, where Λ_t^p denotes the set of $p+1$ uniform mesh-points in $[-\tau, 0]$. The boundary points of $\overline{\mathfrak{G}}^{N,M}$ are $\Upsilon^N = \{\overline{\mathfrak{G}}^{N,M} \cap \Upsilon\} \cup \Upsilon_b^N$. We further discretize $\overline{\mathfrak{G}}_s^{N,M} = \mathfrak{D}^N \times \Lambda_{s,t}^p$, where $\Lambda_{s,t}^p$ denotes the set of $p+1$ uniform mesh-points in $[(s-1)\tau, s\tau]$, for $s = 1, 2, \cdots, k$. From the above discretization we can observe that $\overline{\mathfrak{G}}^{N,M} = \bigcup_{s=1}^k \overline{\mathfrak{G}}_s^{N,M}$.

6.2.1 Numerical scheme

By replacing the time derivative by the implicit-Euler scheme and the spatial derivatives by the upwind scheme in (6.1.1), we obtain the following discrete problem:

$$\begin{cases} (\delta_t^- + \mathcal{L}_\varepsilon^N)U_{i,j}^{n+1} = -c_{i,j}U_{i,j}^{n+1-p} + f_{i,j}^{n+1}, \quad \text{on} \quad \mathfrak{G}^{N,M}, \\ U_{i,j}^{-s} = \varphi_b(x_i, y_j, -t_s), \quad i,j = 0, \cdots, N, \text{ and } s = 0, \cdots, p, \\ U_{i,j}^{n+1} = 0, \quad i = 0,\ N \text{ or } j = 0,\ N, \text{ and } n = 0, \cdots, M-1, \end{cases} \tag{6.2.2}$$

where

$$\mathcal{L}_\varepsilon^N U_{i,j}^{n+1} = -\varepsilon(\delta_x^2 + \delta_y^2)U_{i,j}^{n+1} + a_{1;i,j}\delta_x^- U_{i,j}^{n+1} + a_{2;i,j}\delta_y^- U_{i,j}^{n+1} + b_{i,j}U_{i,j}^{n+1}.$$

After rearranging the terms in (6.2.2), we obtain the following system of linear algebraic equations:

$$\begin{cases} r_{i,j-}U_{i,j-1}^{n+1} + r_{i-,j}U_{i-1,j}^{n+1} + r_{i,j}U_{i,j}^{n+1} + r_{i+,j}U_{i+1,j}^{n+1} + r_{i,j+}U_{i,j+1}^{n+1} = g_{i,j}^{n+1}, \\ \qquad \text{for} \quad i,j = 1, \cdots, N-1, \text{ and } n = 0, \cdots, M-1, \\ U_{i,j}^{-s} = \varphi_b(x_i, y_j, -t_s), \quad i,j = 0, \cdots, N, \text{ and } s = 0, \cdots, p, \\ U_{i,j}^{n+1} = 0, \quad i = 0,\ N \text{ or } j = 0,\ N, \text{ and } n = 0, \cdots, M-1, \end{cases} \tag{6.2.3}$$

where

$$\begin{cases} r_{i-,j} = \left(-\dfrac{2\varepsilon}{\widehat{h}_{x,i}h_{x,i}} - \dfrac{a_{1;i,j}}{h_{x,i}}\right), & r_{i+,j} = \left(-\dfrac{2\varepsilon}{\widehat{h}_{x,i}h_{x,i+1}}\right), \\ r_{i,j-} = \left(-\dfrac{2\varepsilon}{\widehat{h}_{y,j}h_{y,j}} - \dfrac{a_{2;i,j}}{h_{y,j}}\right), & r_{i,j+} = \left(-\dfrac{2\varepsilon}{\widehat{h}_{y,j}h_{y,j+1}}\right), \\ r_{i,j} = \dfrac{1}{\Delta t} - r_{i-,j} - r_{i+,j} - r_{i,j-} - r_{i,j+} + b_{i,j}, \\ g_{i,j}^{n+1} = \dfrac{U_{i,j}^{n}}{\Delta t} - c_{i,j}U_{i,j}^{n-p+1} + f_{i,j}^{n+1}. \end{cases}$$

The finite difference operator $(\delta_t^- + \mathcal{L}_\varepsilon^N)$ defined in (6.2.2) satisfies the following discrete maximum principle on $\mathfrak{G}^{N,M}$, which provides the ε-uniform stability of the difference operator $(\delta_t^- + \mathcal{L}_\varepsilon^N)$.

Lemma 6.2.3. *(**Discrete maximum principle**) Assume that the discrete function $\Psi_{i,j}^n$ satisfies $\Psi_{i,j}^n \geq 0$ on Υ^N. Then $(\delta_t^- + \mathcal{L}_\varepsilon^N)\Psi_{i,j}^n \geq 0$ on $\mathfrak{G}^{N,M}$ implies that $\Psi_{i,j}^n \geq 0$ at each point of $\overline{\mathfrak{G}}^{N,M}$.*

Proof. The proof is given in Chapter 5. ∎

Now, we shall state the lemma which will be used to bound the truncation error. For convenience we decompose the spatial operator $\mathcal{L}_\varepsilon$ as $\mathcal{L}_\varepsilon = \mathcal{L}_{x,\varepsilon} + \mathcal{L}_{y,\varepsilon}$, where

$$\mathcal{L}_{x,\varepsilon} \equiv -\varepsilon\frac{\partial^2}{\partial x^2} + a_1(x,y)\frac{\partial}{\partial x} + b_1(x,y),$$
$$\mathcal{L}_{y,\varepsilon} \equiv -\varepsilon\frac{\partial^2}{\partial y^2} + a_2(x,y)\frac{\partial}{\partial y} + b_2(x,y),$$

and $b(x,y) = b_1(x,y) + b_1(x,y)$. Corresponding discrete operators are defined by $\mathcal{L}_{x,\varepsilon}^N = -\varepsilon\delta_x^2 + a_1(x_i,y_j)\delta_x^- + b_1(x_i,y_j)$ and $\mathcal{L}_{y,\varepsilon}^N = -\varepsilon\delta_y^2 + a_2(x_i,y_j)\delta_y^- + b_2(x_i,y_j)$.

Lemma 6.2.4. *Let $\phi(x,y)$ be a smooth function defined on $\overline{\mathfrak{D}}$ and also let $\phi_{i,j} = \phi(x_i,y_j)$ on $\overline{\mathfrak{D}}^N$. Then the following estimate holds true:*

$$\left|\mathcal{L}_{x,\varepsilon}^N\phi_{i,j} - (\mathcal{L}_{x,\varepsilon}\phi)_{i,j}\right| \leq C\left\{\varepsilon\int_{x_{i-1}}^{x_{i+1}}\left|\frac{\partial^3\phi}{\partial x^3}(\zeta,y_j)\right|d\zeta + \int_{x_{i-1}}^{x_i}\left|\frac{\partial^2\phi}{\partial x^2}(\zeta,y_j)\right|d\zeta\right\},$$

for $0 < i,\, j < N$, with analogous estimates for $\left|\mathcal{L}_{y,\varepsilon}^N\phi_{i,j} - (\mathcal{L}_{y,\varepsilon}\phi)_{i,j}\right|$.

Lemma 6.2.5. *Let $S_{x,i}$ be the mesh function defined by*

$$S_{x,i} = \prod_{j=i+1}^{N}\left(1 + \frac{\alpha_x h_{x,i}}{2\varepsilon}\right)^{-1},$$

where $i = 1,\cdots,N-1$, with the usual convention that, $S_{x,N} = 1$. Then

$$\mathcal{L}_{x,\varepsilon}^N S_{x,i} \geq \frac{C}{\max\{\varepsilon, h_{x,i}\}}S_{x,i}.$$

Proof. We know that

$$\mathcal{L}^N_{x,\varepsilon} S_{x,i} = -\frac{2\varepsilon}{h_{x,i}+h_{x,i+1}}\left(\frac{S_{x,i+1}-S_{x,i}}{h_{x,i+1}} - \frac{S_{x,i}-S_{x,i-1}}{h_{x,i}}\right) + a_1\frac{S_{x,i}-S_{x,i-1}}{h_{x,i}} + b_1 S_{x,i}.$$

Now, by using $(S_{x,i+1}-S_{x,i}) = \left((\alpha_x h_{x,i+1})/2\varepsilon\right) S_{x,i}$ in the above expression, we can obtain the required result. ∎

In an analogous way, we can get the similar result for $\mathcal{L}^N_{y,\varepsilon}$.

Lemma 6.2.6. *The following inequality relates mesh-size and the perturbation parameter with the mesh-generating functions holds true:*

$$\sum_{i=N/2+1}^{N}\left(\frac{h_{x,i}}{\varepsilon}\right)^2 \le \rho^2_{x,0} N^{-1}\int_{1/2}^{1}\{\varphi'(\sigma)\}^2 d\sigma. \tag{6.2.4}$$

Proof. Express the mesh-size by the following representation

$$\frac{h_{x,i}}{\varepsilon} = \rho_{x,0}\int_{\sigma_{i-1}}^{\sigma_i}\varphi'(\sigma)d\sigma, \quad \text{for } i = N/2+1,\cdots,N.$$

Summing up both sides, we get

$$\begin{aligned}\sum_{i=N/2+1}^{N}\left(\frac{h_{x,i}}{\varepsilon}\right)^2 &\le \rho^2_{x,0}\sum_{i=N/2+1}^{N}(\sigma_i-\sigma_{i-1})\int_{\sigma_{i-1}}^{\sigma_i}\{\varphi'(\sigma)\}^2 d\sigma \\ &= \rho^2_{x,0}N^{-1}\int_{1/2}^{1}\{\varphi'(\sigma)\}^2 d\sigma.\end{aligned}$$

This completes the proof. ∎

Lemma 6.2.7. *Suppose (6.2.1) holds true, then there exist a constant C such that*

$$\prod_{j=N/2+1}^{N}\left(1+\frac{\alpha_x h_{x,j}}{2\varepsilon}\right)^{-1} \le CN^{-1}.$$

Proof. We know that, $\ln(1+x) \ge x - \frac{x^2}{2}$, for $x \ge 0$. Now, by using this property, we have

$$\begin{aligned}\ln\left(\prod_{j=N/2+1}^{N}\left(1+\frac{\alpha_x h_{x,j}}{2\varepsilon}\right)\right) &\ge \sum_{j=N/2+1}^{N}\left[\frac{\alpha_x h_{x,j}}{2\varepsilon} - \frac{1}{2}\left(\frac{\alpha_x h_{x,j}}{2\varepsilon}\right)^2\right] \\ &= \left[\frac{\alpha_x}{2\varepsilon}(1-x_{N/2}) - \frac{1}{2}\sum_{j=N/2+1}^{N}\left(\frac{\alpha_x h_{x,j}}{2\varepsilon}\right)^2\right] \\ &= \left[\frac{\alpha_x\rho_{x,0}}{2}\ln N - \frac{\alpha_x^2}{8}\sum_{j=N/2+1}^{N}\left(\frac{h_{x,j}}{\varepsilon}\right)^2\right].\end{aligned}$$

So, we have

$$\prod_{j=N/2+1}^{N}\left(1+\frac{\alpha_x h_{x,j}}{2\varepsilon}\right)^{-1} \le CN^{-\left(\alpha_x\rho_{x,0}\right)/2}\exp\left(\frac{\alpha_x^2}{8}\sum_{j=N/2+1}^{N}\left(\frac{h_{x,j}}{\varepsilon}\right)^2\right).$$

Now, by using (6.2.1) and (6.2.4), we can obtain the required result. ∎

Lemma 6.2.8. *For $i = 0, \cdots, N-1$, we have*

$$\exp(-\alpha_x(1-x_i)/2\varepsilon) \le \prod_{j=i+1}^{N}\left(1+\frac{\alpha_x h_{x,j}}{2\varepsilon}\right)^{-1}.$$

Proof. For each j, we have

$$\exp(-\alpha_x h_{x,j}/2\varepsilon) = \exp(\alpha_x h_{x,j}/2\varepsilon)^{-1} \le \left(1+\frac{\alpha_x h_{x,j}}{2\varepsilon}\right)^{-1}.$$

Multiplying the above inequality for $j = i+1, \cdots, N$, we obtain the required result. ∎

Lemma 6.2.9. *Let the integers i and j be satisfy $i < j$. Then for $i, j \in \{N/2, \cdots, N\}$, we have*

$$\int_{x_i}^{x_j}\exp\left(-\alpha_x(1-x)/\varepsilon\right)dx \le C\varepsilon N^{-1}\exp(-\alpha_x(1-x_j)/2\varepsilon)\max_{\sigma\in[\sigma_i,\sigma_j]}\{|\psi'(\sigma)|\}.$$

Proof. First we substitute $x = 1+\rho_{x,0}\varepsilon\varphi(\sigma)$ in the left hand side of the above equation. Therefore, we get

$$\begin{aligned}
\int_{x_i}^{x_j}\exp\left(-(1-x)\alpha_x/\varepsilon\right)dx &= \rho_{x,0}\varepsilon\int_{\sigma_i}^{\sigma_j}\exp(\alpha_x\rho_{x,0}\varphi(\sigma))\varphi'(\sigma)d\sigma \\
&= \rho_{x,0}\varepsilon\int_{\sigma_i}^{\sigma_j}\exp(\alpha_x\rho_{x,0}\varphi(\sigma))\frac{\psi'(\sigma)}{\psi(\sigma)}d\sigma \\
&\le \rho_{x,0}\varepsilon\int_{\sigma_i}^{\sigma_j}\exp((\alpha_x\rho_{x,0}-1)\varphi(\sigma))\,|\psi'(\sigma)|\,d\sigma \\
&\le \rho_{x,0}\varepsilon\int_{\sigma_i}^{\sigma_j}\exp(\varphi(\sigma))\,|\psi'(\sigma)|\,d\sigma, \\
&\qquad\qquad (\text{since } (\alpha_x\rho_{x,0}-1)\ge 1) \\
&\le \rho_{x,0}\varepsilon(\sigma_i-\sigma_j)\max_{\sigma\in[\sigma_i,\sigma_j]}\{\exp(\varphi(\sigma))\,|\psi'(\sigma)|\} \\
&= \rho_{x,0}\varepsilon(\sigma_i-\sigma_j)\exp(-(1-x_j)/\rho_{x,0}\varepsilon)\max_{\sigma\in[\sigma_i,\sigma_j]}\{|\psi'(\sigma)|\},
\end{aligned}$$

which follows the required result. ∎

6.3 Error Analysis

In this section, we provide the important theorem for the ε-uniform convergence of the numerical solution in the discrete maximum norm. Before that, without loss of generality, we assume that the initial and boundary conditions are zero.

Theorem 6.3.1. *Let $u \in \mathfrak{C}^{4,2}(\overline{\mathfrak{G}})$ be the solution of the continuous problem (6.1.1) and U be the discrete solution of the fully discrete scheme (6.2.2). Then the global error satisfies*

$$||u(x_i, y_j, t_n) - U^n_{i,j}||_\infty \leq C(N^{-1} + \Delta t),$$

for $(x_i, y_j, t_n) \in \mathfrak{G}^{N,M}$.

Proof. We divide the proof of this theorem into different time intervals, because of the presence of the time delay.

Case 1. Consider the first time interval, *i.e.*, for $t \in [0, \tau]$. On the domain $\mathfrak{G}_1 = \mathfrak{D} \times (0, \tau)$, we consider the following singularly perturbed delay parabolic equation:

$$\begin{cases} u_t + \mathcal{L}_\varepsilon u(x,y,t) = -c(x,y)u(x,y,t-\tau) + f(x,y,t), & (x,y,t) \in \mathfrak{G}_1, \\ u(x,y,t) = 0, & (x,y,t) \in \Upsilon_b, \\ u(x,y,t) = 0, & (x,y,t) \in \partial\mathfrak{D} \times (0,\tau). \end{cases} \tag{6.3.1}$$

We apply the implicit-Euler scheme for the time derivative and the upwind scheme for the spatial derivatives to determine the numerical solution U of (6.3.1) at ${\mathfrak{G}_1}^{N,M}$. The discrete problem corresponding to (6.3.1) is given by

$$\begin{cases} \delta_t^- U^n_{i,j} - \varepsilon(\delta_x^2 + \delta_y^2)U^n_{i,j} + a_{1;i,j}\delta_x^- U^n_{i,j} + a_{2;i,j}\delta_y^- U^n_{i,j} + b_{i,j}U^n_{i,j} = -c_{i,j}U^{n-p}_{i,j} + f^n_{i,j}, \text{ on } {\mathfrak{G}_1}^{N,M}, \\ U(x_i, y_j, t_n) = 0, \quad \text{on } \Upsilon_b^N, \\ U(x_i, y_j, t_n) = 0, \quad i = 0,\ N \text{ or } j = 0,\ N, \text{ and } t_n \in \Lambda^p_{1,t}. \end{cases} \tag{6.3.2}$$

Now, we split the solution of (6.3.1) as $u = G + E_1 + E_2 + E_{12}$, where the initial conditions in Υ_b are $G = 0$, $E_1 = 0$, $E_2 = 0$ and $E_{12} = 0$. Similarly the solution of (6.3.2) can be decomposed as $U^n_{i,j} = G^n_{i,j} + {E_1}^n_{i,j} + {E_2}^n_{i,j} + {E_{12}}^n_{i,j}$, where $G^n_{i,j}$ is the solution of

$$\begin{cases} \delta_t^- G^n_{i,j} - \varepsilon(\delta_x^2 + \delta_y^2)G^n_{i,j} & +a_{1;i,j}\delta_x^- G^n_{i,j} + a_{2;i,j}\delta_y^- G^n_{i,j} + b_{i,j}G^n_{i,j} = -c_{i,j}G^{n-p}_{i,j} + f^n_{i,j}, \text{ on } \mathfrak{G}_1^{N,M}, \\ G^n_{i,j} = 0, & \text{on } \Upsilon_b^N, \\ G^n_{i,j} = G(x_i, y_j, t_n), & i = 0,\ N \text{ or } j = 0,\ N, \text{ and } t_n \in \Lambda^p_{1,t}, \end{cases} \tag{6.3.3}$$

and $E^n_{\ell_{i,j}}$, $\ell = 1,\ 2,\ 12$, satisfy

$$\begin{cases} \delta_t^- E^n_{\ell_{i,j}} - \varepsilon(\delta_x^2 + \delta_y^2)E^n_{\ell_{i,j}} + a_{1;i,j}\delta_x^- E^n_{\ell_{i,j}} + a_{2;i,j}\delta_y^- E^n_{\ell_{i,j}} + b_{i,j}E^n_{\ell_{i,j}} = -c_{i,j}E^{n-p}_{\ell_{i,j}},\ \text{on}\ \mathfrak{G}_1^{N,M}, \\ E^n_{\ell_{i,j}} = E_\ell(x_i, y_j, t_n), \quad \text{on}\ \Upsilon_b^N, \\ E^n_{\ell_{i,j}} = E_\ell(x_i, y_j, t_n), \quad i = 0,\ N \,\text{or}\, j = 0,\ N,\ \text{and}\, t_n \in \Lambda_{1,t}^p. \end{cases} \tag{6.3.4}$$

Then the error can be splitted as

$$\begin{aligned} \|u(x_i, y_j, t_n) - U^n_{i,j}\|_\infty \leq\ & \|G(x_i, y_j, t_n) - G^n_{i,j}\|_\infty + \|E_1(x_i, y_j, t_n) - E_{1_{i,j}}^n\|_\infty \\ & + \|E_2(x_i, y_j, t_n) - E_{2_{i,j}}^n\|_\infty + \|E_{12}(x_i, y_j, t_n) - E_{12_{i,j}}^n\|_\infty. \end{aligned} \tag{6.3.5}$$

We will find the error separately for each term in the above equation.

Error estimate for the smooth part

For the smooth component G, the truncation error for the difference equation (6.3.3) can be written as

$$\begin{aligned} (\delta_t^- + \mathcal{L}_\varepsilon^N)(G(x_i, y_j, t_n) - G^n_{i,j}) &= (\delta_t^- + \mathcal{L}_\varepsilon^N)G(x_i, y_j, t_n) - (\delta_t^- + \mathcal{L}_\varepsilon^N)G^n_{i,j} \\ &= (\delta_t^- + \mathcal{L}_\varepsilon^N)G(x_i, y_j, t_n) - f(x_i, y_j, t_n) \\ &= \left((\delta_t^- + \mathcal{L}_\varepsilon^N) - \left(\frac{\partial}{\partial t} + \mathcal{L}_\varepsilon\right)\right) G(x_i, y_j, t_n). \end{aligned}$$

Now, by using the Taylor's formula, we obtain

$$\begin{aligned} \|(\delta_t^- + \mathcal{L}_\varepsilon^N)(G(x_i, y_j, t_n) - G^n_{i,j})\|_\infty \leq & \left[\Delta t \left\|\frac{\partial^2 G}{\partial t^2}\right\|_\infty + \frac{\varepsilon}{3}(h_{x,i} + h_{x,i+1}) \left\|\frac{\partial^3 G}{\partial x^3}\right\|_\infty \right. \\ & + \frac{\varepsilon}{3}(h_{y,j} + h_{y,j+1}) \left\|\frac{\partial^3 G}{\partial y^3}\right\|_\infty \\ & \left. + a_{1;i,j}\frac{h_{x,i}}{2} \left\|\frac{\partial^2 G}{\partial x^2}\right\|_\infty + a_{2;i,j}\frac{h_{y,j}}{2} \left\|\frac{\partial^2 G}{\partial y^2}\right\|_\infty \right]. \end{aligned}$$

By applying the results of Lemma 6.2.2 and Theorem 5.2.1 and using $\varepsilon \leq N^{-1}$, we obtain

$$\|(\delta_t^- + \mathcal{L}_\varepsilon^N)(G(x_i, y_j, t_n) - G^n_{i,j})\|_\infty \leq C(N^{-1} + \Delta t).$$

Now, we choose the barrier function as

$$\Psi(x_i, y_j, t_n) = C(N^{-1}(x_i + y_j) + t_n\Delta t),$$

and apply the discrete maximum principle (Lemma 6.2.3), we obtain that

$$\|G(x_i, y_j, t_n) - G^n_{i,j}\|_\infty \leq C(N^{-1} + \Delta t). \tag{6.3.6}$$

Next, we shall estimate the error associated to the layer component E_1 in two spatial subregions depending on the location of the mesh-point x_i.

Error estimate for the boundary layer components

For $0 \le i \le N/2$ and $0 \le j \le N$, by following the proof of bound for E_1 in fixed time level t_n from [57], we get

$$|E_1(x_i, y_j, t_n) - E_{1_{i,j}}^n| \le CN^{-1}. \tag{6.3.7}$$

Now, we shall estimate $|E_1(x_i, y_j, t_n) - E_{1_{i,j}}^n|$ for $N/2 < i < N$ and $0 < j < N$, by means of consistency and barrier function argument. For the difference equation (6.3.4), we obtain the truncation error

$$\begin{aligned}
&(\delta_t^- + \mathcal{L}_\varepsilon^N)\left(E_1(x_i, y_j, t_n) - E_{1_{i,j}}^n\right) \\
&\quad = \left(\left(\frac{\partial}{\partial t} + \mathcal{L}_\varepsilon\right) - (\delta_t^- + \mathcal{L}_\varepsilon^N)\right) E_1 \\
&\quad \le C\left(\Delta t \left\|\frac{\partial^2 E_1}{\partial t^2}\right\|_\infty + \varepsilon \int_{x_{i-1}}^{x_{i+1}} \left|\frac{\partial^3 E_1}{\partial x^3}\right| dx + \int_{x_{i-1}}^{x_i} \left|\frac{\partial^2 E_1}{\partial x^2}\right| dx\right. \\
&\quad \left. + \varepsilon \int_{y_{j-1}}^{y_{j+1}} \left|\frac{\partial^3 E_1}{\partial y^3}\right| dy + \int_{y_{j-1}}^{y_j} \left|\frac{\partial^2 E_1}{\partial y^2}\right| dy\right) \\
&\quad \le C(\Delta t + \varepsilon^{-1} N^{-1} \exp(-\alpha_x (1 - x_{i+1})/2\varepsilon) \max_{\sigma \in [\sigma_{i-1}, \sigma_{i+1}]} |\psi'(\sigma)|), \\
&\qquad \text{(by using Theorem 5.2.1 and Lemma 6.2.9)} \\
&\quad \le C\left(\Delta t + \varepsilon^{-1} N^{-1} S_{x,i+1} \max_{\sigma \in [\sigma_{i-1}, \sigma_{i+1}]} |\psi'(\sigma)|\right),
\end{aligned}$$

by Lemma 6.2.8. Now, by choosing the barrier function

$$\Psi = C(N^{-1} S_{x,i+1} \max_{\sigma \in [1/2,1]} |\psi'(\sigma)| + \Delta t),$$

and by applying the discrete maximum principle (Lemma 6.2.3), we obtain

$$\| \left(E_1(x_i, y_j, t_n) - E_{1_{i,j}}^n\right) \|_\infty \le C(N^{-1} + \Delta t). \tag{6.3.8}$$

We can get the bound for the other boundary layer part E_2 in an analogous way. Therefore, for $0 \le i, j \le N$, we have

$$\| \left(E_2(x_i, y_j, t_n) - E_{2_{i,j}}^n\right) \|_\infty \le C(N^{-1} + \Delta t). \tag{6.3.9}$$

Error estimate for the corner layer part

For $0 \le i + j \le 3N/2$, by following the proof of bound for E_{12} in fixed time level t_n from [57], we get

$$\left|E_{12}(x_i, y_j, t_n) - E_{12_{i,j}}^n\right| \le CN^{-1}. \tag{6.3.10}$$

Now to estimate the truncation error for $i+j > 3N/2$, we use the Taylor series expansion. From the difference equation (6.3.4), we obtain the truncation error

$$
\begin{aligned}
&(\delta_t^- + \mathcal{L}_\varepsilon^N)\left(E_{12}(x_i, y_j, t_n) - {E_{12}}_{i,j}^n\right) \\
&\qquad = \left(\left(\frac{\partial}{\partial t} + \mathcal{L}_\varepsilon\right) - \left(\delta_t^- + \mathcal{L}_\varepsilon^N\right)\right) E_{12} \\
&\qquad \le C\left(\Delta t \left\|\frac{\partial^2 E_{12}}{\partial t^2}\right\|_\infty + \varepsilon \int_{x_{i-1}}^{x_{i+1}} \left|\frac{\partial^3 E_{12}}{\partial x^3}\right| dx + \int_{x_{i-1}}^{x_i} \left|\frac{\partial^2 E_{12}}{\partial x^2}\right| dx\right. \\
&\qquad \left. + \varepsilon \int_{y_{j-1}}^{y_{j+1}} \left|\frac{\partial^3 E_{12}}{\partial y^3}\right| dy + \int_{y_{j-1}}^{y_j} \left|\frac{\partial^2 E_{12}}{\partial y^2}\right| dy\right) \\
&\qquad = C\left(\Delta t + \varepsilon^{-1} N^{-1} \exp(-\alpha_x (1 - x_{i+1})/2\varepsilon) \max_{\sigma \in [\sigma_{i-1}, \sigma_{i+1}]} |\psi'(\sigma)|\right. \\
&\qquad \left. + \varepsilon^{-1} N^{-1} \exp(-\alpha_y (1 - y_{j+1})/2\varepsilon) \max_{\sigma \in [\sigma_{j-1}, \sigma_{j+1}]} |\psi'(\sigma)|\right), \\
&\qquad\qquad \text{(by using Theorem 5.2.1 and Lemma 6.2.9)} \\
&\qquad \le C\left(\Delta t + \varepsilon^{-1} N^{-1} S_{x,i+1} \max_{\sigma \in [\sigma_{i-1}, \sigma_{i+1}]} |\psi'(\sigma)|\right. \\
&\qquad \left. + \varepsilon^{-1} N^{-1} S_{y,j+1} \max_{\sigma \in [\sigma_{j-1}, \sigma_{j+1}]} |\psi'(\sigma)|\right),
\end{aligned}
$$

by Lemma 6.2.8. Now by choosing the barrier function

$$
\Psi = C\left(N^{-1} S_{x,i+1} \max_{\sigma \in [1/2,1]} |\psi'(\sigma)| + N^{-1} S_{y,j+1} \max_{\sigma \in [1/2,1]} |\psi'(\sigma)| + \Delta t\right),
$$

and by applying the discrete maximum principle (Lemma 6.2.3), we obtain

$$
\| \left(E_{12}(x_i, y_j, t_n) - {E_{12}}_{i,j}^n\right) \|_\infty \le C(N^{-1} + \Delta t). \tag{6.3.11}
$$

From (6.3.5), (6.3.6), (6.3.7), (6.3.8), (6.3.9), (6.3.10) and (6.3.11), we obtain the error estimate

$$
||u(x_i, y_j, t_n) - U_{i,j}^n||_\infty \le C(N^{-1} + \Delta t), \quad (x_i, y_j, t_n) \in \mathfrak{G}_1^{N,M}. \tag{6.3.12}
$$

Case 2. On the domain $\mathfrak{G}_2 = \mathfrak{D} \times (\tau, 2\tau)$, we consider the following singularly perturbed delay parabolic equation:

$$
\begin{cases}
u_t + \mathcal{L}_\varepsilon u(x, y, t) = -c(x, y) u(x, y, t - \tau) + f(x, y, t), & (x, y, t) \in \mathfrak{G}_2, \\
u(x, y, t) = u_\tau(x, y, t), & (x, y, t) \in \overline{\mathfrak{G}}_1 = \overline{\mathfrak{D}} \times [0, \tau], \\
u(x, y, t) = 0, & (x, y, t) \in \partial\mathfrak{D} \times (\tau, 2\tau),
\end{cases} \tag{6.3.13}
$$

where u_τ is the exact solution on $\mathfrak{G}_1$.

We apply the implicit-Euler scheme for the time derivative and the upwind scheme for the spatial derivatives to determine the numerical solution U of (6.3.13) at ${\mathfrak{G}_2}^{N,M}$. The discrete problem corresponding to (6.3.13) is given by

$$\begin{cases} \delta_t^- U_{i,j}^n - \varepsilon(\delta_x^2 + \delta_y^2)U_{i,j}^n + a_{1;i,j}\delta_x^- U_{i,j}^n + a_{2;i,j}\delta_y^- U_{i,j}^n + b_{i,j}U_{i,j}^n = -c_{i,j}U_{i,j}^{n-p} + f_{i,j}^n, \text{ on } {\mathfrak{G}_2}^{N,M}, \\ U(x_i, y_j, t_n) = U_1(x_i, y_j, t_n), \quad (x_i, y_j, t_n) \in {\overline{\mathfrak{G}}_1}^{N,M}, \\ U(x_i, y_j, t_n) = 0, \quad i = 0,\ N \text{ or } j = 0,\ N, \text{ and } t_n \in \Lambda_{2,t}^p, \end{cases} \tag{6.3.14}$$

where $U_1(\cdot,\cdot,\cdot)$ is the numerical solution calculated on ${\mathfrak{G}_1}^{N,M}$.

We split the solution in a similar way as done in previous case as $u = G+E_1+E_2+E_{12}$, where the initial conditions in $\mathfrak{G}_1$ are $G = u_\tau(x,y,t)$, $E_1 = 0$, $E_2 = 0$ and $E_{12} = 0$.

Error estimate for the smooth part

For the smooth component G, the truncation error can be written as

$$\begin{aligned} (\delta_t^- + \mathcal{L}_\varepsilon^N)(G &(x_i, y_j, t_n) - G_{i,j}^n) \\ &= (\delta_t^- + \mathcal{L}_\varepsilon^N)G(x_i, y_j, t_n) - (\delta_t^- + \mathcal{L}_\varepsilon^N)G_{i,j}^n \\ &= (\delta_t^- + \mathcal{L}_\varepsilon^N)G(x_i, y_j, t_n) - \left(-c(x_i, y_j)G_{i,j}^{n-p} + f(x_i, y_j, t_n)\right) \\ &= (\delta_t^- + \mathcal{L}_\varepsilon^N)G(x_i, y_j, t_n) - \Bigg(- c(x_i, y_j)G_{i,j}^{n-p} \\ &+ \left(\frac{\partial}{\partial t} + \mathcal{L}_\varepsilon\right) G(x_i, y_j, t_n) + c(x_i, y_j)G(x_i, y_j, t_{n-p})\Bigg) \\ &= c(x_i, y_j)(G_{i,j}^{n-p} - G(x_i, y_j, t_{n-p})) \\ &+ \left((\delta_t^- + \mathcal{L}_\varepsilon^N) - \left(\frac{\partial}{\partial t} + \mathcal{L}_\varepsilon\right)\right) G(x_i, y_j, t_n). \end{aligned}$$

By using the initial condition for the smooth part of the solution and using the error estimate obtained in (6.3.12), we get

$$\begin{aligned} \|(\delta_t^- + \mathcal{L}_\varepsilon^N)(G(x_i, y_j, t_n) - G_{i,j}^n)\|_\infty \leq \Bigg[& C\left(N^{-1} + \Delta t\right) + \Delta t \left\| \frac{\partial^2 G}{\partial t^2} \right\|_\infty \\ & + \frac{\varepsilon}{3}(h_{x,i} + h_{x,i+1}) \left\| \frac{\partial^3 G}{\partial x^3} \right\|_\infty + a_{1;i,j}\frac{h_{x,i}}{2} \left\| \frac{\partial^2 G}{\partial x^2} \right\|_\infty \\ & + \frac{\varepsilon}{3}(h_{y,j} + h_{y,j+1}) \left\| \frac{\partial^3 G}{\partial y^3} \right\|_\infty + a_{2;i,j}\frac{h_{y,j}}{2} \left\| \frac{\partial^2 G}{\partial y^2} \right\|_\infty \Bigg]. \end{aligned}$$

Now, proceeding in the same way as done in the previous case for the smooth component G, we can obtain

$$\|G(x_i, y_j, t_n) - G_{i,j}^n\|_\infty \leq C(N^{-1} + \Delta t), \tag{6.3.15}$$

for $t \in (\tau, 2\tau)$.

Error estimate for the boundary layer components

For $0 \leq i \leq N/2$ and $0 \leq j \leq N$, by following the proof of bound for E_1 in fixed time level t_n from [57], we get

$$|E_1(x_i, y_j, t_n) - E_{1_{i,j}}^n| \leq CN^{-1}. \tag{6.3.16}$$

Now, we shall estimate $|E_1(x_i, y_j, t_n) - E_{1_{i,j}}^n|$ for $N/2 < i < N$ and $0 < j < N$. We can obtain the truncation error from

$$\begin{aligned}(\delta_t^- + \mathcal{L}_\varepsilon^N)\left(E_1(x_i, y_j, t_n) - E_{1_{i,j}}^n\right) &= c_{i,j}\left(E_1(x_i, y_j, t_{n-p}) - {E_{1}}_{i,j}^{n-p}\right)\\ &+ \left(\left(\frac{\partial}{\partial t} + \mathcal{L}_\varepsilon\right) - \left(\delta_t^- + \mathcal{L}_\varepsilon^N\right)\right) E_1.\end{aligned}$$

Now, by using the initial condition in the above equation, we get

$$(\delta_t^- + \mathcal{L}_\varepsilon^N)\left(E_1(x_i, y_j, t_n) - E_{1_{i,j}}^n\right) = \left(\left(\frac{\partial}{\partial t} + \mathcal{L}_\varepsilon\right) - \left(\delta_t^- + \mathcal{L}_\varepsilon^N\right)\right) E_1.$$

Following a similar approach done in the previous case for the boundary layer part E_1, we can obtain

$$\| \left(E_1(x_i, y_j, t_n) - E_{1_{i,j}}^n\right) \|_\infty \leq C(N^{-1} + \Delta t), \tag{6.3.17}$$

for $t \in (\tau, 2\tau)$. We can get the bound for the other boundary layer part E_2 in an analogous way. Therefore, for $0 \leq i, j \leq N$

$$\| \left(E_2(x_i, y_j, t_n) - E_{2_{i,j}}^n\right) \|_\infty \leq C(N^{-1} + \Delta t). \tag{6.3.18}$$

Error estimate for the corner layer part

For $0 \leq i + j \leq 3N/2$, by following the proof of bound for E_{12} in fixed time level t_n from [57], we get

$$\left|E_{12}(x_i, y_j, t_n) - E_{12_{i,j}}^n\right| \leq CN^{-1}. \tag{6.3.19}$$

Now to estimate the truncation error for $i + j > 3N/2$, we will do the Taylor series approach. Then, the truncation error can be obtained from

$$\begin{aligned}(\delta_t^- + \mathcal{L}_\varepsilon^N)\left(E_{12}(x_i, y_j, t_n) - E_{12_{i,j}}^n\right) &= c_{i,j}\left(E_{12}(x_i, y_j, t_{n-p}) - {E_{12}}_{i,j}^{n-p}\right)\\ &+ \left(\left(\frac{\partial}{\partial t} + \mathcal{L}_\varepsilon\right) - \left(\delta_t^- + \mathcal{L}_\varepsilon^N\right)\right) E_{12}.\end{aligned}$$

Using the initial condition in the above equation, we get

$$(\delta_t^- + \mathcal{L}_\varepsilon^N)\left(E_{12}(x_i, y_j, t_n) - E_{12_{i,j}}^n\right) = \left(\left(\frac{\partial}{\partial t} + \mathcal{L}_\varepsilon\right) - \left(\delta_t^- + \mathcal{L}_\varepsilon^N\right)\right) E_{12}.$$

Now, proceeding in an analogous way as done in the previous case for the corner layer part E_{12}, we can obtain

$$\| \left(E_{12}(x_i, y_j, t_n) - E_{12}{}^n_{i,j} \right) \|_\infty \leq C(N^{-1} + \Delta t), \tag{6.3.20}$$

for $t \in (\tau, 2\tau)$.

Hence, by collecting all the bounds from (6.3.15), (6.3.16), (6.3.17), (6.3.18), (6.3.19) and (6.3.20), we can get the desired bound on ${\mathfrak{G}_2}^{N,M}$.

For $t \geq 2\tau$, we can find the error bound in a similar way as done above. ∎

The estimate obtained in the previous theorem is optimal in the sense, it does not contain the logarithmic term in the right hand side of the error bound.

6.4 Numerical Results

In this section, we present the results of numerical experiments carried out to validate the finding of Theorem 6.3.1 for the following 2D test problems. We choose the transition parameter $\rho_{l,0} = 2.2$, $l = x, y$. In the tables, we begin with $N = 8$, $\Delta t = 0.2$ and $p = 1/\Delta t$ and we multiply N by two and divide Δt by two. Since, we have taken $\Delta t = 1.6/N$, the theoretical error bound obtained in Theorem 6.3.1 will be of order $O(N^{-1})$. Therefore, in this section, we will write only the spatial order of convergence, *i.e.*, $O(N^{-1})$ instead of $O(N^{-1} + \Delta t)$.

Example 6.4.1. *Consider the following singularly perturbed 2D delay parabolic IBVP with constant coefficients:*

$$\begin{cases} u_t - \varepsilon \Delta u + u_x + u_y = u(x, y, t-1) + f(x, y, t), & (x, y, t) \in \mathfrak{D} \times (0, 2], \\ u(x, y, t) = \varphi_b(x, y, t), & (x, y, t) \in \overline{\mathfrak{D}} \times [-1, 0], \\ u(x, y, t) = 0, & (x, y, t) \in \partial\mathfrak{D} \times [0, 2]. \end{cases} \tag{6.4.1}$$

We choose the initial data $\varphi_b(x, y, t)$ and the source function $f(x, y, t)$ to fit with the exact solution

$$u(x, y, t) = (1 - \exp(-t)) \left(m_1 + m_2 x + \exp(-(1-x)/\varepsilon) \right) \left(m_1 + m_2 y + \exp(-(1-y)/\varepsilon) \right),$$

where $m_1 = -\exp(-1/\varepsilon)$, $m_2 = -1 - m_1$.

We calculate the maximum pointwise error and the corresponding order of convergence in the same way as calculated in the previous chapter.

Next, we consider an example where the convection coefficients are function of x and y.

Example 6.4.2. *Consider the following singularly perturbed 2D delay parabolic IBVP:*

$$\begin{cases} u_t - \varepsilon\Delta u + (1+x(1-x))u_x + (1+y(1-y))u_y = & u(x,y,t-1) + f(x,y,t), \\ & (x,y,t) \in \mathfrak{D} \times (0,2], \\ u(x,y,t) = \varphi_b(x,y,t), & (x,y,t) \in \overline{\mathfrak{D}} \times [-1,0], \\ u(x,y,t) = 0, & (x,y,t) \in \partial\mathfrak{D} \times [0,2]. \end{cases} \tag{6.4.2}$$

Here also, we choose the initial data $\varphi_b(x,y,t)$ and the source function $f(x,y,t)$ in such a way, so that they fit with the same exact solution as mentioned in the previous example.

To visualize the appearance of the boundary layer and its behavior for different ε, we have given the surface plots for $\varepsilon = 10^{-2}$, 10^{-4} and $N = 32$ in Figures 6.1 and 6.3.

The calculated maximum pointwise errors and the corresponding order of convergence for Examples 6.4.1 and 6.4.2 are presented for the Bakhvalov-Shishkin mesh in Tables 6.1 and 6.2, respectively, for various values of ε and N. To understand the improvement due to the Bakhvalov-Shishkin mesh, we compare the results tabulated in Table 6.1 with Table 5.1 and Table 6.2 with Table 5.2. We observe that the order of convergence obtained on the Bakhvalov-Shishkin mesh are better than that obtained on the Shishkin mesh, which verifies the estimate proved in Theorem 6.3.1. From the Tables 6.1 and 6.2, we notice that for a fixed ε, the maximum pointwise errors decrease monotonically as N increases, which confirm that the implicit upwind scheme (6.3.2) is ε-uniform convergent.

For the sake of fulfillment of this observation, we have plotted the maximum pointwise errors in loglog scale for the Examples 6.4.1 and 6.4.2 in the Figures 6.2 and 6.4. Indeed, we can conclude that the upwind finite difference scheme on the Bakhvalov-Shishkin mesh surpass the Shishkin mesh, irrespective of the perturbation parameter ε.

6.5 Conclusions

In this chapter, we have provided the characterization of the Bakhvalov-Shishkin mesh for the singularly perturbed 2D delay parabolic convection-diffusion problem of the form (6.1.1). This is executed by forming this mesh with the help of an appropriate mesh-generating function. To discretize the continuous problem, we have applied the implicit-Euler scheme and the classical upwind scheme for the temporal and spatial derivatives, respectively. We have shown numerically that the error bound obtained for the proposed scheme on the Bakhvalov-Shishkin mesh is optimal, that is, the errors are smaller than the results obtained on the standard Shishkin mesh.

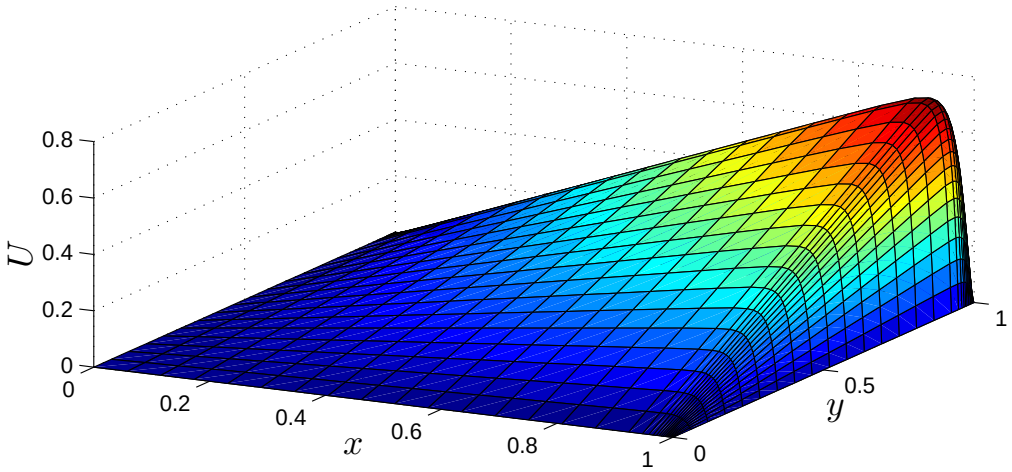

(a) $\varepsilon = 1e-2$.

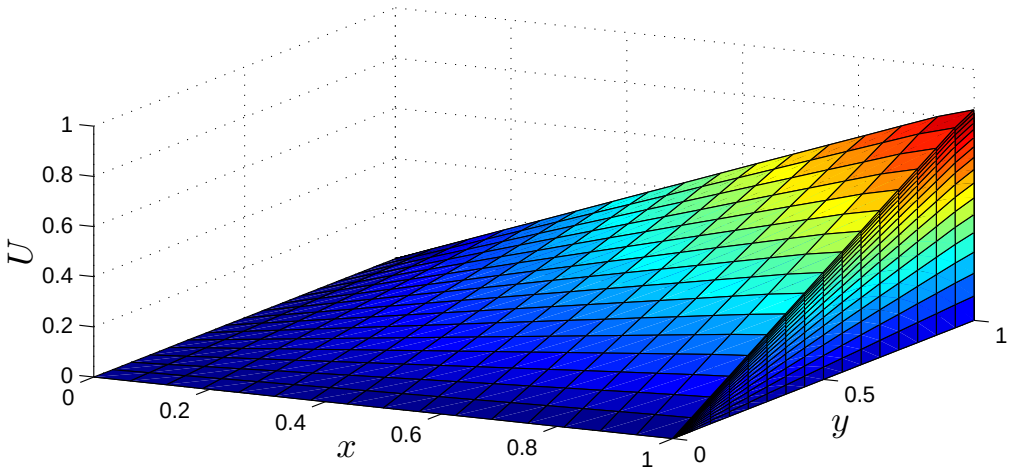

(b) $\varepsilon = 1e-4$.

Figure 6.1: *Surface plots of the numerical solutions* U *at* $t = 2$ *and* $N = 32$ *for Example 6.4.1.*

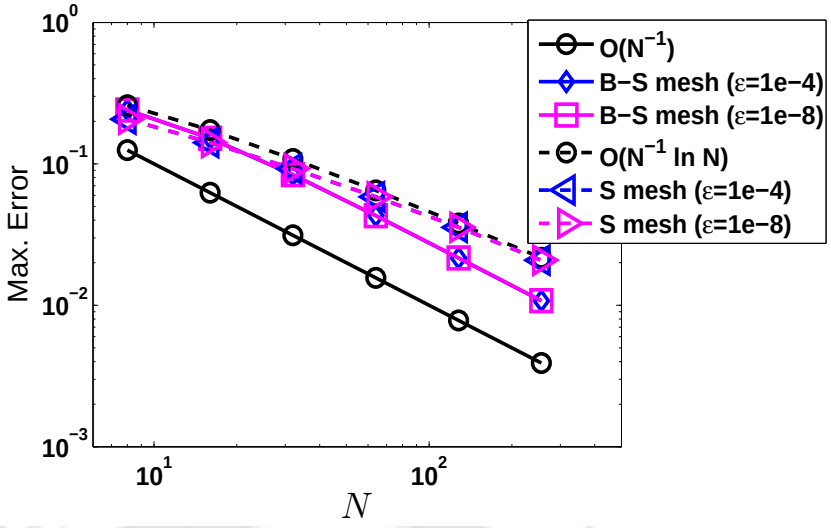

Figure 6.2: *Comparison of the order of convergence through loglog plot for Example 6.4.1.*

Table 6.1: *Maximum pointwise errors and the corresponding order of convergence for Example 6.4.1 on the Bakhvalov-Shishkin mesh.*

ε	Number of mesh-intervals N/temporal mesh-size Δt					
	$8/\frac{1}{5}$	$16/\frac{1}{10}$	$32/\frac{1}{20}$	$64/\frac{1}{40}$	$128/\frac{1}{80}$	$256/\frac{1}{160}$
10^{-1}	9.8602e-2	7.1832e-2	4.0928e-2	2.2042e-2	1.1445e-2	5.8295e-3
	0.4570	0.8116	0.8928	0.9456	0.9732	
10^{-2}	2.1718e-1	1.3625e-1	7.5411e-2	3.9490e-2	2.0204e-2	1.0217e-2
	0.6727	0.8534	0.9333	0.9669	0.9836	
10^{-3}	2.3810e-1	1.4985e-1	8.2815e-2	4.2513e-2	2.1359e-2	1.0678e-2
	0.6680	0.8555	0.9620	0.9931	1.0002	
10^{-4}	2.4035e-1	1.5144e-1	8.3817e-2	4.3002e-2	2.1574e-2	1.0766e-2
	0.6664	0.8534	0.9629	0.9951	1.0028	
10^{-5}	2.4057e-1	1.5160e-1	8.3922e-2	4.3055e-2	2.1599e-2	1.0778e-2
	0.6662	0.8532	0.9629	0.9952	1.0029	
10^{-6}	2.4060e-1	1.5162e-1	8.3932e-2	4.3060e-2	2.1602e-2	1.0779e-2
	0.6662	0.8532	0.9629	0.9952	1.0029	
10^{-7}	2.4060e-1	1.5162e-1	8.3933e-2	4.3061e-2	2.1602e-2	1.0779e-2
	0.6662	0.8531	0.9629	0.9952	1.0029	
10^{-8}	2.4060e-1	1.5162e-1	8.3933e-2	4.3061e-2	2.1602e-2	1.0779e-2
	0.6662	0.8531	0.9629	0.9952	1.0029	
$e^{N,\Delta t}$	**2.4060e-1**	**1.5162e-1**	**8.3933e-2**	**4.3061e-2**	**2.1602e-2**	**1.0779e-2**
$p^{N,\Delta t}$	**0.6662**	**0.8531**	**0.9629**	**0.9952**	**1.0029**	

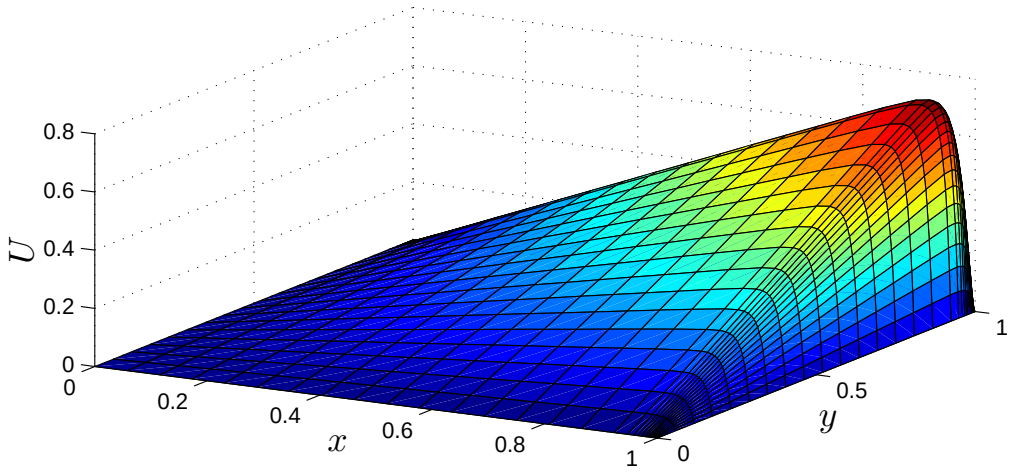

(a) $\varepsilon = 1e-2$.

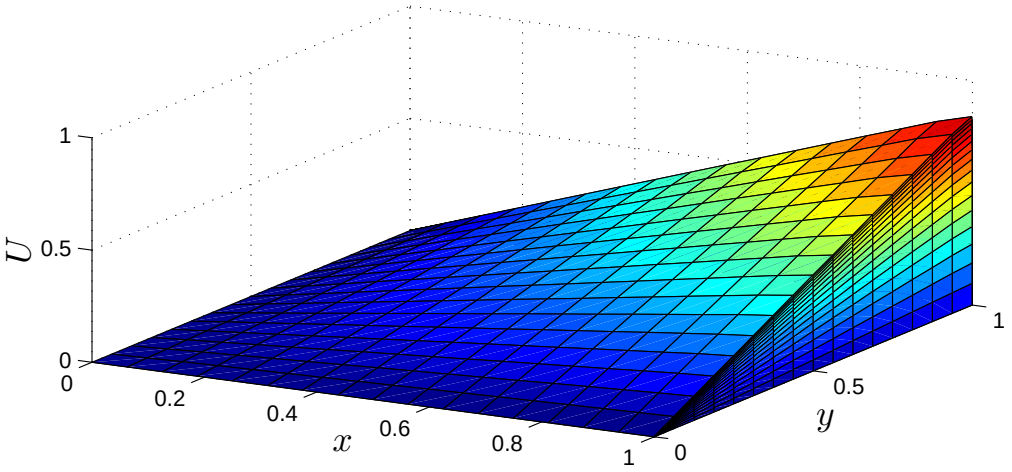

(b) $\varepsilon = 1e-4$.

Figure 6.3: *Surface plots of the numerical solutions U at $t = 2$ and $N = 32$ for Example 6.4.2.*

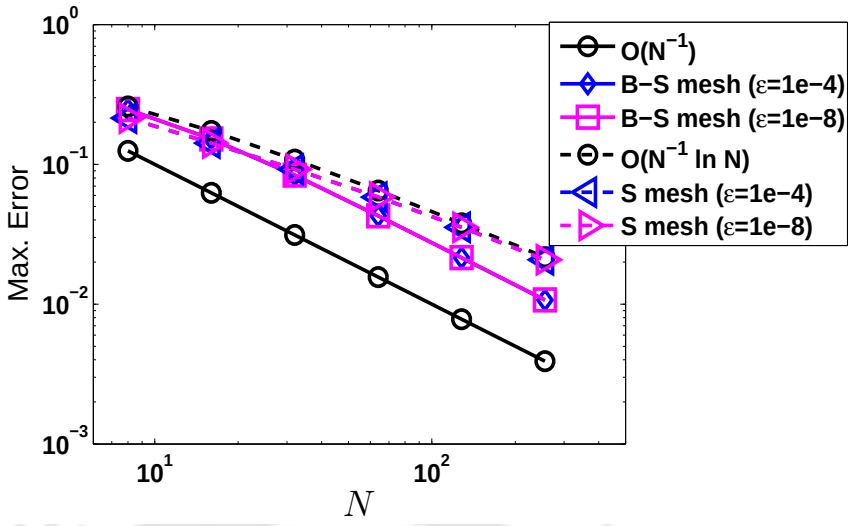

Figure 6.4: *Comparison of the order of convergence through loglog plot for Example 6.4.2.*

Table 6.2: *Maximum pointwise errors and the corresponding order of convergence for Example 6.4.2 on the Bakhvalov-Shishkin mesh.*

ε	Number of mesh-intervals N/temporal mesh-size Δt					
	$8/\frac{1}{5}$	$16/\frac{1}{10}$	$32/\frac{1}{20}$	$64/\frac{1}{40}$	$128/\frac{1}{80}$	$256/\frac{1}{160}$
10^{-1}	1.0571e-1	7.3729e-2	4.1932e-2	2.2514e-2	1.1689e-2	5.9596e-3
	0.5198	0.8142	0.8972	0.9457	0.9718	
10^{-2}	2.2134e-1	1.3621e-1	7.4915e-2	3.9204e-2	2.0054e-2	1.0141e-2
	0.7004	0.8625	0.9343	0.9671	0.9837	
10^{-3}	2.4413e-1	1.5026e-1	8.2578e-2	4.2316e-2	2.1249e-2	1.0622e-2
	0.7002	0.8636	0.9645	0.9938	1.0004	
10^{-4}	2.4663e-1	1.5196e-1	8.3650e-2	4.2833e-2	2.1475e-2	1.0714e-2
	0.6987	0.8612	0.9656	0.9961	1.0032	
10^{-5}	2.4688e-1	1.5213e-1	8.3762e-2	4.2890e-2	2.1501e-2	1.0726e-2
	0.6985	0.8609	0.9657	0.9962	1.0033	
10^{-6}	2.4691e-1	1.5215e-1	8.3773e-2	4.2895e-2	2.1504e-2	1.0727e-2
	0.6985	0.8609	0.9657	0.9962	1.0033	
10^{-7}	2.4691e-1	1.5215e-1	8.3775e-2	4.2896e-2	2.1504e-2	1.0727e-2
	0.6985	0.8609	0.9657	0.9962	1.0033	
10^{-8}	2.4691e-1	1.5215e-1	8.3775e-2	4.2896e-2	2.1504e-2	1.0727e-2
	0.6985	0.8609	0.9657	0.9962	1.0033	
$e^{N,\Delta t}$	**2.4691e-1**	**1.5215e-1**	**8.3775e-2**	**4.2896e-2**	**2.1504e-2**	**1.0727e-2**
$p^{N,\Delta t}$	**0.6985**	**0.8609**	**0.9657**	**0.9962**	**1.0033**	

CHAPTER 7

Fractional-Step Method for Singularly Perturbed 2D Delay Parabolic Convection-Diffusion Problems on Shishkin Mesh

In previous chapter we observed that, to solve a singularly perturbed 2D delay parabolic convection-diffusion problem numerically, we need to handle a banded pentadiagonal matrix. Dealing with such matrix is a costly task in computational perspective. For this reason, to solve the singularly perturbed 2D delay problem in this chapter, first, we use a fractional-step method for discretizing the time derivative of the continuous problem on the uniform mesh in the temporal direction, then, we apply the classical finite difference scheme on a special mesh to discretize those 1D problems resulting of the first step. We derive the truncation errors for the scheme to obtain the error estimates, which shows that the scheme is uniformly convergent of almost first-order (up to a logarithmic factor) in space and first-order in time. Numerical examples are carried out to verify the theoretical results.

7.1 Introduction

In this chapter, we consider the following singularly perturbed 2D delay parabolic convection-diffusion IBVP posed on the domain $\mathfrak{G} = \mathfrak{D} \times \Lambda_t$, $\mathfrak{D} = (0,1)^2$, $\Lambda_t = (0,T]$ and $\Upsilon = \partial\mathfrak{D} \cup \Upsilon_b$, where $\Upsilon_b = \overline{\mathfrak{D}} \times [-\tau, 0]$:

$$\begin{cases} u_t + \mathcal{L}_\varepsilon u(x,y,t) = -c(x,y)u(x,y,t-\tau) + f(x,y,t), & (x,y,t) \in \mathfrak{G}, \\ u(x,y,t) = \varphi_b(x,y,t), & (x,y,t) \in \Upsilon_b, \\ u(x,y,t) = 0, & (x,y,t) \in \partial\mathfrak{D} \times \overline{\Lambda}_t, \end{cases} \tag{7.1.1}$$

where

$$\mathcal{L}_\varepsilon u = -\varepsilon\Delta u + \mathbf{a}(x,y).\nabla u + b(x,y)u,$$

$0 < \varepsilon \ll 1$ is the singular perturbation parameter and $\tau > 0$ is the delay parameter. The coefficients $\mathbf{a} = (a_1, a_2)$, b and c are sufficiently smooth and bounded functions such that $a_1(x, y) \geq \alpha_{_x} > 0$, $a_2(x, y) \geq \alpha_{_y} > 0$, $b(x, y) \geq 0$ and $c(x, y)$ is nonzero on $\overline{\mathfrak{D}}$.

Under sufficient smoothness and necessary compatibility conditions imposed on the functions f and φ_b, the delay parabolic IBVP (7.1.1) admits a unique solution $u(x, y, t)$, which exhibits a regular boundary layer of width $O(\varepsilon)$ along the sides $x = 1$ and $y = 1$, and a corner layer at $(x, y) = (1, 1)$.

The rest part of this chapter is organized as follows: In Section 7.2, the time semidiscretization process through the fractional-step method has been discussed and the uniform convergence of this scheme has been studied. Section 7.3 deals with the piecewise-uniform Shishkin mesh and the classical upwind scheme. The main proof of convergence has been provided in Section 7.4. Numerical results are presented in Section 7.5 and the chapter ends with Section 7.6, that summarizes the main conclusions.

7.2 Time Semidiscretization

In this section, we study the semidiscretization of the singularly perturbed 2D delay parabolic IBVP (7.1.1) which is essential for the analysis of the fully discrete scheme, since it will contribute to the decomposition of the global error for the spatial and temporal variables. Also, we provide the asymptotic behavior of the solution of the semidiscrete problems. Before proceeding for time semidiscretization, we state the bounds for the time derivatives of exact solution.

Lemma 7.2.1. *For $0 \leq i \leq 2$, the time derivatives of the exact solution $u(x, y, t)$ of the IBVP (7.1.1) satisfy the estimate*

$$\left| \frac{\partial^i}{\partial t^i} u(x, y, t) \right| \leq C, \quad (x, y, t) \in \overline{\mathfrak{G}}.$$

Proof. The process is similar to the approach used in Theorem 2.2.3 for obtaining the bounds of the time derivatives. ∎

7.2.1 The semidiscrete problem

First, we discretize the time domain $\overline{\Lambda}_t$ by uniform mesh with mesh-size Δt, such that

$$\Lambda_t^M = \{t_n = n\Delta t, n = 0, \cdots, M, \Delta t = T/M\},$$

where M is the number of mesh-points in the t-direction on the interval $[0, T]$ and the temporal mesh-size Δt satisfies the constraint $p\Delta t = \tau$, where p is a positive integer, $t_n = n\Delta t$, $n \geq -p$.

Now, we split the differential operator $\mathcal{L}_\varepsilon$ as $\mathcal{L}_\varepsilon = \mathcal{L}_{x,\varepsilon} + \mathcal{L}_{y,\varepsilon}$, where

$$\mathcal{L}_{x,\varepsilon} \equiv -\varepsilon\frac{\partial^2}{\partial x^2} + a_1(x,y)\frac{\partial}{\partial x} + b_1(x,y),$$
$$\mathcal{L}_{y,\varepsilon} \equiv -\varepsilon\frac{\partial^2}{\partial y^2} + a_2(x,y)\frac{\partial}{\partial y} + b_2(x,y),$$

with $b(x,y) = b_1(x,y) + b_2(x,y)$, $c(x,y) = c_1(x,y) + c_2(x,y)$ and $f(x,y,t) = f_1(x,y,t) + f_2(x,y,t)$, such that

$$f_1(x,0,t) = f_1(x,1,t) = f_2(0,y,t) = f_2(1,y,t) = 0. \tag{7.2.1}$$

The operator $\mathcal{L}_{x,\varepsilon}$ can be considered as a family of one-dimensional differential operators with one parameter $y \in (0,1)$ (similarly for $\mathcal{L}_{y,\varepsilon}$).

Now, we introduce a time discretization process by means of the following fractional-step scheme:

$$u^{-m} = \varphi_b(x,y,-t_m), \quad m = 0,\cdots,p,$$

$$\begin{cases} (I + \Delta t\mathcal{L}_{x,\varepsilon})u^{n+1/2} = u^n - \Delta t c_1(x,y)u^{n+1-p} + \Delta t f_1(x,y,t_{n+1}), \ y \in (0,1), \\ u^{n+1/2}(0,y) = u^{n+1/2}(1,y) = 0, \end{cases} \tag{7.2.2}$$

$$\begin{cases} (I + \Delta t\mathcal{L}_{y,\varepsilon})u^{n+1} = u^{n+1/2} - \Delta t c_2(x,y)u^{n+1-p} + \Delta t f_2(x,y,t_{n+1}), \ x \in (0,1), \\ u^{n+1}(x,0) = u^{n+1}(x,1) = 0. \end{cases} \tag{7.2.3}$$

The above scheme provides the approximation $u^n(x,y)$ to the solution $u(x,y,t)$ of (7.1.1) at the time level $t_n = n\Delta t$.

The operators $(I + \Delta t\mathcal{L}_{i,\varepsilon})$, $i = x,\ y$, satisfy the following maximum principle.

Lemma 7.2.2. *(**Maximum principle**) Let $\Psi(x,y) \geq 0$ on the boundary $\partial\mathfrak{D}$ and $(I + \Delta t\mathcal{L}_{i,\varepsilon})\Psi(x,y) \geq 0$, $i = x,\ y$ on $\mathfrak{D}$. Then $\Psi(x,y) \geq 0$ on $\overline{\mathfrak{D}}$.*

Proof. First we prove the maximum principle for the operator $(I + \Delta t\mathcal{L}_{x,\varepsilon})$. Let $(x^*,y^*) \in \overline{\mathfrak{D}}$ be such that $\Psi(x^*,y^*) = \min_{\overline{\mathfrak{D}}}\Psi(x,y) < 0$. It is clear that the point $(x^*,y^*) \notin \partial\mathfrak{D}$, which implies $(x^*,y^*) \in \mathfrak{D}$. Since $\Psi_x(x^*,y^*) = 0$ and $\Psi_{xx}(x^*,y^*) \geq 0$, we get

$$\begin{aligned}(I + \Delta t\mathcal{L}_{x,\varepsilon})\Psi(x^*,y^*) \ &= \Psi(x^*,y^*) - \varepsilon\Delta t\Psi_{xx}(x^*,y^*) + \Delta t a_1(x^*,y^*)\Psi_x(x^*,y^*) \\ &\quad + \Delta t b_1(x^*,y^*)\Psi(x^*,y^*) < 0,\end{aligned}$$

which is a contradiction. Hence the required result follows for the operator $(I + \Delta t\mathcal{L}_{x,\varepsilon})$. Similarly, we can prove the maximum principle for the operator $(I + \Delta t\mathcal{L}_{y,\varepsilon})$. ∎

In order to analyze the convergence of the semidiscrete scheme (7.2.2)-(7.2.3), we introduce the local truncation error e_{n+1} defined by $e_{n+1} = u(t_{n+1}) - \widehat{u}^{n+1}$, where $\widehat{u}^{n+1}$ is the solution of the following system:

$$\begin{cases} (I + \Delta t\mathcal{L}_{x,\varepsilon})\widehat{u}^{n+1/2} = u(x,y,t_n) - \Delta t c_1(x,y)\widehat{u}(x,y,t_{n+1-p}) \\ \qquad\qquad + \Delta t f_1(x,y,t_{n+1}),\ y \in (0,1), \\ \widehat{u}^{n+1/2}(0,y) = \widehat{u}^{n+1/2}(1,y) = 0, \end{cases} \tag{7.2.4}$$

$$\begin{cases} (I + \Delta t\mathcal{L}_{y,\varepsilon})\widehat{u}^{n+1} = \widehat{u}^{n+1/2} - \Delta t c_2(x,y)\widehat{u}(x,y,t_{n+1-p}) \\ \qquad\qquad + \Delta t f_2(x,y,t_{n+1}),\ x \in (0,1), \\ \widehat{u}^{n+1}(x,0) = \widehat{u}^{n+1}(x,1) = 0, \end{cases} \tag{7.2.5}$$

where $\widehat{u}(x,y,t_{-m}) = u(x,y,-t_m)$, for $m = 0, \cdots, p$.

Now, one can obtain the following consistency result.

Lemma 7.2.3. *The local error corresponding to the scheme (7.2.4)-(7.2.5) satisfies* $\|e_{n+1}\|_\infty \leq C(\Delta t)^2$.

Proof. Since the function $\widehat{u}^{n+1/2}$ satisfies

$$(I + \Delta t\mathcal{L}_{x,\varepsilon})\widehat{u}^{n+1/2} = u(x,y,t_n) - \Delta t c_1(x,y)\widehat{u}(x,y,t_{n+1-p}) + \Delta t f_1(x,y,t_{n+1}),$$

therefore, from (7.2.5), we obtain

$$\begin{aligned} u(x,y,t_n) &= (I + \Delta t\mathcal{L}_{x,\varepsilon})(I + \Delta t\mathcal{L}_{y,\varepsilon})\widehat{u}^{n+1} - \Delta t f_1(t_{n+1}) + c_1\Delta t\widehat{u}(x,y,t_{n+1-p}) \\ &\quad -\Delta t(I + \Delta t\mathcal{L}_{x,\varepsilon})f_2(t_{n+1}) + c_2\Delta t(I + \Delta t\mathcal{L}_{x,\varepsilon})\widehat{u}(x,y,t_{n+1-p}). \end{aligned}$$

On the other hand, since the solution of (7.1.1) is smooth enough, we have

$$\begin{aligned} u(t_n) &= u(t_{n+1} - \Delta t) = u(t_{n+1}) - \Delta t\frac{\partial u}{\partial t}\Big|_{t_{n+1}} + \int_{t_{n+1}}^{t_n}(t_n - s)\frac{\partial^2 u}{\partial t^2}(s)ds \\ &= u(t_{n+1}) + \Delta t\left[(\mathcal{L}_{x,\varepsilon} + \mathcal{L}_{y,\varepsilon})u(t_{n+1}) - (f_1(t_{n+1}) + f_2(t_{n+1}))\right. \\ &\quad \left. + c_1(x,y)u(x,y,t_{n+1-p}) + c_2(x,y)u(x,y,t_{n+1-p})\right] \\ &\quad + \int_{t_{n+1}}^{t_n}(t_n - s)\frac{\partial^2 u}{\partial t^2}(s)ds \\ &= (I + \Delta t\mathcal{L}_{x,\varepsilon})\left[(I + \Delta t\mathcal{L}_{y,\varepsilon})u(t_{n+1}) - \Delta t f_2(t_{n+1})\right. \\ &\quad \left. + c_2\Delta t u(x,y,t_{n+1-p})\right] - \Delta t f_1(t_{n+1}) + c_1\Delta t u(x,y,t_{n+1-p}) + O(\Delta t^2). \end{aligned}$$

Hence, e_{n+1} satisfies

$$\begin{cases} (I+\Delta t\mathcal{L}_{x,\varepsilon})(I+\Delta t\mathcal{L}_{y,\varepsilon})e_{n+1} = -c_2\Delta t(I+\Delta t\mathcal{L}_{x,\varepsilon})e_{n+1-p} - c_1\Delta t e_{n+1-p} + O(\Delta t^2), \\ e_{n+1}(0,y) = e_{n+1}(1,y) = e_{n+1}(x,0) = e_{n+1}(x,1) = 0. \end{cases} \tag{7.2.6}$$

For the first time interval, *i.e.*, when $t_n \in [0,\tau]$, the delay terms of both the continuous and semidiscrete equations will take value from given initial condition. So, $e_{n+1-p} = 0$. Therefore, the above equation reduces to

$$\begin{cases} (I+\Delta t\mathcal{L}_{x,\varepsilon})(I+\Delta t\mathcal{L}_{y,\varepsilon})e_{n+1} = O(\Delta t^2), \\ e_{n+1}(0,y) = e_{n+1}(1,y) = e_{n+1}(x,0) = e_{n+1}(x,1) = 0. \end{cases}$$

Finally, by applying the maximum principle given in Lemma 7.2.2 for the operators, $(I+\Delta t\mathcal{L}_{i,\varepsilon})$, $i = x, y$, we obtain

$$\|e_{n+1}\|_\infty \le C(\Delta t)^2, \tag{7.2.7}$$

for $t_n \in [0,\tau]$.

For the second time interval, *i.e.*, when $t_n \in (\tau, 2\tau]$, we obtain the required bound by using (7.2.7) and the maximum principle (Lemma 7.2.2) on (7.2.6).

In a similar way, we can prove the required bound for $t_n > 2\tau$. ∎

Lemma 7.2.4. *Under the hypothesis of Lemma 7.2.3, we have*

$$\sup_{n\le T/(\Delta t)} \|u(t_n) - u^n\|_\infty \le C\Delta t.$$

Proof. Let $E_n = u(t_n) - u^n$. Now, subtracting and adding $\widehat{u}^n$, we have

$$E_n = e_n + \widehat{u}^n - u^n = e_n + R_1E_{n-1} + R_1\left(-\Delta t c_1(x,y)e_{n-p}\right) + R_2\left(-\Delta t c_2(x,y)e_{n-p}\right), \tag{7.2.8}$$

where $R_1 \equiv (I+\Delta t\mathcal{L}_{x,\varepsilon})^{-1}(I+\Delta t\mathcal{L}_{y,\varepsilon})^{-1}$ and $R_2 \equiv (I+\Delta t\mathcal{L}_{y,\varepsilon})^{-1}$. We know $e_{n-p} = 0$, when the time discretization parameter n varies from 0 to p. Therefore, we get

$$E_n = e_n + R_1E_{n-1}.$$

Using the above recurrence, we get $E_n = \sum_{i=1}^{n} R_1^{n-i}e_i$. Now, by using the idea given in [12], we get

$$\sup_{0\le n\le p} \|u(t_n) - u^n\|_\infty \le C\Delta t. \tag{7.2.9}$$

For the next time interval, *i.e.*, when n varies from $p+1$ to $2p$, by using the bound given in Lemma 7.2.3 and (7.2.9) to (7.2.8), and proceeding in an analogous way as

done above, we can get the required bound. In a similar way one can get the required bound for the entire time domain Λ_t^M. ∎

Therefore, the time semidiscretization process is uniformly convergent of first-order in time.

Before proceeding, we present a lemma which gives the bounds of the derivatives of the solution of (7.2.4). To prove that without loss of generality we assume that the initial condition of (7.2.4) is zero.

Lemma 7.2.5. *The solution of (7.2.4) satisfies the following bound:*

$$\left|\frac{\partial^i \widehat{u}^{n+1/2}}{\partial x^i}\right| \leq C\left(1+\varepsilon^{-i}\exp\left(-\alpha_{_x}(1-x)/\varepsilon\right)\right), \quad (x,y)\in\overline{\mathfrak{D}}, \quad 0\leq i\leq 4.$$

Proof. To prove the above bound, we will consider several cases.

Case (i). Here, we consider the case, when $i=0$. By using the maximum principle (Lemma 7.2.2), it is easy to show that $|\widehat{u}^{n+1/2}|\leq C$.

Case (ii). Let us take $i=1$. To obtain the bound for the first derivative of $\widehat{u}^{n+1/2}$ with respect to x, let

$$\kappa(x,y)=\frac{\widehat{u}^{n+1/2}(x,y)-u(x,y,t_n)}{\Delta t}, \tag{7.2.10}$$

be the solution of

$$\begin{cases} (I+\Delta t\mathcal{L}_{x,\varepsilon})\kappa=-\mathcal{L}_{x,\varepsilon}u(x,y,t_n)+f_1(x,y,t_{n+1})-c_1(x,y)\widehat{u}(x,y,t_{n+1-p}), \\ \kappa(0,y)=\kappa(1,y)=0. \end{cases} \tag{7.2.11}$$

Since, the right hand side is containing a delay term, we will proceed step by step.

In the first time level, *i.e.*, $t\in(0,\tau)$, since the initial condition is zero, therefore, (7.2.11) reduces to

$$\begin{cases} (I+\Delta t\mathcal{L}_{x,\varepsilon})\kappa=-\mathcal{L}_{x,\varepsilon}u(x,y,t_n)+f_1(x,y,t_{n+1}), \\ \kappa(0,y)=\kappa(1,y)=0. \end{cases}$$

Taking into account that $|\mathcal{L}_{x,\varepsilon}u(x,y,t_n)|\leq C$ [14, Appendix A], the maximum principle (Lemma 7.2.2) implies that $|\kappa|\leq C$.

Now, to find a bound for $\widehat{u}^{n+1/2}$ we apply $\mathcal{L}_{x,\varepsilon}$ on (7.2.10). Simple calculation shows that $\widehat{u}^{n+1/2}$ satisfies the following problem:

$$\begin{cases} \mathcal{L}_{x,\varepsilon}\widehat{u}^{n+1/2}=-\kappa+f_1(x,y,t_{n+1})-c_1(x,y)\widehat{u}(x,y,t_{n+1-p}), \\ \widehat{u}^{n+1/2}(0,y)=\widehat{u}^{n+1/2}(1,y)=0. \end{cases} \tag{7.2.12}$$

Now, for the first time level, $(0,\tau)$, we know $\widehat{u}(x,y,t_{n+1-p})=0$. Therefore, (7.2.12) reduces to

$$\begin{cases} \mathcal{L}_{x,\varepsilon}\widehat{u}^{n+1/2} = -\kappa + f_1(x,y,t_{n+1}), \\ \widehat{u}^{n+1/2}(0,y) = \widehat{u}^{n+1/2}(1,y) = 0. \end{cases}$$

By proceeding in an analogous way as in [41], we can prove that

$$\left|\frac{\partial^i \widehat{u}^{n+1/2}}{\partial x^i}(0,y)\right| \le C, \qquad 0 \le i \le 1,$$
$$\left|\frac{\partial^i \widehat{u}^{n+1/2}}{\partial x^i}(1,y)\right| \le C\varepsilon^{-i}, \quad 0 \le i \le 2,$$

and

$$\left|\frac{\partial \widehat{u}^{n+1/2}}{\partial x}\right| \le C\left[1+\varepsilon^{-1}\exp\left(-\alpha_{_x}(1-x)/\varepsilon\right)\right]. \tag{7.2.13}$$

In the next time level, *i.e.*, when $t\in(\tau,2\tau)$, one can write (7.2.11) as

$$\begin{cases} (I+\Delta t\mathcal{L}_{x,\varepsilon})\kappa = -\mathcal{L}_{x,\varepsilon}u(x,y,t_n) + f_1(x,y,t_{n+1}) - c_1(x,y)\widehat{u}_\tau(x,y,t_{n+1-p}), \\ \kappa(0,y) = \kappa(1,y) = 0, \end{cases}$$

where, $\widehat{u}_\tau(x,y,t_{n+1-p})$ is the semidiscrete solution in $(0,\tau)$. We know that $\widehat{u}_\tau(x,y,t_{n+1-p})$ is bounded. Therefore, using the same argument as done in previous time interval, we can prove that $|\kappa|\le C$.

For $t\in(\tau,2\tau)$, (7.2.12) can be written as

$$\begin{cases} \mathcal{L}_{x,\varepsilon}\widehat{u}^{n+1/2} = -\kappa + f_1(x,y,t_{n+1}) - c_1(x,y)\widehat{u}_\tau(x,y,t_{n+1-p}), \\ \widehat{u}^{n+1/2}(0,y) = \widehat{u}^{n+1/2}(1,y) = 0. \end{cases}$$

Since $\widehat{u}_\tau(x,y,t_{n+1-p})$ is bounded, the right hand side of the above equation is bounded. Now, by using the similar idea used in [41], one can obtain the required bound for the second time interval, *i.e.*, $t\in(\tau,2\tau)$.

In an analogous way, we can get the bound (7.2.13) for $t\ge 2\tau$ as well.

Case (iii). Now, we consider the case for $i=2$. To obtain the bounds for the second-order derivative of $\widehat{u}^{n+1/2}$ with respect to x, we differentiate (7.2.12) with respect to x and obtain

$$\mathcal{L}_{x,\varepsilon}\left(\frac{\partial \widehat{u}^{n+1/2}}{\partial x}\right) = \frac{1}{\Delta t}\left(\frac{\partial u(x,y,t_n)}{\partial x} - \frac{\partial \widehat{u}^{n+1/2}}{\partial x}\right) + \frac{\partial f_1}{\partial x} - \frac{\partial a_1}{\partial x}\frac{\partial \widehat{u}^{n+1/2}}{\partial x} - \frac{\partial b_1}{\partial x}\widehat{u}^{n+1/2} - \frac{\partial c_1}{\partial x}\widehat{u}(x,y,t_{n+1-p}) - c_1\frac{\partial \widehat{u}}{\partial x}(x,y,t_{n+1-p}).$$

By using the same idea as we applied for (7.2.13), we can obtain

$$\left|\frac{\partial^2 \widehat{u}^{n+1/2}}{\partial x^2}\right| \leq C\left[1+\varepsilon^{-2}\exp\left(-\alpha_{_x}(1-x)/\varepsilon\right)\right].$$

But, the above bound can only be obtained if we can prove that

$$\left|\frac{1}{\Delta t}\left(\frac{\partial u(x,y,t_n)}{\partial x}-\frac{\partial \widehat{u}^{n+1/2}}{\partial x}\right)\right| \leq C\left[1+\varepsilon^{-1}\exp\left(-\alpha_{_x}(1-x)/\varepsilon\right)\right]. \tag{7.2.14}$$

For that we assume, $\overline{\kappa}(x,y)=\mathcal{L}_{x,\varepsilon}\kappa$, which satisfies

$$\begin{cases} (I+\Delta t\mathcal{L}_{x,\varepsilon})\overline{\kappa}=\mathcal{L}_{x,\varepsilon}f_1-\mathcal{L}^2_{x,\varepsilon}u(x,y,t_n)-c_1\mathcal{L}_{x,\varepsilon}\widehat{u}(x,y,t_{n+1-p}),\\ \overline{\kappa}(0,y)=\dfrac{1}{\Delta t}\left(f_1(0,y,t_{n+1})-\mathcal{L}_{x,\varepsilon}u(0,y,t_n)-c_1\widehat{u}(0,y,t_{n+1-p})\right),\\ \overline{\kappa}(1,y)=\dfrac{1}{\Delta t}\left(f_1(1,y,t_{n+1})-\mathcal{L}_{x,\varepsilon}u(1,y,t_n)-c_1\widehat{u}(1,y,t_{n+1-p})\right). \end{cases} \tag{7.2.15}$$

In the first time level, *i.e.*, $t\in(0,\tau)$, the IBVP (7.2.15) can be rewritten as

$$\begin{cases} (I+\Delta t\mathcal{L}_{x,\varepsilon})\overline{\kappa}=\mathcal{L}_{x,\varepsilon}f_1-\mathcal{L}^2_{x,\varepsilon}u(x,y,t_n),\\ \overline{\kappa}(0,y)=\dfrac{1}{\Delta t}\left(f_1(0,y,t_{n+1})-\mathcal{L}_{x,\varepsilon}u(0,y,t_n)\right),\\ \overline{\kappa}(1,y)=\dfrac{1}{\Delta t}\left(f_1(1,y,t_{n+1})-\mathcal{L}_{x,\varepsilon}u(1,y,t_n)\right). \end{cases}$$

Now, by using the same idea used in [14], we can prove $|\overline{\kappa}|\leq C$.

Now, one can verify that κ satisfies the following problem:

$$\begin{cases} \mathcal{L}_{x,\varepsilon}\kappa=\overline{\kappa},\\ \kappa(0,y)=\kappa(1,y)=0. \end{cases}$$

So, again proceeding in a similar way as in [41], we can show that

$$\left|\frac{\partial \kappa}{\partial x}\right| \leq C\left[1+\varepsilon^{-1}\exp\left(-\alpha_{_x}(1-x)/\varepsilon\right)\right],$$

and hence

$$\left|\frac{\partial^2 \widehat{u}^{n+1/2}}{\partial x^2}\right| \leq C\left[1+\varepsilon^{-2}\exp\left(-\alpha_{_x}(1-x)/\varepsilon\right)\right].$$

In the next time level, *i.e.*, when $t\in(\tau,2\tau)$, (7.2.15) can be expressed as

$$\begin{cases} (I+\Delta t\mathcal{L}_{x,\varepsilon})\overline{\kappa}=\mathcal{L}_{x,\varepsilon}f_1-\mathcal{L}^2_{x,\varepsilon}u(x,y,t_n)-c_1\mathcal{L}_{x,\varepsilon}\widehat{u}_\tau(x,y,t_{n+1-p}),\\ \overline{\kappa}(0,y)=\dfrac{1}{\Delta t}\left(f_1(0,y,t_{n+1})-\mathcal{L}_{x,\varepsilon}u(0,y,t_n)-c_1\widehat{u}_\tau(0,y,t_{n+1-p})\right),\\ \overline{\kappa}(1,y)=\dfrac{1}{\Delta t}\left(f_1(1,y,t_{n+1})-\mathcal{L}_{x,\varepsilon}u(1,y,t_n)-c_1\widehat{u}_\tau(1,y,t_{n+1-p})\right). \end{cases}$$

Since, we know $\widehat{u}_\tau(x,y,t_{n+1-p})$ is bounded, by using the same idea used in [14], it is easy to show that $|\overline{\kappa}| \leq C$. By following the same way as done for previous time interval $(0,\tau)$, we can obtain the required bound.

In an analogous way, we can prove the required bound for $t \geq 2\tau$.

To obtain the corresponding bounds for higher-order derivatives of $\widehat{u}^{n+1/2}$ with respect to x, we can use the similar idea. ∎

We decompose the solution $\widehat{u}^{n+1/2}$ of (7.2.4) into the smooth and singular components, *i.e.*, $\widehat{u}^{n+1/2} = \widehat{v}^{n+1/2} + \widehat{w}^{n+1/2}$, similarly, we decompose u as $u = v + w$ and $\widehat{u}(x,y,t_{n+1-p})$ as $\widehat{u}(x,y,t_{n+1-p}) = \widehat{v}(x,y,t_{n+1-p}) + \widehat{w}(x,y,t_{n+1-p})$.

We further express the smooth components in the form $\widehat{v}^{n+1/2} = \sum_{k=0}^{3} \varepsilon^k \widehat{v}_k^{n+1/2}$, $v = \sum_{k=0}^{3} \varepsilon^k v_k$ and $\widehat{v}(x,y,t_{n+1-p}) = \sum_{k=0}^{3} \varepsilon^k \widehat{v}_k(x,y,t_{n+1-p})$, where they satisfy the following problem for $y \in (0,1)$:

$$\begin{cases} (I + \Delta t \mathcal{L}_{x,\varepsilon})\widehat{v}^{n+1/2} = v(x,y,t_n) - \Delta t c_1(x,y)\widehat{v}(x,y,t_{n+1-p}) + \Delta t f_1(x,y,t_{n+1}), \\ \widehat{v}^{n+1/2}(0) = 0, \quad \widehat{v}^{n+1/2}(1) = \displaystyle\sum_{i=0}^{3} \varepsilon^i \widehat{v}_i^{n+1/2}(1), \quad \widehat{v}(x,y,t_{n+1-p}) = \widehat{u}(x,y,t_{n+1-p}), \end{cases} \tag{7.2.16}$$

and the singular components satisfy the following problem:

$$\begin{cases} (I + \Delta t \mathcal{L}_{x,\varepsilon})\widehat{w}^{n+1/2} = w(x,y,t_n) - \Delta t c_1(x,y)\widehat{w}(x,y,t_{n+1-p}), \quad y \in (0,1), \\ \widehat{w}^{n+1/2}(0) = 0, \quad \widehat{w}^{n+1/2}(1) = \widehat{u}^{n+1/2}|_{x=1} - \widehat{v}^{n+1/2}(1), \quad \widehat{w}(x,y,t_{n+1-p}) = 0. \end{cases} \tag{7.2.17}$$

The following lemma provides the bounds for the derivatives of the smooth and singular components.

Lemma 7.2.6. *The smooth component $\widehat{v}^{n+1/2}$ and the singular component $\widehat{w}^{n+1/2}$ defined in (7.2.16) and (7.2.17), respectively, satisfy the following bounds:*

$$\left|\left| \frac{\partial^i \widehat{v}^{n+1/2}}{\partial x^i} \right|\right|_\infty \leq C\left(1 + \varepsilon^{3-i}\right),$$

and

$$\left| \frac{\partial^i \widehat{w}^{n+1/2}}{\partial x^i} \right| \leq C\varepsilon^{-i} \exp(-\alpha_x(1-x)/\varepsilon), \quad 0 \leq i \leq 4.$$

Proof. Since, we have obtained the bounds of the derivatives of $\widehat{u}^{n+1/2}$, one can easily obtain the required bounds by the same idea as given in Theorem 2.2.4 of Chapter 2. ∎

7.3 The Discrete Problem

In this section, we describe the layer-adapted Shishkin meshes for the spatial directions, then we discretize the spatial derivatives in the semidiscrete scheme (7.2.4)-(7.2.5).

7.3.1 Discretization of the domain

Let the rectangular mesh $\overline{\mathfrak{D}}^N$ be defined by the tensor product of the 1D Shishkin meshes, *i.e.*, $\overline{\mathfrak{D}}^N = \overline{\Omega}_x^N \times \overline{\Omega}_y^N$, which is constructed as follows:

First, define the transition parameters

$$\rho_l = \min\left\{\frac{1}{2}, \rho_{l,0}\varepsilon \ln N\right\}, \; l = x, \, y,$$

where $\rho_{l,0} \geq 1/\alpha_l$. In the analysis, we shall assume that $\rho_l = \rho_{l,0}\varepsilon \ln N$. Note that if $\rho_l = 1/2$, $l = x, \, y$, then the mesh is uniform and in this case the error estimates can be obtained in the classical way.

To obtain the piecewise-uniform Shishkin mesh, we divide the domain $\overline{\Omega}_x^N$ into two sub-domains $[0, 1-\rho_x]$ and $(1-\rho_x, 1]$ and each sub-domain will have $N/2$ uniform mesh-intervals, and denote it by

$$\overline{\Omega}_x^N = \left\{0 = x_0, \, x_1, \, \cdots, \, x_{N/2} = 1-\rho_x, \, \cdots, \, x_N = 1\right\}.$$

Similarly, we define $\overline{\Omega}_y^N = \left\{0 = y_0, \, y_1, \, \cdots, \, y_{N/2} = 1-\rho_y, \, \cdots, \, y_N = 1\right\}$.

We denote the mesh-sizes in both the spatial directions by

$$h_{x,i} = x_i - x_{i-1}, \; i = 1, \cdots, N, \quad \widehat{h}_{x,i} = h_{x,i} + h_{x,i+1}, i = 1, \cdots, N-1,$$

$$h_{y,j} = y_j - y_{j-1}, \; j = 1, \cdots, N, \quad \widehat{h}_{y,j} = h_{y,j} + h_{y,j+1}, j = 1, \cdots, N-1,$$

and let $H_l = 2(1-\rho_l)/N$ and $h_l = 2\rho_l/N$, $l = x, \, y$, be the mesh-sizes in $[0, 1-\rho_l]$ and $[1-\rho_l, 1]$ respectively. Then it is easy to see that

$$N^{-1} \leq H_l \leq 2N^{-1}, \quad h_l = 2\rho_{l,0}\varepsilon N^{-1} \ln N, \quad l = x, \, y.$$

We define the discrete domain by $\mathfrak{G}^{N,M} = \overline{\mathfrak{G}}^{N,M} \cap \mathfrak{G}$ where $\overline{\mathfrak{G}}^{N,M} = \overline{\Omega}_x^N \times \overline{\Omega}_y^N \times \Lambda_t^M$, and $\Upsilon_b^N = \overline{\Omega}_x^N \times \overline{\Omega}_y^N \times \Lambda_t^p$, where Λ_t^p denotes the set of $p+1$ uniform mesh-points in $[-\tau, 0]$ and $\Omega_x^N = \overline{\Omega}_x^N \cap \Omega_x$, $\Omega_y^N = \overline{\Omega}_y^N \cap \Omega_y$. The boundary points of $\overline{\mathfrak{G}}^{N,M}$ are $\Upsilon^N = \{\overline{\mathfrak{G}}^{N,M} \cap \Upsilon\} \cup \Upsilon_b^N$. We further discretize $\overline{\mathfrak{G}}_s{}^{N,M} = \mathfrak{D}^N \times \Lambda_{s,t}^p$, where $\Lambda_{s,t}^p$ denotes the set of $p+1$ uniform mesh-points in $[(s-1)\tau, s\tau]$, for $s = 1, 2, \cdots, k$. From the above discretization we can observe that $\overline{\mathfrak{G}}^{N,M} = \bigcup_{s=1}^{k} \overline{\mathfrak{G}}_s{}^{N,M}$.

7.3.2 Numerical scheme

Let $\mathcal{L}_{x,\varepsilon}^N$ denotes the discretization of the differential operator $\mathcal{L}_{x,\varepsilon}$ after replacing the spatial derivatives by the upwind finite difference scheme on Ω_x^N. Then the discretized

equation can be written as follows: For $y \in \Omega_y^N$,

$$\begin{cases} (I + \Delta t \mathcal{L}_{x,\varepsilon}^N)\widehat{U}_{x_i,y}^{n+1/2} & = (I + \Delta t(-\varepsilon\delta_x^2 + a_1(x_i,y)\delta_x^- + b_1(x_i,y)))\widehat{U}_{x_i,y}^{n+1/2} \\ & = u(x_i,y,t_n) - \Delta t c_1(x_i,y)\widehat{U}(x_i,y,t_{n+1-p}) \\ & \quad + \Delta t f_1(x_i,y,t_{n+1}), \quad i = 1,\cdots,N-1, \\ \widehat{U}_{0,y}^{n+1/2} = \widehat{U}_{1,y}^{n+1/2} = 0, \end{cases} \tag{7.3.1}$$

and, for $x \in \Omega_x^N$,

$$\begin{cases} (I + \Delta t \mathcal{L}_{y,\varepsilon}^N)\widehat{U}_{x,y_j}^{n+1} & = (I + \Delta t(-\varepsilon\delta_y^2 + a_2(x,y_j)\delta_y^- + b_2(x,y_j)))\widehat{U}_{x,y_j}^{n+1} \\ & = \widehat{U}_{x,y_j}^{n+1/2} - \Delta t c_2(x,y_j)\widehat{U}(x,y_j,t_{n+1-p}) \\ & \quad + \Delta t f_2(x,y_j,t_{n+1}), \quad j = 1,\cdots,N-1, \\ \widehat{U}_{x,0}^{n+1} = \widehat{U}_{x,1}^{n+1} = 0, \end{cases} \tag{7.3.2}$$

where $\widehat{U}(x,y,t_{-m}) = u(x,y,-t_m)$, for $m = 0,\cdots,p$.

After rearranging the terms in (7.3.1), for $i = 1,\cdots,N-1$, we get

$$\begin{cases} (I + \Delta t \mathcal{L}_{x,\varepsilon}^N)\widehat{U}_{x_i,y}^{n+1/2} \equiv r_i^{1,-}\widehat{U}_{x_{i-1},y}^{n+1/2} + r_i^{1,0}\widehat{U}_{x_i,y}^{n+1/2} + r_i^{1,+}\widehat{U}_{x_{i+1},y}^{n+1/2} = F_{1x_i,y}, \\ \widehat{U}_{0,y}^{n+1/2} = \widehat{U}_{1,y}^{n+1/2} = 0, \end{cases} \tag{7.3.3}$$

where

$$\begin{cases} r_i^{1,-} = \Delta t\left(-\dfrac{2\varepsilon}{\widehat{h}_{x,i}h_{x,i}} - \dfrac{a_1(x_i,y)}{h_{x,i}}\right), \quad r_i^{1,+} = \Delta t\left(-\dfrac{2\varepsilon}{\widehat{h}_{x,i}h_{x,i+1}}\right), \\ r_i^{1,0} = 1 + \Delta t b_1(x_i,y) - r_i^{1,-} - r_i^{1,+}, \\ F_{1x_i,y} = u(x_i,y,t_n) + \Delta t\left(-c_1(x_i,y)\widehat{U}(x_i,y,t_{n+1-p}) + f_1(x_i,y,t_{n+1})\right). \end{cases} \tag{7.3.4}$$

Similarly, after rearranging the terms in (7.3.2), for $j = 1,\cdots,N-1$, we get

$$\begin{cases} (I + \Delta t \mathcal{L}_{y,\varepsilon}^N)\widehat{U}_{x,y_j}^{n+1} \equiv r_j^{2,-}\widehat{U}_{x,y_{j-1}}^{n+1} + r_j^{2,0}\widehat{U}_{x,y_j}^{n+1} + r_j^{2,+}\widehat{U}_{x,y_{j+1}}^{n+1} = F_{2x,y_j}, \\ \widehat{U}_{x,0}^{n+1} = \widehat{U}_{x,1}^{n+1} = 0, \end{cases} \tag{7.3.5}$$

where

$$\begin{cases} r_j^{2,-} = \Delta t\left(-\dfrac{2\varepsilon}{\widehat{h}_{y,j}h_{y,j}} - \dfrac{a_2(x,y_j)}{h_{y,j}}\right), \quad r_j^{2,+} = \Delta t\left(-\dfrac{2\varepsilon}{\widehat{h}_{y,j}h_{y,j+1}}\right), \\ r_j^{2,0} = 1 + \Delta t b_2(x,y_j) - r_j^{2,-} - r_j^{2,+}, \\ F_{2x,y_j} = \widehat{U}_{x,y_j}^{n+1/2} - \Delta t\left(c_2(x,y_j)\widehat{U}(x,y_j,t_{n+1-p}) + f_2(x,y_j,t_{n+1})\right). \end{cases} \tag{7.3.6}$$

Lemma 7.3.1. *The matrices associated with the finite difference schemes (7.3.1) and (7.3.2) are M-matrices.*

Proof. For $\ell = 1, 2$, it is clear from (7.3.3)-(7.3.6) that,

$$r_l^{\ell,-} < 0,\ r_l^{\ell,+} < 0 \,\text{and}\, r_l^{\ell,0} > 0$$

along with

$$|r_1^{\ell,0}| - |r_1^{\ell,+}| > 0,\ |r_{N-1}^{\ell,0}| - |r_{N-1}^{\ell,-}| > 0 \text{ and } |r_l^{\ell,0}| - |r_l^{\ell,+}| - |r_l^{\ell,-}| > 0, \text{ for } l = 1, \cdots, N-1.$$

Therefore, the matrices associated with the finite difference schemes are M-matrices. ∎

As a consequence, the difference operator given in (7.3.1) satisfies the following discrete maximum principle.

Lemma 7.3.2. *(***Discrete maximum principle***) Assume that the discrete function Ψ_i satisfies $\Psi_i \geq 0$ on $i = 0, N$. Then $(I + \Delta t \mathcal{L}_{x,\varepsilon}^N)\Psi_i \geq 0$ on Ω_x^N implies that $\Psi_i \geq 0$ at each point of $\overline{\Omega}_x^N$.*

Hence the method is uniformly stable in the supremum norm. Similar property holds for the difference operator defined in (7.3.2).

7.4 Convergence Analysis

This section provides the ε-uniform error estimate for the numerical solution of the following fully discrete scheme:

$$U_{i,j}^{-m} = \varphi_b(x_i, y_j, -t_m), \quad m = 0, \cdots, p, \quad \text{and} \quad i, j = 0, \cdots, N,$$

$$\begin{cases} (I + \Delta t \mathcal{L}_{x,\varepsilon}^N) U_{i,j}^{n+1/2} = U_{i,j}^n - \Delta t c_1(x_i, y_j) U_{i,j}^{n+1-p} + \Delta t f_1(x_i, y_j, t_{n+1}),\ 1 \leq i \leq N-1, \\ U_{0,j}^{n+1/2} = U_{N,j}^{n+1/2} = 0, \quad 0 \leq j \leq N, \end{cases} \tag{7.4.1}$$

$$\begin{cases} (I + \Delta t \mathcal{L}_{y,\varepsilon}^N) U_{i,j}^{n+1} = U_{i,j}^{n+1/2} - \Delta t c_2(x_i, y_j) U_{i,j}^{n+1-p} + \Delta t f_2(x_i, y_j, t_{n+1}),\ 1 \leq j \leq N-1, \\ U_{i,0}^{n+1} = U_{i,N}^{n+1} = 0, \quad 0 \leq i \leq N. \end{cases} \tag{7.4.2}$$

The following theorem provides the error bounds, when $t \in [0, \tau]$.

Theorem 7.4.1. *Let u be the exact solution of (7.1.1) and $\{U^n\}$ be the numerical solution of the fully discrete scheme (7.4.1)-(7.4.2) at time level $t_n = n\Delta t$. Then there exists a positive constant C, independent of ε, N, with $0 < q < 1$ such that*

$$\left\| u(x_i, y_j, t_n) - U_{i,j}^n \right\|_\infty \leq C(\Delta t + N^{-1+q} \ln N),$$

for $(x_i, y_j, t_n) \in \Omega_x^N \times \Omega_y^N \times \Lambda_{1,t}^p$.

Proof. For the first time interval $[0,\tau]$, the delay terms present in the right hand side of (7.1.1) and (7.4.1)-(7.4.2) will get replaced by the given initial condition. So, the analysis can be carried out in the same way as one can do for a problem with out delay. Therefore, for $t \in [0,\tau]$ we can adapt the proof of convergence as given in [14], that is, we can have the following error bound:

$$\left\|u(x_i,y_j,t_n) - U_{i,j}^n\right\|_\infty \leq C(\Delta t + N^{-1+q}\ln N),$$

for $(x_i,y_j,t_n) \in \Omega_x^N \times \Omega_y^N \times \Lambda_{1,t}^p$. ∎

On the second interval $(\tau,2\tau]$, the approach of [14] is not applicable because, the value of the delay terms present in the right hand side of (7.4.1)-(7.4.2) will be the numerical solution obtained in previous time interval $[0,\tau]$. Therefore, we will do the detailed analysis to get the error over the interval $(\tau,2\tau]$.

On the domain $\mathfrak{D}\times(\tau,2\tau)$, the equation (7.2.4) becomes

$$\begin{cases} (I+\Delta t\mathcal{L}_{x,\varepsilon})\widehat{u}^{n+1/2} = u(x,y,t_n) - \Delta t c_1(x,y)\widehat{u}(x,y,t_{n+1-p}) \\ \qquad\qquad\qquad\qquad + \Delta t f_1(x,y,t_{n+1}), \quad y\in(0,1), \\ \widehat{u}^{n+1/2}(0,y) = \widehat{u}^{n+1/2}(1,y) = 0, \quad \widehat{u}(x,y,t_{n+1-p}) = \widehat{u}_\tau(x,y,t_{n+1-p}), \end{cases} \tag{7.4.3}$$

and

$$\begin{cases} (I+\Delta t\mathcal{L}_{y,\varepsilon})\widehat{u}^{n+1} = \widehat{u}^{n+1/2} - \Delta t c_2(x,y)\,\widehat{u}(x,y,t_{n+1-p}) \\ \qquad\qquad\qquad\qquad + \Delta t f_2(x,y,t_{n+1}), \quad x\in(0,1), \\ \widehat{u}^{n+1}(x,0) = \widehat{u}^{n+1}(x,1) = 0, \qquad \widehat{u}(x,y,t_{n+1-p}) = \widehat{u}_\tau(x,y,t_{n+1-p}), \end{cases} \tag{7.4.4}$$

respectively, where $\widehat{u}_\tau(x,y,t_{n+1-p})$ is the semidiscrete solution of (7.2.4)-(7.2.5) on the domain $\mathfrak{D}\times(0,\tau)$.

The discrete problems corresponding to (7.4.3) and (7.4.4) are given by

$$\begin{cases} (I+\Delta t\mathcal{L}_{x,\varepsilon}^N)\widehat{U}_{x_i,y}^{n+1/2} &= (I+\Delta t(-\varepsilon\delta_x^2 + a_1(x_i,y)\delta_x^- + b_1(x_i,y)))\widehat{U}_{x_i,y}^{n+1/2} \\ &= u(x_i,y,t_n) - \Delta t c_1(x_i,y)\widehat{U}(x_i,y,t_{n+1-p}) \\ &\quad + \Delta t f_1(x_i,y,t_{n+1}), \quad i=1,\cdots,N-1, \\ \widehat{U}_{0,y}^{n+1/2} = \widehat{U}_{1,y}^{n+1/2} = 0, & \widehat{U}(x_i,y,t_{n+1-p}) = \widehat{U}_1(x_i,y,t_{n+1-p}), \end{cases} \tag{7.4.5}$$

and

$$\begin{cases} (I+\Delta t\mathcal{L}_{y,\varepsilon}^N)\widehat{U}_{x,y_j}^{n+1} &= (I+\Delta t(-\varepsilon\delta_y^2 + a_2(x,y_j)\delta_y^- + b_2(x,y_j)))\widehat{U}_{x,y_j}^{n+1} \\ &= \widehat{U}_{x,y_j}^{n+1/2} - \Delta t c_2(x,y_j)\widehat{U}(x,y_j,t_{n+1-p}) \\ &\quad + \Delta t f_2(x,y_j,t_{n+1}), \quad j=1,\cdots,N-1, \\ \widehat{U}_{x,0}^{n+1} = \widehat{U}_{x,1}^{n+1} = 0, & \widehat{U}(x,y_j,t_{n+1-p}) = \widehat{U}_1(x,y_j,t_{n+1-p}), \end{cases} \tag{7.4.6}$$

respectively, where $\widehat{U}_1(\cdot,\cdot,t_{n+1-p})$ is the numerical solution of (7.3.1)-(7.3.2) calculated on the time interval $[0,\tau]$

Similarly, the equations (7.2.16) and (7.2.17) become

$$\begin{cases} (I+\Delta t\mathcal{L}_{x,\varepsilon})\widehat{v}^{n+1/2} = v(x,y,t_n) - \Delta t c_1(x,y)\widehat{v}(x,y,t_{n+1-p}) \\ \qquad\qquad +\Delta t f_1(x,y,t_{n+1}), \quad y\in(0,1), \\ \widehat{v}^{n+1/2}(0)=0, \quad \widehat{v}^{n+1/2}(1) = \sum_{i=0}^{3}\varepsilon^i\,\widehat{v}_i^{n+1/2}(1), \quad \widehat{v}(x,y,t_{n+1-p}) = \widehat{u}_\tau(x,y,t_{n+1-p}), \end{cases} \tag{7.4.7}$$

and

$$\begin{cases} (I+\Delta t\mathcal{L}_{x,\varepsilon})\widehat{w}^{n+1/2} = w(x,y,t_n) - \Delta t c_1(x,y)\widehat{w}(x,y,t_{n+1-p}), \quad y\in(0,1), \\ \widehat{w}^{n+1/2}(0)=0, \quad \widehat{w}^{n+1/2}(1) = \widehat{u}^{n+1/2}|_{x=1} - \widehat{v}^{n+1/2}(1), \quad \widehat{w}(x,y,t_{n+1-p})=0, \end{cases} \tag{7.4.8}$$

respectively.

The discrete problems corresponding to (7.4.7) and (7.4.8) are given by

$$\begin{cases} (I+\Delta t\mathcal{L}^N_{x,\varepsilon})\widehat{V}^{n+1/2} &= (I+\Delta t(-\varepsilon\delta_x^2 + a_1(x_i,y)\delta_x^- + b_1(x_i,y)))\widehat{V}^{n+1/2} \\ &= v(x_i,y,t_n) - \Delta t c_1(x_i,y)\widehat{V}(x_i,y,t_{n+1-p}) \\ &\quad +\Delta t f_1(x_i,y,t_{n+1}), \quad i=1,\cdots,N-1, \\ \widehat{V}_0^{n+1/2} = \widehat{v}^{n+1/2}(0), & \widehat{V}_1^{n+1/2} = \widehat{v}^{n+1/2}(1), \quad \widehat{V}(x_i,y,t_{n+1-p}) = \widehat{U}_1(x_i,y,t_{n+1-p}), \end{cases} \tag{7.4.9}$$

and

$$\begin{cases} (I+\Delta t\mathcal{L}^N_{x,\varepsilon})\widehat{W}^{n+1/2} &= (I+\Delta t(-\varepsilon\delta_x^2 + a_1(x_i,y)\delta_x^- + b_1(x_i,y)))\widehat{W}^{n+1/2} \\ &= w(x_i,y,t_n) - \Delta t c_1(x_i,y)\widehat{W}(x_i,y,t_{n+1-p}), \ i=1,\cdots,N-1, \\ \widehat{W}_0^{n+1/2} = \widehat{w}^{n+1/2}(0), & \widehat{W}_1^{n+1/2} = \widehat{w}^{n+1/2}(1), \quad \widehat{W}(x_i,y,t_{n+1-p}) = 0, \end{cases} \tag{7.4.10}$$

respectively, where $\widehat{V}^{n+1/2}$, $\widehat{W}^{n+1/2}$, $\widehat{V}(x_i,y,t_{n+1-p})$ and $\widehat{W}(x_i,y,t_{n+1-p})$ are the discrete versions of $\widehat{v}^{n+1/2}$, $\widehat{w}^{n+1/2}$, $\widehat{v}(x,y,t_{n+1-p})$ and $\widehat{w}(x,y,t_{n+1-p})$, respectively.

At the node $(x_i,y,t_{n+1/2})$ the errors can be written in the form

$$(\widehat{U}-\widehat{u})(x_i,y,t_{n+1/2}) = (\widehat{V}-\widehat{v})(x_i,y,t_{n+1/2}) + (\widehat{W}-\widehat{w})(x_i,y,t_{n+1/2}).$$

Now, before proceeding further, we give some technical lemmas which will be required for the error bound.

Lemma 7.4.2. *The solution of (7.4.8) satisfies*

$$|\widehat{w}(x_i, y, t_{n+1/2})| \leq CN^{-1}, \quad 1 \leq i \leq N/2.$$

Proof. We know from Lemma 7.2.6, the singular component satisfies

$$|\widehat{w}(x_i, y, t_{n+1/2})| \leq C \exp(-\alpha_{_x}(1 - x_i)/\varepsilon) \leq C \exp(-\alpha_{_x}\rho_{_x}/\varepsilon).$$

Since $\rho_{_x} \geq (\varepsilon/\alpha_{_x}) \ln N$, we get $|\widehat{w}(x_i, y, t_{n+1/2})| \leq CN^{-1}$. ∎

Lemma 7.4.3. *Numerical solution of (7.4.10) satisfies*

$$|\widehat{W}(x_i, y, t_{n+1/2})| \leq \prod_{j=i+1}^{N} \left(1 + \frac{\alpha_{_x} h_{x,j}}{\varepsilon}\right)^{-1}, \text{ for } i = 0, 1, \cdots, N-1.$$

Proof. Define the Padé approximation of the boundary layer function $\exp(-\alpha_{_x}(1 - x_i)/\varepsilon)$ as $S_i = \prod_{j=1}^{i} \left(1 + \frac{\alpha_{_x} h_{x,j}}{\varepsilon}\right)$, with $S_0 = 1$.

Therefore,

$$\begin{aligned} \frac{S_i}{S_N} &= \prod_{j=i+1}^{N} \left(1 + \frac{\alpha_{_x} h_{x,j}}{\varepsilon}\right)^{-1} \\ &\geq \prod_{j=i+1}^{N} \exp\left(-\alpha_{_x} h_{x,j}/\varepsilon\right) \\ &= \exp\left(-\alpha_{_x}(1 - x_i)/\varepsilon\right). \end{aligned}$$

Assume $Y_i = CS_i/S_N$, for $i = 0, 1, \cdots, N-1$. Therefore, we have

$$(I + \Delta t \mathcal{L}^N_{x,\varepsilon}) Y_i = \frac{C}{S_N} (I + \Delta t \mathcal{L}^N_{x,\varepsilon}) S_i.$$

Now, by applying the difference operator to S_i, we obtain

$$\begin{aligned} (I + \Delta t \mathcal{L}^N_{x,\varepsilon}) S_i &= \left(I + \Delta t(-\varepsilon \delta_x^2 + a_1(x_i, y)\delta_x^- + b_1(x_i, y))\right) S_i \\ &= (1 + \Delta t b_1(x_i, y)) S_i - \Delta t \varepsilon \delta_x^2 S_i + \Delta t a_1(x_i, y) \delta_x^- S_i. \quad (7.4.11) \end{aligned}$$

It is easy to derive that

$$\delta_x^- S_i = \frac{\alpha_{_x}}{(\varepsilon + \alpha_{_x} h_{x,i})} S_i, \quad \delta_x^+ S_i = \frac{\alpha_{_x}}{\varepsilon} S_i, \quad \text{and} \quad \varepsilon \delta_x^2 S_i = \frac{-\alpha_{_x}^2 h_{x,i}}{\widehat{h}_{x,i}(\varepsilon + \alpha_{_x} h_{x,i})} S_i.$$

Therefore, from (7.4.11), we get that

$$(I + \Delta t \mathcal{L}^N_{x,\varepsilon}) S_i \geq \frac{C}{\max\{\varepsilon, h_{x,i}\}} S_i.$$

Now, for $t \in (\tau, 2\tau)$, by using the initial condition given in (7.4.10), and the bound for the singular component, (7.4.10) can be written as

$$(I + \Delta t \mathcal{L}^N_{x,\varepsilon})\widehat{W}(x_i, y, t_{n+1/2}) \leq C \exp\left(-\alpha_x(1 - x_i)/\varepsilon\right) \leq C\frac{S_i}{S_N} \leq (I + \Delta t \mathcal{L}^N_{x,\varepsilon})Y_i.$$

By using the discrete maximum principle (Lemma 7.3.2), we obtain that $\widehat{W}(x_i, y, t_{n+1/2}) \leq CY_i$. With the same argument, we can have $-\widehat{W}(x_i, y, t_{n+1/2}) \leq CY_i$.

Hence, we have $|\widehat{W}(x_i, y, t_{n+1/2})| \leq CY_i$, which is the required bound. ∎

Lemma 7.4.4. *The error of the singular component satisfies*

$$|(\widehat{W} - \widehat{w})(x_i, y, t_{n+1/2})| \leq CN^{-1}, \quad \text{for } i = 1, \cdots, N/2.$$

Proof. For $i = 1, \cdots, N/2$, we have

$$|(\widehat{W} - \widehat{w})(x_i, y, t_{n+1/2})| \leq |\widehat{W}| + |\widehat{w}| \leq CY_i + CN^{-1}, \tag{7.4.12}$$

by using the result of Lemma 7.4.2 and Lemma 7.4.3.

From the definition of Y_i and the monotonicity of Y_i, we have

$$\frac{S_i}{S_N} \leq \frac{S_{N/2}}{S_N} = \prod_{j=N/2+1}^{N}\left(1 + \frac{\alpha_x h_{x,j}}{\varepsilon}\right)^{-1} = (1 + 2N^{-1}\ln N)^{-N/2}.$$

We know that $\ln(1 + m) \geq m - m^2/2$ for $m \geq 0$. Therefore,

$$-\frac{N}{2}\ln(1 + 2N^{-1}\ln N) \leq -\frac{N}{2}\left[2N^{-1}\ln N - \frac{(2N^{-1}\ln N)^2}{2}\right] = -\ln N + N^{-1}\ln^2 N.$$

Now, by taking exponential on the both sides, we get $Y_i \leq CN^{-1}$. Using this bound in (7.4.12), one can get the required result. ∎

Theorem 7.4.5. *Let $\widehat{u}^{n+1/2}$ be the exact solution of the problem (7.4.3) and $\widehat{U}^{n+1/2}_{x_i,y}$ be the numerical solution of the upwind scheme (7.4.5) defined on the special mesh Ω^N_x. Then we have the following error bound*

$$|\widehat{u}^{n+1/2}(x_i, y) - \widehat{U}^{n+1/2}_{x_i,y}| \leq CN^{-1}\ln N.$$

Proof. The local truncation error for the smooth component can be written as

$$\begin{aligned}(I + \Delta t \mathcal{L}^N_{x,\varepsilon})(\widehat{V} - \widehat{v})(x_i, y, t_{n+1/2}) &= \left((I + \Delta t \mathcal{L}^N_{x,\varepsilon}) - (I + \Delta t \mathcal{L}_{x,\varepsilon})\right)\widehat{v}(x_i, y, t_{n+1/2}) \\ &\quad -c_1\Delta t(\widehat{V} - \widehat{v})(x_i, y, t_{n+1-p}).\end{aligned}$$

By using the initial conditions from (7.4.7) and (7.4.9), we get

$$\begin{aligned}(I + \Delta t \mathcal{L}^N_{x,\varepsilon})(\widehat{V} - \widehat{v})(x_i, y, t_{n+1/2}) &= \left((I + \Delta t \mathcal{L}^N_{x,\varepsilon}) - (I + \Delta t \mathcal{L}_{x,\varepsilon})\right)\widehat{v}(x_i, y, t_{n+1/2}) \\ &\quad -c_1\Delta t(\widehat{U}_1 - \widehat{u}_\tau)(x_i, y, t_{n+1-p}).\end{aligned}$$

Since, we are estimating the error in $\Lambda_{2,t}$, the delay term in the right hand side of the above equation will be in $\Lambda_{1,t}$. From [14], we know

$$\left|\left(\widehat{U}-\widehat{u}\right)(x_i,y_j,t_n)\right| \leq CN^{-1}\ln N, \tag{7.4.13}$$

for $(x_i,y_j,t_n) \in \Omega_x^N \times \Omega_y^N \times \Lambda_{1,t}^p$.

Now, by using (7.4.13) along with the Taylor's formula we get

$$(I+\Delta t\mathcal{L}_{x,\varepsilon}^N)(\widehat{V}-\widehat{v})(x_i,y,t_{n+1/2}) \leq CN^{-1}\ln N.$$

Now by choosing an appropriate barrier function and applying the discrete maximum principle (Lemma 7.3.2), we can obtain

$$\left|(\widehat{V}-\widehat{v})(x_i,y,t_{n+1/2})\right| \leq CN^{-1}\ln N. \tag{7.4.14}$$

To find the error bound of the singular component, we will consider two cases as follows:

If $i \leq N/2$, then we can find

$$|(\widehat{W}-\widehat{w})(x_i,y,t_{n+1/2})| \leq CN^{-1}, \text{ for } i=1,\cdots,N/2.$$

by using Lemma 7.4.4.

In the second case, when $i = N/2+1,\cdots,N$, the local truncation error for the singular component can be written as

$$\begin{aligned}(I+\Delta t\mathcal{L}_{x,\varepsilon}^N)(\widehat{W}-\widehat{w})(x_i,y,t_{n+1/2}) &= \left((I+\Delta t\mathcal{L}_{x,\varepsilon}^N)-(I+\Delta t\mathcal{L}_{x,\varepsilon})\right)\widehat{w}(x_i,y,t_{n+1/2}) \\ &\quad -c_1\Delta t(\widehat{W}-\widehat{w})(x_i,y,t_{n+1-p}).\end{aligned}$$

By using the initial conditions from (7.4.8) and (7.4.10), we get

$$(I+\Delta t\mathcal{L}_{x,\varepsilon}^N)(\widehat{W}-\widehat{w})(x_i,y,t_{n+1/2}) = \left((I+\Delta t\mathcal{L}_{x,\varepsilon}^N)-(I+\Delta t\mathcal{L}_{x,\varepsilon})\right)\widehat{w}(x_i,y,t_{n+1/2}).$$

Then, by applying the Taylor's expansion formula and using the bound of the singular component we get

$$(I+\Delta t\mathcal{L}_{x,\varepsilon}^N)(\widehat{W}-\widehat{w})(x_i,y,t_{n+1/2}) \leq C\varepsilon^{-1}N^{-1}(\ln N)\exp\left(-\alpha_{_x}(1-x_i)/\varepsilon\right).$$

Now, by choosing the barrier function

$$\phi_i = CN^{-1}(\ln N)(1+Y_i), \quad \text{for } i = N/2,\cdots,N,$$

and applying the discrete maximum principle (Lemma 7.3.2), we get

$$|(\widehat{W}-\widehat{w})(x_i,y,t_{n+1/2})| \leq CN^{-1}\ln N, \quad \text{for } i = N/2+1,\cdots,N. \tag{7.4.15}$$

Therefore, combining the results obtained in (7.4.14), Lemma 7.4.4 and (7.4.15), one can obtain the required error bound. ∎

The following theorem provides the error bound for the solution of (7.4.6).

Theorem 7.4.6. *Let $\widehat{u}^{n+1}$ be the exact solution of the problem (7.4.4) and $\widehat{U}^{n+1}_{x,y_j}$ be the numerical solution of the upwind scheme (7.4.6) defined on the special mesh Ω^N_y. Then we have the following error bound:*

$$|\widehat{u}^{n+1}(x,y_j) - \widehat{U}^{n+1}_{x,y_j}| \leq CN^{-1}\ln N.$$

Proof. The semidiscrete problems (7.4.3) and (7.4.4) are almost of the same type except the first term in the right hand side of both the equations, *i.e.*, the right hand side of (7.4.4) contains $\widehat{u}^{n+1/2}$ instead of $u(x,y,t_n)$ as in (7.4.3). So, by decomposing $\widehat{u}(x,y,\cdot)$ and $\widehat{U}(x,y_j,\cdot)$ of (7.4.4) and (7.4.6) into the smooth and singular components and using the bounds given in (7.4.14), Lemma 7.4.4, (7.4.15) and proceeding in a similar way as done in Theorem 7.4.5, we can obtain the required bound. ∎

Note that, if we take $N^{-q} \leq C\Delta t$ with $0 < q < 1$, from Theorems 7.4.5 and 7.4.6, we can deduce that

$$|\widehat{u}^{n+1/2}(x_i,y) - \widehat{U}^{n+1/2}_{x_i,y}| \leq C\Delta t N^{-1+q}\ln N, \quad \text{for } 1 \leq i \leq N-1, \tag{7.4.16}$$

and

$$|\widehat{u}^{n+1}(x,y_j) - \widehat{U}^{n+1}_{x,y_j}| \leq C\Delta t N^{-1+q}\ln N, \quad \text{for } 1 \leq j \leq N-1, \tag{7.4.17}$$

respectively.

We prove the uniform convergence of the fully discrete scheme (7.4.1)-(7.4.2), by using (7.4.16) and (7.4.17).

Theorem 7.4.7. *Let u be the exact solution of (7.1.1) and $\{U^n\}$ be the numerical solution of the fully discrete scheme (7.4.1)-(7.4.2) at time level $t_n = n\Delta t$. Then there exists a positive constant C, independent of ε, N, with $0 < q < 1$ such that*

$$\left\|u(x_i,y_j,t_n) - U^n_{i,j}\right\|_\infty \leq C(\Delta t + N^{-1+q}\ln N),$$

for $(x_i,y_j,t_n) \in \Omega^N_x \times \Omega^N_y \times \Lambda^p_{2,t}$.

Proof. The global error at time level $t_n = n\Delta t$ can be written as

$$\begin{aligned}\left\|u(x_i,y_j,t_n) - U^n_{i,j}\right\|_\infty &\leq \left\|u(x_i,y_j,t_n) - \widehat{u}^n_{i,j}\right\|_\infty + \left\|\widehat{u}^n_{i,j} - \widehat{U}^n_{x_i,y_j}\right\|_\infty \\ &\quad + \left\|\widehat{U}^n_{x_i,y_j} - U^n_{i,j}\right\|_\infty.\end{aligned}$$

Now using Lemma 7.2.3 along with the bounds given in (7.4.16) and (7.4.17), we get

$$\left\|u(x_i,y_j,t_n) - U^n_{i,j}\right\|_\infty \leq C\Delta t(\Delta t + N^{-1+q}\ln N) + \left\|\widehat{U}^n_{x_i,y_j} - U^n_{i,j}\right\|_\infty. \tag{7.4.18}$$

Then, by using the stability of the fully discrete scheme (7.4.1)-(7.4.2), it can be shown that

$$\left\|\widehat{U}^n_{x_i,y_j} - U^n_{i,j}\right\|_\infty \leq \left\|u(x_i,y_j,t_{n-1}) - U^{n-1}_{i,j}\right\|_\infty + C\Delta t \left\|\widehat{U}^{n-p}_{x_i,y_j} - U^{n-p}_{i,j}\right\|_\infty. \tag{7.4.19}$$

Since $t_n \in \Lambda^p_{2,t}$, it is obvious that $t_{n-p} \in \Lambda^p_{1,t}$. Now, by using the result of Theorem 7.4.1 in (7.4.19), we get

$$\left\|\widehat{U}^n_{x_i,y_j} - U^n_{i,j}\right\|_\infty \leq \left\|u(x_i,y_j,t_{n-1}) - U^{n-1}_{i,j}\right\|_\infty + C\Delta t(\Delta t + N^{-1+q}\ln N). \tag{7.4.20}$$

Therefore, from (7.4.18) and (7.4.20), we get

$$\left\|u(x_i,y_j,t_n) - U^n_{i,j}\right\|_\infty \leq C(\Delta t + N^{-1+q}\ln N),$$

for $1 \leq i,j \leq N-1$. Hence, the proof is completed. ∎

The above theorem provides the convergence result on the interval $[\tau, 2\tau]$. If we proceed in an analogous way, we can achieve the same convergence result for $t > 2\tau$. Hence, we can have the following convergence result for $t \in (0,T]$.

Theorem 7.4.8. *Let u be the exact solution of (7.1.1) and $\{U^n\}$ be the numerical solution of the fully discrete scheme (7.4.1)-(7.4.2) at time level $t_n = n\Delta t$. Then there exists a positive constant C, independent of ε, N, with $0 < q < 1$ such that*

$$\left\|u(x_i,y_j,t_n) - U^n_{i,j}\right\|_\infty \leq C(\Delta t + N^{-1+q}\ln N),$$

for $(x_i,y_j,t_n) \in \mathfrak{G}^{N,M}$.

7.5 Numerical Results

To validate the theoretical results proved in the previous section, here we present the numerical result obtained by the proposed method for two 2D test problems. We perform the numerical experiments by choosing the constant $\rho_{l,0} = 1.5$, $l = x, y$. Moreover, in the tables, we begin with $N = 32$, $\Delta t = 0.025$ and $p = 1/\Delta t$ and we multiply N by two and divide Δt by two. Since, we have taken $\Delta t = 0.8/N$, the theoretical error bound obtained in Theorem 7.4.8 will be of order $O(N^{-1}\ln N)$. Therefore, in this section, we will write only the spatial order of convergence, *i.e.*, $O(N^{-1}\ln N)$ instead of $O(N^{-1}\ln N + \Delta t)$. Note that in the following examples, we decompose the source term $f(x,y,t)$ in the form

$$f_2(x,y,t) = f(x,0,t) + y\left(f(x,1,t) - f(x,0,t)\right),\ f_1(x,y,t) = f(x,y,t) - f_2(x,y,t),$$

so that the property (7.2.1) is satisfied under the following compatibility condition:

$$f(0,0,t) = f(0,1,t) = f(1,0,t) = f(1,1,t) = 0, \quad \text{for } t \in [0,T].$$

Example 7.5.1. *Consider the following singularly perturbed 2D delay parabolic IBVP with constant coefficients:*

$$\begin{cases} u_t - \varepsilon\Delta u + u_x + u_y = u(x,y,t-1) + f(x,y,t), & (x,y,t) \in \mathfrak{D} \times (0,2], \\ u(x,y,t) = \varphi_b(x,y,t), & (x,y,t) \in \overline{\mathfrak{D}} \times [-1,0], \\ u(x,y,t) = 0, & (x,y,t) \in \partial\mathfrak{D} \times [0,2]. \end{cases} \tag{7.5.1}$$

We choose the initial data $\varphi_b(x,y,t)$ and the source function $f(x,y,t)$ to fit with the exact solution

$$u(x,y,t) = (1-\exp(-t))\left(m_1 + m_2 x + \exp(-(1-x)/\varepsilon)\right)\left(m_1 + m_2 y + \exp(-(1-y)/\varepsilon)\right),$$

where $m_1 = -\exp(-1/\varepsilon)$, $m_2 = -1 - m_1$.

We calculate the maximum pointwise error for each ε by

$$e_\varepsilon^{N,\Delta t} = \max_{(x_i,y_j,t_n)\in\mathfrak{G}^{N,M}} \left|u(x_i,y_j,t_n) - U(x_i,y_j,t_n)\right|,$$

where $u(x_i,y_j,t_n)$ and $U(x_i,y_j,t_n)$ denote the exact solution and the numerical solution obtained in $\mathfrak{G}^{N,M}$ with N mesh-intervals in the spatial directions and M mesh-intervals in the temporal direction, such that $\Delta t = T/M$ is the uniform mesh-size. We determine the corresponding order of convergence for each ε by

$$p_\varepsilon^{N,\Delta t} = \log_2\left(\frac{e_\varepsilon^{N,\Delta t}}{e_\varepsilon^{2N,\Delta t/2}}\right).$$

Now, for each N and Δt, we define the ε-uniform maximum pointwise error by

$$e^{N,\Delta t} = \max_\varepsilon e_\varepsilon^{N,\Delta t},$$

and the corresponding ε-uniform order of convergence by

$$p^{N,\Delta t} = \log_2\left(\frac{e^{N,\Delta t}}{e^{2N,\Delta t/2}}\right).$$

Next, we consider an example with variable coefficients.

Example 7.5.2. *Consider the following singularly perturbed 2D delay parabolic IBVP:*

$$\begin{cases} u_t - \varepsilon\Delta u + (1+x)u_x + (2-y)u_y + (x^2+y^2+1)u = u(x,y,t-1) + f(x,y,t), \\ \qquad\qquad (x,y,t) \in \mathfrak{D} \times (0,2], \\ u(x,y,t) = \varphi_b(x,y,t), \qquad (x,y,t) \in \overline{\mathfrak{D}} \times [-1,0], \\ u(x,y,t) = 0, \qquad (x,y,t) \in \partial\mathfrak{D} \times [0,2]. \end{cases} \tag{7.5.2}$$

We choose the initial data $\varphi_b(x, y, t)$ and the source function $f(x, y, t)$ to fit with the exact solution

$$u(x, y, t) = \exp(-t)xy(\gamma_1(x) - 1)(\gamma_2(y) - 1),$$

with

$$\gamma_1(x) = \exp(-(3 - 2x - x^2)/(2\varepsilon)) \quad \text{and} \quad \gamma_2(y) = \exp(-(3 - 4y + y^2)/(2\varepsilon)).$$

We calculate the maximum pointwise errors and the corresponding orders of convergence in a similar way as discussed earlier. Tables 7.1 and 7.2 display the maximum pointwise errors and the corresponding orders of convergence of the computed solution U for Examples 7.5.1 and 7.5.2, respectively.

In both the Tables 7.1 and 7.2, we can observe that for fixed ε, the maximum pointwise errors decrease monotonically as N increases, which confirms that the proposed method is ε-uniform convergent. It also reflects the fact that the fractional-step method along with classical upwind scheme applied on this class of problem results almost first-order convergence.

The numerical solutions of both the Examples 7.5.1 and 7.5.2 are plotted in Figures 7.1 and 7.3, respectively, for $\varepsilon = 10^{-2}, 10^{-8}$, $t = 1$, 2, and $N = 32$. These figures show the appearance of the boundary layer and its behavior for different ε and t.

As a complement of these observations, Figures 7.2 and 7.4 display the plot of N versus the maximum pointwise errors in loglog scale for both the Examples 7.5.1 and 7.5.2, respectively. As N increases, the monotonically decreasing behavior of the maximum pointwise errors can be observed from both the Figures 7.2 and 7.4. Moreover, these two figures also confirm that the proposed method is almost first-order accurate.

7.6 Conclusions

In this chapter, we have proposed an efficient numerical scheme for the singularly perturbed 2D delay parabolic convection-diffusion problem of the form (7.1.1), using the uniform mesh for the temporal domain and the piecewise-uniform Shishkin mesh for the spatial domain. For discretizing the time derivative a fractional-step method has been used and then the classical upwind scheme has been used for the 1D stationary problems resulting of the first step. This method has an advantage of solving only the tridiagonal linear systems instead of handling a banded pentadiagonal matrix, which therefore reduces the computational cost. It has been theoretically proved that the newly proposed scheme is ε-uniformly convergent with almost first-order (up to a logarithmic factor) in space and first-order in time. Along with the analysis, we have presented two numerical examples to verify the theoretical findings.

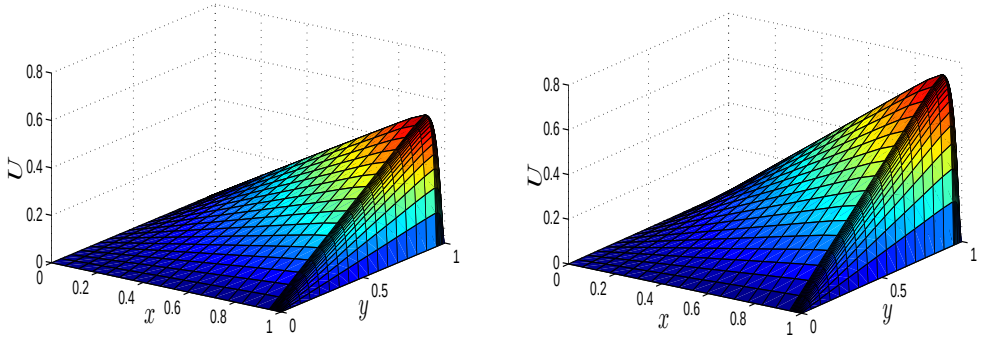

(a) $\varepsilon = 1e-2,\ t = 1.$ (b) $\varepsilon = 1e-2,\ t = 2.$

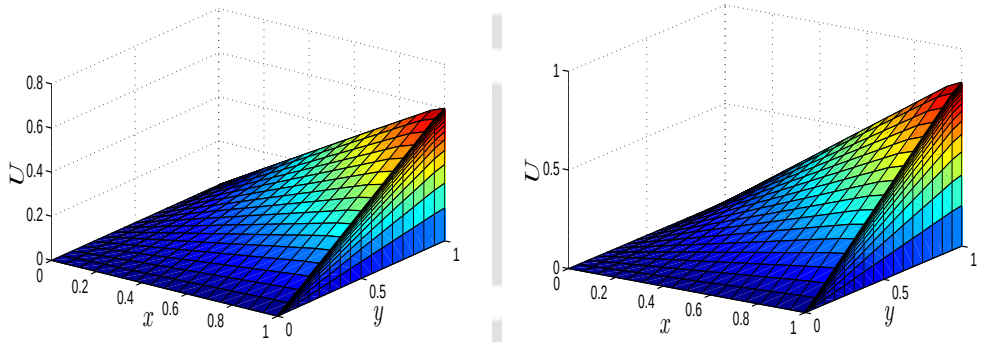

(c) $\varepsilon = 1e-8,\ t = 1.$ (d) $\varepsilon = 1e-8,\ t = 2.$

Figure 7.1: *Surface plots of the numerical solutions U at $N = 32$ for Example 7.5.1.*

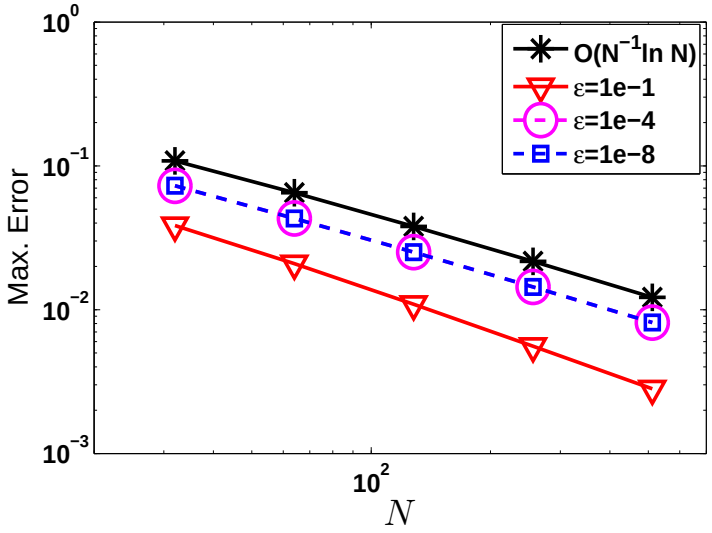

Figure 7.2: *Visualization of the order of convergence through loglog plot for Example 7.5.1.*

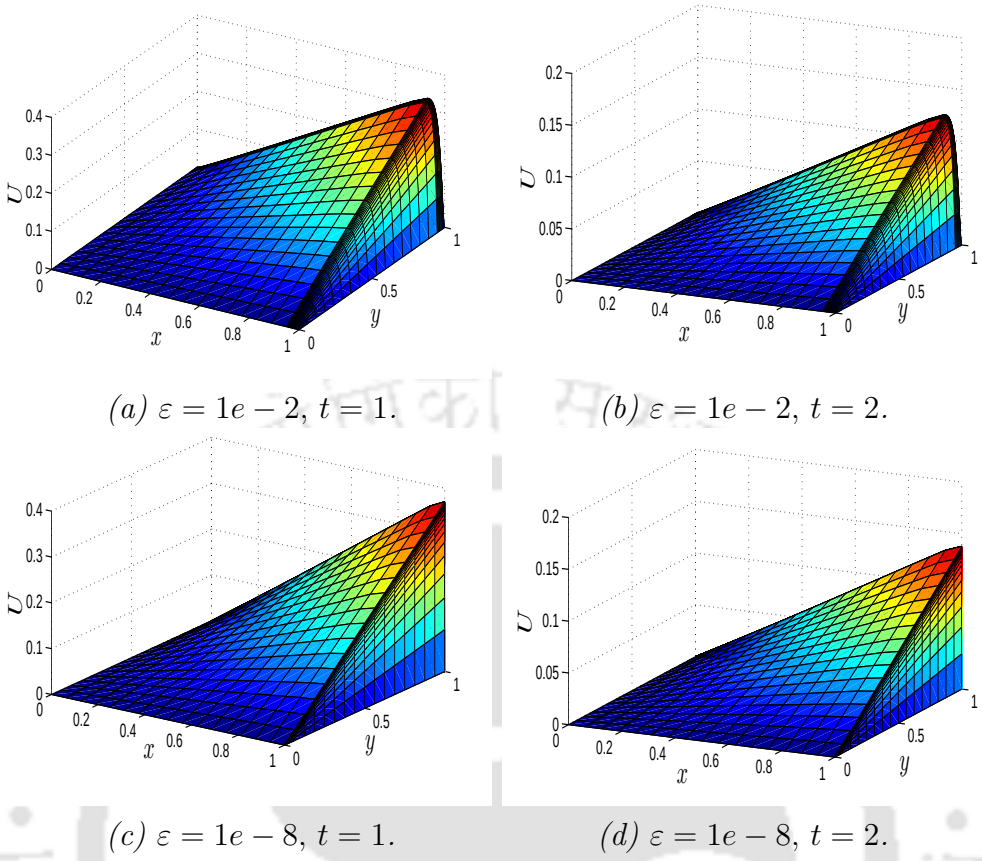

(a) $\varepsilon = 1e-2$, $t = 1$. (b) $\varepsilon = 1e-2$, $t = 2$.

(c) $\varepsilon = 1e-8$, $t = 1$. (d) $\varepsilon = 1e-8$, $t = 2$.

Figure 7.3: *Surface plots of the numerical solutions U at $N = 32$ for Example 7.5.2.*

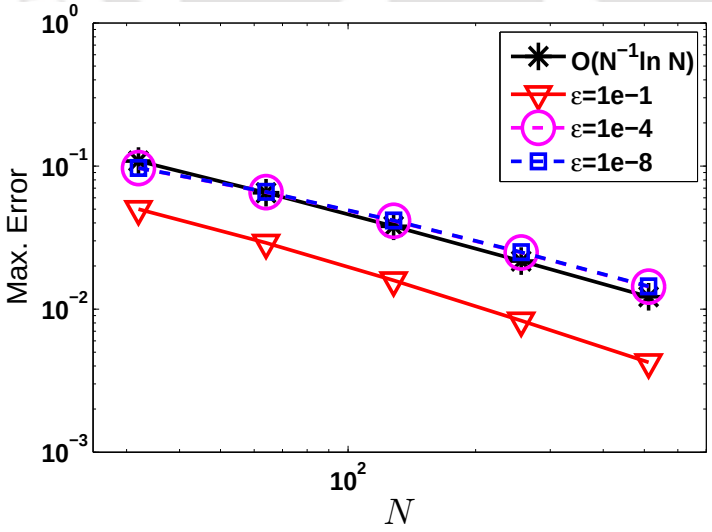

Figure 7.4: *Visualization of the order of convergence through loglog plot for Example 7.5.2.*

Table 7.1: *Maximum pointwise errors and the corresponding order of convergence for Example 7.5.1.*

ε	Number of mesh-intervals N/temporal mesh-size Δt				
	$32/\frac{1}{40}$	$64/\frac{1}{80}$	$128/\frac{1}{160}$	$256/\frac{1}{320}$	$512/\frac{1}{640}$
10^{-1}	3.8524e-2	2.0897e-2	1.0902e-2	5.5691e-3	2.8148e-3
	0.8824	0.9387	0.9691	0.9844	
10^{-2}	6.6775e-2	4.0097e-2	2.3696e-2	1.3720e-2	7.8000e-3
	0.7358	0.7589	0.7883	0.8147	
10^{-3}	7.2054e-2	4.2686e-2	2.4903e-2	1.4295e-2	8.0778e-3
	0.7553	0.7775	0.8008	0.8235	
10^{-4}	7.2681e-2	4.3029e-2	2.5086e-2	1.4396e-2	8.1308e-3
	0.7563	0.7784	0.8012	0.8242	
10^{-5}	7.2745e-2	4.3064e-2	2.5106e-2	1.4408e-2	8.1377e-3
	0.7563	0.7785	0.8012	0.8242	
10^{-6}	7.2751e-2	4.3068e-2	2.5107e-2	1.4409e-2	8.1384e-3
	0.7564	0.7785	0.8012	0.8241	
10^{-7}	7.2752e-2	4.3068e-2	2.5108e-2	1.4409e-2	8.1385e-3
	0.7564	0.7785	0.8012	0.8241	
10^{-8}	7.2752e-2	4.3068e-2	2.5108e-2	1.4409e-2	8.1385e-3
	0.7564	0.7785	0.8012	0.8241	
$e^{N,\Delta t}$	**7.2752e-2**	**4.3068e-2**	**2.5108e-2**	**1.4409e-2**	**8.1385e-3**
$p^{N,\Delta t}$	**0.7564**	**0.7785**	**0.8012**	**0.8241**	

Table 7.2: *Maximum pointwise errors and the corresponding order of convergence for Example 7.5.2.*

ε	Number of mesh-intervals N/temporal mesh-size Δt				
	$32/\frac{1}{40}$	$64/\frac{1}{80}$	$128/\frac{1}{160}$	$256/\frac{1}{320}$	$512/\frac{1}{640}$
10^{-1}	4.9930e-2	2.9034e-2	1.5886e-2	8.3027e-3	4.2476e-3
	0.7822	0.8700	0.9361	0.9669	
10^{-2}	8.4968e-2	5.8123e-2	3.6785e-2	2.2100e-2	1.2794e-2
	0.5478	0.6600	0.7351	0.7886	
10^{-3}	9.4080e-2	6.4490e-2	4.0709e-2	2.4412e-2	1.4111e-2
	0.5448	0.6637	0.7378	0.7907	
10^{-4}	9.6667e-2	6.5608e-2	4.1396e-2	2.4861e-2	1.4364e-2
	0.5591	0.6644	0.7356	0.7914	
10^{-5}	9.6963e-2	6.5981e-2	4.1604e-2	2.4909e-2	1.4402e-2
	0.5554	0.6653	0.7401	0.7903	
10^{-6}	9.6993e-2	6.6018e-2	4.1650e-2	2.4964e-2	1.4413e-2
	0.5550	0.6645	0.7385	0.7925	
10^{-7}	9.6996e-2	6.6022e-2	4.1655e-2	2.4970e-2	1.4419e-2
	0.5550	0.6645	0.7383	0.7922	
10^{-8}	9.6997e-2	6.6023e-2	4.1656e-2	2.4970e-2	1.4420e-2
	0.5550	0.6644	0.7383	0.7921	
$e^{N,\Delta t}$	**9.6997e-2**	**6.6023e-2**	**4.1656e-2**	**2.4970e-2**	**1.4420e-2**
$p^{N,\Delta t}$	**0.5550**	**0.6644**	**0.7383**	**0.7921**	

CHAPTER 8

Summary and Future Scopes

A brief summary of the results made in this thesis along with the techniques used in deriving the results is given in this chapter. It also contains the possible extensions of the present work and their further investigations.

8.1 Summary of the Results

The results of this thesis with some important observations are briefly described below:

- A parameter-uniform numerical scheme is analyzed on the Shishkin mesh for solving a one-dimensional singularly perturbed delay parabolic convection-diffusion problem. The scheme consists of the implicit-Euler scheme for the time derivative and the hybrid numerical scheme for the spatial derivatives. It is shown that the discrete solution obtained by this technique is almost second-order spatial accurate in the discrete supremum norm, provided the perturbation parameter ε satisfies $\varepsilon \leq N^{-1}$, which is the most demandable case from practical point of view. Numerical results are produced to validate theoretical error estimates. Numerically, it is shown that the result obtained by the proposed scheme is also valid for semilinear delay parabolic problems.

- Then, a post-processing technique known as the Richardson extrapolation technique is analyzed for solving a one-dimensional singularly perturbed delay parabolic convection-diffusion problem, on the piecewise-uniform Shishkin mesh. Theoretically and numerically it is proved that the order of convergence of the classical upwind scheme is enhanced from almost first-order to almost second-order, after extrapolation. Numerical experiments are carried out to validate the theoretical findings. This method is applied on semilinear delay parabolic problems also.

- The idea of the Richardson extrapolation technique is used to obtain second-order accurate (both in space and time) numerical solution of a singularly perturbed 2D parabolic convection-diffusion problem. To discretize the time derivative, we used the fractional-step method, then to solve the 1D stationary problems resulting of the first step, we used the classical upwind scheme on the piecewise-uniform Shishkin meshes in the spatial directions. Numerical results are produced to validate theoretical error estimates.

- In the literature, so far there exist no result where a singularly perturbed 2D delay parabolic convection-diffusion problem is considered. To solve such problems in this thesis, we used the classical upwind scheme to discretize the spatial derivatives on the piecewise-uniform Shishkin mesh and the implicit-Euler scheme to discretize the temporal derivatives on the uniform mesh. It is shown both theoretically and numerically that the method applied on the Shishkin mesh is almost first-order (up to a logarithmic factor) accurate in space and first-order accurate in time.

- One can notice, the order reduction occurred due to the Shishkin mesh, which was used to discretize the spatial domain. To overcome the reduction of order, we used the Bakhvalov-Shishkin mesh for the discretization of spatial domain. Theoretically and numerically it is shown that the error estimate obtained for the classical upwind scheme is first-order accurate in space as well as in time.

- An efficient numerical scheme is proposed to solve a singularly perturbed 2D delay parabolic convection-diffusion problem. To discretize the time derivative, the fractional-step method is used. Then the classical upwind scheme is used on the piecewise-uniform Shishkin meshes in the spatial directions, for the 1D stationary problems resulting of the first step. The parameter-uniform error estimates are derived for the numerical solution. Numerical experiments are carried out to validate the theoretical findings.

8.2 Future Scope

The possible extensions of the works carried out in this thesis are presented below:

In Chapter 2, we analyzed a singularly perturbed delay parabolic convection-diffusion problem using the implicit-Euler scheme for the time derivative and the hybrid scheme for the spatial derivative on the piecewise-uniform Shishkin mesh. The order of convergence in time can be increased by applying the Richardson extrapolation technique and appropriate analysis can be done.

The scheme applied in Chapter 2 can be used to solve a two-parameter delay convection-diffusion problem of the form

$$\begin{cases} (u_t - \varepsilon u_{xx} + \mu a(x)u_x + b(x,t)u)(x,t) = f(x,t) - c(x,t)u(x,t-\tau), & (x,t) \in D, \\ u(x,t) = \phi_b(x,t), & (x,t) \in \Gamma_b, \\ u(0,t) = \phi_l(t), & \text{on } \Gamma_l = \{(0,t) : 0 \le t \le T\}, \\ u(1,t) = \phi_r(t), & \text{on } \Gamma_r = \{(1,t) : 0 \le t \le T\}, \end{cases} \tag{8.2.1}$$

where $0 < \varepsilon, \mu \ll 1$ are the singular perturbation parameters and $\tau > 0$ is the delay parameter. $a(x)$, $b(x,t)$, $c(x,t)$, $f(x,t)$ on $\overline{D}$, and $\phi_l(t)$, $\phi_r(t)$, $\phi_b(x,t)$ on Γ, are sufficiently smooth and bounded functions, such that $a(x) \ge \alpha > 0$, $b(x,t) \ge 0$ and $c(x,t)$ is nonzero on $\overline{D}$.

The Richardson extrapolation technique used in Chapter 3 can be applied to the above problem (8.2.1).

The analysis done in this thesis can be extended to a coupled system of equations. One may think to use the higher-order schemes used in Chapter 2 and Chapter 3 to solve the following model equation:

$$\begin{cases} L_{\vec{\varepsilon}}\vec{u} \equiv \dfrac{\partial \vec{u}}{\partial t} + L_{x,\vec{\varepsilon}}\vec{u} = \vec{f} - \tilde{B}(x)\vec{u}(x,t-\tau), & (x,t) \in D = \Omega_x \times \Lambda_t = (0,1) \times (0,T], \\ \vec{u}(x,t) = \vec{\phi}_b(x,t), & (x,t) \in \Gamma_b, \\ \vec{u}(0,t) = \vec{\phi}_l(t), & \text{on } \Gamma_l = \{(0,t) : 0 \le t \le T\}, \\ \vec{u}(1,t) = \vec{\phi}_r(t), & \text{on } \Gamma_r = \{(1,t) : 0 \le t \le T\}, \end{cases} \tag{8.2.2}$$

where the spatial differential operator $L_{x,\vec{\varepsilon}}$ is given by

$$L_{x,\vec{\varepsilon}} \equiv -\mathcal{E}\frac{\partial^2}{\partial x^2} - A(x)\frac{\partial}{\partial x} + B(x),$$

and the coefficient matrices $\mathcal{E} = \text{diag}(\varepsilon_1, \varepsilon_2)$, $A(x) = \text{diag}(a_1(x), a_2(x))$, $B(x) = (b_{ij}(x))_{2\times 2}$, and $\tilde{B}(x) = (\tilde{b}_{ij}(x))_{2\times 2}$. We shall assume that convection matrix A satisfies following conditions:

$$a_1(x) \ge \alpha > 0, \qquad a_2(x) \ge \alpha > 0.$$

In addition, we assume that $B = \{b_{ij}\}_{i,j=1}^{2}$ is an L_0-matrix (*i.e.*, off-diagonals are non-positive and diagonals are positive) with

$$\min_{x\in[0,1]} \{b_{11}(x) + b_{12}(x), b_{21}(x) + b_{22}(x)\} > \beta > 0,$$

In Chapter 4, we used the Richardson extrapolation technique for singularly perturbed 2D parabolic convection-diffusion PDE with homogeneous Dirichlet boundary condition. One can use the fractional-step method along with the hybrid scheme to solve the following singularly perturbed 2D parabolic convection-diffusion problem with nonhomogeneous Robin type boundary conditions, posed on the domain $\mathfrak{G} = \mathfrak{D} \times \Lambda_t$,

$$\begin{cases} u_t + \mathcal{L}_\varepsilon u(x,y,t) = f(x,y,t), & (x,y,t) \in \mathfrak{G}, \\ u(x,y,0) = s(x,y), & (x,y) \in \overline{\mathfrak{D}}, \\ \lambda(x,y,t)u(x,y,t) + \varepsilon\gamma(x,y,t)\dfrac{\partial u}{\partial n}(x,y,t) = \tilde{s}(x,y,t), & (x,y,t) \in \partial\mathfrak{D} \times \overline{\Lambda}_t, \end{cases}$$

where

$$\mathcal{L}_\varepsilon u = -\varepsilon\Delta u + \mathbf{a}(x,y).\nabla u + b(x,y)u,$$

and $\dfrac{\partial u}{\partial n}$ denotes the derivative of u in the outward normal direction to the boundary $\partial\mathfrak{D} \times \overline{\Lambda}_t$. The coefficients $\mathbf{a} = (a_1, a_2)$, b and the functions $\lambda(x,y,t)$, $\gamma(x,y,t)$ are sufficiently smooth and bounded function such that $a_1(x,y) \geq \alpha_x > 0$, $a_2(x,y) \geq \alpha_y > 0$ and $b(x,y) \geq 0$, on $\overline{\mathfrak{D}}$ and $\lambda(x,y,t)$, $\gamma(x,y,t) \geq 0$, $\lambda(x,y,t) + \gamma(x,y,t) > 0$, on $\partial\mathfrak{D} \times \overline{\Lambda}_t$.

Finally, in Chapter 7, we analyzed singularly perturbed 2D delay parabolic convection-diffusion problem using the fractional-step method and the upwind scheme. It will be much interesting to enhance the order of convergence by using the technique done in Chapter 4.

[1] L. R. Abrahamsson, H. B. Keller, and H. O. Kreiss. Difference approximations for singular perturbations of systems of ordinary differential equations. *Numer. Math.*, 22:367–391, 1974.

[2] G. M. Amiraliyev and F. Erdogan. Uniform numerical method for singularly perturbed delay differential equations. *Comput. Math. Appl.*, 53(8):1251–1259, 2007.

[3] A. R. Ansari, S. A. Bakr, and G. I. Shishkin. A parameter-robust finite difference method for singularly perturbed delay parabolic partial differential equations. *J. Comput. Appl. Math.*, 205(1):552–566, 2007.

[4] N. S. Bakhvalov. The optimization of methods of solving boundary value problems with a boundary layer. *Comput. Math. Math. Phys.*, 9(4):139–166, 1969.

[5] R. K. Bawa and S. Natesan. A computational method for self-adjoint singular perturbation problems using quintic spline. *Comput. Math. Appl.*, 50(8-9):1371–1382, 2005.

[6] R. Bellman and K. L. Cooke. *Differential-Difference Equations*. Academic Press, New York-London, 1963.

[7] C. M. Bender and S. A. Orszag. *Advance Mathematical Methods for Scientists and Engineers*. McGraw-Hill, New York, 1978.

[8] N. F. Britton. Spatial structures and periodic travelling waves in an integro-differential reaction-diffusion population model. *SIAM J. Appl. Math.*, 50(6):1663–1688, 1990.

[9] A. W. Bush. *Perturbation Methods for Engineers and Scientists*. CRC Press, London, 1992.

[10] X. Cai and F. Liu. A Reynolds uniform scheme for singularly perturbed parabolic differential equation. *ANZIAM J.*, 47((C)):C633–C648, 2005.

[11] Z. Cen. A second-order finite difference scheme for a class of singularly perturbed delay differential equations. *Int. J. Comput. Math.*, 87(1-3):173–185, 2010.

[12] C. Clavero, J. L. Gracia, and J. C. Jorge. A uniformly convergent alternating direction HODIE finite difference scheme for 2D time-dependent convection-diffusion problems. *IMA J. Numer. Anal.*, 26(1):155–172, 2006.

[13] C. Clavero and J. C. Jorge. Another uniform convergence analysis technique of some numerical methods for parabolic singularly perturbed problems. *Comput. Math. Appl.*, 70(3):222–235, 2015.

[14] C. Clavero, J. C. Jorge, F. Lisbona, and G. I. Shishkin. A fractional step method on a special mesh for the resolution of multidimensional evolutionary convection-diffusion problems. *Appl. Numer. Math.*, 27(3):211–231, 1998.

[15] C. Clavero, J. C. Jorge, F. Lisbona, and G. I. Shishkin. An alternating direction scheme on a nonuniform mesh for reaction-diffusion parabolic problems. *IMA J. Numer. Anal.*, 20(2):263–280, 2000.

[16] P. Das and S. Natesan. Richardson extrapolation method for singularly perturbed convection-diffusion problems on adaptively generated mesh. *CMES Comput. Model. Eng. Sci.*, 90(6):463–485, 2013.

[17] P. Das and S. Natesan. A uniformly convergent hybrid scheme for singularly perturbed system of reaction-diffusion Robin type boundary-value problems. *J. Appl. Math. Comput.*, 41(1-2):447–471, 2013.

[18] B. S. Deb and S. Natesan. Richardson extrapolation method for singularly perturbed coupled system of convection-diffusion boundary-value problems. *CMES Comput. Model. Eng. Sci.*, 38(2):179–199, 2008.

[19] O. Diekmann, S. A. van Gils, S. M. Verduyn Lunel, and H.-O. Walther. *Delay Equations*. Springer-Verlag, New York, 1995.

[20] E. P. Doolan, J. J. H. Miller, and W. H. A. Schilders. *Uniform Numerical Methods for Problems with Initial and Boundary Layers*. Boole Press, Dublin, 1980.

[21] R. D. Driver. *Ordinary and Delay Differential Equations*. Springer-Verlag, Berlin, 1977.

[22] W. Eckhaus. *Matched Asymptotic Expansions and Singular Perturbations*. North Holland, Amsterdam, 1973.

[23] W. Eckhaus. *Asymptotic Analysis of Singular Perturbations*. North Holland, Amsterdam, 1979.

[24] L. E. El'sgol'ts and S. B. Norkin. *Introduction to the Theory and Application of Differential Equations with Deviating Arguments*. Academic Press, New York-London, 1973.

[25] F. Erdogan. A parameter robust method for singularly perturbed delay differential equations. *J. Inequal. Appl.*, pages 14, Art. ID 325654, 2010.

[26] R. E. Ewing and H. Wang. A summary of numerical methods for time-dependent advection-dominated partial differential equations. *J. Comput. Appl. Math.*, 128(1-2):423–445, 2001.

[27] P. A. Farrell. Sufficient conditions for uniform convergence of a class of difference schemes for a singularly perturbed problem. *IMA J. Numer. Anal.*, 7(4):459–472, 1987.

[28] P. A. Farrell, A. F. Hegarty, J. J. H. Miller, E. O'Riordan, and G. I. Shishkin. *Robust Computational Techniques for Boundary Layers*. Chapman & Hall/CRC, Boca Raton, FL, 2000.

[29] A. Friedman. *Partial Differential Equations of Parabolic Type*. Prentice-Hall, Inc., Englewood Cliffs, N.J., 1964.

[30] K. O. Friedrichs and W. R. Wasow. Singular perturbations of nonlinear oscillations. *Duke Math. J.*, 13:367–381, 1946.

[31] S. Gowrisankar and S. Natesan. A robust numerical scheme for singularly perturbed delay parabolic initial-boundary-value problems on equidistributed grids. *Electron. Trans. Numer. Anal.*, 41:376–395, 2014.

[32] S. Gowrisankar and S. Natesan. ε-Uniformly convergent numerical scheme for singularly perturbed delay parabolic partial differential equations. *Int. J. Comput. Math.*, 94(5):902–921, 2017.

[33] J. Hale. *Theory of Functional Differential Equations*. Springer-Verlag, New York-Heidelberg, 1977.

[34] J. K. Hale and S. M. Verduyn Lunel. *Introduction to Functional Differential Equations*. Springer-Verlag, New York, 1977.

[35] M. K. Kadalbajoo and K. C. Patidar. Singularly perturbed problems in partial differential equations: a survey. *Appl. Math. Comput.*, 134(2-3):371–429, 2003.

[36] M. K. Kadalbajoo and V. P. Ramesh. Hybrid method for numerical solution of singularly perturbed delay differential equations. *Appl. Math. Comput.*, 187(2):797–814, 2007.

[37] M. K. Kadalbajoo and V. P. Ramesh. Numerical methods on Shishkin mesh for singularly perturbed delay differential equations with a grid adaptation strategy. *Appl. Math. Comput.*, 188(2):1816–1831, 2007.

[38] M. K. Kadalbajoo and K. K. Sharma. An ε-uniform fitted operator method for solving boundary-value problems for singularly perturbed delay differential equations: layer behavior. *Int. J. Comput. Math.*, 80(10):1261–1276, 2003.

[39] M. K. Kadalbajoo and K. K. Sharma. Numerical analysis of singularly perturbed delay differential equations with layer behavior. *Appl. Math. Comput.*, 157(1):11–28, 2004.

[40] H. B. Keller. *Numerical Methods for Two-Point Boundary Value Problems*. Dover Publications, Inc., New York, 1992.

[41] R. B. Kellogg and A. Tsan. Analysis of some difference approximations for a singular perturbation problem without turning points. *Math. Comp.*, 32(144):1025–1039, 1978.

[42] J. Kevorkian and J. D. Cole. *Multiple Scale and Singular Perturbation Methods*. Springer-Verlag, New York, 1996.

[43] V. Kolmanovskii and A. Myshkis. *Applied Theory of Functional Differential Equations*. Kluwer, Dordrecht, 1992.

[44] V. Kolmanovskii and V. Nosov. *Stability of Functional Differential Equations*. Academic Press, London, 1986.

[45] N. Kopteva and M. Stynes. Approximation of derivatives in a convection-diffusion two-point boundary value problem. *Appl. Numer. Math.*, 39(1):47–60, 2001.

[46] Y. Kuang. *Delay Differential Equations with Applications in Population Dynamics.* Academic Press, Inc., Boston, MA, 1993.

[47] D. Kumar and M. K. Kadalbajoo. A parameter-uniform numerical method for time-dependent singularly perturbed differential-difference equations. *Appl. Math. Model.*, 35(6):2805–2819, 2011.

[48] O. A. Ladyženskaja, V. A. Solonnikov, and N. N. Ural′ceva. *Linear and Quasilinear Equations of Parabolic Type.* American Mathematical Society, Providence, R.I., 1968.

[49] P. A. Lagerstrom and R. G. Casten. Basic concepts underlying singular perturbation techniques. *SIAM Rev.*, 14:63–120, 1972.

[50] C. G. Lange and R. M. Miura. Singular perturbation analysis of boundary value problems for differential-difference equations. *SIAM J. Appl. Math.*, 42(3):502–531, 1982.

[51] C. G. Lange and R. M. Miura. Singular perturbation analysis of boundary value problems for differential-difference equations. II. Rapid oscillations and resonances. *SIAM J. Appl. Math.*, 45(5):687–707, 1985.

[52] C. G. Lange and R. M. Miura. Singular perturbation analysis of boundary value problems for differential-difference equations. III. Turning point problems. *SIAM J. Appl. Math.*, 45(5):708–734, 1985.

[53] C. G. Lange and R. M. Miura. Singular perturbation analysis of boundary value problems for differential-difference equations. V. Small shifts with layer behavior. *SIAM J. Appl. Math.*, 54(1):249–272, 1994.

[54] C. G. Lange and R. M. Miura. Singular perturbation analysis of boundary value problems for differential-difference equations. VI. Small shifts with rapid oscillations. *SIAM J. Appl. Math.*, 54(1):273–283, 1994.

[55] T. Linß. An upwind difference scheme on a novel Shishkin-type mesh for a linear convection-diffusion problem. *J. Comput. Appl. Math.*, 110(1):93–104, 1999.

[56] T. Linß. Layer-adapted meshes for convection-diffusion problems. *Comput. Methods Appl. Mech. Engrg.*, 192(9-10):1061–1105, 2003.

[57] T. Linß and M. Stynes. A hybrid difference scheme on a Shishkin mesh for linear convection-diffusion problems. *Appl. Numer. Math.*, 31(3):255–270, 1999.

[58] J. J. H. Miller. Sufficient conditions for the convergence, uniformly in ε, of a three-point difference scheme for a singular perturbation problem. In *Numerical Treatment of Differential Equations in Applications*, volume 679 of *Lect. Notes in Maths.*, pages 85–91. Springer, Berlin, 1978.

[59] J. J. H. Miller, E. O'Riordan, and G. I. Shishkin. On piecewise-uniform meshes for upwind- and central-difference operators for solving singularly perturbed problems. *IMA J. Numer. Anal.*, 15(1):89–99, 1995.

[60] J. J. H. Miller, E. O'Riordan, and G. I. Shishkin. *Fitted Numerical Methods for Singular Perturbation Problems*. World Scientific Publishing Co. Pte. Ltd., Singapore, 2012.

[61] P. D. Miller. *Applied Asymptotic Analysis*. Graduate Studies in Mathematics. American Mathematical Society, Providence, RI, 2006.

[62] J. Mohapatra and S. Natesan. Uniformly convergent second-order numerical method for singularly perturbed delay differential equations. *Neural Parallel Sci. Comput.*, 16(3):353–370, 2008.

[63] J. Mohapatra and S. Natesan. Uniformly convergent numerical method for singularly perturbed differential-difference equation using grid equidistribution. *Int. J. Numer. Methods Biomed. Eng.*, 27(9):1427–1445, 2011.

[64] K. W. Morton. *Numerical Solution of Convection-Diffusion Problems*. Chapman & Hall, London, 1996.

[65] K. Mukherjee and S. Natesan. Parameter-uniform hybrid numerical scheme for time-dependent convection-dominated initial-boundary-value problems. *Computing*, 84(3-4):209–230, 2009.

[66] K. Mukherjee and S. Natesan. Richardson extrapolation technique for singularly perturbed parabolic convection-diffusion problems. *Computing*, 92(1):1–32, 2011.

[67] K. Mukherjee and S. Natesan. ε-uniform error estimate of hybrid numerical scheme for singularly perturbed parabolic problems with interior layers. *Numer. Algorithms*, 58(1):103–141, 2011.

[68] J. D. Murray. *Mathematical Biology*. Springer-Verlag, Berlin, 1989.

[69] S. Natesan and N. Ramanujam. Booster method for singularly-perturbed one-dimensional convection-diffusion Neumann problems. *J. Optim. Theory Appl.*, 99(1):53–72, 1998.

[70] S. Natesan and N. Ramanujam. "Shooting method" for singular perturbation problems arising in chemical reactor theory. *Int. J. Comput. Math.*, 70(2):251–262, 1998.

[71] S. Natesan and N. Ramanujam. A "booster method" for singular perturbation problems arising in chemical reactor theory. *Appl. Math. Comput.*, 100(1):27–48, 1999.

[72] S. Natesan and N. Ramanujam. Improvement of numerical solution of self-adjoint singular perturbation problems by incorporation of asymptotic approximations. *Appl. Math. Comput.*, 98(2-3):119–137, 1999.

[73] M. C. Natividad and M. Stynes. Richardson extrapolation for a convection-diffusion problem using a Shishkin mesh. *Appl. Numer. Math.*, 45(2-3):315–329, 2003.

[74] A. H. Nayfeh. *Perturbation Methods*. John Wiley & Sons, New York, 1973.

[75] A. H. Nayfeh. *Introduction to Perturbation Methods*. John Wiley & Sons, New York, 1981.

[76] P. W. Nelson and A. S. Perelson. Mathematical analysis of delay differential equation models of HIV-1 infection. *Math. Biosci.*, 179(1):73–94, 2002.

[77] M. J. Ng-Stynes, E. O'Riordan, and M. Stynes. Numerical methods for time-dependent convection-diffusion equations. *J. Comput. Appl. Math.*, 21(3):289–310, 1988.

[78] R. E. O'Malley, Jr. *Introduction to Singular Perturbations*. Academic Press, New York, 1974.

[79] R. E. O'Malley, Jr. *Singular Perturbation Methods for Ordinary Differential Equations*. Applied Mathematical Sciences. Springer-Verlag, New York, 1991.

[80] K. C. Patidar and K. K. Sharma. Uniformly convergent non-standard finite difference methods for singularly perturbed differential-difference equations with delay and advance. *Internat. J. Numer. Methods Engrg.*, 66(2):272–296, 2006.

[81] K. C. Patidar and K. K. Sharma. ε-uniformly convergent non-standard finite difference methods for singularly perturbed differential difference equations with small delay. *Appl. Math. Comput.*, 175(1):864–890, 2006.

[82] L. Prandtl. Uber flussigkeits-bewegung bei kleiner reibung. In *Verhandlungen, III Inter. Math. Kongresses, Tuebner, Leipzig*, pages 484–491, 1905.

[83] V. P. Ramesh and M. K. Kadalbajoo. Upwind and midpoint upwind difference methods for time-dependent differential difference equations with layer behavior. *Appl. Math. Comput.*, 202(2):453–471, 2008.

[84] H.-G. Roos and T. Linß. Sufficient conditions for uniform convergence on layer-adapted grids. *Computing*, 63(1):27–45, 1999.

[85] H.-G. Roos, M. Stynes, and L. Tobiska. *Robust Numerical Methods for Singularly Perturbed Differential Equations*. Springer-Verlag, Berlin, 2008.

[86] G. I. Shishkin and L. P. Shishkina. *Difference Methods for Singular Perturbation Problems*. CRC Press, Boca Raton, FL, 2009.

[87] R. B. Stein. Some models of neuronal variability. *Biophys. J.*, 7:37–68, 1967.

[88] M. Stynes. Steady-state convection-diffusion problems. *Acta Numer.*, 14:445–508, 2005.

[89] M. Stynes and H.-G. Roos. The midpoint upwind scheme. *Appl. Numer. Math.*, 23(3):361–374, 1997.

[90] H. Tian. The exponential asymptotic stability of singularly perturbed delay differential equations with a bounded lag. *J. Math. Anal. Appl.*, 270(1):143–149, 2002.

[91] J. Vigo-Aguiar and S. Natesan. A parallel boundary value technique for singularly perturbed two-point boundary value problems. *J. Supercomput.*, 27(2):195–206, 2004.

[92] J. Vigo-Aguiar and S. Natesan. An efficient numerical method for singular perturbation problems. *J. Comput. Appl. Math.*, 192(1):132–141, 2006.

[93] M. Villasana and A. Radunskaya. A delay differential equation model for tumor growth. *J. Math. Biol.*, 47(3):270–294, 2003.

[94] R. Vulanović. *Mesh Construction for Discretization of Singularly Perturbed Boundary Value Problems*. PhD thesis, University of Novi Sad, 1986.

[95] P. K. C. Wang. Asymptotic stability of a time-delayed diffusion system. *Trans. ASME Ser. E.J. Appl. Mech.*, 30:500–504, 1963.

[96] T. Zhao. Global periodic solutions for a differential delay system modeling a microbial population in the chemostat. *J. Math. Anal. Appl.*, 193(1):329–352, 1995.

List of published and communicated papers

Based on the work in this thesis, the following research articles are published or communicated.

1. A. Das and S. Natesan. Uniformly convergent hybrid numerical scheme for singularly perturbed delay parabolic convection-diffusion problems on Shishkin mesh. *Appl. Math. Comput.*, 271:168-186, 2015.
2. A. Das and S. Natesan. Second-order uniformly convergent numerical method for singularly perturbed delay parabolic partial differential equations. *Int. J. Comput. Math.*, doi:10.1080/00207160.2017.1290439.
3. A. Das and S. Natesan. Parameter-uniform numerical method for singularly perturbed 2D delay parabolic convection-diffusion problems on Shishkin mesh (communicated).
4. A. Das and S. Natesan. Fractional-step method for singularly perturbed 2D delay parabolic convection-diffusion problems on Shishkin mesh (communicated).
5. A. Das and S. Natesan. The parameter-uniform numerical method for singularly perturbed 2D delay parabolic convection-diffusion problems on Bakhvalov-Shishkin mesh (communicated).
6. A. Das and S. Natesan. Higher-order convergence with fractional-step method for singularly perturbed 2D parabolic convection-diffusion problems on Shishkin mesh (communicated).